MONITORING OF DAMAGE IN REINFORCEMENT IN CONCRETE

A

Thesis

Submitted in fulfillment of the requirement

for the award of degree of

DOCTOR OF PHILOSOPHY

By

SHRUTI SHARMA

Regd. No 90602502

SUPERVISOR

Dr. Abhijit Mukherjee

Director, Thapar University

Patiala-147004

DEPARTMENT OF CIVIL ENGINEERING

THAPAR UNIVERSITY, PATIALA-147004

AUGUST- 2010

CERTIFICATE

Certified that the work presented in the thesis titled, **"MONITORING OF DAMAGE IN REINFORCEMENT IN CONCRETE"** which is being submitted by **Ms. Shruti Sharma**, **Regd. No 90602502**, in fulfillment of the requirement for the award of the degree of 'Doctor of Philosophy' in the Department of Civil Engineering, Thapar University, Patiala, is an authentic record of the candidate's own work carried out from April, 2007 to June, 2010 in this university under my supervision. The matter presented in this thesis has not been submitted for the award of any other degree in any other university.

(Dr. Abhijit Mukherjee)
Director
Thapar University
Patiala-147004

ACKNOWLEDGEMENTS

Time has provided me cherished opportunity to express feelings of gratefulness and submit my acknowledgements for those who helped me earning this day in my life. First and foremost, I wish to express my deep sense of gratitude with reverence towards my supervisor **Prof. Abhijit Mukherjee**, Director, Thapar University, Patiala, for his valuable guidance and inspiring encouragement in pursuance of this work. Despite his busy schedule, he always spared time for me and his guidance, precious and genial, which always kept me on the right track. I shall remain grateful to him for providing valuable and remarkable support throughout my thesis work. I am indeed highly indebted to him for his support and thought provoking suggestions during many exigent circumstances. His systematic approach and unconditional co-operation made me work hard. It was a great pleasure working with him and for me; it is the beginning of research. I shall remain grateful to him forever.

I am also very thankful to Dr. Maneek Kumar, Prof. & Head, Department of Civil Engineering, for providing excellent academic environment and laboratory facilities for experimentation. I have no words to express my sincere gratitude to all the staff of Dynamics Lab and Concrete Structures Lab. Without their active support and enthusiasm, it would not have been possible to carry out the experimental work. I am extremely thankful to Sh. Vinod Billa, Sh. Om Prakash, Sh. Udham Singh, Sh. Ram Sumiran, Sh. Amarjit, Sh. Surinder and all other manpower for their support and much needed help.

Constructive suggestions and help of my students, Ms. Garima Vermani, Mr. Raghuram, Mr. S. Arjun, Mr. Sameer Sharma towards amelioration of this work is deeply acknowledged. I am highly obliged to them for their support in carrying out present research work.

I am also grateful to the Dr. K. K Raina, Deputy Director whose motivating words and encouragement always kept me rolling. Thanks are also due to Dr. Sushil Mittal, Dean (RSP) for giving me the opportunity and co-operation and support in pursuing this work. I also thank all my fellows, friends, colleagues at Thapar University and relatives who directly or indirectly helped me carry out this research.

I am indeed indebted to my parents, Sh. V.R Sharma and Ms. Sneh Sharma and my

parent in-laws, Sh. Hari Om Sharma and Ms. Darshana Sharma without whose encouraging words and timely support this would not have been possible. Thanks are also due to my brother in-laws, Sh. Munish Kaushal, Dr. Paras Khullar & Dr. Sumit Bedi for their encouraging words. My sisters, Dr. Ritu Kaushal, Dr. Smriti Khullar and Dr. Sonali Bedi also require a special mention for providing cheerful support during the tenure of my work. I am also thankful to my brother, Er. Mayank for providing emotional support and help whenever required.

I owe special thanks to my son, Sanyam for patiently bearing inattentiveness towards him during my doctoral work. I acknowledge my heartiest gratitude to my husband and best colleague, Sh. Sandeep Sharma, without whose untiring support, enduring patience and valuable suggestions, I would ever have been able to complete this work successfully.

Last but not the least, I wish to express my thanks to all those who remained behind the screen but whose work has been quoted and consulted in the present research. In the end, I am thankful and grateful to the Almighty for bringing this day in my life.

Shruti Sharma

(Shruti Sharma)

ABSTRACT

One of the major causes of catastrophic failures in reinforced concrete structures such as bridges, dams and buildings is the deterioration of reinforcing bars due to corrosion. If the degradation remains unnoticed inside concrete, it further accelerates and causes huge loss of life and property. Removal of concrete to visually inspect the reinforcement is detrimental to the structure. Hence, it is imperative to develop a non-intrusive health monitoring technique for early detection of corrosion related damages in steel embedded in concrete. Guided ultrasonic waves offer a potentially attractive solution.

In the present study, bars embedded in concrete are subjected to corrosion and monitored ultrasonically using longitudinal guided waves. A mode with minimal attenuation and mode shape that is suitable for detection of a particular type of damage is chosen from dispersion curves. The reinforcements have been excited at one end with an ultrasonic pulse using piezoelectric transducers and are received at the other end (pulse transmission technique). In pulse echo technique same transducer is used as transmitter and receiver. Ultrasonic testing is carried out on bars in concrete by simulating corrosion in the form of area loss (notches) and delamination (tape wrapped on embedded bar).The developed methodology is applied to reinforced concrete beams specimens undergoing accelerated corrosion. Two corrosion environments- i.e. presence of chlorides (referred to as chloride corrosion, CC) and absence of chlorides (referred to as oxide corrosion, OC) are chosen. To investigate the ability of ultrasonics in predicting the level of deterioration, a correlation is attempted between ultrasonic voltages and destructive tests such as mass loss, pull out strength and tensile strength at different stages and ages of corrosion

It is observed that corrosion of reinforcing bars in concrete is discernible using ultrasonic guided waves. Through a judicious selection of different ultrasonic modes, not only the corrosion phenomenon can be monitored but also different types of corrosion occurring in different environments can be successfully identified. From the limited experimental data approximate relations between ultrasonic signals and physical conditions of the corroded bars have been developed.

CONTENTS

LIST OF PUBLICATIONS

International Journals

1. Sharma, S. and Mukherjee, A. (2011) , 'Monitoring progression of corrosion in chloride and oxide environment using ultrasonic guided waves', Technical Note in *ASCE-Journal of Materials in Civil Engineering*, Vol. 23(2), February 2011.
2. Sharma, S. and Mukherjee, A. (2010), 'Longitudinal Guided Waves for Monitoring Chloride Corrosion in reinforcing bars in concrete', *Structural Health Monitoring*, Vol. 9 (6), 555-567, November-December 2010.
3. Sharma, S. and Mukherjee, A. (2010), 'Propagating ultrasonic guided waves through concrete reinforcements with simulated and actual corrosion', *Canadian Institute of Non-Destructive Evaluation Journal*, March-April-2010.
4. Sharma, S. and Mukherjee, A., Ultrasonic Guided Waves for Corrosion Monitoring in Chloride Environment', *ACI Materials Journal*, In Review after Revision.

National Journals

5. Sharma, S., Bhise, P.C. and Mukherjee, A. (2011), 'Damage Detection in steel bars using ultrasonic guided waves: An Experimental and Analytical study', *Journal of Structural Engineering, SERC, Chennai*, June-July 2011.
6. Sharma, S. and Mukherjee, A. (2009), 'Damage Detection in Reinforcing Bars in Concrete using Ultrasonic Waves', *Journal of Pure and Applied Ultrasonics*, Vol. 3, August – September, 2009.

International Conferences

7. Sharma, S. and Mukherjee, A. (2009), 'Damage Monitoring in Reinforcing Bars in Concrete using Longitudinal Guided Waves', *International Conference on Structural Health Monitoring SHMII-4, 22nd -24th July- 2009, Zurich, Switzerland*.
8. Sharma, S. and Mukherjee, A. (2009), 'Ultrasonics for Corrosion Monitoring of Embedded Reinforcements', *International Conference on Advances in Structures and Geotechnical Engineering, ACSGE-2009, Oct 25-27, 2009 at BITS, Pilani, India.*

Book Chapter

9. Mukherjee, A., Sharma, S. and Sharma, S. (2009), 'Health Monitoring of Steel Structures using Ultrasonic Waves', *INSDAG Year Book-2009.*

ABBREVIATIONS USED

P/E	Pulse Echo
NE	Notch Echo
BWE	Back Wall Echo
NE-Notch	Notch Echo in simulated notch specimens
BWE-Notch	Back Wall Echo in simulated notch specimens
NE-Corrosion	Notch Echo in actual corrosion specimens
BWE-Corrosion	Back Wall Echo in actual corrosion specimens
P/T	Pulse Transmission
P/T-1	I^{st} Pulse Transmission Peak
P/T-2	II^{nd} Pulse Transmission Peak
P/T-Notch	Transmitted Peak in simulated notch specimens
P/T-Delam-Simulated	Transmitted Peak in simulated debond specimens
P/T- Corrosion	Transmitted Peak in actually corroding specimens
P/T-Delam-Corrosion	Transmitted Peak in actually corroding specimens with L(0,1) mode
CC	Chloride Corrosion
OC	Oxide Corrosion
DAC	Data Acquisition Card

LIST OF FIGURES

LIST OF TABLES

CHAPTER 1

INTRODUCTION

1.1 GENERAL

Steel reinforced concrete is the most popular construction material today, in which steel bars are used as reinforcements. With the passage of time, deterioration and damage occurs in the embedded bars in concrete due to a variety of factors such as environmental degradation resulting from corrosion, fatigue, excessive loads, and natural calamities or simply due to long endurance combined with intensive usage. If this deterioration inside the concrete goes unnoticed, it can lead to catastrophic failure of the structures leading to large scale loss of life and property. To alleviate this risk, rigorous inspection of the embedded reinforcements in RC structures is imperative. However, the size and limited accessibility of civil engineering installations prevent the adoption of rigorous techniques like C-Scan. Thus, there is a great necessity of a reliable, non-invasive and real time non-destructive testing methodology that can detect, locate and quantify damage in embedded steel bars.

Usually embedded steel is as durable as concrete because it is protected by a passivating layer of iron oxide that forms in the alkaline environment of cement based concrete. But concrete is permeable and when exposed to corrosive agents, they penetrate through the concrete cover and reach the reinforcing steel. In some cases, this may result in a rapid deterioration in the strength and integrity of the concrete structure. This phenomenon is called corrosion of reinforcements in concrete and it now figures heavily in the maintenance of existing buildings and it has contributed to a number of structural collapses. It assumes greater significance when the reinforcing bar in concrete is exposed to the chlorides either contributed from the concrete ingredients or penetrated from the surrounding chloride-bearing environment. Carbonation of concrete or penetration of acidic gases into it are other causes of reinforcement corrosion. Besides these, there are a few more factors, some related to concrete quality, such as water–cement ratio, cement content, impurities in the concrete ingredients, presence of surface cracks etc. Some factors related to the external environment

are moisture, oxygen, humidity, temperature, bacterial attack, stray currents, etc. also affect reinforcement corrosion. Moreover, steel embedded in concrete may be subjected to cracks due to repeated loading or fatigue or overloading, though corrosion is, by far, the biggest culprit.

Concrete normally provides a high degree of protection to the reinforcing steel against corrosion, by virtue of the high alkalinity (pH > 13) of the pore solution. Under such high alkalinity conditions, steel remains passivated. In addition, well-consolidated and properly cured concrete with a low water-cement ratio has a low permeability, which minimizes penetration of corrosion inducing agents, such as chloride, carbon dioxide, moisture, etc. to the steel surface. Further, the high electrical resistivity of concrete restricts the rate of corrosion by reducing the flow of electrical current from the anodic to the cathodic sites. Usually in a properly designed, constructed and maintained structure, there should be little problem of steel corrosion during its design life. Unfortunately, the durability requirement is not always achieved in practice due to which corrosion of reinforcement in concrete has become a commonly encountered cause of deterioration in many RC structures in the recent years. According to a study conducted by US Strategic Highway Research Program, about $450 to $550 million per year can be saved by correcting corrosion problems in existing bridges. In some situations it may seem to be more economic to replace and remove the areas of active reinforcement corrosion only, rather than to remove all the chloride contaminated concrete, particularly in areas where active reinforcement corrosion had not yet started. In fact it can be considered that the most cost effective action is to manage the risk by monitoring the condition of the reinforcement following the refurbishment work.

In general, there are two major factors, which cause corrosion of reinforcement in concrete to proceed to an unacceptable degree. They are: (i) carbonation, and (ii) presence of chloride ions, which may either have been present in the concrete constituents right from the beginning or are introduced into the concrete through ingress during the service life. The quality of concrete, mainly the permeability, nature and intensity of cracks, and the cover thickness, have also a great bearing upon the initiation and sustenance of reinforcement corrosion. Once reinforcement corrosion is initiated, it progresses at a steady rate and shortens the service life of the structure in the following two major detrimental ways:

- The rust produced as a result of corrosion has a volume 6-10 (Broomfield, 1997) times than that of steel. It causes volume expansion developing tensile stresses in concrete, which ultimately results in cracking and spalling of the cover concrete. Due to the loss of cover concrete, there may be significant reduction in the load bearing capacity of the structure. Further, steel becomes more accessible to the aggressive agents leading to corrosion at an accelerated rate.
- Corrosion reduces the cross-sections of the steel and thereby the load carrying capacity of the structure. Pitting (i.e., localized) corrosion of the rebar is more dangerous than uniform corrosion because it progressively reduces the cross-sectional area of rebar to a point where it can no longer withstand the applied load, leading to a catastrophic failure of the structure.

Corrosion affects the steel-concrete interface and the bond between them is reduced. As a result, the composite action between steel and concrete is lost leading to premature failure. Hence, the manifestation of corrosion is evident in the formation of corrosion products on the surface of the rebar whereby the steel-concrete interface is altered with the formation of rust. The resulting corrosion products cause the processes of cracking, spalling and delamination of the bar from the surrounding concrete. Another distinguishing feature is pitting where crevices are formed in the bar leading to local loss of material.

In a tropical country like India, where approximately 80% of the annual rainfall takes place in the two monsoon months, rusting related problems are more alarming, especially in RC bridges etc. India also has a very long coastline where marine weather prevails. Typically, a structure requires major restoration work within fifteen years of its construction. Consequently, it has become urgent to have a reliable method for accurately measuring condition of reinforcement in existing as well as new concrete structures.

The rate of corrosion directly affects the extent of the remaining service life of a corroding RC structure. The assessment of the causes and extent of corrosion is usually carried out using various techniques discussed briefly in **Section 1.2**. They may be suitably employed for the monitoring of corrosion of steel in concrete structures for the purpose of diagnosing the cause and extent of the reinforcement corrosion, but have certain limitations. Also, for assessment of corrosion related damages, in addition to debond, any corrosion monitoring methodology should also identify local weakening and loss of strength and

ductility of the bar.

1.2 EXISTING CORROSION DAMAGE MONITORING METHODOLOGIES

Techniques and methods currently used for damage detection in steel use either visual examination or non-destructive testing methods comprising physical and chemical techniques. Visual examination would rely on manifestation of corrosion on the surface of structure in the form of staining, cracking or spalling of concrete. The techniques of conducting condition survey on reinforced concrete structures suffering from corrosion vary greatly in principle and the purpose they serve:

- Visual Inspection - Surface Cracks
- Hammer/ Chain - Delamination
- Cover meter - Rebar Depth
- Phenolphthalein spray - Carbonation depth
- Chloride content - Chloride induced corrosion
- Permeability - Diffusion rate
- Petrography - Concrete properties
- Half Cell Potential - Corrosion risk
- Linear polarization - Corrosion rate
- Resistivity - Concrete resistivity

All of the techniques can be used either in isolation or in combination to provide a 'snapshot' of the condition of the structure. They are either electrochemical in nature or typically fail or encounter problems when applied for in- situ damage monitoring of steel embedded in concrete. They give idea only about the initiation and progression of corrosion but the quantification of corrosion still remains a vital issue. There is a difficulty in interpreting the results in half cell potential methods. Further, for RC systems, a number of probes have to be installed before the system can be effectively utilized. The infrastructure involved in measurement is bulky. Also the measured electrochemical potentials are affected by a number of factors like the quality of concrete, relative humidity, cover of concrete and its contamination by chlorides or carbonation etc.

Various non-destructive methods used for condition assessment of steel are as follows:

- Impact Echo - Defects/Cracks
- Radiography - X- Ray image
- Remanent Magnetism - Fractures in steel
- Reflectometrical Impulse Measurement (RIMT) - Anomalies in steel
- Acoustic Monitoring - General defects
- Thermography - Delamination / Debonding
- Acoustic Tomography - Imaging of concrete

These non-destructive techniques for condition monitoring of steel, as recommended and described by various researchers, have specific applications only. They are either too expensive or they require highly skilled personnel or have limited practical application like in radiography, thermography and acoustic tomography. So the measurement of state of reinforcement in concrete structures needs a method which can determine simply, accurately, and non-destructively not only whether or not deterioration of reinforcement is taking place but also the extent of damage and its characterization. The technique developed should be applicable for new structures with long time requirements and for older structures to find out the corrosion damage, locate it and finally quantify it so that the service life prediction of the subject RC structure can be done.

Hence, there is a need to supplement or replace these methods with an efficient, reliable, in-situ and non-destructive damage monitoring technique for reinforcement in concrete typically for corrosion induced damages. The thesis is an attempt to develop a complete corrosion monitoring methodology for reinforced concrete structures using ultrasonic guided waves.

1.3 ULTRASONIC GUIDED WAVES – A POTENTIAL SOLUTION

Currently used methods of nondestructive testing used for embedded steel are indirect indicators of likelihood of corrosion. They cannot be used for large structures either due to scale up problems or huge cost associated with their implementation and maintenance.

Corrosion, if undiscovered can cause catastrophic failure of the structure. The degradation accelerates unless early remedial action is taken. A wide range of techniques have been reported in the literature that may be suitably employed for the monitoring of corrosion of steel in concrete structures for the purpose of diagnosing the cause and extent of the reinforcement corrosion. But none of the techniques concentrate on corrosion monitoring through direct measurements on embedded steel. Removal of concrete to visually inspect the reinforcement is detrimental to the structure. Therefore, it is imperative to develop a non-intrusive technique for early detection of corrosion in steel embedded in concrete.

Assessing the integrity of reinforcing bars poses practical difficulties since the reinforcements are typically embedded inside concrete. Many non-destructive testing methods currently used such as radiography, acoustic emission, X-ray etc cannot be adopted due to the huge size and limited accessibility of civil engineering installations. These techniques either require skilled labor or are costly and difficult to apply on civil infrastructure. Hence, there is a need for non-intrusive, in-situ and real time corrosion monitoring system for RC structures. Towards the development of such a technique, ultrasonic wave propagation is explored in this work. The ultrasonic wave characteristics change when the reinforcing bars deteriorate due to corrosion. They are sensitive to the location, extent and character of corrosion.

In reinforcing bars, the ultrasonic waves are constrained by the bar geometry and travels as guided waves. Sound propagation is complex and it travels in a large number of ‘modes’, which can be determined by the solution of the wave propagation equation. Guided waves are dispersive and the frequency dependence of their properties such as velocity and attenuation must be known so that test results can be accurately interpreted. A major advantage of guided waves is that they propagate in the bar as a whole, and therefore have the potential to inspect the whole bar from a single point. Thus, a guided wave excited at the exposed end of a reinforcing bar would be reflected from any defect in the bar, allowing defects to be accurately located. The defect location can be estimated from the time taken by the wave to travel. This technique of testing is called Pulse Echo method. It is observed that for the steel bars in air the attenuation is primarily due to material scattering and absorption. But when the bars are embedded in concrete, both longitudinal and shear waves leak into the surrounding concrete. Thus, the lack of leakage and increase in the transmitted signal

strength (called Pulse Transmission method) can indicate delamination between concrete and bars. Hence, by using conventional techniques of pulse echo as well as pulse transmission, the location as well as extent of damage can be evaluated using guided waves. The two main limitations are decay of the signal due to leakage into the embedding material and the reflection coefficient for defects such as breaks and corrosion patches. The recent discovery of high frequency, low-leakage guided modes (Pavlakovic et al., 2001) has the potential to reduce the attenuation due to leakage, although the reflection coefficients from defects need to be determined. In addition, lower frequency modes may offer an alternative to the high frequency modes for detection of surface/interfacial damages. Hence, in the present work, it is proposed to use high and low frequency guided wave modes for corrosion detection in steel embedded in concrete.

Ultrasonic guided wave propagation is beginning to gain popularity among researchers in the detection of corrosion related damage in reinforcing bars. But most of the researchers have simulated corrosion as delamination /debond of reinforcing bars. It is widely conjectured that debond impedes the leakage of waves into concrete. Thus, higher signal strength at the receiving end indicates debond and corrosion. It has been validated by introducing debond in the form of PVC pipes (Wu et al., 2006) or by wrapping a tape around the bar (Reis et al., 2005). Other effects such as loading conditions, reinforcing ribs, corrosion products and anchorages on the guided waves also have been reported. Use of both low and high frequency guided wave modes to monitor corrosion damage in reinforced mortar specimens after subjecting them to accelerated corrosion has been suggested (Ervin et al., 2008; 2009). It was found that some modes were sensitive to the combined effect of bond deterioration and mortar stiffness reduction while some other modes related well to change in cross-sectional area.

But the effect of corrosion has mainly been viewed as loss of interfacial bond. Limited experimental evidence of actually corroded RC specimens indicates that in addition to loss of bond, loss of cross-sectional area of bars has also significant influence. But the phenomenon of corrosion as interpreted by various researchers is not only cracking and spalling of concrete cover and delamination of the reinforcing bar from the surrounding concrete. Another distinguishing feature is pitting where crevices are formed in the bar leading to local loss of material. Thus, in addition to debond, any corrosion monitoring

methodology should also identify local weakening and loss of strength and ductility of the bar. This thesis is an attempt to develop a complete corrosion monitoring methodology using ultrasonic guided waves and various issues related to it have been investigated.

Also, mechanism and progression of corrosion in the absence and presence of chlorides is very different. Prognosis of these two types of corrosion would be vastly different. The manifestation of corrosion in oxide and chloride environments is in the formation of the corrosion products on the surface of the rebar. Thus, the steel-concrete interface is altered where rust is formed. The resulting corrosion products and accompanying processes of cracking, spalling and delamination of concrete occurring in both types of corrosion are similar but the rate and the mode of occurrence of various aspects of corrosion are different in the two cases. Hence, a non-destructive technique that is able to discern these two modes of corrosion will also be of great benefit and ultrasonic guided waves have been explored in this work for the same.

1.4 AIMS AND OBJECTIVES

The aim of the present work is to develop an in-situ corrosion monitoring methodology for steel reinforced in concrete using ultrasonic guided waves. The developed technique should detect, localize and finally quantify the extent of deterioration of steel embedded in concrete. Current work proposes to use cylindrical piezoelectric actuators to generate guided waves through the reinforcement embedded in concrete. The resulting signals are obtained through the similar piezoelectric sensor at the other end of the reinforcing bar. Wave signatures are first obtained for healthy bars embedded in concrete. Thereafter, signatures for bars embedded in concrete with simulated corrosion damages in the form of area reduction and delamination are taken. The variation in the received signals should lead one to identify, locate and evaluate the state of rebar in concrete.

The methodology developed is then extended to RC beams undergoing actual accelerated corrosion in the absence and presence of chlorides. A comparison is drawn between simulated and actual corrosion studies in the two corrosion environments. Also, the difference in the mechanism and progression of corrosion in two vastly different environments using guided wave modes is investigated. After exposure to different corrosive environments for specified durations, the extracted bars are subjected to destructive tests to

determine mass loss, tensile strength and pull out strength. Calibration of ultrasonic test data is done with destructive tests to relate the ultrasonic voltages measured at a particular instant to the physical condition of the bar in terms of residual mass, tensile strength and residual pull out strength. However, key technologies must be established before the wave propagation techniques are effectively utilized in the monitoring of reinforcing steel in RC beams. A large number of specimens must be investigated with different amounts and rates of damage, different depths and locations of damages etc. and characterization of the same needs to be done. Hence, the objectives of the present work can be outlined as:

- Investigation of propagation of guided ultrasonic waves through healthy and damaged reinforcing steel bar specimens, simulating area reduction and delamination effects of corrosion.
- Characterizing corrosion in reinforcing bars and its extent through the analysis and comparison of wave signatures of healthy bars and bars with simulated corrosion damages.
- Application of above developed methodology to bars embedded in concrete.
- Extension of the developed methodology to RC beams undergoing actual corrosion.
- Study of difference in corrosion mechanism in the absence and presence of chlorides using guided waves.
- Comparison of actual and simulated corrosion studies.
- Calibration of ultrasonic data with destructive tests to relate to the physical condition of the bar at any instant.
- Development of semi-empirical relationships between corrosion state and ultrasonic signals.
- Recommend a non-invasive and in-situ corrosion monitoring methodology for embedded steel reinforcements in concrete.

1.5 LAYOUT OF THE THESIS

In Chapter 1, the significance and need of a non-intrusive corrosion monitoring technique is established by highlighting the drawbacks of the existing methods by ultrasonic guided waves. The scope and objectives of the present work have been detailed.

Chapter 2 highlights the theory and background of ultrasonic for damage detection and introduces ultrasonic guided waves as a potential solution for corrosion monitoring in embedded reinforcements in concrete.

Chapter 3 explains in detail the mechanism of corrosion, its types and forms and existing corrosion monitoring techniques. The drawbacks of the existing methods are brought out highlighting the importance of a non-invasive monitoring technique.

A detailed experimental study utilizing ultrasonic guided waves is carried out first on bars in air with simulated notch damages relating to area reduction/pitting due to corrosion. Then the study is extended to reinforcing bars embedded in concrete with simulated pitting and delaminated damages due to corrosion. Conventional ultrasonic techniques of pulse echo and transmission are used to characterize simulated damages in embedded bars in Chapter 4.

In Chapter 5, the methodology of damage detection established above is extended to RC beams undergoing actual corrosion. Ultrasonic investigations are carried out on RC beams undergoing actual accelerated corrosion in the presence and absence of chlorides and the difference in ultrasonic voltages in the two environments is studied. Ultrasonic data obtained is also calibrated with destructive test results of mass loss, tensile and pull out strength of the embedded bar.

Chapter 6 draws out a comparative study of the ultrasonic test results of simulated and actual corroding reinforcing bar specimens in concrete.

Chapter 7 briefly summarizes the entire work. The conclusions drawn from the investigation are reported and the scope for future investigations in the area is highlighted in this chapter.

In the end, references cited in the entire work have been presented.

CHAPTER 2

ULTRASONICS FOR STRUCTURAL HEALTH MONITORING

2.1 INTRODUCTION

Although many NDE techniques such as liquid penetrant dye, radiography, holography, eddy current, magnetic flux, thermography are available but elastic wave based techniques have become most popular for Structural Health Monitoring applications. It is observed that crack initiation and propagation generate detectable sonic and ultrasonic waves. These waves can propagate large distances through the structure under investigation and can be picked up by a sensor placed at another location. The received signal at the sensor can be analyzed in order to locate and estimate the degree of damage in the structure. Ultrasonic waves are vibrational waves having frequencies higher than the human audible range above 20 kHz. Upper range of these waves can be as high as 15-30 GHz. However, for most SHM applications, the upper bound of frequency rarely exceeds 20MHz. It is important to note that there are no changes in the dimensions and structure of the object when the test is performed. This can be achieved only when the maximum applied stresses do not exceed the elastic limit so that the resultant strain is proportional to the applied stress. Hence, it is necessary that the ultrasonic intensity is sufficiently low for the elastic limit not to be exceeded. It involves introducing a very low energy level, high frequency stress pulse or 'wave packet' into a material and observing the subsequent propagation and reflection of this energy. The means for introducing and detecting the stress waves are based generally on the piezoelectric effect. By studying the propagation, reflection, and attenuation of ultrasonic pulses, it is possible to determine the fundamental properties of the materials such as elastic constants and damping characteristics and also employ them for damage diagnosis.

Various types of methods based on audible sound and ultrasound are applied for non-destructive testing (NDT). Acoustic Emission and Ultrasonic Inspection are the most widely used techniques in industrial applications. The first technique is passive and does not require any external excitation; stress waves are structure-born and produced internally by defects.

The second approach requires high-frequency external excitation. The maturity and proven damage detection applications are the major advantages of these techniques. The Acousto-Ultrasonic approach combines elements of Acoustic Emission and Ultrasonic Inspection. In this report, only ultrasonic wave propagation has been considered. Using ultrasonic wave propagation as a means for monitoring the soundness/ health of structure involves the propagation of acoustic waves through structures. The wave characteristics change due to the deterioration in the structure and they are sensitive to the location, extent and character of damage. However, for a successful monitoring a prior knowledge of the wave characteristic due to different cases is imperative.

2.2 ULTRASONIC WAVES

Elastic waves in all frequency ranges-ultrasonic, sonic and subsonic-can be classified into two groups: Body Waves or Bulk waves and Surface Waves or Guided Waves **(Fig. 2.1)**. Body waves travel through the bulk material while surface waves propagate along the surface. Sound waves travel as a bulk wave in any elastic material where the sound does not interact with the edges of material therefore acting as infinite extent of material. The velocity of sound in materials varies with its elastic properties which can be calculated by measuring the time of flight between the two points. Velocity can be related to a variety of different material properties and conditions and is often used as a test of concrete uniformity, where velocity is usually displayed on a contour map. Large cracks and voids can be detected by an increase in travel time. Surface waves are often called guided waves because of the geometry of the boundary which guides them. The use of ultrasound in civil engineering is widespread but is limited to use of bulk waves rather than guided waves.

Ultrasonic testing of materials utilizes mechanical waves. They are simply organized mechanical vibrations traveling through a medium, which may be solid, liquid, or gas. These waves will travel through a given medium at a specific speed or velocity, in a predictable direction, and when they encounter a boundary with a different medium they will be reflected or transmitted. This is the principle of physics that underlies ultrasonic flaw detection.

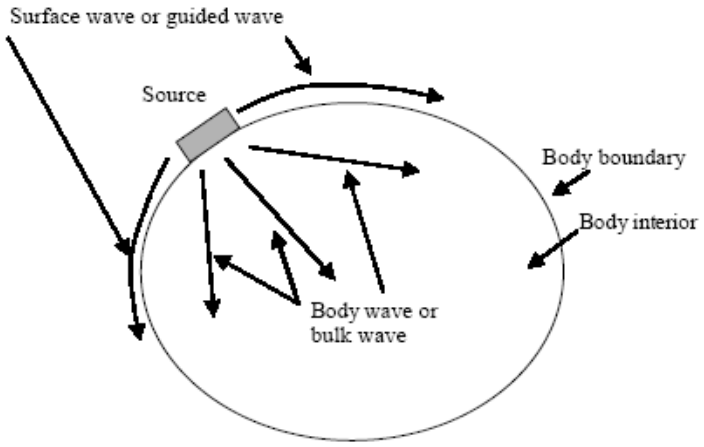

Fig. 2.1: Body waves and Surface waves generated by an ultrasonic source (Kundu , 2004)

Some of the common terms associated with ultrasonic bulk wave propagation are as follows (Bindal, 1999):

1. **Frequency (f):** All sound waves oscillate at a specific frequency, or number of vibrations or cycles per second, which is experienced as pitch in the familiar range of audible sound. Human hearing extends to a maximum frequency of about 20,000 cycles per second (20 KHz), while the majority of ultrasonic flaw detection applications utilize frequencies between 500 KHz to 10 MHz. At frequencies in the Megahertz range, sound energy does not travel efficiently through air or other gasses, but it travels freely through most liquids and common engineering materials.
2. **Wave Velocity (V):** The speed of a sound wave varies depending on the medium through which it is traveling, affected by the medium's density and elastic properties. Different types of sound waves will travel at different velocities.
3. **Wavelength (λ):** Wavelength is related to frequency and velocity by the simple equation Wavelength (λ) = Velocity (V)/frequency (f). In ultrasonic flaw detection, the generally accepted lower limit of detection for a small flaw is one-half wavelength, and anything smaller than that will be invisible. In ultrasonic thickness gauging, the theoretical minimum measurable thickness is one wavelength.

4. **Acoustic impedance (Z):** Sound travels through materials under the influence of sound pressure. Since molecules or atoms of a solid are bound elastically to one another, the excess pressure results in a wave propagating through the solid. Acoustic impedance (Z) of a material is defined as the product of its density (ρ) and acoustic velocity (V).

$$Z = \rho V \tag{2.1}$$

5. **Reflection and transmission coefficients:** Ultrasonic waves are reflected at boundaries where there is a difference in acoustic impedances (Z) of the materials on each side of the boundary as shown in the **Fig. 2.2**. This difference in Z is commonly referred to as the impedance mismatch. The greater the impedance mismatch, the greater the percentage of energy that will be reflected at the interface or boundary between one medium and another. The fraction of the incident wave intensity that is refracted can be derived since particle velocity and local particle pressure are continuous across the boundary.

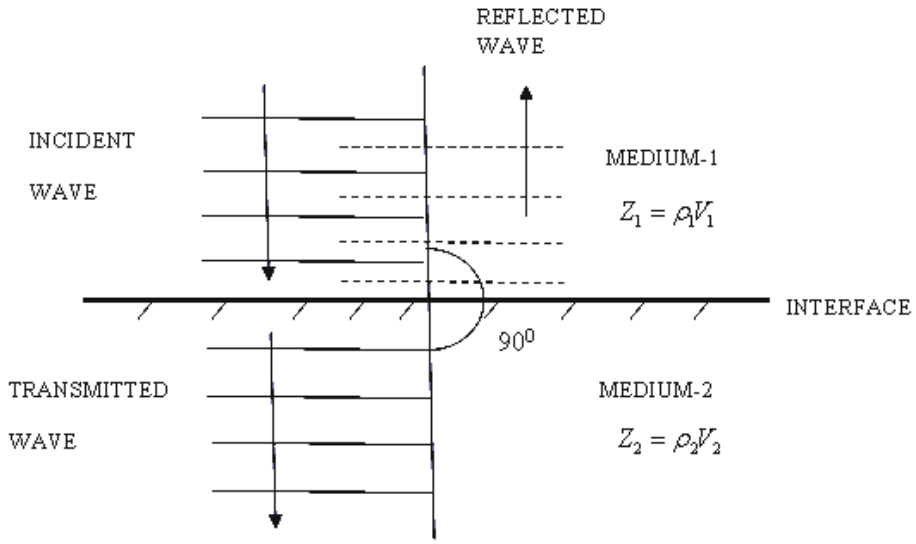

Fig. 2.2: Reflection and Transmission of sound wave at normal incidence

(Bindal, 1999)

When the acoustic impedances of the materials on both sides of the boundary are known, the fraction of the incident wave intensity that is reflected can be calculated **(Equation 2.2)** and is known as the reflection coefficient. Multiplying the reflection

coefficient by 100 yields the amount of energy reflected as a percentage of the original energy.

$$R = \left[\frac{Z_2 - Z_1}{Z_2 + Z_1} \right]^2 \tag{2.2}$$

Since the amount of reflected energy plus the transmitted energy must equal the total amount of incident energy, the transmission coefficient is calculated by simply subtracting the reflection coefficient from one.

6. **Mode Conversion:** When sound travels in a solid material, one form of wave energy can be transformed into another form. For example, when a longitudinal wave hits an interface at an angle, some of the energy can cause particle movement in the transverse direction to start a shear (transverse) wave. Mode conversion occurs when a wave encounters an interface between materials of different acoustic impedances and the incident angle is not normal to the interface.

When sound waves pass through an interface between materials having different acoustic velocities, refraction takes place at the interface **(Fig. 2.3)**. The larger the difference in acoustic velocities between the two materials, the more the sound is refracted. The shear wave is not refracted as much as the longitudinal wave. This occurs because shear waves travel slower than longitudinal waves. Therefore, the velocity difference between the incident longitudinal wave and the shear wave is not as great as longitudinal waves but it is between the incident and refracted longitudinal waves. Also, when a longitudinal wave is reflected inside the material, the reflected shear wave is reflected at a smaller angle than the reflected longitudinal wave. This is also due to the fact that the shear velocity is less than the longitudinal velocity within a given material. Snell's Law holds true for shear waves as well as longitudinal waves and can be written as follows:

$$\frac{Sin\theta_1}{V_{L1}} = \frac{Sin\theta_2}{V_{L2}} = \frac{Sin\theta_3}{V_{S3}} = \frac{Sin\theta_4}{V_{S4}} \tag{2.3}$$

where:

V_{L1} - is the longitudinal wave velocity in medium 1

V_{L2} - is the longitudinal wave velocity in medium 2

V_{S1} - is the shear wave velocity in medium1

V_{S2} - is the shear wave velocity in medium 2

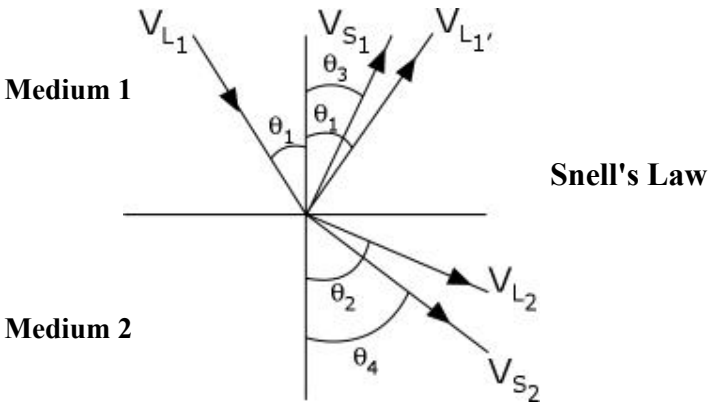

Fig. 2.3: Reflection and Refraction at the boundary of two media

(Bindal, 1999)

2.2.1 Modes of Wave Propagation

The ultrasonic waves propagate in a number of ways in a medium. On the basis of the mode of particle displacement, these waves can be classified as:

- Longitudinal or Compression waves (L-waves)
- Transverse or Shear waves (S-waves)
- Surface or Rayleigh waves
- Lamb or Plate waves

Longitudinal or Compression waves

In longitudinal waves, the oscillations occur in the longitudinal direction or the direction of wave propagation. Since compression and dilatational forces are active in these waves, they are also called pressure or compression waves **(Fig. 2.4)**. Compression waves

can be generated in liquids, as well as solids because the energy travels through the atomic structure by a series of comparison and expansion (rarefaction) movements. They are also some times called **density waves** because their particle density fluctuates as they move. The velocity of longitudinal ultrasonic waves is about 6000 m/s in steel, 1500 m/s in water and 330 m/s in air approximately.

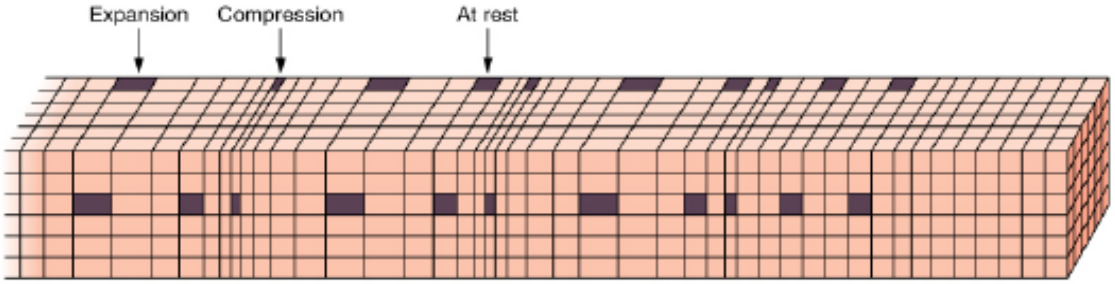

Fig 2.4: Propagation of Longitudinal waves (www.ndt.org)

Transverse or Shear waves

In the transverse or shear wave, the particles oscillate at a right angle or transverse to the direction of propagation **(Fig. 2.5)**. Shear waves require an acoustically solid material for effective propagation, and therefore, are not effectively propagated in materials such as liquids or gasses. Shear waves are relatively weak when compared to longitudinal waves. S-waves polarized in the horizontal plane are classified as SH-waves. If polarized in the vertical plane, they are classified as SV-waves. When an S- or P-wave strikes an interface at an angle other than 90 degrees, a phenomenon known as mode conversion occurs.

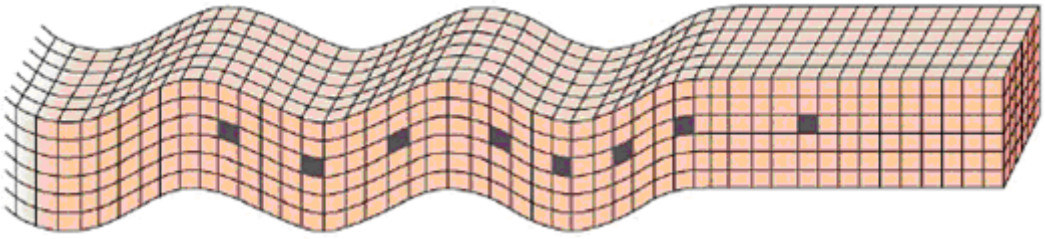

Fig. 2.5: Propagation of Transverse or Shear waves (www.ndt.org)

Surface (or Rayleigh) waves

Surface (or Rayleigh) waves travel the surface of a relatively thick solid material penetrating to a depth of one wavelength. The particle movement has an elliptical orbit as

shown **(Fig. 2.6)**. Rayleigh waves are useful because they are very sensitive to surface defects and they follow the surface around curves. Because of this, Rayleigh waves can be used to inspect areas that other waves might have difficulty reaching.

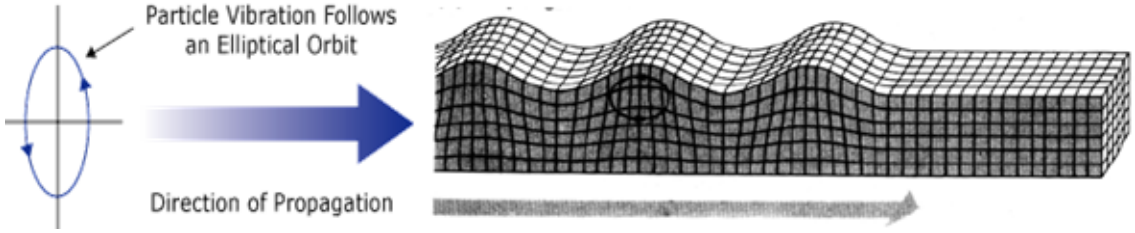

Fig. 2.6: Propagation of Surface or Rayleigh Waves (www.ndt.org)

Lamb waves or Plate waves

Plate waves can be propagated only in very thin metals. Lamb waves are the most commonly used plate waves in NDT. Lamb waves are complex vibrational waves that travel through the entire thickness of a material. Propagation of lamb waves depends on the density and the elastic material properties of a component. They are also influenced a great deal by the test frequency and material thickness.

With Lamb Waves, a number of modes of particle vibration are possible, but the two most common are symmetrical and asymmetrical. The complex motion of the particles is similar to the elliptical orbits for surface waves. Symmetrical lamb waves move in a symmetrical fashion about the median plane of the plate. This is sometimes called the extensional mode because the wave is "stretching and compressing" the plate in the wave motion direction. Wave motion in the symmetrical mode is most efficiently produced when the exciting force is parallel to the plate. The asymmetrical lamb wave mode is often called the "flexural mode" because a large portion of the motion moves in a normal direction to the plate, and a little motion occurs in the direction parallel to the plate. In this mode, the body of the plate bends as the two surfaces move in the same direction **(Fig. 2.7)**.

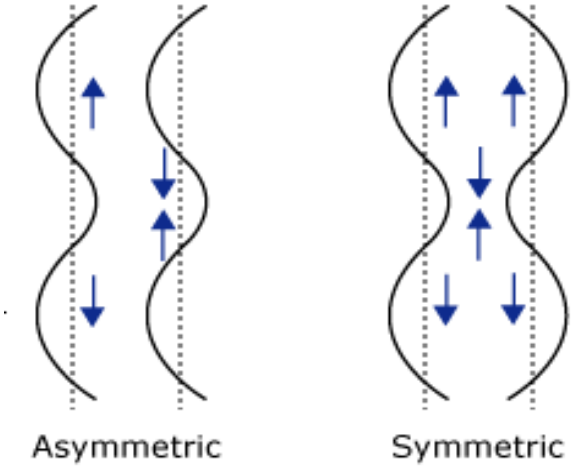

(a) **(b)**

Fig. 2.7: Lamb Wave propagation (a) Asymmetrical (Bending) (b) Symmetrical (Dilatational) waves (www.ndt.org)

2.3 ULTRASONIC TESTING

2.3.1 Basic Principles

Ultrasonic non-destructive testing introduces high frequency sound waves into a test object to obtain information about the object without altering or damaging it in any way. For this, a typical Ultrasonic Testing (UT) inspection system comprises several functional units, such as the pulser/receiver, transducer, and display devices. A pulser/receiver is an electronic device that can produce high voltage electrical pulses. Driven by the pulser, the transducer generates high frequency ultrasonic energy, which is introduced and propagated through the materials in the form of waves. When there is a discontinuity (such as a crack) in the wave path, part of the energy will be reflected back from the flaw surface. The reflected wave signal is transformed into an electrical signal by the transducer and is displayed on a screen **(Fig. 2.8)**.

Two basic quantities are measured in ultrasonic testing; they are time of flight or the amount of time for the sound to travel through the sample, and amplitude of received signal. Based on velocity of travel through the material and round trip time of flight through the material the material, thickness can be calculated as follows:

$$T = \frac{Vt}{2} \tag{2.4}$$

T = Material Thickness

V = Material Sound Velocity

t = Time of Flight

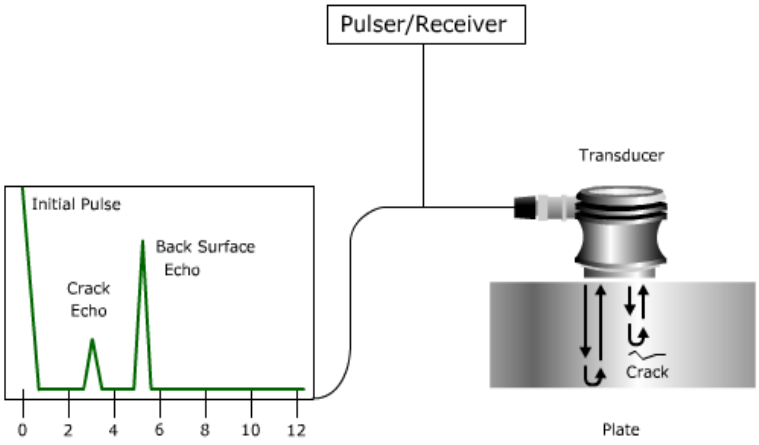

Fig. 2.8: General ultrasonic inspection principle (www.ndt.net)

Measurement of the relative change in signal amplitude can be used in sizing flaws or measuring the attenuation of a material. The relative change in signal amplitude is commonly measured in decibels. Decibel values are the logarithmic value of the ratio of two signal amplitudes. This can be calculated using the following equation.

$$dB = 20\log_{10}\frac{A_1}{A_2} \tag{2.5}$$

dB = Decibels

A_1 = Amplitude of Input Signal

A_2 = Amplitude of Transmitted/ Received Signal

2.3.2 Methods of Ultrasonic Testing

Most commonly used methods of ultrasonic testing are:

- Pulse Echo method
- Pulse Transmission method

Pulse Echo method

In the pulse-echo method, a piezoelectric transducer with its longitudinal axis located perpendicular to and mounted on or near the surface of the test material is used to transmit and receive ultrasonic energy **(Fig.2.9)**. The ultrasonic waves are reflected by the opposite face of the material or by discontinuities, layers, voids, or inclusions in the material, and received by the same transducer where the reflected energy is converted into an electrical signal. The electrical signal is computer processed for display on a video monitor or TV screen. The display can show the relative thickness of the material, depth into the material where flaws are located, and (with proper scanning hardware and software), where the flaws are located in the X-Y plane.

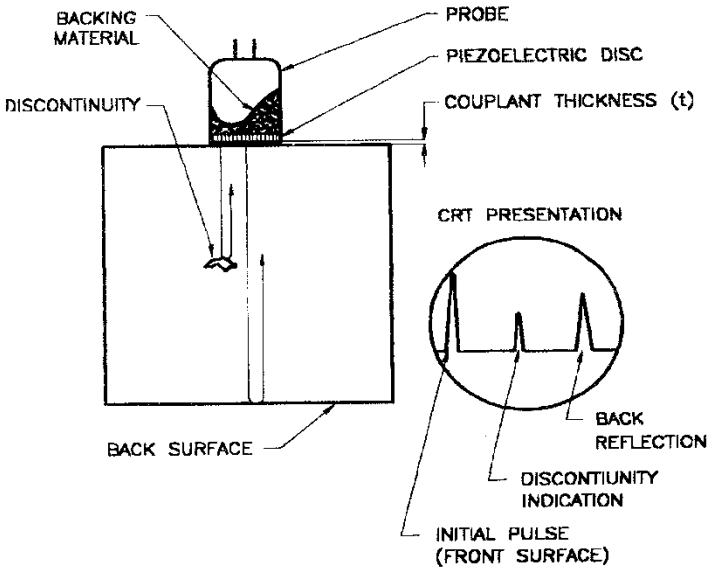

Fig 2.9: Pulse Echo method of testing (Bindal, 1999)

When there is an interface such as a crack, void or flaw in the wave path, part of the energy is reflected back from the interface and received by the same transmitting transducer. The reflected energy is converted into an electrical signal which is processed in a computer and digitized for display. From the display, the time of flight between the excitation and reflected pulse is measured. Knowing the velocity of the wave, the location of the defect can be calculated as follows:

$$D = \frac{Vt}{2} \tag{2.6}$$

Where D = Distance of defect from transducer end, V = Velocity of wave and t = Time of Flight

Pulse Transmission method

In the pulse-transmission method, an ultrasonic transmitter is used on one side of the material while a detector is placed on the opposite side. One unit acts as transmitter and the other unit as receiver. The beam from the transmitter T travels through the material to its opposite surface where the receiving transducer R is placed. Scanning of the material using this method will result in the location of defects, flaws, and inclusions in the X-Y plane **(Fig. 2.10)**

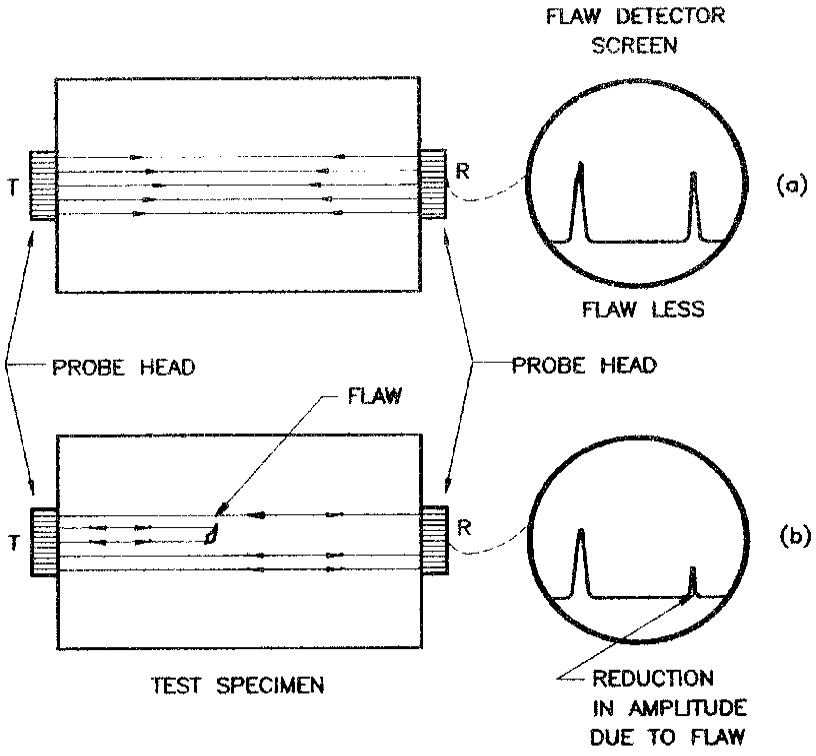

Fig 2.10: Pulse Transmission method of testing (Bindal, 1999)

By measuring the relative change of the amplitudes of the input and the received signals, the relative severity of the flaw is assessed.

2.3.3 Attenuation of Sound Waves

When sound travels through a medium, its intensity diminishes with distance. In idealized materials, sound pressure is only reduced by spreading of wave. Natural materials, however, produce an effect which further weakens the sound. This further weakening results from scattering and absorption. Scattering is the reflection of sound in the direction other than its original direction of propagation. Absorption is the conversion of sound energy to other forms of energy. The combined effect of scattering and absorption is called attenuation.

- **Scattering-** Most of the materials are not homogenous. They contain boundaries on which acoustic impedance changes because two materials of different densities or sound velocities occur at these interfaces. Scattering is highly dependent on the relation of crystalline size to ultrasonic wavelength. When the grain size is less than 0.01 times the wavelength, scatter is negligible. Scattering effects vary approximately with the third power of grain size and when the grain size is 0.1 times the wavelength or larger, excessive scattering make it impossible to perform ultrasonic inspections.

- **Absorption-** If a sound wave propagates through a medium, alternately the regions of compressions and rarefactions are formed. During compression, heat is generated in that region and in the region of rarefaction, cooling is created. Due to rapid occurrence of compressions and rarefactions, the heat generated during compression does not get enough time to dissipate as heat flows much slower than ultrasonic wave. This energy converted into heat is lost to the medium which progressively reduces energy in the propagating ultrasonic wave.

2.4 ULTRASONIC GUIDED WAVES

2.4.1 Introduction

When ultrasonic wave is constrained within the boundaries and is guided by the geometry of the structure, it becomes a guided wave. If the structure is a homogenous half space, then the guided wave propagating along the surface of the half space is called Rayleigh wave, named after its inventor. Waves propagating through a plate like structure

with two parallel stress free boundaries are known as Lamb waves. Elastic waves propagating through a hollow cylindrical or pipe structure is called cylindrical guided waves. When the guided waves propagate through a solid rod or bar, they are known as bar waves. **Fig. 2.11** shows the different types of guided waves propagating through various structures that are also known as waveguides.

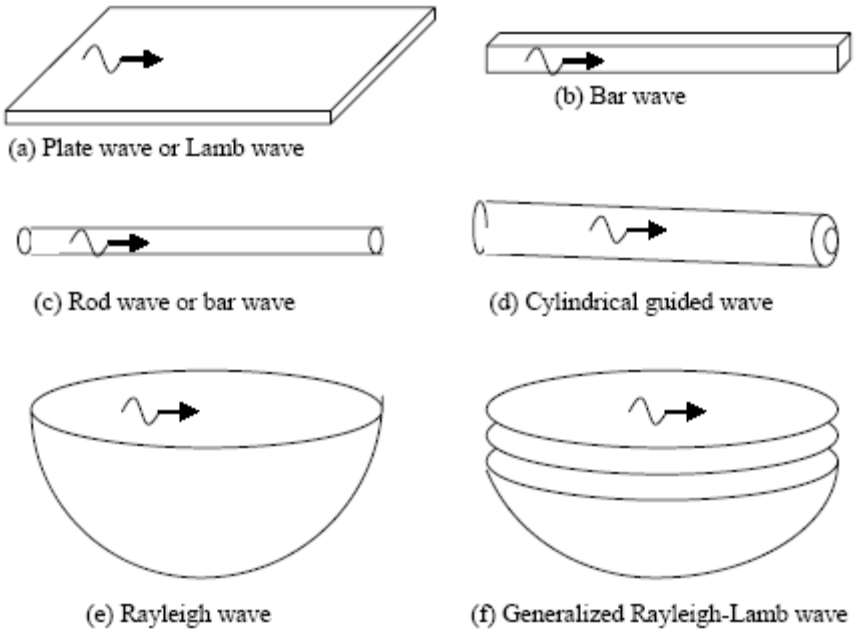

Fig. 2.11: Different types of guided waves in various geometries (Kundu , 2004)

Guided waves exist in structures that do not behave as an infinite mass of material, and the sound propagation is constrained by one or more material boundaries. In such cases, sound propagation is complex and sound can travel in a large number of 'modes' that can be determined by the solution of the wave propagation equation. The complications arise from the fact that these guided waves are dispersive, and the frequency dependence of their properties such as velocity and attenuation must be known so that test results can be accurately interpreted. Use of guided ultrasonic waves is more complicated than bulk waves and has limited its use in NDT. It is still in research phase and has not developed into a full fledged practical method.

A major advantage of guided waves is that they propagate in the structure as a whole,

and, therefore, have the potential to inspect the entire structure from a single point. Thus, a guided wave excited at the exposed end of a rebar would be reflected from any defect in the bar, allowing defects to be accurately located. The proposed inspection technique in the thesis involves damage monitoring in reinforcing bars embedded in concrete by exciting suitable guided wave modes at the ends. The waves will then be reflected back from the defects or notches simulating area reduction due to pitting caused as a result of corrosion. Amplitude and time of arrival of these reflections can be used to identify or locate defects. Ultrasonic pulse transmission utilizing two transducers at the two ends of the reinforcing bars is also used in conjunction with pulse echo testing method to quantify the extent of corrosion induced defects in embedded bars. The development of a guided wave testing methodology involves identifying suitable guided wave modes through modeling which are sensitive to different types of corrosion induced damages encountered in reinforcing bars.

2.4.2 Historical Development of Cylindrical Guided Waves

Guided wave propagation in a free bar was first studied numerically in the late 19th century by Pochhammer (1876) and Chree (1889). The next major achievements were made by Hudson (1943), who studied the fundamental flexural mode in a free bar and by Davies (1948), who studied the longitudinal modes. Later papers by Onoe et al.(1962), Pao et al. (1960), Pao (1962) and Meeker et al. (1972) reported further developments in the understanding of elastic wave dispersion in a three dimensional solid bar. Hollow isotropic cylinders were first studied by Gazis (1959) and his predictions were validated by Fitch (1963) for both flexural and longitudinal modes. Kumar (1971, 1972) investigated the case of a hollow cylinder filled with fluid, such as would be found in a pipeline. Numerous developments have also taken place in the treatment of anisotropic materials (Gazis, 1959; Morse, 1954; Mirsky, 1954; Xu et al., 1991; Dayal, 1993; Nagy, 1995; Berliner, 1996). The extension of solution methods to the leaky case of embedded bars was limited by the ability to calculate complex Bessel functions. Thurton (1978) was able to calculate dispersion curves for a clad rod, but only in the regions where the Bessel functions had wholly real arguments. Developments in the ability to calculate Bessel functions with complex arguments (Amos, 1995) has allowed researchers to calculate dispersion relationships more fully (Safaii-Jazi et al., 1986; Simmons et al., 1992; Viens et al., 1994). The discovery of

high frequency low loss modes in embedded bars (Pavlakovic et al., 2001) was made possible by the ability to calculate these functions efficiently. The calculation of dispersion curves for systems with an arbitrary number of layers has been made much easier with the development of Disperse (Pavlakovic et al., 2000), a general purpose program for tracing dispersion curves. The software was originally developed by Lowe (1995), who used the global matrix method to solve the wave propagation equation. The general purpose nature of the software is a significant improvement over previous reported solutions, which were generally case specific. This software allows the modeling of elastic isotropic materials (with or without material damping), transversely isotropic materials, spring boundaries and fluids. Dispersion curves can be calculated in both Cartesian and cylindrical co-ordinates, and the solution method is valid for all mode types. The inclusion of multi-layered cylindrical embedded systems is a recent addition to the software (Pavlakovic et al., 1999), allowing leakage from a bar into an embedding material to be considered.

2.4.3 Guided Waves in Reinforcing Bars

In an infinite bulk of a perfectly elastic material, a sound wave will spread out through the material as a bulk wave, decaying in amplitude because of the spread of the wave front. However, in a finite structure such as a perfectly elastic steel bar, the sound wave is reflected from the structure boundaries, and the energy is contained within the bar as a guided wave. The complex effect of the boundaries means that the energy propagates in modes that have predictable properties such as mode shapes and frequencies. They can be calculated by solution of the wave propagation equation. The mathematical solution to the wave propagation equation yields a number of solutions that form continuous propagating modes.

For a cylindrical system, waves propagate in three modes due to dispersive effect of boundaries i.e longitudinal (L), flexural (F) and torsional (T) modes. The modes are numbered according to the format used by Disperse, which closely follows that defined by Silk and Bainton [6]. Each mode is identified by the use of a letter and two reference numbers. The three waveforms are represented by L (m, n), T (m, n) and F (m, n) for longitudinal, torsional and flexural modes respectively. The ‘m’ variable refers to the variation in displacement around the circumference of the bar. This variable is zero by definition for the axially-symmetric longitudinal modes. For the flexural modes the ‘m’

variable is determined by the number of displacement cycles around the outside of the bar, hence the displacement varies as cos(mθ) around the bar circumference. The second reference number 'n' is a counter variable, the modes being numbered sequentially as they appear with increasing frequency. The lowest frequency axially symmetric mode is therefore numbered L (0, 1). Specific modes can be excited selectively by choosing a frequency band. The velocity-frequency relationships of guided waves can be displayed as **dispersion curves.**

Adding finite layers around the steel bar, such as concrete, further complicates the waveguide, as energy can now be passed between the layers. In this case, a guided wave will still propagate in the structure as a whole, but with properties that depend on the elastic and damping properties of all the layers. Stress and displacement boundary conditions must be satisfied at the boundaries between layers. Generally, the level of interaction between two adjacent layers will be high if the bulk wave speed and density of the materials is similar, giving a low contrast in acoustic impedance between the layers. Attenuation through leakage can occur if the outermost layer maybe considered infinite in extent.

The remainder of this section discusses properties that are commonly used to describe guided wave behavior. The properties of wave number, phase velocity and group velocity are introduced through the examination of the dispersion curves for a free, perfectly elastic bar. The properties of attenuation and energy velocity are introduced by extending this simple model to include an elastic embedding material, which introduces the possibility of leakage.

2.4.3.1 Free Elastic Systems

This section examines the dispersion curves for a perfectly elastic, steel bar in vacuum, and defines the quantities of real wave number, phase velocity and group velocity. In this example, the bar diameter considered is 12mm.

- ***Real Wavenumber***

The tracing routines that are used by Disperse (Pavlakovic et al., 2000) to search for solutions to the wave propagation problem in elastic systems operate in frequency-wavenumber space, or frequency-wavenumber- attenuation space in attenuative systems. The real wavenumber is simply inversely proportional to the wavelength of the guided wave **(Equation 2.7)** where ξ is the real wavenumber in radians per meter, and λ is the wavelength

in meters.

$$\xi = \frac{2\pi}{\lambda} \tag{2.7}$$

Dispersion curves are often displayed as wave number plots in the literature. This solution space is also the one chosen by Disperse because it is the space in which the curves appear mostly linear, and therefore the easiest to trace. However, the wave number plot does not contain much useful information for the application of guided waves to NDT; therefore, other projections and derived data are also required.

- ***Phase Velocity***

The phase velocity, V_{ph}, is calculated from the real wave number, ξ (Equation 2.8), where ω is the circular frequency in radians/metre. Physically, the phase velocity is the speed at which the individual wave crests travel.

$$V_{ph} = \frac{\omega}{\xi} \tag{2.8}$$

The phase velocity dispersion curves for a 12 mm steel bar in a vacuum **(Fig. 2.12)** shows number of propagating modes that can be categorized into two groups. The red lines represent modes with an axially symmetric mode shape (longitudinal modes), and the blue lines represent modes with a non-axially symmetric mode shape (flexural modes). An infinite number of modes exist at higher frequencies, but only modes up to 4 MHz are shown.

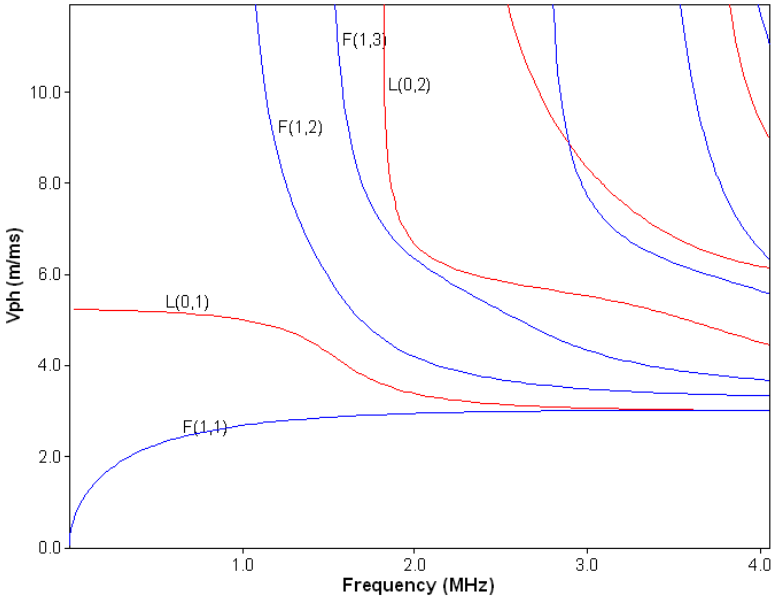

Fig. 2.12: Phase Velocity Vs Frequency (Pavlakovic et al., 2000)

- ***Group Velocity***

The phase velocity is the velocity of the propagating monochromatic wave and tells us the speed at which the individual wave crests travel but it does not tell us how fast the wave will propagate along a structure as a whole. In a perfectly elastic system, the group velocity is the rate of energy propagation along a structure, and is therefore the speed at which a guided wave packet will travel. The group velocity, V_{gr}, is defined by Equation 2.9, where ω is the circular frequency and ξ is the real wave number in radians per metre.

$$V_{gr} = \frac{\partial \omega}{\partial \xi} \tag{2.9}$$

2.4.3.2 Leaky Elastic Systems

If a structure is embedded in a material and not in vacuum, energy is able to leak from the waveguide into the embedding material. In reality, this happens for simple cases such as a steel bar in air, but because the acoustic properties of the air and steel are very different, the amount of leakage is small. However, if the acoustic properties are more closely matched, as in the case for embedding the steel in another elastic solid, the leakage becomes very significant. The embedding material may alter all the other properties of the guided wave as well as introducing leakage. Energy can cross the boundary from the structure to the embedding material, but no energy will cross back from the embedding material to the structure. The leaked energy that crosses the boundary travels as a bulk wave in the embedding material, resulting in attenuation of the guided wave contained within the structure. Two additional properties that are useful to describe the behavior of leaky waves are attenuation and energy velocity.

- ***Attenuation***

This section introduces the concept of wave attenuation through leakage into an embedding material. There is also another mechanism of attenuation that occurs due to damping inherent in the waveguide material. This effect occurs because real materials are not perfectly elastic, and some attenuation of sound waves occurs because of visco-elastic losses. This effect will occur in a bulk wave and a guided wave, and can be calculated if the damping properties of the material are known. The standard model of damping used by Disperse assumes a constant attenuation per wavelength, which in a bulk wave means that

attenuation generally increases with frequency. Although this effect has some influence on guided waves, the frequency-attenuation relationship of guided waves is much more complex and is controlled by many other factors, including leakage. The attenuation dispersion curves for a perfectly elastic 12 mm diameter steel bar, embedded in concrete are shown in **Fig. 2.13** The attenuation is expressed in dB/m, therefore showing the decrease in the amplitude of a guided wave that would occur over any given propagation distance. In this leaky elastic case, the attenuation is purely due to leakage as well as material damping. For a 12mm bar in concrete, the least attenuative mode is L(0,7) mode as shown in **Fig. 2.13**.

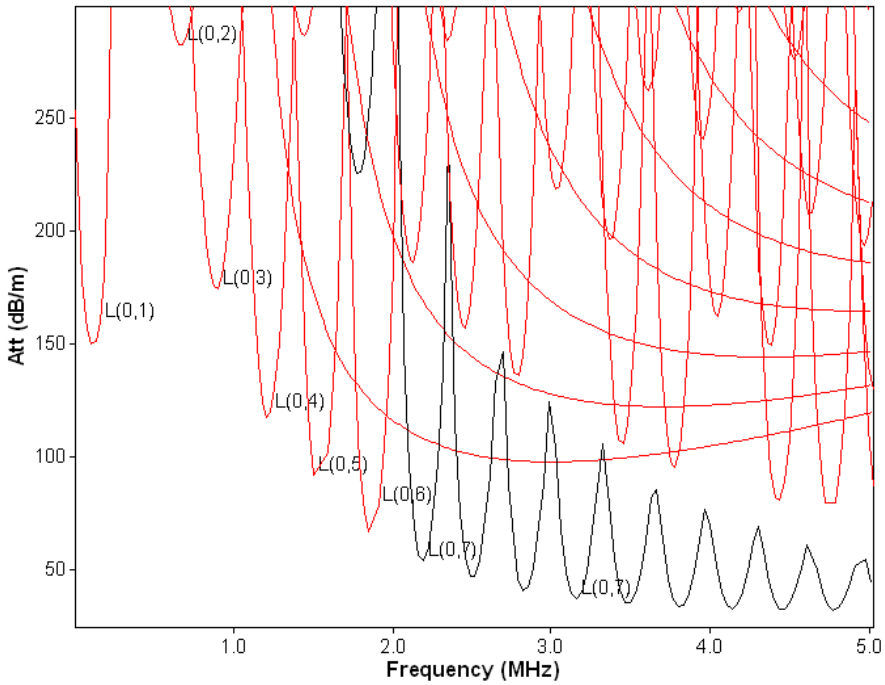

Fig. 2.13: Attenuation Vs Frequency (Pavlakovic et al., 2000)

- ***Energy Velocity***

The group velocity calculation is not valid for waves which are attenuating. The speed at which a wave packet will propagate along a structure is known as the energy velocity, and can be obtained from data derived from the mode shapes (stress and displacement fields). The energy velocity is defined as the ratio of the power flowing along the structure to the strain energy stored in the structure as it passes. In cases such as the perfectly elastic steel bar in a vacuum, the energy velocity is equal to the group velocity. However, in leaky or attenuative systems there are differences between the group and energy velocities. The

energy velocity dispersion curves for a perfectly elastic, 12 mm diameter steel bar embedded in concrete are shown in **Fig. 2.14.** Again L (0, 7) mode shows a energy velocity maxima and hence should be used for ultrasonic investigations for a 12mm bar in concrete.

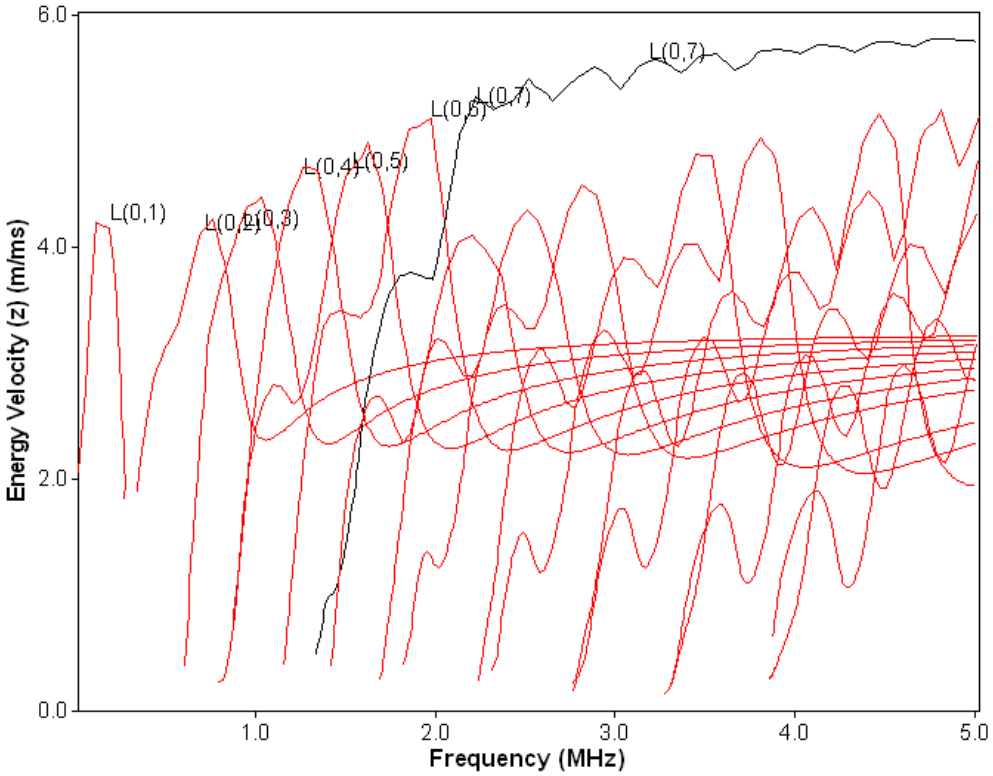

Fig. 2.14: Energy Velocity Vs Frequency (Pavlakovic et al., 2000)

2.5 CLOSING REMARKS

This chapter highlights the basics of ultrasonic waves and the principal issues associated with it to be adopted as a NDT tool for civil engineering purposes. Ultrasonics can be exploited as bulk waves or guided waves for health monitoring. They have normally been employed as bulk waves since the use of guided ultrasonic waves is more complicated, thus limiting its use in NDT. It is still in research phases and has not developed into a full fledged practical method because sound propagation is complex. Sound can travel in a large number of 'modes', which can be determined by the solution of the wave propagation equation. The complications arise from the fact that these guided waves are dispersive, and the frequency dependence of their properties such as velocity and attenuation must be known so that test results can be accurately interpreted.

However, ultrasonic guided wave propagation is slowly gaining popularity among researchers in the detection of corrosion related damage in reinforcing bars. But most of the work has remained confined to simulated studies in which corrosion is mainly modeled as delamination in reinforcing bars. Effect of corrosion has mainly been viewed as loss of interfacial bond. Limited experimental evidence of actually corroded RC specimens indicates that in addition to loss of bond, loss of cross-sectional area of bars has also significant influence. The thesis is a step forward in the monitoring of corrosion induced damages in reinforcing bars in concrete using ultrasonic guided waves and various issues related to it have been investigated. The following chapter gives a brief account of the mechanism of corrosion of steel in concrete, various techniques used for corrosion monitoring in RC structures and an account of recent research in utilizing guided waves for the same.

CHAPTER 3

CORROSION OF STEEL IN CONCRETE

3.1 INTRODUCTION

Corrosion of reinforcing steel in concrete is one of the biggest durability challenges faced by construction industry. The resulting corrosion products occupy volumes 6-10 (Broomfield, 1997) times that of the steel. The increased volume induces tensile stresses in the concrete resulting in cracking, spalling and delamination. As a consequence, the reinforcements get exposed to direct environmental attack and corrosion is accelerated. Along with unpleasant appearance it weakens the concrete structure to a high degree. Moreover, bond between the steel and the concrete is reduced (Okba et al. 2003; Fang et al. 2004). Pitting corrosion may also reduce the ductility of the steel bar by introducing notches on the surface of the steel bars that leads to a premature necking (Andrade et al. 1993).

Corrosion related problems are also alarming in a tropical country like India that has more than 3000 km of coastline where approximately 80% of the annual rainfall takes place in the two monsoon months,. In metro cities, the carbon and nitrogen oxide emissions aggravate the situation further by neutralizing the concrete cover. A large proportion of such damage is caused due to insufficient planning and incorrect assessment of the environmental attack such as carbonation and chloride exposure. Unlike other devices and facilities that are renewed periodically with newer ones, human endeavor has been to maintain centuries old structures. As a result, structural engineers dealing with ageing infrastructure and corrosion is one of the major problems. Typically, an RC structure that is subjected to heavy environmental loading requires major restoration work within fifteen years of its construction. Also, overall repair and maintenance of reinforced concrete structures is 1-2% of the cost of new construction per year (Gadve et al., 2008). The economic loss and damage caused by corrosion of steel in concrete makes it arguably the largest single infrastructural problem facing industrialized countries.

Corrosion, if undiscovered can cause catastrophic failure of the structure. The degradation accelerates unless early remedial action is taken. A wide range of techniques

have been reported in literature that may be suitably employed for the monitoring of corrosion of steel in concrete structures in order to diagnose the cause and extent of reinforcement corrosion. But these existing techniques are electrochemical in nature which relates corrosion rate and extent through assessment on surrounding concrete medium. None of the techniques concentrate on corrosion monitoring through direct measurement on embedded steel. Removal of concrete to visually inspect the reinforcement is detrimental to the structure. Also, many currently used nondestructive testing methods such as radiography, acoustic emission, X-ray etc (Aktan et al.1999; Matt 2001; Griffiths 1998; Vurpillot et al. 1996) cannot be used due to the huge size and limited accessibility of civil engineering installations. These techniques either require skilled labour or are costly and difficult to apply on civil infrastructure.

Hence, there is a need for developing a non-intrusive, in-situ and real time corrosion monitoring technique for embedded reinforcements in concrete structures. To develop and appreciate the technique, a review of the following aspects of reinforcement corrosion is discussed:

- Mechanism of reinforcement corrosion
- Initiation and progress of reinforcement corrosion
- Need for corrosion monitoring
- Existing corrosion monitoring techniques

3.2 CORROSION MECHANISM OF STEEL IN CONCRETE

3.2.1 Corrosion Initiation

Concrete is alkaline due to the presence of hydroxides of Calcium, Potassium and Sodium ($Ca(OH)_2$, KOH and NaOH) and the alkalinity typically ranges between pH 12 and 13. Due to the high alkalinity of the concrete pore water, the steel reinforcing bars are passivated by an iron oxide film (Fe_2O_3) that protects the steel. The passive layer is a dense, impenetrable film which if fully established and maintained, prevents the further corrosion of steel. The layer formed on steel in concrete is probably part metal oxide/hydroxide and part mineral from the cement. However, the passivating environment is not always maintained. In

the presence of oxygen, water and aggressive ions such as chlorides, steel bars are depassivated and corrosion is initiated. Corrosion is basically an electrochemical process where the anode and the cathode are on the same steel bar. At the anode, iron atoms lose electrons to become iron ions (Fe^{++}). At the cathode, oxygen in the presence of water accepts electrons to form hydroxyl ions (OH^-). Therefore, reinforcement corrosion cell is formed as shown in **Fig 3.1**.

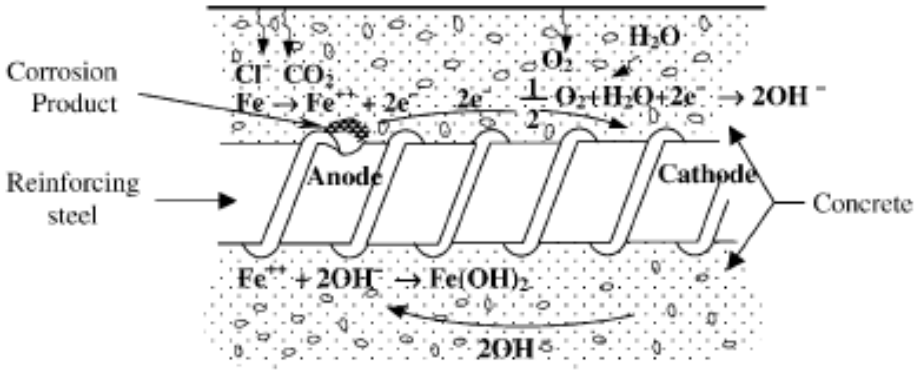

Fig. 3.1: Schematic illustration of corrosion of reinforcement in concrete

(Shamsad, 2003)

Concrete works as an electrolyte that facilitates the flow of electrons between the anode and the cathode. Concrete, when exposed to wet and dry cycles, has sufficient conductivity to serve as an electrolyte. Both the anodic and cathodic reactions are necessary for the corrosion to occur and they need to take place simultaneously. The anode and cathode can be located next to each other or can be separated. When they are located next to each other, i.e., on microscopic scale, the resulting corrosion cell is referred to as a micro cell. When they are separated by some finite distance, the resulting corrosion cell is referred to as macro cell. Corrosion of steel reinforcing bars embedded in concrete may be due to a combination of macro cells and micro cells **(Fig 3.2).** The initiation and continuation of the corrosion process are controlled by the environment in the concrete surrounding the steel reinforcing bars. The distribution of chlorides in concrete is not uniform. The chlorides enter the concrete from the exposed surface. The concentration of chlorides is not uniform along the length of steel bars due to the heterogeneity of the concrete. These differences in chloride concentrations establish anodes and cathodes on individual steel bars and result in the formation of micro cells.

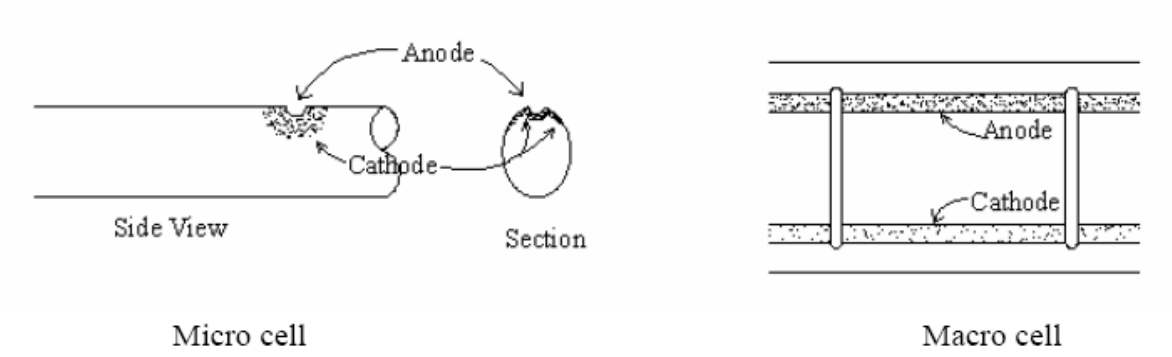

Fig. 3.2: Micro Cell and Macro Cell (Gadve, 2008)

3.2.2 The Corrosion Process

Oxygen, water and aggressive ions such as chlorides need to be available, and the concrete needs to have low resistivity. Also all these conditions must be present simultaneously. However, the intrusion of chloride ions is the most important factor in the corrosion of steel reinforcing bars embedded in concrete. Possible sources of chlorides include: aggregates, mix water, admixtures (accelerators), deicing chemicals, seawater. The chloride content of Portland cement, fly ash and silica fume is typically very low. However, the chloride content of ground granulated blast-furnace slag is variable. The water used in the mixing process can be a major contributor. The chloride content can be significantly high if saltwater is used. Aggregates may contain chlorides, especially if they are obtained from sites associated with seawater or ground water containing chlorides. Potable water can contain small amounts of chlorides (20 to 100 ppm). This amount of chloride is generally considered insignificant and when used in concrete of typical mix proportions, the resulting concrete would have chloride concentration much lower than the threshold limit. In addition to the admixtures based on calcium chloride ($CaCl_2$), some water reducers and setting admixtures also contain chlorides. It is considered insignificant if the chloride content is less than 0.01% of mass of cementitious material.

Several theories have been presented to explain the role of chloride ions. Chloride ions reach the reinforcing steel by penetrating the concrete via the pore water and through cracks in the concrete. According to the oxide film theory, the chloride ions breakdown the passive oxide film. At this point, the steel reinforcing bar becomes depassivated and corrosion gets initiated. In accordance with the adsorption theory, chloride ions are adsorbed

onto the surface of the steel reinforcing bar and they attack the steel directly. As per the transitory complex theory, chloride ions act as a catalyst. The chloride ions combine with the ferrous ions to form a soluble iron chloride complex that diffuses away from the anode. Subsequent breakdown of the iron chloride complex frees the chloride ions for reuse when ferrous hydroxide is formed.

When carbon dioxide (CO_2) from the atmosphere penetrates concrete and dissolves in the pore solution, carbonic acid is formed. This acid reacts with the alkali in the cement to form carbonates and lower the pH of concrete. When the alkalinity reaches a low enough level, the steel reinforcing bar becomes depassivated and in the presence of sufficient water and oxygen, corrosion is initiated and propagated. However, carbonation advances very slowly in sound concrete and is generally not a big factor in corrosion initiation.

The corrosion of steel in concrete in the presence of oxygen but without chlorides takes place in several steps and is referred as ***Oxide Corrosion (OC).***

At the anode, iron is oxidized to ferrous state and releases electrons:

***Anodic Reaction*:** $Fe \rightarrow Fe^{2+} + 2e^-$ (3.1)

***Cathodic Reaction*:** $2e^- + H_2O + \frac{1}{2}O_2 \rightarrow 2OH^-$ (3.2)

Both the anodic and cathodic reactions are necessary for corrosion to occur and they need to take place simultaneously. The hydroxyl ions combine with the ferrous ions to form ferrous hydroxide:

$Fe^{2+} + 2OH^- \rightarrow Fe(OH)_2$ (3.3)

In the presence of water and oxygen, the ferrous hydroxide is further oxidized to form Fe_2O_3.

$4Fe(OH)_2 + O_2 + H_2O \rightarrow 4Fe(OH)_3$ (Ferric Hydroxide) (3.4)

$Fe(OH)_3 \rightarrow Fe_2O_3.2H_2O$ (Hydrated Ferric Oxide- Rust) (3.5)

Whenever spontaneous reaction occurs, all the electrons released in the anodic reaction are consumed in the cathodic reaction; no excess or deficiency is found. Therefore, no net current can be measured externally. Moreover the metal normally takes up more or less uniform electrode potential often called corrosion or mixed potential (E_{corr}). The corresponding rate of metal dissolution at this potential is called corrosion rate (I_{corr}).

The manifestation of oxide corrosion is in the formation of these corrosion products on the surface of the rebar. Thus, the steel-concrete interface is altered where rust is formed. In the initial stages, the corrosion products increase the friction coefficient at the interface through the roughening of the bar surface. As corrosion progresses, an outward pressure is generated on the concrete due to higher volume of corrosion products than the corresponding volume of steel. This might initially improve the interfacial bond. However, the pressure results in tensile stresses in concrete. As concrete is weak in tension, cracks develop in it leading to debond. Most researchers have simulated debond by artificially introducing an element at the interface.

Corrosion of steel in concrete in the presence of chlorides, but with no oxygen (at the anode) and referred to as ***Chloride Corrosion (CC)*** takes place in several steps. At the anode, iron reacts with chloride ions to form an intermediate soluble iron-chloride complex:

Anodic Reaction: $Fe + 2Cl^- \rightarrow (Fe^{2+} + 2Cl^-) + 2e^-$ (3.6)

When the iron-chloride complex diffuses away from the bar to an area with higher pH and concentration of oxygen, it reacts with hydroxyl ions to form $Fe(OH)_2$. This complex reacts with water to form ferrous hydroxide:

Cathodic Reaction: $(Fe^{2+} + 2Cl^-) + 2e^- + 2H_2O \rightarrow Fe(OH)_2 + 2H^+ 2Cl^-$ (3.7)

This ferrous hydroxide is oxidized to rust in the presence of oxygen and water. As in the case of oxide corrosion of steel, ferrous hydroxide is oxidized to rust in the presence of oxygen and water. The resulting corrosion products and accompanying processes of cracking, spalling and delamination of concrete occurring in both types of corrosion are similar but the rate and mode of occurrence of various aspects of corrosion are different in the two cases. The rate of chloride corrosion is much faster than oxide corrosion. Although it also leads to debond as described in oxide corrosion, its distinguishing feature is pitting where crevices are formed in the bar leading to local loss of material. Thus, in addition to debond, chloride corrosion leads to local weakening and loss of strength and ductility of the bar.

3.2.3 Time Dependant States of Reinforcement Corrosion

A typical model for the corrosion process in RC structures was set forth (Tuutti , 1982) and **Fig. 3.3** is a close derivative of the original model (Rostam, 2003; Morcous et al., 2005). The model defines two periods during the corrosion process: initiation and propagation. When bare steel is initially exposed to oxygen and water, it forms a very thin (1 μm) dense layer of either metal oxide or hydroxide on its surface (Bazant, 1979). This film, referred to as the passive layer, protects the steel while it is contained in the proper environment. The initiation period is the amount of time that the passive layer on the embedded steel is protected by the surrounding concrete which provides a highly alkaline environment to protect the passive layer. The length of the initiation period is determined by the amount of time that deleterious substances (e.g., chlorides and carbon dioxide) take to ingress through the concrete pore structure and/or cracks and reach a critical threshold at the reinforcement depth. Both chlorides and carbon dioxide can eventually destroy the passive layer and lead to the initiation of corrosion.

An illustration of the corrosion process is depicted in **Fig. 3.4** (Ervin et al., 2009). Point (a) reflects a moment during the ingress of the deleterious substances prior to reaching the reinforcement depth. Once the chlorides or carbonation have reached the reinforcement depth and destroyed the passive layer, both oxygen and water must be present in order for the steel to corrode. It must be noted that the type of corrosion is dependent on whether carbon dioxide or chlorides are present and on the quantity ingressed. Carbon dioxide and a high concentration of chlorides usually remove the passive layer more uniformly which leads to uniform corrosion (i.e. general or homogeneous), while a lower concentration of chlorides remove the passive layer in select locations which leads to localized (i.e. pitting) corrosion. Cracks connecting the concrete cover to the depth of reinforcement, usually caused by other sources of deterioration (e.g., shrinkage, overloading, freezing/thawing and settling), will lead to more localized corrosion as well. Once the passive layer has been destroyed, point (b), the initiation period is over and the propagation period begins. The propagation period tracks the progression of reinforcement corrosion over its service life. Point (c) is an example of corrosion product accumulation after the breakdown of the passive layer. Corrosion products are more voluminous than iron, confines the amount of volume expansion, creating hoop stresses from the pressure. Cracks are created, point (d), in the concrete from the hoop

stress. The cracks degrade the ability of the surrounding concrete to confine the corrosion product and subsequently reduce the interfacial bond. The crack patterns created are dependent on the reinforcement location, the ratio of the depth of cover to the reinforcement diameter and the type of corrosion (Bentur et al., 1997). Multiple cracks, point (e), can eventually lead to concrete section loss (spalling). The end of the propagation period is determined by how service life is defined for the particular structure (e.g., crack width limit, deflection limit and excessive spalling). The main factors contributing to structural damage in the RC infrastructure from uniform corrosion are loss of the steel cross-sectional area during the corrosion reaction, cracking and spalling of the concrete from corrosion product accumulation, and destruction of bond between the steel and concrete from corrosion product accumulation.

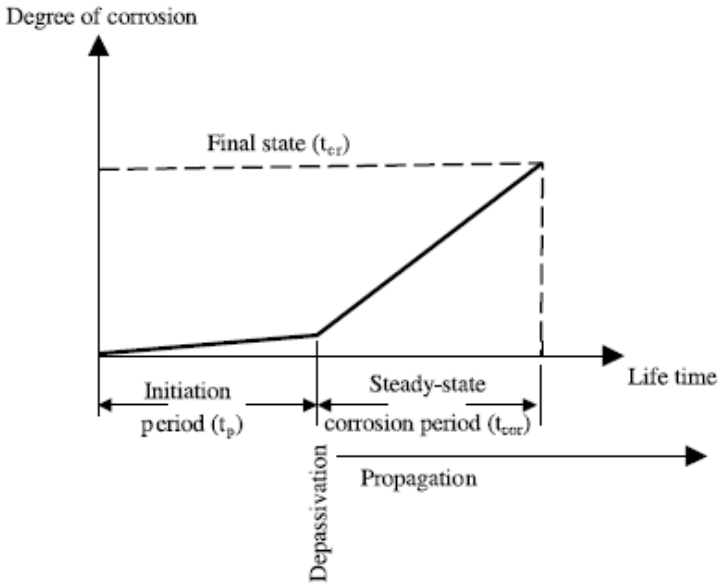

Fig 3.3: Stages of reinforcing bar corrosion (Schiessl, 1988)

Hence, the state of corrosion of steel in concrete may be expected to change as a function of time. Corrosion process has three distinct stages, namely, depassivation, propagation, and final state (Schiessl, 1988) as shown in **Fig. 3.3**. Depassivation is the loss of oxide (passive) layer over the rebar, which is initially formed due to the high alkalinity of concrete. The process of depassivation takes an initiation period, t_p, which is the time from construction to the time of initiation of corrosion (depassivation). The propagation phase starts from the time of depassivation, t_p, to the final state, is reached at a critical time, t_{cr}, at

which corrosion would produce spalling of concrete cover or cracking through the whole of concrete cover. During the propagation period, i.e. corrosion period, t_{cor}, which begins at the moment of depassivation, the rebar corrosion is usually assumed to be in a steady state. The critical time, t_{cr}, as defined above can be expressed as:

$$t_{cr} = t_p + t_{cor} \quad (3.8)$$

For reinforced concrete, it has been assumed reasonable to equate the unacceptable corrosion damage to the onset of spalling of concrete cover (Schiessl, 1975). Therefore, the service life can be equated to the critical time **(Equation 3.8)**.

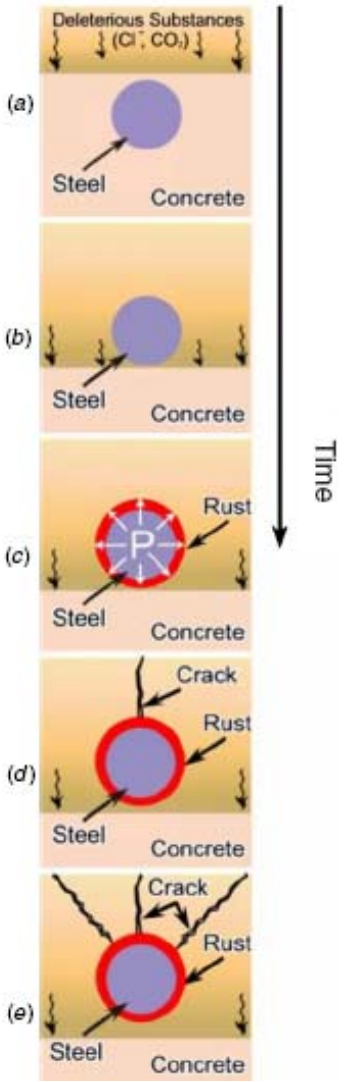

Fig. 3.4: Progressive stages of corrosion process in RC structures (Ervin et al., 2009)

3.2.4 Effect of Corrosion on Concrete

The important factor in corrosion of steel in concrete compared to most other corrosion problems is the volume of oxide and where it is formed. A dense oxide formed at high temperatures usually has twice the volume of the steel consumed. In most aqueous environments the excess volume of oxide is transported away and deposits on open surfaces within the structure (Ahmad, 2003). In the case of steel in concrete two factors predominate:

- The main problem is that the pore water is static and there is no transport mechanism to move the oxide away from the steel surface. This means that all the oxide is deposited at the metal oxide interface.
- The second problem is that the oxide is not dense. It is very porous and takes up a very large volume; up to ten times that of steel consumed when the porosity of the corrosion products is taken into account.

Since reinforcing steel is doing its job in areas of tension in the structure, small cracks will occur in concrete as shown in **Fig. 3.5** as the tension load increases the tensile strength of the steel. Most of these are small cracks (< 0.5mm) at right angle to the reinforcing steel. They should not significantly affect the rate of corrosion of the steel as any local ingress of chlorides, moisture and carbonation is limited and contained by the local alkalinity. Obviously there is a limit to this 'self healing' ability. If there are large cracks (> 0.5mm) that stay open, or excessive shrinkage cracks along the bars, then corrosion can be accelerated. Corrosion also causes horizontal cracking along the plane of the rebar and the corner cracking around the end rebar. This leads to loss of concrete cover. Corners tend to crack first on corroding reinforced concrete structures. This is because the oxygen, water, chlorides and carbon dioxide have two faces as pathways to the steel. Delaminations occur as corrosion proceeds on the neighboring reinforcing bars and the horizontal cracks join up.

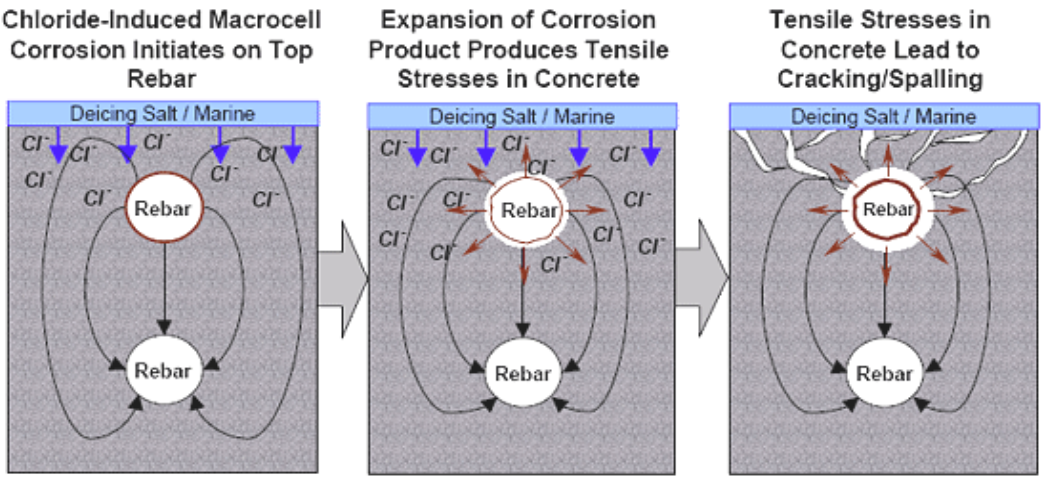

Fig 3.5: Cracking and Spalling of corrosion effected concrete

(www.googleimages.com)

3.2.5 Effect of Corrosion on Structural Behavior

The corrosion of reinforcing steel has the following major detrimental effects on the durability of RC structures (Ahmad, 2003):

- Since the rust produced as a result of corrosion has a volume 6 – 10 times than that of steel (Broomfield,1997) it causes volume expansion developing tensile stresses in concrete, which ultimately results in cracking and spalling of the cover concrete as shown in **Fig 3.6** and delamination or debonding of the bar from the surrounding concrete. Due to the loss of cover concrete, there may be significant reduction in the load bearing capacity of the structure, and besides this, steel may be more accessible to the aggressive agents leading to further corrosion at an accelerated rate.
- Corrosion reduces the cross-sections of the steel and thereby the load carrying capacity of the structure. Pitting (i.e., localized) corrosion of the rebar is more dangerous than uniform corrosion because it progressively reduces the cross-sectional area of rebar to a point where the rebar can no longer withstand the applied load leading to a catastrophic failure of the structure.

Fig 3.7 shows the various shapes of pitting in corroded reinforcement.

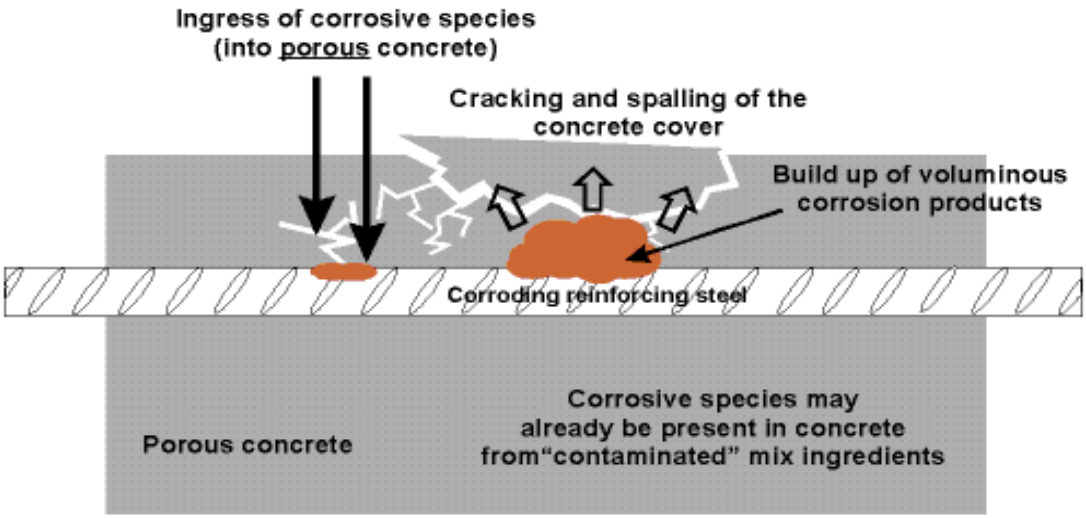

Fig. 3.6: Effect of Reinforcement Corrosion on steel and concrete

(www.googleimages.com)

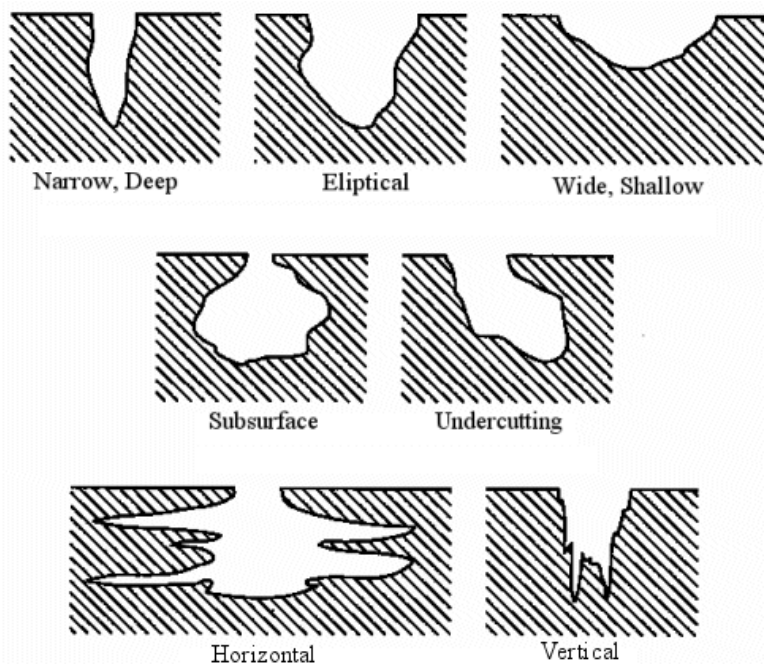

Fig. 3.7: Various types of shapes of pitting in corroded reinforcement

(www.googleimages.com)

3.2.6 Strategies for investigation of a corroding RC structure (Ahmad, 2003)

A visual survey of a corroding structure provides valuable information as to, whether the corrosion of rebar is really a cause of distress or there is some other cause of distress.

This survey consists of a careful investigation of the structure for any sign of distress, such as cracking, spalling, and rust staining.

If visual inspection of the structure suggests that the cause of distress is the corrosion of rebar only, the next step is to undertake a careful examination of the structure and carry out detailed tests which will positively identify the cause and extent of the distress, and allow prediction to be made about the remaining service life of the structure. A widely accepted flowchart for investigation of a corroding RC structure, suggested by Pullar-Strecker (1987), is reproduced in **Fig. 3.8**.

3.2.7 Need for Corrosion Monitoring

To counteract the destructive corrosion process, standard practices for reinforced concrete design have improved over the last 25 years. The quality of the concrete cover with respect to mix design, placement, compaction, depth, sealants and curing practices will tremendously delay the ingress of deleterious substances. Carbon fibre-reinforced polymer wraps (Wootton et al., 2003) and electrochemical chloride removal sytems (Bennett et al., 1993) have been used to protect and restore reinforced concrete in corrosive environments. Protection of the reinforcement by polymer/metallic coatings (Sanjurjo et al., 1993) and/or cathodic protection (Broomfield et al., 1992) have also been effectively used. Ultimately, however, these practices generally only *delay* the onset of corrosion rather than prevent the process entirely.

Monitoring the corrosion process over time is necessary to ensure serviceability and safety requirements. Millions of dollars are spent worldwide annually in the repair, rehabilitation, restoration and maintenance of structures affected by corrosion. The economic loss and damage caused by corrosion of steel in concrete makes it arguably the largest single infrastructural problem facing industrialized countries (Gadve, 2008). Furthering the need for monitoring is the industry goal to push service design lives of reinforced concrete structures well over 100 years.

Ultimately, the public demands RC structures those are functional, cost effective, reliable and safe. To date, numerous on-site non-destructive and semi-destructive testing methods exist. Many of the methods are time-consuming procedures that require the structure to be temporarily shut down. The closure will create indirect costs associated with the use of the method. Most of the methods rely very heavily on the inspector's expertise to visually

assess damage and his knowledge of the equipment used to inspect the structure. Other methods that can avoid on-site inspections, such as ground penetrating radar from a moving vehicle, are generally structure specific, allowing for inspection of only certain parts of a structure (e.g., bridge deck).

3.3 CORROSION MONITORING - CHEMICAL TECHNIQUES

Reinforcement corrosion has been widely reported in the literature over the last two to three decades. The assessment of the causes and extent of corrosion is carried out using various electrochemical techniques. In this section, a review of the electrochemical techniques utilized to monitor reinforcement corrosion is presented. A wide range of electrochemical techniques have been reported in the literature that may be suitably employed for the monitoring of corrosion of steel in concrete structures for the purpose of diagnosing the cause and extent of the reinforcement corrosion.

3.3.1 Corrosion measurement parameters

The information about the state of reinforcement corrosion is obtained usually in terms of three measurement parameters (Ahmad, 2003), namely

(i) Half-cell potential, E_{corr}

(ii) Concrete resistivity, ρ

(iii) Corrosion current density, I_{corr}

(i) Half-cell potential (E_{corr}): The half-cell potential, also called the open-circuit potential or rest potential or corrosion potential, is measured at several distinct points over a given area to be surveyed, and is used as a qualitative index for ascertaining whether or not reinforcement is likely to be corroding. It is also used for obtaining a contour plot to delineate anodic (corroding) and cathodic (non-corroding or passive) portions of the RC structure under investigation. Interpretation of half-cell potential test results is carried out as per the ASTM C876 (1987) guidelines, as presented in **Table 3.1.**

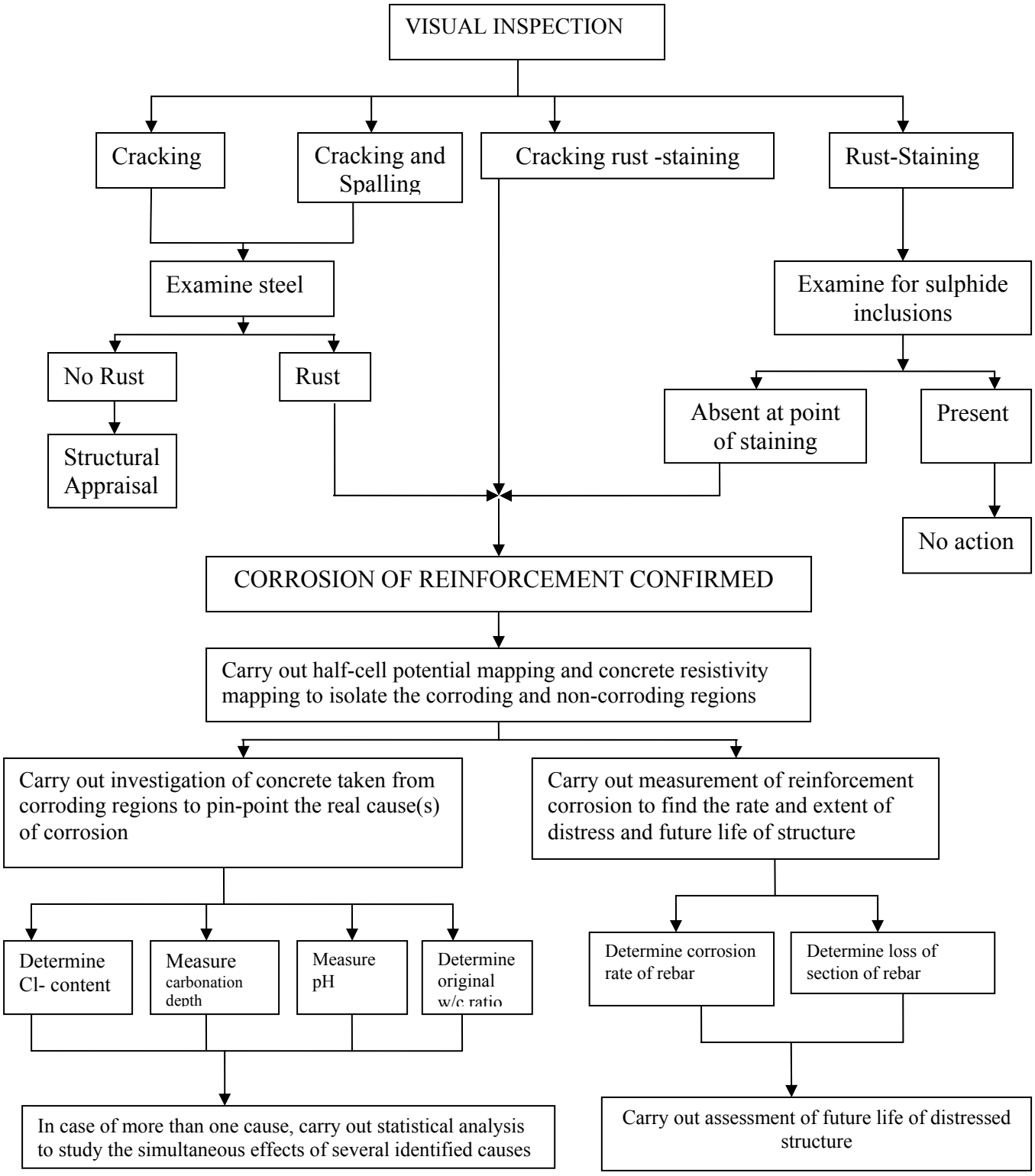

Fig. 3.8: Flowchart of investigation strategies of a corroding RC structure

(Pullar-Strecker, 1987)

Table 3.1: Interpretation of half-cell potential values as per ASTM C876 (1991)

Half-cell potential relative to Cu-/$CuSO_4$ reference electrode (mV)	Percentage Chance of Active Corrosion (%)
< -350	90
-200 to -350	50
>-200	10

(ii) Concrete resistivity (ρ): The corrosion of a specific length of reinforcement is dependent on the algebraic summation of the electrical currents originating from the corroding sites on the steel and flowing through the surrounding concrete to the non-corroding sites. Hence, the electrical resistance of the concrete plays an important role in determining the magnitude of corrosion at any one specific location (Berkeley, 1990). This factor is measured in terms of electrolytic resistivity of concrete and is usually expressed in ohm-centimeters. Classification of the likelihood of corrosion, actually occurring, can be obtained on the basis of the values given in **Table 3.2**, and this is best suited when half-cell potential measurements indicates that corrosion is possible (Bungey, 1989).

Table 3.2: Interpretation of concrete resistivity values (Bungey, 1989)

Resistivity (ohm-cm)	Likelihood of corrosion (non-saturated concrete when steel is activated)
<5000	Very High
5000-10,000	High
10,000-20,000	Low/Moderate
>20,000	Low

(iii) Corrosion current density (I_{corr}): The corrosion rate is measured in terms of the corrosion current density, I_{corr}, and is a quantitative index, which represents an overall estimate of the corrosion attack of reinforcement. I_{corr} is measured electrochemically and can be converted (Ijsseling, 1986) to the instantaneous corrosion rate, J_r, and penetration rate, P_r, through Faraday's law, as follows:

$$J_r = \left(\frac{W}{F}\right) I_{corr} \quad (3.9)$$

$$P_r = \left(\frac{W}{F\rho_{st}}\right) I_{corr} \quad (3.10)$$

Where

W= equivalent weight of steel = 55:85/2 = 27:925 g, F = Faraday's constant = 96487 C,

ρ_{st}= Density of steel (7.85 gm/cm^3), I_{corr} = corrosion current density (Amp/cm^2),

J_r = instantaneous corrosion rate (gm/cm^2/s), P_r = penetration rate (cm/s).

The corrosion rate measured may be either passive or active depending on the corrosion rate (Rodriguez, 1994). Passive state rate of corrosion of rebar is found to be relatively low in the order of 10^{-9} to 10^{-7} Amp/cm^2, whereas the active state corrosion rate is found to be relatively high, compared to that of passive state, in the order of 10^{-6} to 10^{-5} Amp/cm^2.

3.3.2 Methods of Corrosion Monitoring

Measurement of reinforcement corrosion in concrete needs a method which can not only simply, accurately and non-destructively determine whether or not corrosion of reinforcement is taking place but also to evaluate the extent of damage. Of all the techniques of corrosion monitoring, half cell potential mapping is the simplest and most widely used. But it does not give any quantitative information on corrosion. Corrosion rate, I_{corr} is the most useful quantitative parameter for measuring corrosion and the fastest and best method to measure it is 'Linear polarization method' (Schiessl, 1988; Rodriguez, 1994). But application of this technique to RC specimens poses a number of difficulties. The various methods of corrosion monitoring developed over a period of time with their drawbacks are listed below:

3.3.2.1 Half Cell Potential Mapping

This method was first developed in late 1950's (Stratfull, 1957) and since then has been extensively used for the assessment of concrete bridges. It was adopted as an ASTM standard method C876. The method as discussed, measures the electrochemical potential of reinforcement against a reference electrode placed on concrete surface. The basic setup of this method is shown in **Fig. 3.9.** Prior, to testing, electrical continuity of reinforcement is checked by applying a potential difference across a rebar at different sections of the structure.

A measured resistance of less than 1 ohm is used to indicate continuous electrical connection of reinforcement. In order to ensure a good contact with the reference electrode, the concrete surface requires pre-wetting. A number of reference electrodes may be used but $Cu/CuSO_4$ is most commonly used. **Table 3.1** is used for assessing corrosion. But there is a difficulty in interpreting the results which lies between -200 and -350mV. Comparing the neighboring surface potentials (i.e potential gradients) is a more appropriate procedure. Measurements are presented in the form of equipotential contour maps **(Fig. 3.10)** by which areas of suspected corrosion are identified. It is a common practice now to embed half cells in the concrete to monitor the performance of cathodic protection systems for atmospherically exposed steel in concrete.

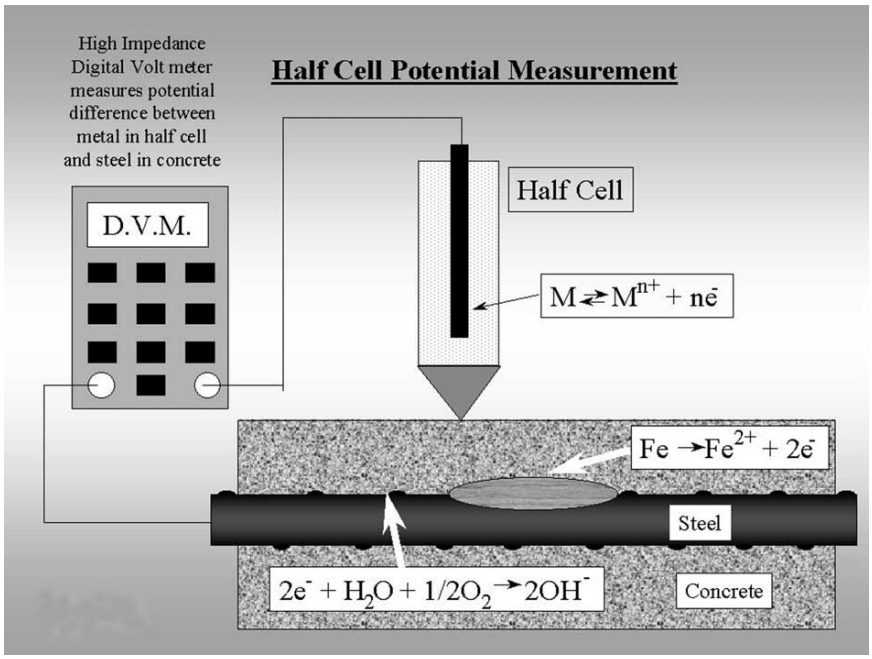

Fig. 3.9: Half cell potential measurement (Broomfield, 2002)

But it is not economical to install half cells all over a structure to monitor its changing corrosion condition. Also measured potentials are affected by a number of methods and these should be considered in interpreting the results. One of the most important factors is the quality of cover concrete, particularly its moisture content and contamination by carbonation or chlorides and oxygen access. Also, this method only gives an indication of whether corrosion is thermodynamically possible and no information relating to corrosion kinetics can be obtained.

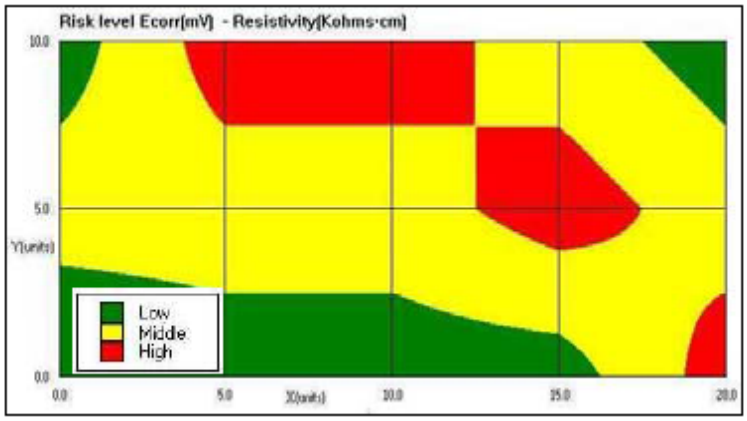

Fig 3.10: Corrosion risk map on a reinforcement slab in terms of E_{corr} and ρ (Martínez, 2009)

3.3.2.2 Linear Polarization Method (LPR method)

Linear polarisation is simple in principle although the underlying theory is complex and its use in practice is also complex. The theory of linear polarisation, also known as polarisation resistance, relies on the relationship between the half cell potential of a piece of corroding steel and an external current applied to it, i.e., the corrosion rate is proportional to the applied current divided by the potential shift. This can be expressed by the equations:

$$I_{corr} = \frac{B}{Rp} \tag{3.11}$$

Where I_{corr} is the corrosion current, B is a constant related to the anodic and cathodic Tafel slopes and Rp, the polarisation resistance= dE/dI, where dI is the change in current and dE is the change in potential.

Linear polarisation (LP) is usually conducted in aqueous solutions on small, uniformly corroding specimens. A number of LP devices are now available for use in steel in concrete. One of the most sophisticated device is illustrated in **Fig. 3.11**. The system consists of a half cell to measure the potential and its change, an auxiliary electrode to pass the current and, in this case, a guard ring around the auxiliary electrode to constrain the electric field from the auxiliary electrode because of the size of the corroding rebar. This ensures that a measurement is taken from a defined area of steel and prevents gross errors in the area of measurement (Broomfield, 1997, 2002; Flis et al., 1993).

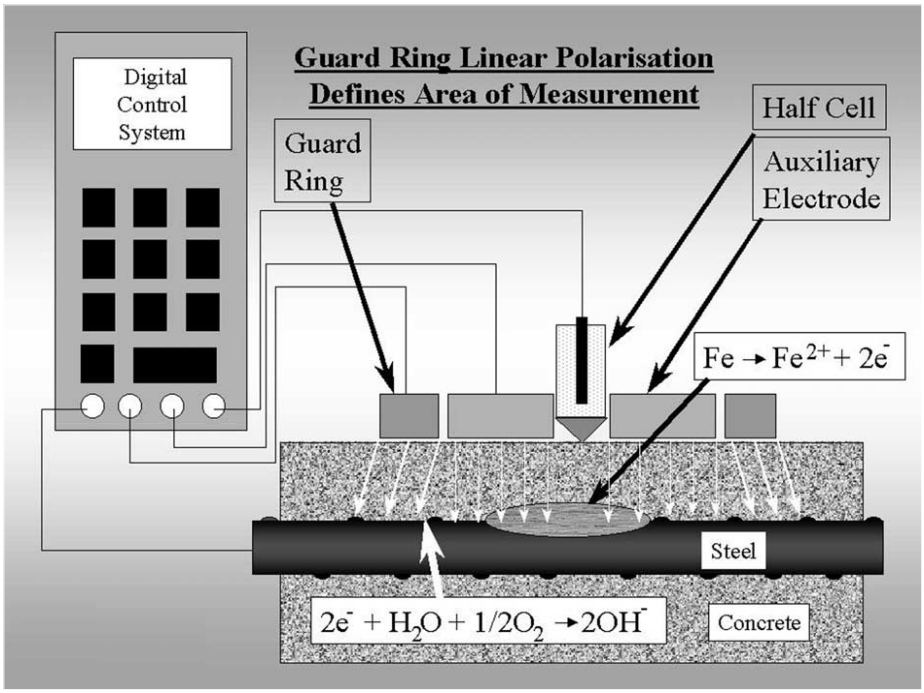

Fig. 3.11: Guard Ring Linear Polarisation Measurement Method

(Broomfield, 2002)

If linear polarization method is used in corrosion monitoring, then in new construction the measurement can be made with an embedded half cell against a mild steel ‘‘working electrode’’ with one or more stainless steel auxiliary electrodes. The mild steel working electrode should be fully representative of the actual reinforcement and should accurately represent the corrosion rate of the steel around it if embedded at the same cover. There may be slight differences due to variations in the steel surface between ribbed slightly corroded bars and a smooth electrode, and macrocell effects may be different if the electrode is left unconnected to the steel between readings.

Some of the difficulties associated with the method which are difficult to achieve practically are:

(1) When the steel surface is passivated, Tafel slope is often difficult to determine.

(2) Maintaining constant electrochemical current at a fixed potential during the entire polarization period

(3) Ensuring uniform current distribution around the steel bar

(4) Precisely correcting the effect of high electrical resistance of concrete

Moreover, this technique measures only the instantaneous corrosion rates of reinforcement; it does not reflect the long term corrosion rate.

3.3.2.3 AC/Electrochemical Impedance Spectroscopy (EIS)

AC impedance spectroscopy has been widely used in fundamental and applied studies in electrochemistry and for studying corrosion mechanisms and determining corrosion rate of reinforcing steel in concrete (Wenger et al., 1990; John et al., 1981; Macdonald et al., 1991; Hachani et al., 1994) This method applies small amplitude sinusoidal signals over a large range of frequencies of a system and records the impedance response. The complex plane (imaginary Vs real) and bode plots (phase and amplitude Vs frequency) can be obtained for data analysis which can be used to provide information about corrosion kinetics and mechanism. A simple electrochemical interface between liquid (pore solution) and solid steel can be modeled with an equivalent circuit as shown in **Fig. 3.12**. The impedance of the circuit is given by:

$$Z(\omega) = \mathrm{Rs} + \frac{Rp}{1+(\omega C_{dl} Rp)^2} - j\frac{\omega C_{dl} Rp^2}{1+(\omega C_{dl} Rp)^2} \qquad (3.12)$$

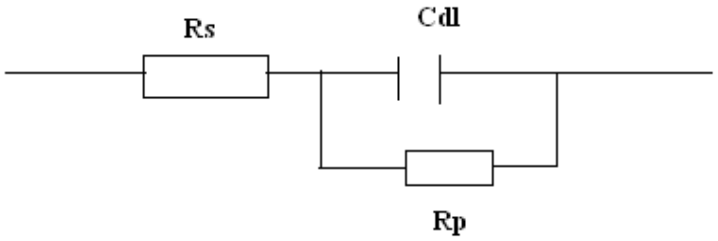

Fig. 3.12: Simple Equivalent circuit for modeling steel/concrete interface (Hong et al., 2007)

Where

Rs is the concrete solution resistance between RE and measured reinforcing steel, C_{dl} is the doulble layer capacitance at the steel concrete interface, Rp is the polarization resistance, ω is $2\pi f$ and $j = \sqrt{-1}$.

A plot of Equation (3.12) yields a perfect semicircle in the complex plane which intercepts on the real axis at Rs and Rs+Rp with Rp as its diameter **(Fig. 3.13)**.Therefore the corrosion rate can be calculated by Stern-Geary (1957) equation as

$$Rp = \left(\frac{\Delta E}{\Delta I} \right)_{E_{corr}} \quad (3.13)$$

The A.C. impedance technique has the advantage that it can give more information than DC LPR measurements, but it can be very time-consuming to perform and its use has been generally confined to the laboratory rather than on structures in the field (Mac Donald, 1991). EIS has been extensively used to evaluate the corrosion rate of the steel/concrete system. This technique may be very attractive because, used in a wide range of frequencies; it can give detailed information about the mechanism and kinetics of the electrochemical reactions. Not only is it able to give Rp values, but it may also give complementary information on the corrosion process, the dielectric properties of the concrete (high frequency range) or the characteristics of the passivating film (very low frequency) (Andrade et al., 1996). Many researchers have used Impedance Spectroscopy for the characterization of the corrosion behavior of steel in concrete (Gu et al., 1994, Mac Donald et al. 1988, Montemor et al., 1993, Kranc et al., 1993 and Lay et al., 1985). An advantage of the EIS technique is the very small excitation amplitudes, generally in the range of 5 to 10mV peaks to peaks, minimally disturbs the steel, attached corrosion products or absorbed species during testing (Husain et al., 2004).

But in situations where oxide films and interfacial films are present, the impedance spectra becomes more complicated, mandating a more complex equivalent circuit to model the steel concrete interface. A potentiostat coupled with a frequency response analyzer can perform complicated tests for such systems but the complete frequency scan is too time consuming and the equipment overly expensive. At this point, there is no AC impedance instrument suitable for field tests over the entire frequency range.

3.3.2.4 Concrete Resistance and Resistivity Measurements

The electrical resistivity of concrete is an important parameter concerning determination of intensity of the initiated corrosion process. In concretes with high electrical resistivity the corrosion process will be slow compared to concrete with low resistivity in which the current can easily pass between anode and cathode areas. Two different techniques, namely AC and DC measurements are used for determination of electrical resistivity. In these measurements both surface and embedded probes are applied. Applying a constant electric field between the two embedded electrodes and measuring the resulting current as a voltage drop over a small

resistance accomplish the DC measurements. The AC measurements can be conducted both by means of two and four pin methods. The most common surface mounted probe is known as the Werner Probe. An alternating current is passed between the outer electrodes and the potential between the inner electrodes is measured. Concrete resistivity is generally measured by using the Wenner four probe method as shown in **Fig. 3.14**.

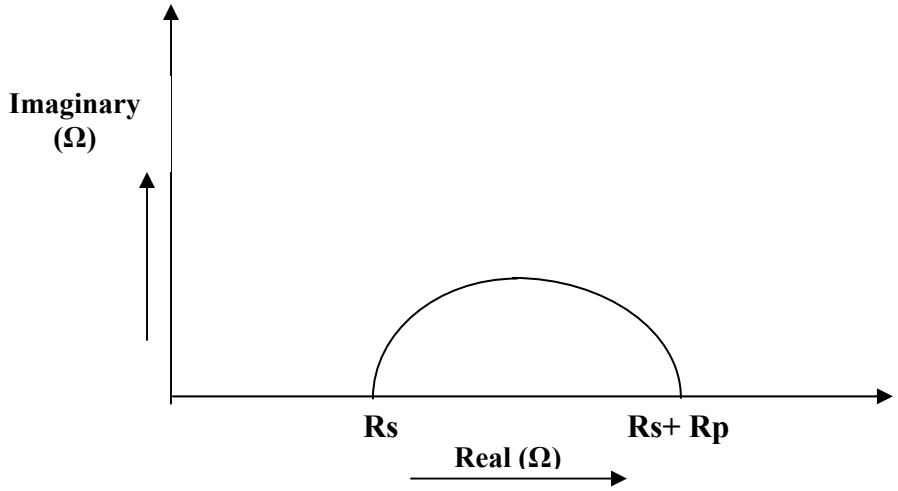

Fig. 3.13: Impedance Plot in the complex plane from simple equivalent circuit (Hong et al., 2007)

A known current 'I' is impressed on the outer probes and the resulting potential drop 'V' between the inner probes is measured and resistance 'R' is given by V/I

Resistivity of concrete (ρ) = $2\pi aR$ (3.14)

Where, a = Inner electrode distance (in cm)

R = Measured Resistance (in ohm)

The electrical resistivity of concrete is being increasingly used indirectly to evaluate concrete characteristics such as the chloride ion diffusivity, the degree of concrete saturation and its aggressiveness (Berke et al., 1992). This parameter may also provide useful information regarding the rebar corrosion performance in concrete (Millard et al., 1989). As indicated by Feliu et al. (1996), the electrical resistivity of concrete is inversely proportional to the corrosion rate. This observation was supported by Glass et al. (1991), who showed that the effect of mortar resistivity on the rebar corrosion rate was strongly dependent on the

environmental relative humidity. Lopez et al., (1993) have shown that the concrete pores saturation level governs the resistivity and the corrosion rate. Even when the influence of concrete resistivity on the rebar corrosion rate is evident, there are important differences in the threshold values of ρ proposed by several authors in order to evaluate the degree of rebar corrosion (Hope et al., 1985; Stratfull, 1974; Browne, 1982).

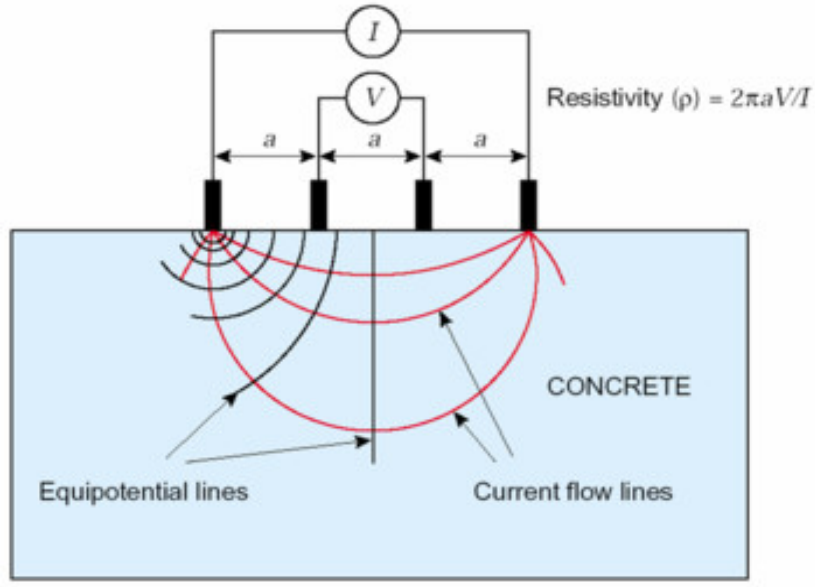

Fig. 3.14: Circuit for electrical resistance measurements (Martinez et al., 2009)

It was reported that the electrical resistivity of concrete was proposed as an effective parameter to evaluate the risk of reinforcing steel corrosion, particularly when corrosion is induced by chloride attack (Morris et al., 2002). The resistivity of concrete is strongly dependent on the concrete quality and exposure conditions, such as relative humidity and temperature which affects the degree of concrete pore saturation (Hussain et al., 1995; Hope et al., 1985) and thus impacts resistivity values. Corrosion and resistivity are related as shown in **Table 3.2**. The resistivity measurement is a useful additional aide in identifying problem areas or confirming concerns about poor quality concrete. Measurements can only be considered alongside other measurements. Reinforcing bars will interfere with resistivity measurements.

3.3.2.5 Galvanostatic Pulse Technique

It is a rapid non-destructive polarization technique. When steady fixed levels of current are applied and the potential is monitored the measurement is called 'galvanostatic'

pulse technique. The method set-up is shown in **Fig. 3.15.** A short time anodic current pulse is impressed galvanostatically from a counter electrode placed on concrete surface together with a reference electrode of the same type as described in potential mapping. Applied current is normally in the range of 10-100μA and the typical pulse duration is 5-30 seconds. The small anodic current results in change of reinforcement potential which is recorded by means of data logger. Reinforcement is polarized in anodic direction compared to its free corrosion potential.

Galvanostatic pulse method yields better information on corrosion behavior. It can be applied to wet concretes where the problem of low potentials is encountered by potential mapping technique. Together with better reliable qualitative information concerning classification of passive and corroding areas, it gives better quantitative qualification namely the corrosion current (Newton et al., 1988). Under the assumption that the area of polarized reinforcement is known, corrosion current can be converted to corrosion rate.

When the constant current I_{app} is applied to the system, the polarized potential Vt, at a given time can be expressed as

$$Vt = I_{app} [Rp[1-exp(-t/RpC_{dl})] + R_{ohm}] \quad (3.15)$$

Where R_p and R_{ohm} is the ohmic and polarization resistance in ohms.

Corrosion current can be calculated from **Equation 3.11**. It is a better non-destructive method of corrosion monitoring than LPR method which gives lower corrosion rates of steel in concrete due to the inclusion of resistance of concrete in measurement. But there are still many practical difficulties associated with it like interference of electromagnetic influences, stray currents, reliable contacts and electrodes etc.

3.3.2.6 Other Measurements

It is common practice to use temperature sensors in the RC systems. Chloride and pH sensitive electrodes, as well as relative humidity probes have also been used in some installations. However, the stability of the sensors is difficult to guarantee over a period of years, and recalibration is almost impossible.

Fig 3.15: Galvanostatic pulse instrument with probe and concrete sample

(Sathiyanarayanan et al., 2006)

3.4 CORROSION MONITORING – PHYSICAL TECHNIQUES

There are many different physical non-destructive testing (NDT) techniques in use for assessing the condition of concrete structures for corrosion related damages. The techniques are well documented. This section gives a brief summary of the more common physical NDT methods in use and brings out their merits and limitations for civil engineering applications.

3.4.1 Visual Inspection

The visual inspection is the first step in any investigation. It may start out as a casual 'look over' that spots a problem and end up as a rigorous logging of every defect seen on the concrete surface. The aim of the visual survey is to give a first indication of what is wrong and how extensive the damage is. If concrete is spalling off, then that can be used as a measure of extent of damage. In some cases, weighing the amount of spalled concrete with the time can be a direct measure of the deterioration rate. In most cases loose concrete should be removed to avoid safety problems.

Fig. 3.16 shows critical stages of damage in main beams of the span structure in On Dock Elements.

(a) Span T- reinforcement

(b) Cracks on the span beam

(c) Columns with corrosion damage

Fig. 3.16: Critical Stages of corrosion in main beams of a dock structure

(Bjegovic et al., 2009)

3.4.2 Georadar and Covermeter

Experience with practical applications has shown that georadar is suitable only for the location of rebars, which often is a prerequisite for a detailed RC structures inspection. A cover survey requires the location of rebars three dimensionally, i.e. their position with regard to each other and plane of surface and depth of surface. According to Matt (2001), georadar allows the location of reinforcements to a depth of up to 300 mm under favorable conditions, i.e. no congestion of reinforcement. Powerful cover meters are generally capable of detecting reinforcements and tendons at concrete covers of 40- 50 mm provided that light reinforcement is present. Hence, overall, the georadar and cover meter applications have been highly limited to special conditions that may not be the case in the field and have therefore not become popular in the concrete world. They are difficult to use as they are slow and deep covers and closely spaced reinforcements affect the readings. Congestion of rebars gives misleading information. Iron bearing aggregates give misleading readings as they influence the magnetic field. Problems can also arise when the reinforcements are not vertical

or horizontal. **Fig. 3.17** shows the cover meter used for measuring the cover thickness as well diameter and size of the rebar.

Fig. 3.17: Cover meter (www.googleimages.com)

3.4.3 Impact Echo method

Impact echo is a method for non-destructive evaluation of concrete and masonry structures, based on the use of impact generated stress waves that propagate through the structure and are reflected by internal flaws and external surfaces. It can determine the location of flaws such as cracks, delamination, voids, honeycombing and debonding in plain, reinforced and post-tensioned concrete structures. It is not adversely affected by presence of reinforcing bars. Carino (2001) provides an overview of this technique and discusses the important parameters involved in this type of testing.

This method has been under development primarily in the United States since 1983 and can be used to detect grout voids in tendons. Researchers in Europe have verified the applicability of the method in post-tensioned structures. It is a delicate operation requiring skilled personnel. The presence of cracks and other concrete defects as often found in real structures influences significantly the test results and can make the evaluation impossible at times. Intimate contact is required between the impactor and the surface. **Fig. 3.18** shows a typical Impact-Echo system.

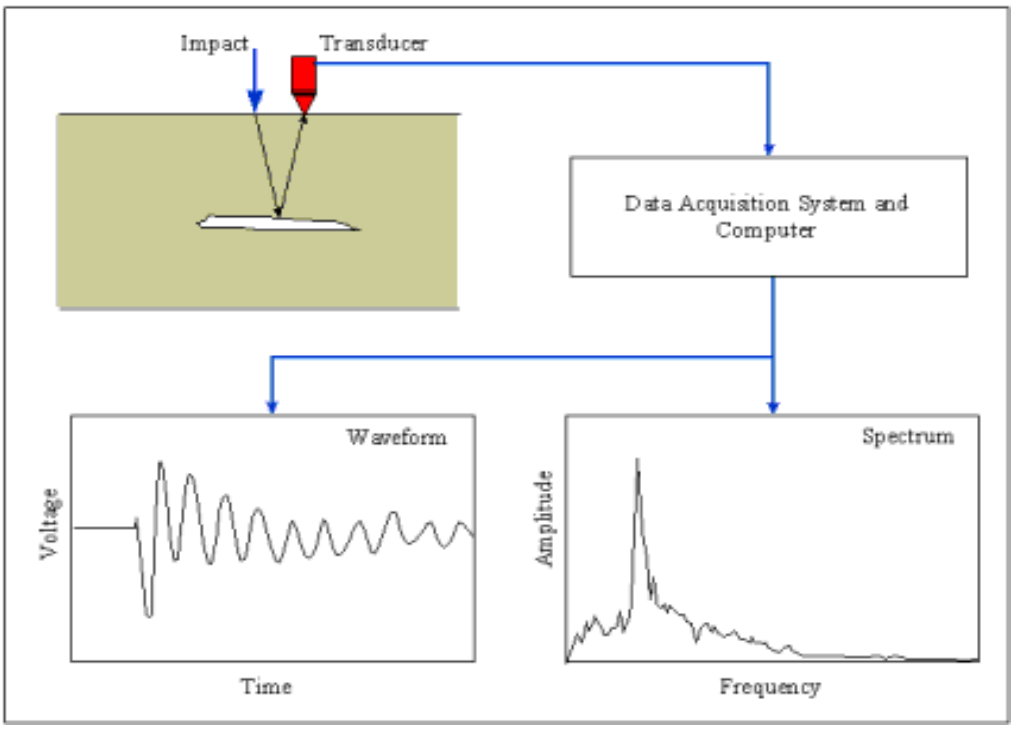

Fig. 3.18: Typical Impact-Echo System (www.googleimages.com)

3.4.4 Remanent Magnetism Method

This method developed in Germany detects fractures in steel. The magnetizing and recording equipment has to be moved along the tendon path on auxiliary guidance rails and scaffolding fixed to the concrete surface in order to measure a magnetic leakage field generated by the formation of magnetic dipole distribution around the fracture area. Fracture patterns have typical signatures that are matched and interpreted by experienced personal or pattern recognition (PR) software. Sometimes magnetic testing methods require the magnetization of the object. Often pulse magnetization proves to be the best technique. The method is suitable to locate fractures of prestressing strands and reinforcing steel bars and to detect real corrosion. It works for concrete covers of up to 18 cm. The major constraint of this method is the difficulty in coping with the disturbing magnetic signals originating from other embedded steel elements such as normal reinforcement, anchorage elements, duct couplers, steel plates, nails, etc (Scheel, 1995).

3.4.5 X-Ray and Gamma Radiography

Radiography uses high frequency electromagnetic radiation in the form of X-rays and gamma rays to gain detailed images of the internal structure of concrete bodies. Despite the highly specialized equipment and safety precautions, radiography produces the most understandable results. The principle behind radiography involves the measurement of attenuation of radiation as it passes through the material under investigation. In this method, a Portable X-Ray Betatron (PXB) is used to produce X-ray beams with an energy level of 7.5 MeV (mega-electron-volt) **(Fig. 3.19)**. With such high energy, the X-rays can penetrate thick concrete and steel, and reveal flaws inside the concrete structure by high-quality X-ray images. The PXB is easy to transport, assemble, operate and maintain. The radiation levels outside the main beam are low.

Fig.3.19: Portable X-Ray Betatron (www.googleimages.com)

The application of radiography is limited nowadays to very special cases. Apart from cost, another important reason for the restricted use of this method is that most countries have regulated the use of X-rays to protect people, animals and environment. Hence, this method holds very special application in detecting corrosion and is rarely used. Also it requires access to the structure from both sides. Multiple layers of reinforcement will be superimposed and may limit interpretation.

3.4.6 Reflectometrical Impulse Measurement Technique (RIMT)

RIMT employs time-domain reflectometry to locate anomalies such as corrosion, breakage in wires or whole tendons in post tensioned bridges as well as in rebars in concrete. It involves the sending of a high-frequency impulse along a bar and allows *in-situ*

measurement of the integrity of reinforcing bars and rock/soil anchors. To perform RIMT measurement, only the rebar ends or anchors need be exposed. Where this is not possible, an electrical connection can be made to the bar nearest to the end in question. Prior to RIMT, the only way to evaluate bonded and unbonded prestressed tendons was to select tendons at random and remove them for visual inspection. This method is both incomplete (only a few tendons are actually examined) and expensive because it requires the destruction and restoration of a part of the structure. Some European researchers who carried out a project aimed at developing an understanding of the fundamentals while applying RIMT to a prestressed concrete structure (Matt, 1991) consider that the recorded signals do not contain information on the condition of the tendon/rebar but are artifacts of the measurement procedure. Thus, Matt disregards it as a complete diagnostic technique for grouted tendons and reinforcing bars in concrete.

3.4.7 Acoustic Monitoring

Corrosion of prestressing wire in prestressed structures and rebars in RC structures including bridges, buildings, parking structures and concrete cylinder pipe is a widespread concern for owners and managers of these facilities. The general inaccessibility of the prestressing wires and rebars makes evaluation difficult, costly and often inconclusive. Random examination of prestressing wires in these structures gives only a much localized knowledge of the prestressing wire condition; conventional investigations can be misleading, resulting often in an underestimation of the extent of corrosion, deterioration or failure. **Fig. 3.20** shows the experimental device of acoustic monitoring measurement.

The operation of a continuous acoustic monitoring system to detect and locate corrosion-induced failures of reinforcing bars has been considered as a favorable alternative in NDT. It can also be successfully applied in practice in equivalent situations. It involves the listening of acoustic events in a structure through permanently attached transducers. The characteristics of the signals can be correlated to identify failure event. Use of many transducers allows the events to be located accurately. Method is limited in use because of difficult data interpretation. Cullington et al. (2001) reported that trials, carried out in Great Britain to assess whether the method can also be used for post tensioned internal bonded tendons, were successful. The authors showed that a single wire fracture can be detected

above the ambient noise level, distinguished from other acoustic events and located in position.

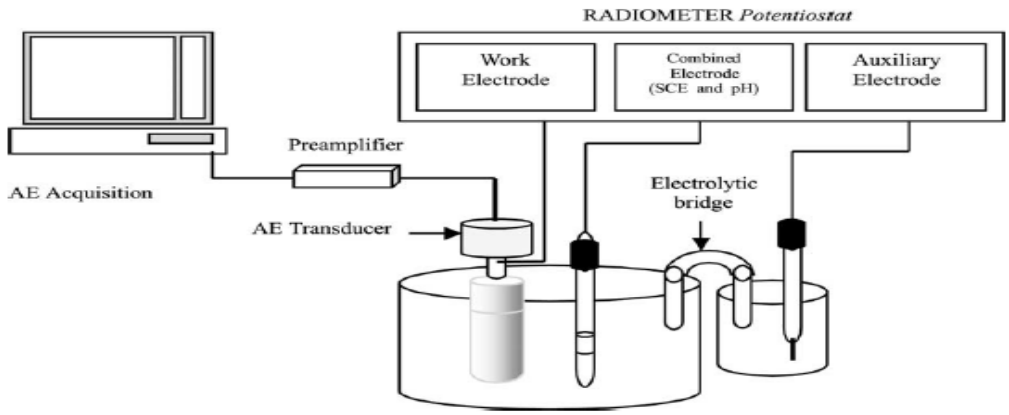

Fig. 3.20: Experimental device for acoustic monitoring measurements (Idrissi et al., 2003)

3.4.8 Thermography (Infrared-Scanning)

All objects naturally emit infrared radiation in proportion to their surface temperature. Thermography measures the emitted radiation and displays the information as a visual image. Today's state-of-the-art equipment can measure radiation from 490,000 points every second and display the information as a TV picture. This can then be recorded for subsequent analysis to provide a permanent record of heat loss and surface temperature. With a temperature range of –30°C to 2000°C and a sensitivity of 0.05°C, there are very few applications beyond the reach of this hi-tech technique. By combining infrared and computer technologies, it is possible to generate thermograms (heat pictures), having up to 256 colors, that clearly show thermal profiles and temperature measurements. A combination of thermography and natural heating/cooling cycle allows areas of delaminated concrete and debonded tendons to be detected. **Fig. 3.21** shows the measurement and result of multi-spectrum camera (Sato, 2001).The advantages of this technique are that it is a remote operation and non-destructive.

3.4.9 Acoustic Tomographic Imaging

Acoustic tomographic imaging of concrete is a developing nondestructive evaluation technology and has a potential to assess the condition of concrete structures (Rens et al.,

2000). Although this technology has been used with great success to image fluid-rich media like biological tissue, the complex behavior of stress waves in solids complicates the imaging of concrete, masonry and other heterogeneous materials such as those used to construct RC structures.

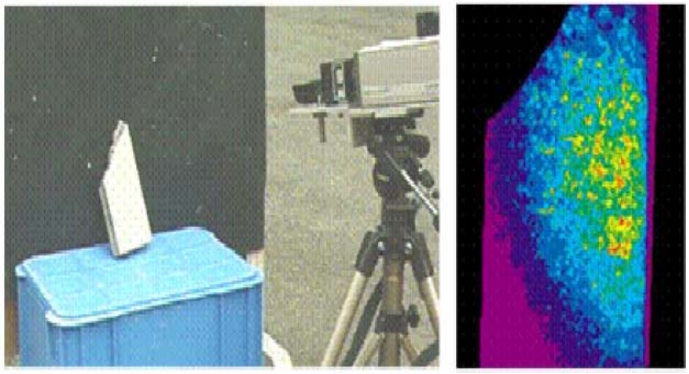

Fig. 3.21: Measurement and result of multi-spectrum camera (Sato, 2001)

3.4.10 GPR (Ground Penetrating Radar)

It is not a standard method as yet for NDT in civil engineering. Research is in progress to fully evaluate the potential of this method. Travel time and amplitude tomography have been applied to stone pillar testing and to geotechnical surveys by using a frequency stepped radar (Valle et al., 1997-1998). However, all applications of this method have experienced the problem of resolution vs. penetration.

3.4.11 Ultrasonic Methods

Ultrasonics is the name given to the study and application of ultrasound, which is the sound of a pitch too high to be detected by the human ear, i.e. of frequencies greater than about 20 kHz. With ultrasonic NDT, which is effectively a mechanical method, periodic mechanical stresses are applied to the object. Ultrasonic testing consists effectively of the propagation of low amplitude waves through a material to measure either or both the time of travel and any change of intensity for a given distance. The use of ultrasound in civil engineering is widespread but is limited to use of bulk waves rather than guided waves. Sound waves travel as a bulk wave in any elastic material where the sound does not interact with edges of material therefore acting as infinite extent of material. The velocity of sound in materials varies with its elastic properties which can be calculated by measuring the time of flight between the two points using the equipment known as Ultrasonic Pulse Velocity

(UPV) Meter. Velocity can be related to a variety of different material properties and conditions and is often used as a test of concrete uniformity, where velocity is usually displayed on a contour map. Large cracks and voids in concrete can be detected by an increase in travel time. Low frequencies of 20-150 kHz are used for testing concrete because shorter wavelengths of higher frequencies would be scattered in concrete. Ultrasound is more often used in pulse transmission rather than pulse echo technique.

Use of guided ultrasonic waves is more complicated than bulk waves and has limited its use in NDT. Guided waves exist in structures that do not behave as an infinite mass of material, and the sound propagation is constrained by one or more material boundaries. Sound propagation is complex and sound travels in a large number of 'modes', which can be determined by the solution of the wave propagation equation. Guided waves are dispersive and the frequency dependence of their properties such as velocity and attenuation must be known so that test results can be accurately interpreted. A major advantage of guided waves is that they propagate in the structure as a whole, and therefore have the potential to inspect the whole structure from a single point. Thus, a guided wave excited at the exposed end of a rebar would be reflected from any defect in the bar, allowing defects to be accurately located.

Ultrasonic wave propagation is beginning to gain popularity among researchers in the detection of corrosion related damage in reinforcing bars. Following section gives a brief account of the same. The embedded reinforcements in concrete can be excited at one end. The bar acts as a waveguide that assists its propagation. The waves leak into concrete and thus attenuate before reaching the receiver at the other end of reinforcement.

3.5 GUIDED WAVES FOR CORROSION MONITORING

As discussed, the existing corrosion monitoring techniques are electrochemical in nature which relates corrosion rate and extent through assessment of surrounding concrete medium and are just indicators of onset of corrosion. They are unable to discern its extent. The size and limited accessibility of civil engineering installations prevent the adoption of many currently used non-destructive testing methods such as radiography, acoustic emission etc. Therefore, it is imperative to develop a non-intrusive technique for early detection of corrosion in steel embedded in concrete.

Towards the development of a non-invasive, in-situ and non-destructive corrosion monitoring methodology, a guided wave approach has been undertaken. Guided waves were chosen because they have the capability of testing over long distances with a sensitivity often greater than conventional non-destructive testing (NDT) techniques, have the ability to test multilayered structures, and are relatively inexpensive due to simplicity and sensor cost (Hay and Rose,2004). Furthermore, frequency and mode tuning can be utilized for evaluation of different types of deterioration or damage. One disadvantage of guided waves for monitoring corrosion in reinforced concrete is the limitation of inspection range for certain modes and frequencies. Unlike guided wave propagation in other multilayered systems, such as a metal pipeline in air, wave energy in steel bars embedded in mortar is lost (i.e. attenuated) at high rates due to leakage into the surrounding concrete. Generally, modes exist that have attenuation minima, or dips, with minimal amounts of wave energy lost due to leakage and material absorption. However, once corrosion begins to occur, the corrosion product accumulation will actually cause an increase in bond and subsequently lead to more energy leaking into the surrounding concrete. Irregularities in the bar profile surface from corrosion can cause more attenuation from reflections, scattering and mode convesions.

Till date, the use of guided waves for continuous monitoring of actual corroding reinforced concrete specimens has not been reported. This section provides a brief overview of previous research pertaining to guided waves used to monitor reinforced concrete (or mortar/grout). While not all of the research reported focused specifically on monitoring corrosion, the test results are relevant due to the similarity in damage mechanisms. However, inducing corrosion quickly to develop a monitoring technique in a controlled manner is challenging. Hence, most of the researchers have concentrated only on simulated corrosion studies. Studies have been conducted to assess the bond level between steel and concrete, attenuation from the surrounding concrete, and the effects of loading conditions and other interfaces such as corrosion products, anchorage (i.e. stirrups) and ribs.

3.5. 1 Bond Assessment

Wu et al. (2006) created a set of reinforced concrete beam specimens with various bond levels and tested using guided waves at lower frequencies. The diameter of the steel rebar was 19.05 mm and the specimen size was 10.16 cm × 10.16 cm × 50.8 cm. Transducers were attached to the steel rebar via silver epoxy in a through transmission arrangement and

then embedded into the concrete. The transducers were spaced 40.64 cm apart. Specimens simulating 0%, 6.25%, 12.5%, 25% and 50% debonding were created. Bond was inhibited between the steel and concrete by surrounding the rebar with a PVC pipe for the necessary length prior to embedment. Longitudinal modes were invoked using 5-cycle tone bursts, primarily around 90 kHz. The results indicated that the received waveform is less attenuated as the amount of debonding increased. However, there was no significant change in the waveform arrival time reported.

He et al., (2006) created a set of reinforced concrete cylinder specimens with various bond levels and tested using guided waves at higher frequencies. The diameters of the steel rebar and concrete cylinder were 19.05 mm and 10.16 cm, respectively. The reinforced concrete specimen was 0.914 m long. Frequencies were tested between 1 and 2 MHz using tone burst excitations. The transducer was attached to the exposed end of the rebar in a pulse-echo arrangement. Specimens simulating 0%, 25%, 33%, 50%, 75% and 100% debonding were created. Bond was inhibited between the steel and concrete by surrounding the rebar with high-density polyethylene for the necessary length prior to embedment. The results indicated that the received waveform is less attenuated as the amount of debonding increased for all frequencies. However, the lowest frequencies tested showed more sensitivity to the change in bond.

Na et al., (2002) created a set of reinforced concrete beam specimens with various bond levels and tested using guided waves at low and high frequencies. The diameter of the steel bar was 22.86 mm and the specimen size was 12.7 cm × 12.7 cm × 60.96 cm. Frequencies were tested at 1 MHz (flexural) and 150 kHz (longitudinal) using tone burst excitations. Transducers were attached to the exposed ends of the rebar, set up in a through-transmission arrangement. Specimens simulating 0%, 25%, 50% and 75% debonding were created. Bond was inhibited between the steel and concrete by surrounding the rebar with a PVC pipe for the necessary length prior to embedment. The results of lower and higher frequencies indicated that the received waveform is less attenuated as the amount of debonding increased. Specimens were tested with lengths of debonding in different locations along the bar. The results indicated that the location was not discernible.

In other words, the amount of bond loss, rather than the location, was the critical factor in determining the guided wave characteristics.

3.5.2 Corrosion Products

Gaydecki et al., (1992) embedded a 7 mm steel wire into a concrete mix with a 4% calcium chloride solution added to induce corrosion. The reinforced concrete specimen was cylindrical, with an outer diameter of 150 mm and a length of 1 m. The steel wire was exposed on either end of the concrete to allow for transducer coupling. After the concrete had initially cured, a transducer with a 200 kHz resonance was used to invoke a longitudinal wave (single cycle pulse). Six months later, after slight corrosion had occurred (confirmed after breaking open), another wave was sent into the specimen. The higher frequency content was most affected (i.e. loss in signal strength) by the corrosion product accumulation. This was attributed to the corrosion pressure creating better acoustic coupling at the interface between the steel and concrete, thereby allowing more energy leakage.

Miller et al., (2002) corroded rebar specimens to different levels using impressed current and then embedded the bars into concrete. The diameter of the steel rebar was 22.23 mm and the specimen size was 12.7 cm× 12.7 cm × 60.96 cm. Tone burst pulses were invoked at 1 MHz. The results indicate that the wave is more attenuated as the corrosion level increases. This was attributed to better bonding between the corroded steel surface and concrete, allowing more energy leakage.

3.5.3 Attenuation Measurement

Beard (2002) embedded different diameter plain steel bars, 0.33 m in length, into grout. The grout size was 0.1 m × 0.1 m × 0.3 m. The embedment length was short enough so that multiple reflections from the end of the bar could be detected and compared to each other for attenuation measurements. Multiple frequencies were invoked for the different bar diameters using a 100-cycle tone burst. All modes of propagation were longitudinal. It was assumed that losses from reflections off of the back wall of the steel bar were less than ±5%. The predicted values for attenuation were used to normalize the measured values. In every case, the predicted values overestimate the amount of attenuation.

In fact, the measured attenuation values were closer to the predicted attenuation values for a free bar. The difference in predicted and measured attenuation values was attributed to two main factors. The first is that the material damping constants are most likely imprecise due to the difficulty in accurate measurements. The second factor is that the

interface conditions between the steel and grout are not completely known (i.e. the bond is most likely less than perfect). It was concluded that the predicted attenuation measurements were not completely reliable and should be used as an upper bound for determining maximum inspection ranges.

3.5. 4 Anchors

Na et al., (2002) tested reinforced concrete specimens with and without stirrups surrounding the reinforcing bars. Using tone burst excitations, tested frequencies were 1 MHz and 150 kHz for flexural and longitudinal waves, respectively. Transducers were attached to the exposed ends of the rebar, set up in a through-transmission arrangement. It was concluded that specimens without stirrups had stronger waveform amplitudes than specimens with stirrups.

3.5.5 Ribs

Beard tested a smooth bar and a rock bolt to examine whether the surface features affected wave propagation (Beard, 2002). The rock bolt tested had threads and mixing ribs along segments of the 2.4 m length. The smooth bar tested was 1.8 m in length. Both bars had a diameter of 20 mm and were excited with a 10-cycle Gaussian-windowed tone burst at 50 kHz. There were no reflections from surface features and the wave amplitude was relatively unaffected. The results indicated that wave propagation is largely unaffected by the presence of surface features when the ratio of the wavelength to the surface feature dimensions is large.

Miller et al., (2002) described strong scattering effects for longitudinal modes (>600 kHz) propagating in rebar, 22.2 mm in diameter. There was particular sensitivity to diagonal rib patterns compared to an orthogonal axi-symmetric rib pattern. Similar filtering of frequency ranges has been studied for guided waves in plates with corrugated patterns (Kundu et al., 2006). Frequency ranges that were filtered out were referred to as stop bands, while frequencies that still effectively propagated in the corrugated plate were referred to as pass bands.

3.5.6 Loading Effects

Wu et al. (2006) investigated what effect loading the rebar would have on the guided wave characteristics. The diameter of the rebar was 19.05 mm and the length was 66.04 cm. A tapered notch was created in the middle of the bar length to ensure that yielding would occur at that location. The transducers were attached to the sides of the rebar in a through-transmission setup. There was spacing between the transducers of 40.64 cm. Longitudinal modes were invoked using 5-cycle tone bursts, primarily around 90 kHz. The results indicate that the applied load does not affect the wave amplitude for the frequency range and mode tested. However, the time of arrival of the waveforms did change once yielding occurred due to the rapid increase in length.

The authors also investigated how guided wave characteristics are affected by bending. The reinforced concrete specimen was subjected to a four-point bending test while monitored with guided waves. The diameter of the rebar was 12.7 mm and the specimen size was 10.16 cm × 10.16 cm × 60.96 cm. The transducers were attached to the sides of the rebar in a through-transmission setup. There was spacing between the transducers of 40.64 cm. Longitudinal modes were invoked using 5-cycle tone bursts, primarily around 90 kHz. The four-point bending test created a crack that was perpendicular to the axis of the reinforced mortar specimen in the tension zone. The crack extended up towards the neutral axis during the test. The results indicate that as the applied loads and cracking of the surrounding concrete matrix increased, the amplitude of the waveform increased.

3.5.7 Accelerated Corrosion Studies

Reis et al. (2005) used fundamental flexural mode at 250 kHz for estimation of corrosion damage in steel reinforced mortar. Debond defects were simulated by wrapping a tape around the rebar. Waveform energy indicative of the attenuation was used to relate to corrosion damage and the loss of bond between steel and surrounding concrete could be detected and evaluated. Ervin et al. (2008, 2009) used both low (<200 kHz) and high (2-9 MHz) guided longitudinal modes to monitor corrosion damage in reinforced mortar specimens. The beams, after subjecting them to accelerated corrosion were monitored ultrasonically. It was found that some modes were sensitive to the combined effect of bond deterioration and mortar stiffness reduction while some other modes related well to change in

crossectional area.

Thus, there is ample evidence that corrosion could be detected by ultrasonics. But most of the researchers have simulated corrosion as delaminated reinforcing bars (Wu et al., 2006; He et al., 2006; Na et al., 2002; Miller et al., 2002; Reis et al., 2005). It is widely conjectured that debond impedes leakage of waves into concrete. Thus, higher signal strength at the receiving end indicates debond and corrosion. It has been validated by introducing debond in the form of PVC pipes (Wu et al., 2006). Other effects such as loading conditions (Wu et al., 2006), reinforcing ribs (Na et al., 2002; Miller et al., 2002, Beard , 2002), corrosion products (Beard, 2002; Gaydecki et al., 1992) and anchorages (Na et al., 2002) on the guided waves have been reported.

But limited experimental evidence exists on utilizing ultrasonics for real time corrosion monitoring in beams undergoing corrosion. Also, mechanism and progression of corrosion in the absence and presence of chlorides is different. Prognosis of these two types of corrosion would be vastly different. The manifestation of corrosion in oxide and chloride environments is in the formation of these corrosion products on the surface of the rebar. Thus, the steel-concrete interface is altered where rust is formed. The resulting corrosion products and accompanying processes of cracking, spalling and delamination of concrete occurring in both types of corrosion are similar but the rate and the mode of occurrence of various aspects of corrosion are different in the two cases. Debond is common in oxide corrosion whereas in chloride corrosion, distinguishing feature is pitting where crevices are formed in the bar leading to local loss of material. Thus, in addition to debond, any corrosion monitoring methodology should also identify local weakening and loss of strength and ductility of the bar. This thesis is an attempt to develop a complete corrosion monitoring methodology using ultrasonic guided waves. Also, a non-destructive technique that is able to discern these two modes of corrosion will be of great benefit.

3.6 CLOSING REMARKS

All the traditional techniques of corrosion monitoring of steel as described are either electrochemical in nature or typically fail or encounter problems when applied for in- situ damage monitoring of steel embedded in concrete. They give an idea only about the initiation of corrosion but the quantification of corrosion remains a vital issue. There is

difficulty in interpreting the results in half cell potential methods. Further, in preview of RC systems, a number of probes have to be installed before the system can be effectively utilized. Also, the infrastructure involved in measurement is bulky. Besides, the measured electrochemical potentials are affected by a number of factors like the quality of concrete, relative humidity, cover of concrete and its contamination by chlorides or carbonation etc.

Similarly non-destructive techniques for condition monitoring of steel, as recommended by various researchers and as described have specific applications only. They are either too expensive or require the use of highly skilled personnel and suffer from practical applications like in radiography, thermography and acoustic tomography. So the measurement of state of reinforcement in concrete structures needs a method which can determine simply, accurately, and non-destructively not only whether or not deterioration of reinforcement is taking place but also the extent of damage and its characterization.

Hence, it is recommended to use ultrasonic guided waves as a non-destructive corrosion monitoring technique in embedded reinforcements. They have the capability of testing over large distances than the conventional non-destructive testing techniques, can be used for multilayered systems as in RC structures and are relatively inexpensive. The ultrasonic investigation of corroded RC beams has mainly remained confined to simulated studies. Effect of corrosion has primarily been viewed as loss of interfacial bond. Limited experimental evidence of actually corroded RC specimens indicates that in addition to loss of bond, loss of cross-sectional area of bars has also significant influence. In this work, both simulated and actually corroded bars have been investigated using ultrasonic guided waves. The following two chapters give a detailed account of the experimental investigations utilizing guided waves for monitoring simulated and actually corroding RC beam specimens.

CHAPTER 4

BARS AND BEAMS WITH SIMULATED CORROSION

4.1 INTRODUCTION

Corrosion of steel reinforcements results in the deterioration of reinforcing bars in concrete which is one of the major causes of catastrophic failures in reinforced concrete structures such as bridges, dams and buildings. It is essential to develop a reliable and non-invasive corrosion monitoring technique for embedded reinforcements in concrete. In this work, ultrasonic guided waves have been explored as a possible solution for the same. Embedded reinforcements in concrete can be excited at one end and received at the same or the opposite end. The bar will act as a waveguide and assists its propagation. The waves leak into concrete and thus attenuate before reaching the receiver at the other end of reinforcement. Also the ultrasonic waves are partially reflected back from the defects. The defect location is estimated from the time taken by the wave to travel. The technique was attempted experimentally by Weight (1994) and then theoretically by Pavlakovic (1998). It is observed that for steel bars in air the attenuation is primarily due to material scattering and absorption (Alleyne et al., 1997, 1998). When the bars are embedded in concrete, both longitudinal and shear waves leak into the surrounding concrete (Bernard et al., 2000) and the lack of leakage can indicate delamination between concrete and the bars.

For bars in concrete, it is important to identify the modes and frequency ranges for ultrasonic monitoring. Wave in a bar in concrete becomes a dispersive guided wave and the calculation of dispersion curves for systems with an arbitrary number of layers has been made much easier with the development of Disperse (Pavlakovic et al., 2000), a general purpose program for tracing dispersion curves. The software allows the modeling of elastic isotropic materials (with or without material damping), transversely isotropic materials, spring boundaries and fluids. Dispersion curves can be calculated in both Cartesian and cylindrical co-ordinates, and the solution method is valid for all mode types. The inclusion of multi-layered cylindrical embedded systems is a recent addition to the software (Pavlakovic et al., 2001) allowing leakage from a bar into an embedding material to be considered.

The ultrasonic investigation of RC beams for corrosion related damages has mainly

remained confined to simulated specimens. As discussed in **Section 3.4**, most of the researchers have simulated corrosion as delaminated reinforcing bars. Effect of corrosion has primarily been viewed as loss of interfacial bond. Limited experimental evidence of actually corroded RC specimens indicates that in addition to loss of bond, loss of cross-sectional area of bars has also significant influence (Ervin et al., 2008 and Ervin et al., 2009)

In this chapter, ultrasonic wave propagation through the reinforcing bars in air is first studied and then extended to bars embedded in concrete. The investigations for bars embedded in concrete are carried out by simulating corrosion. The simulation of corrosion is carried out in two ways- loss of area (analogous to pitting) and loss of bond (analogous to debonding of the bar). The embedded bars are seeded with a range of simulated notches and debond defects in the varying percentages of area reduction and delamination respectively. Conventional techniques of pulse echo and pulse transmission are used in combination to predict the presence, location and magnitude of the defects.

4.2 BARS IN AIR

This section investigates the ultrasonic guided wave propagation in reinforcing bars in air. The bars are seeded with damages in the form of notches in varying percentages of area reduction at a particular location simulating cross section loss (pitting effect) due to corrosion. Ultrasonic testing is done in both pulse echo and pulse transmission modes. Plain mild steel bars of 12 mm and 25 mm diameter are used in the present investigation.

4.2.1 Selection of Excitation Mode

For ultrasonic testing of the bars in air, first step is to select the ideal frequency and mode of testing. As discussed, in an infinite bulk of a perfectly elastic material, ultrasonic waves travel as bulk waves in the form of compressional and shear waves. Both the waves propagate with constant velocities. They are non-dispersive and decay in amplitude because of the spread of the wave front. But in a finite perfectly elastic media like a reinforcing bar, the ultrasonic wave is reflected from its boundaries, and the energy is contained within the bar as a guided wave. The velocity-frequency relationships of guided waves are displayed as dispersion curves. A global matrix method is employed for solution of wave propagation equation using optimization techniques (Lowe, 1995). The method was then developed into a

standard software Disperse (Lowe, 1995; Pavlakovic and Cawley, 2000).

For a cylindrical system, waves propagate in three modes due to dispersive effect of boundaries i.e longitudinal (L), flexural (F) and torsional (T) modes. Longitudinal waveforms have axial and radial displacements but no angular displacements. In order to produce a strong longitudinal wave, a compressional transducer must be placed parallel to axis of the bar. Non-axi-symmetric flexural waves exhibit high attenuation and are produced by placing the transducers normal to the bar. Torsional waveforms have only angular displacements and no radial or axial displacements. To produce a torsional wave, a couple must be created on the circumference of the guiding configuration which is practically difficult to achieve. Hence, longitudinal wave which is easiet to invoke and is least attenuative is chosen for excitation. In the present work, two steel bars of 12 mm and 25 mm diameters with the material properties shown in **Table 4.1** are chosen.

The different longitudinal modes at the ends of the bar are excited by varying the excitation frequencies. The selection of frequencies is done based on the phase velocity dispersion curves **(Fig. 4.1(a))**. They are validated by experimentally confirming the signal fidelity. High frequency low attenuative modes are found to be the best. Phase velocity dispersion curves for 12 mm in air show the fundamental L (0, 1) mode starting at zero frequency with each higher order mode starting from a higher cut off frequency. Each of the higher modes shows a plateau region around the steel longitudinal bulk velocity line.

This becomes more predominant for higher modes and corresponds to the points of maximum energy velocity **(Fig. 4.1(b))** and minimum attenuation **(Fig. 4.1(c))** (Pavlakovic et al., 2001). In these regions, phase velocity is almost equal to longitudinal bulk velocity and longitudinal partial wave is almost parallel to the bar axis. Amplitude of longitudinal partial wave is also much greater than the amplitude of shear partial wave. Hence, the wave propagates with short apparent path length through the material, resulting in less attenuation.

Therefore, a higher order mode L (0, 11) at 3.5 MHz with minimal attenuation and maximum energy velocity is chosen for testing 12 mm bars in air. High signal output is also observed at this frequency experimentally. The group velocity as obtained from dispersion curve at this frequency is 5.52 km/s. Similarly, for 25 mm bar in air, 1 MHz frequency and L (0, 6) mode is chosen due to high energy velocity and minimum attenuation. The group velocity as obtained from dispersion curve at this frequency is 5.33 km/s. The velocities in

the two modes chosen for 12 mm and 25 mm bars are close to the longitudinal bulk velocity of steel.

Table 4.1: Material Properties of steel used for modeling in Disperse (Pavlakovic et al., 2000)

SNo.	Material Property (Extruded Steel)	Value
1.	Modulus, E (GPa)	210
2.	Density(ρ),(kg/m^3)	7932
3.	Longitudinal Attenuation (np /wl)	0.003
4.	Shear Attenuation (np/wl)	0.008
5.	Longitudinal Velocity (m/s)	5960
6.	Shear Velocity (m/s)	3260
7.	Poisson's Ratio	0.2865

4.2.2 Experimental Set-Up and Details

For exciting longitudinal guided waves in the bars in air, a typical ultrasonic testing system (UT) is used. It consists of a pulser/receiver (DPR 300, JSR Make), transducers (Karl Deutsch Make), and display devices. Driven by the pulser, the compressional transducer generates ultrasonic pulse that propagates through the bar in the form of longitudinal waves. Ultrasonic testing of the bar in air is done in both Pulse Echo and Pulse Transmission modes.

Pulse Echo (P/E) testing is done on the bars in air for damage detection, localization and quantification. When there is an interface such as a crack, void or flaw in the wave path, part of the energy is reflected back from the interface and received by the same transmitting transducer. The reflected energy is converted into an electrical signal which is processed in a computer and digitized for display.

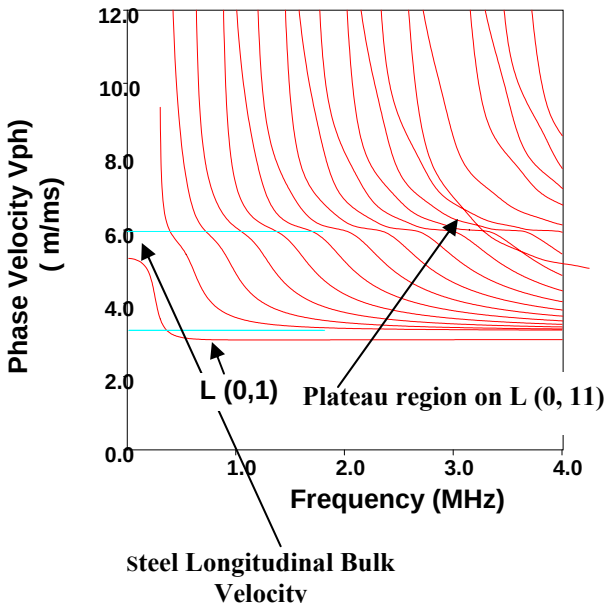

(a)Phase Velocity Dispersion Curve

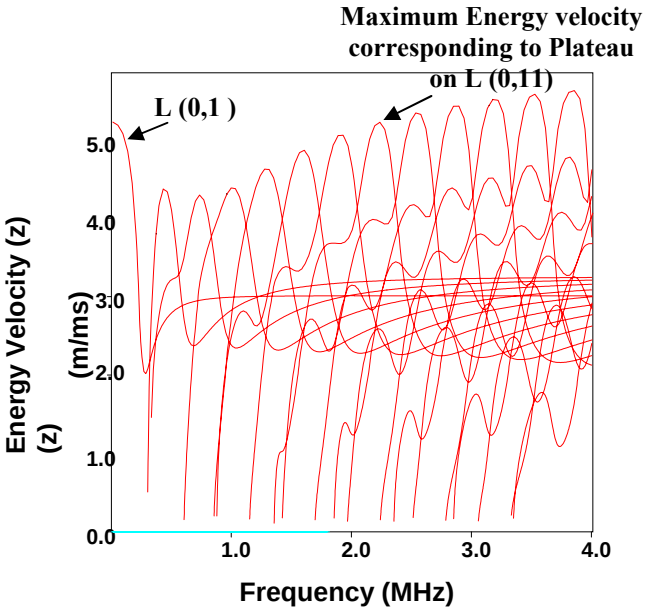

(b) Energy Velocity Dispersion Curve

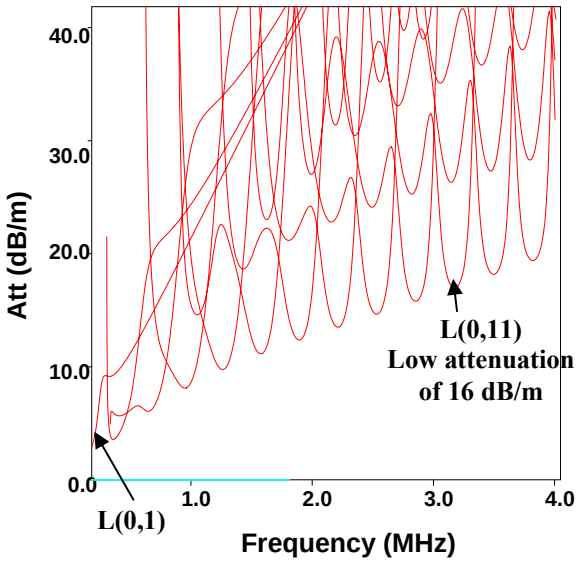

(c) Attenuation Dispersion Curve

Fig. 4.1: Dispersion Curves for 12 mm diameter bar in air (Pavlakovic et al., 2000)

From the display, the time of flight between the excitation and reflected pulse is measured. Knowing the group velocity of the excited longitudinal wave mode, the location of the defect is calculated as follows:

$$D = \frac{Vt}{2} \tag{4.1}$$

Where D = Distance of defect from transducer end, V = Group Velocity of excited mode and t = Time of Flight

In addition to this, testing is also done in Pulse Transmission (P/T) mode in which an ultrasonic transmitter introduces the wave from one end of the bar and a receiver is placed at the opposite end to record the transmitted pulse. By measuring the relative change of the amplitudes of the input and the received signals, the relative severity of the flaw is assessed.

A single contact transducer is used to generate and receive wave signatures in the Pulse-Echo method. Two contact transducers are used for sending and receiving the waveforms in pulse transmission method. Transducers ACCUSCAN "S" series having a longer wave form duration and a relatively narrow frequency bandwidth with center frequency of 3.5 MHz is used for the 12 mm bars and 1MHz frequency is used for 25 mm diameter bars. The transducers are driven by a Pulser/Receiver system with a particular gain (0-66dB) and maximum input voltage of 475V. A computer with a digitizer card (Acquiris Make- 12 Bit Resolution) is used to capture the received signal and its processing. The transducer is mounted in a holder and attached to the specimens using an industrial coupling gel **(Fig 4.2).** The excitation signal consists of a compressive spike pulse with duration ranging from 10-70 ns.

Damages are introduced in the form of notches at a particular location of the bar with 0%, 20%, 40% and 60% diameter reduction **(Fig 4.3)** simulating area loss due to corrosion. The damage is symmetrically induced to minimize experimental complications.

The location of the damage is also varied along the length of the bar as L/2, 2L/3 & L/3 where L is the length of the bar. Extruded mild steel bars of 12 mm diameter and variable lengths are used in the experiments.

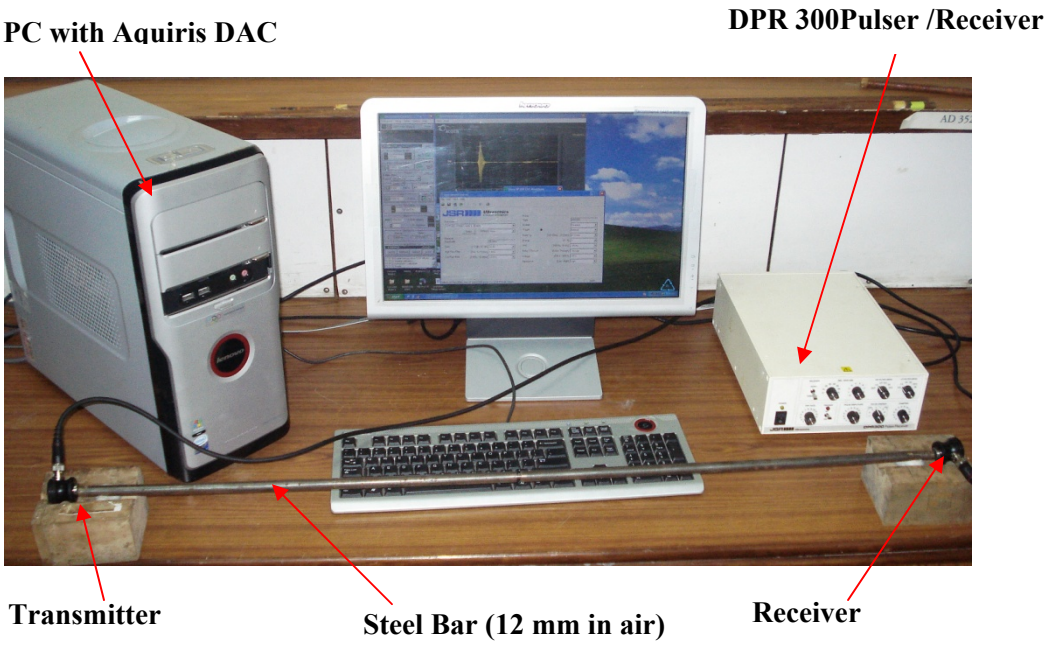

Fig. 4.2: Experimental Set up (Pulse transmission arrangement)

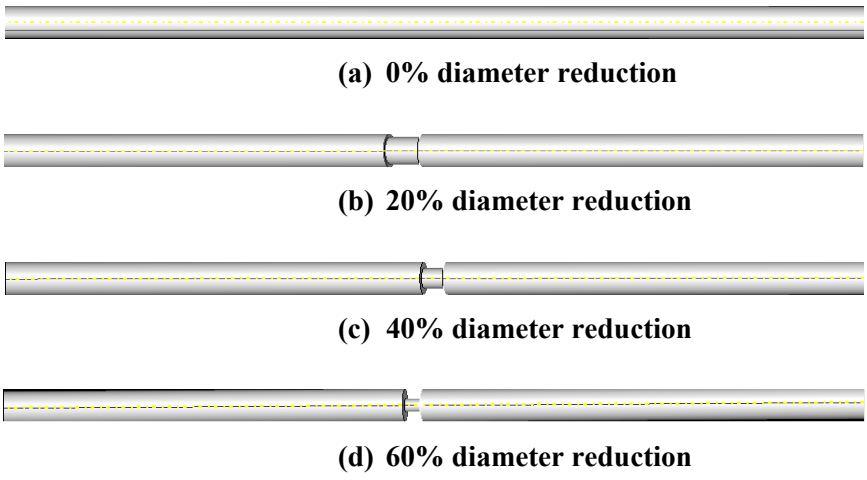

Fig. 4.3: Simulation of area reduction in steel bars with (a) 0%, (b) 20%, (c) 40% and (d) 60% diameter reduction at the centre

Three sets of specimens of 1 m, 1.5 m and 2 m length are fabricated. Two samples of each specimen are tested to examine the repeatability and precision of results. **Fig 4.4** defines the outline of the parametric study done. The results are reported in the form of voltage

amplitude-time signatures (V-t).The voltage time histories of the reflected (Pulse Echo) and transmitted waves (Pulse Transmission) are plotted.

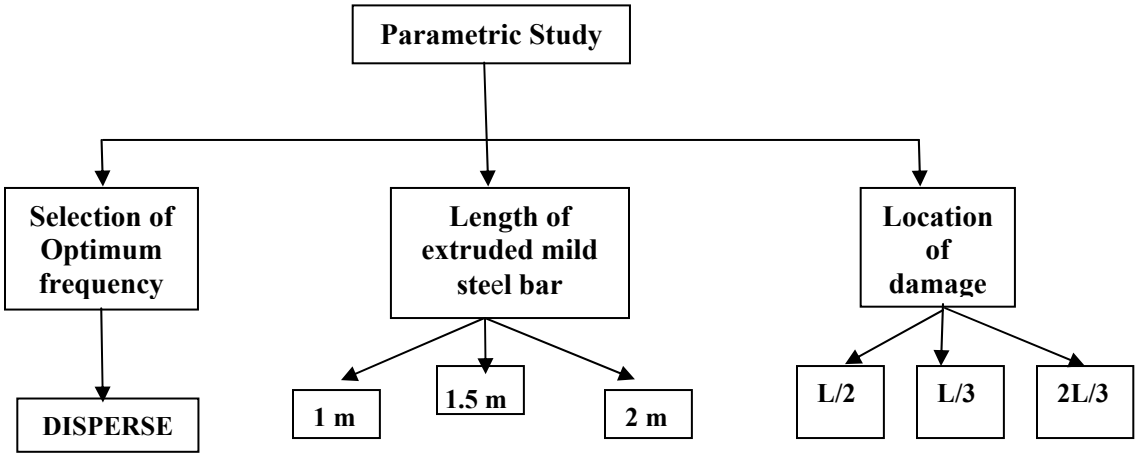

Fig. 4.4: Parametric study for damage detection in bars in air

4.2.3 Results and Discussions

4.2.3.1 Pulse Echo testing

In the pulse echo method of testing, experimentally two reflections are obtained –one from the notch (referred to as Notch Echo, NE) and another from the back wall (referred to as Back Wall Echo, BWE). In a healthy specimen, the peak obtained is only the BWE **(Fig 4. 5 a)**. **Fig 4.6(a)** shows a typical healthy bar signature. In a notched specimen (Notch at L/2), the 1st peak is NE and the 2nd peak is the BWE (**Fig 4.5 b). Fig 4.6 (b-d)** shows the typical pulse echo signatures obtained for 1 m notched bars with notch at the centre**.**

Appearance of a NE indicates the presence of defect in the bar. By knowing the time point of this echo, location of damage can be computed from **Equation 4.1**. Comparing the peak-peak voltage ratio amplitudes of NE's and BWE's with reference to the input pulse, extent of damage can also be estimated.

Hence, it may be noted that it is fairly simple to identify a defect in the pulse echo technique. Appearance of a peak between the initial pulse and BWE in pulse echo indicates the presence of damage or defect in the bar specimen **(Fig 4.6).** Once the damage is detected, its location must be ascertained. From the time of flight of NE, the exact location of the notch can be obtained.

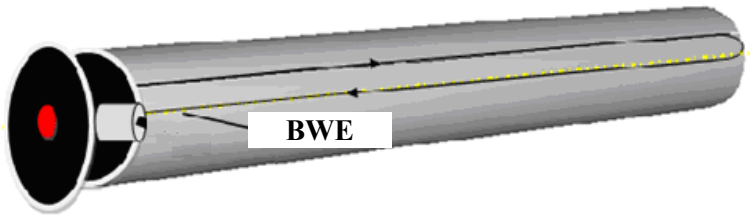

(a) Healthy bar

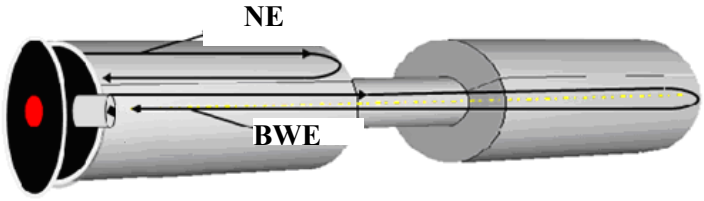

(b) Notched bar (Notch at L/2)

Fig. 4.5: Pulse Echo (P/E) peaks

After ascertaining the presence and location of damage, the next step is to evaluate its extent. The magnitude of damage can be directly related to the magnitude of the peak received after reflection from the notch (NE) as well as BWE. The amplitude of NE increased and that of BWE reduced with the increase in the notch dimensions **(Fig 4.6).** As the depth of the notch increases more energy is reflected back from it and less of it travels to the back wall. This is evident from experimental results. Hence, pulse echo can be effectively used for damage detection in bars. It not only indicates the presence of damage but also gives its exact location and extent.

Testing is extended in pulse echo mode to different lengths of the bar (1m, 1.5m & 2m) with notch at centre. **Table 4.2** shows the comparison of time of flights of NE's in notched specimens obtained experimentally for different lengths of the bar with notch at the centre. It may be noted that for 1m, 1.5m and 2 m lengths of the bars, the times of flights are in close agreement. Pulse echo signatures are also taken by varying the location of the notch from L/2 to L/3 and then to 2L/3 with 0%, 20%, 40% and 60% diameter reductions at respective locations.

Table 4.3 shows the peak to peak ratios of amplitudes with respect to initial pulse in healthy and notched specimens obtained experimentally for all lengths of the bars with notch at the centre. **Fig. 4.7** shows the plotted results for the same. As discussed, the amplitude of NE increased and that of BWE reduced as the percentage diameter of the notch increased for

all the lengths of the bars with notch at the centre. An idea about the extent of the damage can be obtained by relatively comparing the amplitudes of the NE's and BWE's with respect to initial pulse as well as with increasing notch dimensions. Another observation is that with the increase in length of the bar, the amplitudes of the received signals follow a decreasing trend. This is because signal attenuation due to material scattering and absorption increases as the length of the bar increases.

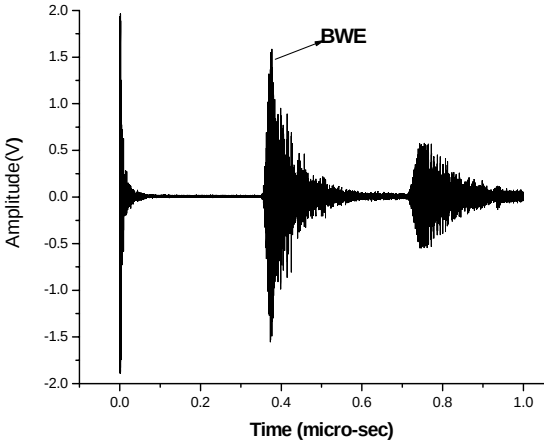

(a) Healthy bar

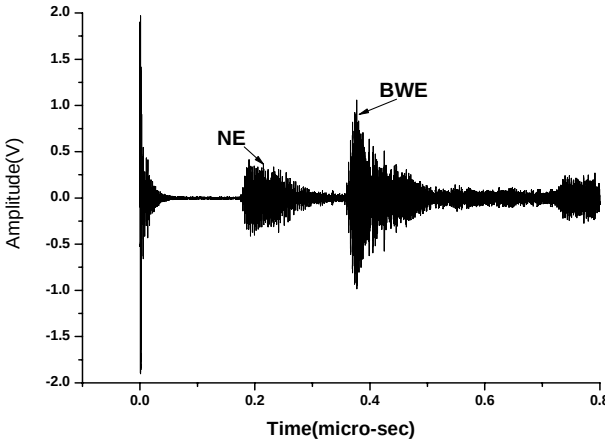

(b) 20% Diameter Reduction

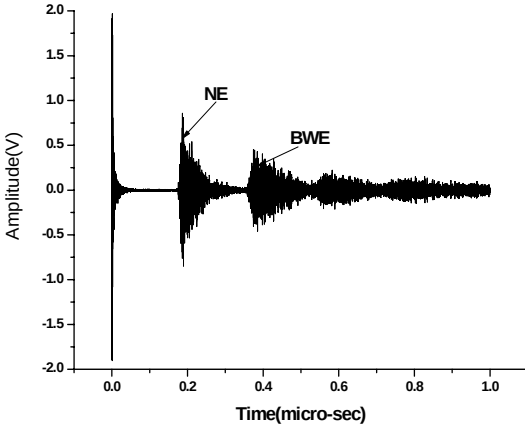

(c) 40% Diameter Reduction

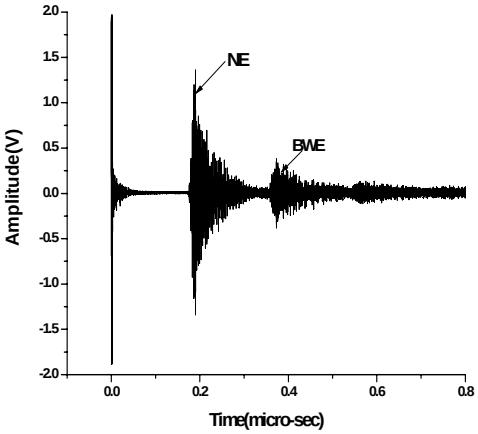

(d) 60% Diameter Reduction

Fig. 4.6 (a-d): Pulse Echo signatures of 12 mm diameter, 1m bar (Notch at L/2)

Table 4.2: Comparison of time of flight of NE in Pulse Echo

Fault Location-L/2	**Time* (μsec)**
Notched specimen	
1 m bar	1.79 – 1.81**
1.5 m bar	2.69-2.71**
2 m bar	3.6-3.62**
Fault location –L/3	
Notched specimen	2.1- 2.16**
Fault location –2L/3	
Notched specimen	2.49-2.5**

***Phase Velocity of L (0, 11) mode = 5520 m/s,**

**** Range of values for different % of defect**

Table 4.3: Peak to peak voltage ratios* in Pulse Echo

Diameter Reduction (%)	**NE**			**BWE**		
	1m	**1.5m**	**2m**	**1m**	**1.5m**	**2m**
0	0	0	0	0.83	0.34	0.22
20	0.207	0.1	0.04	0.53	0.31	0.16
40	0.43	0.318	0.22	0.24	0.159	0.15
60	0.7	0.612	0.371	0.2	0.119	0.08

*** Peak to peak voltage ratios are calculated with respect to voltage amplitude of initial pulse**

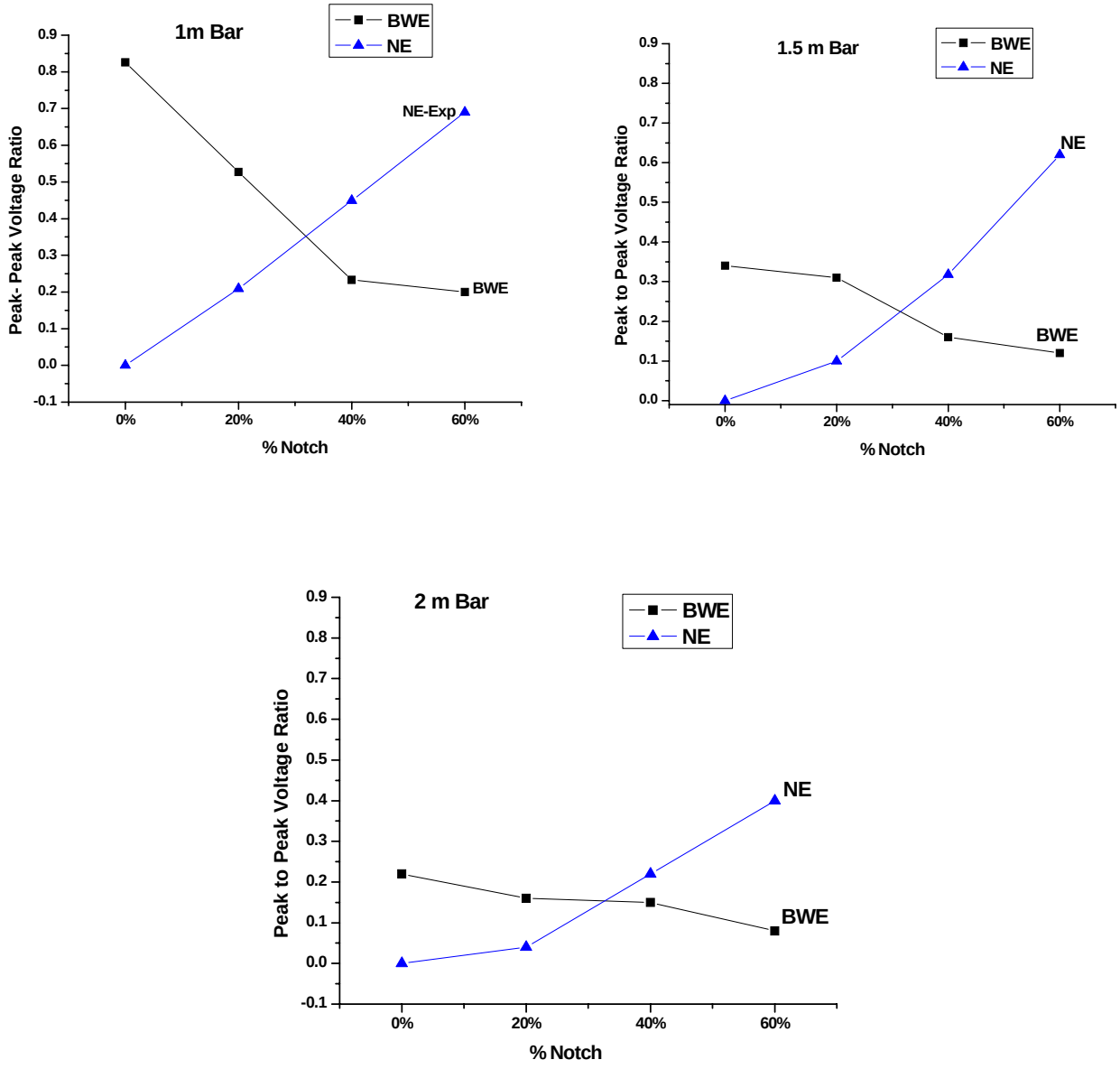

Fig. 4.7: Peak to peak voltage ratio trends of P/E of 12mm diameter bar (1m, 1.5m, 2.0 m) (Notch at L/2)

4.2.3.2 Pulse Transmission testing

In Pulse Transmission (P/T) method of testing, signals are recorded by placing the emitting and receiving transducers at opposite ends of the bars. In a healthy specimen, peaks are obtained after traveling 'L' (P/T-1) and '3L' (P/T-3) distances as transmitted pulses at the receiving end **(Fig 4.8 a, 4.9 a)**. In the notched specimens, a peak appears between the

two peaks. This is due to reflection from the notch (P/T-2) **(Fig 4.8 b). Fig 4.9 (b-d)** shows the pulse transmission signatures of the notched bars with notch at the centre. Therefore, the peak due to the notch should appear in the middle of L and 3L peaks of the healthy bar. The peak is not clearly observed at 20% notch. However, the peak rose considerably with higher depths of notches. When one compares these results with pulse echo results, the NE is very clearly visible at the lowest depth of notch. Hence, pulse echo is a better indicator of the presence of the notch rather than pulse transmission technique.

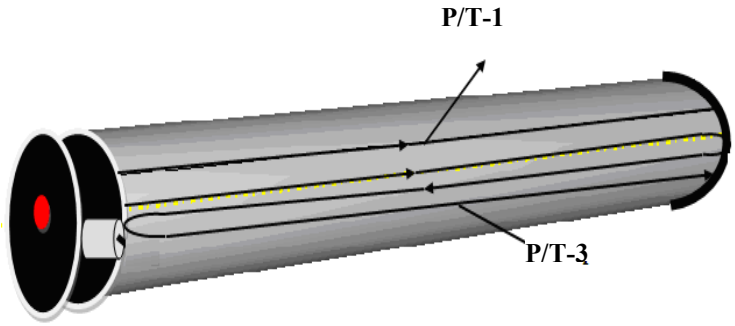

(a) Healthy bar

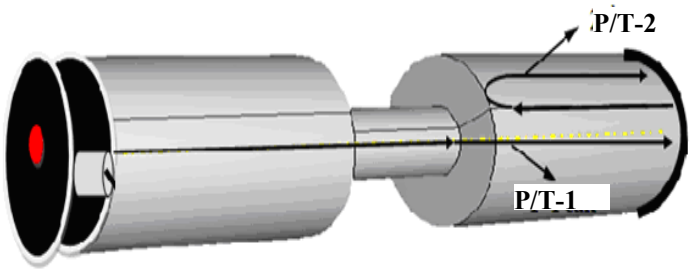

(b) Notched bar

Fig. 4.8: Pulse Transmission (P/T) peaks

Table 4.4 shows the comparison of time of receipt of first peak (P/T-1) in both healthy and notched specimens. **Table 4.5** shows the peak-peak voltage amplitude ratios of first (P/T-1) and second peaks (P/T-2) from healthy and notched specimens experimentally. The comparison of amplitude ratios of P/T-2 for all lengths of specimens is presented. In pulse transmission, arrival time remains unchanged due to varying location of notch. Thus, it is not feasible to ascertain the location of the damage using pulse transmission technique.

However, an indirect technique from the time of flight of P/T-2-Notch can be used to find the location of damage. But pulse echo is a preferred method for damage location since NE is more discernible and it directly gives the location.

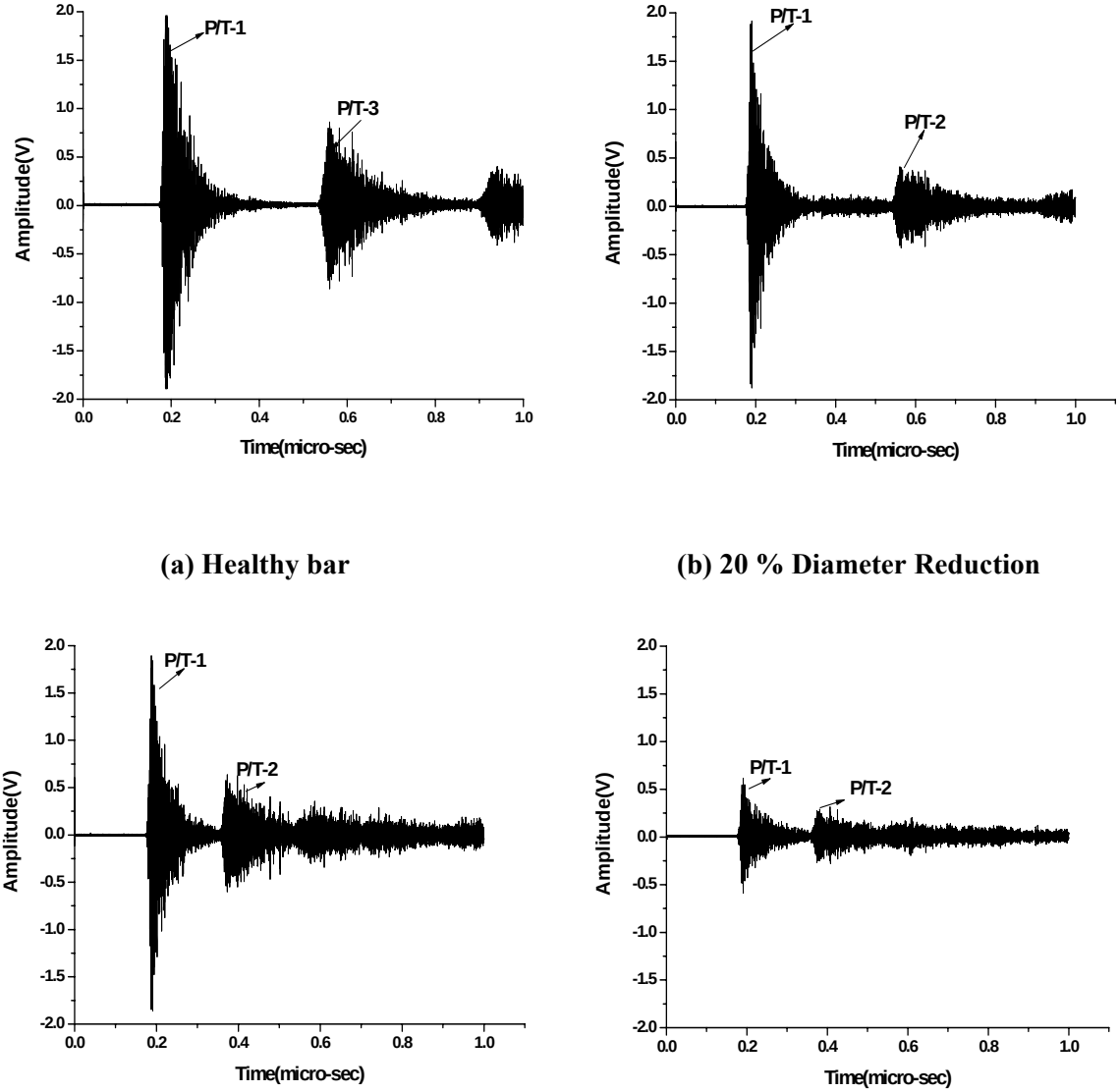

(a) Healthy bar **(b) 20 % Diameter Reduction**

(c) 40 % Diameter Reduction **(d) 60 % Diameter Reduction**

Fig. 4.9 (a-d): Pulse Transmission signatures of 12 mm diameter, 1m bar (Notch at L/2)

The extent of damage in bar can be ascertained by observing the peak to peak voltage trends of P/T-1. As the % of damage increases from 0% to 60%, the magnitude of the transmitted peak reduces continuously **(Fig 4.10)**. This is because, as the notch dimensions increase, more energy is reflected back and less of it travels through the bar to reach at the other end. Hence, relative signal attenuation of P/T-1 can relate to the extent of the damage in the bar. However, the signal attenuation is not linear with the depth of notch. P/T-1 values drops very gradually with increase in notch dimensions. This is attributed to the parabolic input pressure profile generated by the transducer with the maximum energy at its centre. Thus, most of the energy is able to pass through the core portion of the bar even though its periphery is notched leading to lower fall in P/T -1 with increasing notch dimensions.

Table 4.4: Comparison of time of receipt of P/T-1 in Pulse Transmission

Fault location –L/2	**Time (µsec)***		
	1m	**1.5m**	**2.0m**
Healthy specimen	1.82	2.72	3.6
Notched specimen**	1.8-1.82	2.69-2.72	3.6-3.62

*Phase Velocity of L (0, 11) mode in 12 mm diameter bars = 5520m/s

** Range of values for different % of defect

Table 4.5: Peak to peak voltage ratios in Pulse Transmission

Diameter Reduction (%)	**P/T-1**			**P/T-2**		
	1m	**1.5m**	**2m**	**1m**	**1.5m**	**2m**
0	0.98	0.96	0.936	0	0	0
20	0.94	0.811	0.858	0.19	0.08	0.059
40	0.787	0.66	0.6	0.270	0.17	0.094
60	0.36	0.238	0.18	0.18	0.11	0.06

* Peak to peak voltage ratios are calculated with respect to voltage amplitude of initial pulse

4.2.4 Variation in Damage Location

As the damage location is varied from L/2 to L/3 and 2L/3 in the bar, the results follow same trends for peak to peak voltage ratio amplitudes in pulse echo and pulse

transmission testing as for bar with notch at center **(Fig 4.11, 4.12).** Location of damage can be ascertained from the time of flight of NE from pulse echo signatures. Extent of damage can be judged from the peak to peak voltage amplitude ratios of the P/T-1 and NE in pulse transmission and pulse echo respectively

4.2.5 Variation in Diameter of Bar

Experiments are also done on 25 mm diameter bars and L (0, 6) mode is excited with 1MHz frequency transducer of 25 mm diameter. Damages are inflicted in the form of notches at L/2 as 0%, 20%, 40% and 60% and testing is done to ascertain the location and magnitude of damage with pulse echo and transmission testing. The results follow same trends as shown in **Fig 4.13.** Hence, the methodology can be generalized for any bar diameter.

4.2.6 Closing Remarks - Bars in air

This section described an experimental technique for monitoring damages in a bar in air that has flaws in the form of notches. The methodology established by the study utilizing the pulse echo and pulse transmission techniques for damage detection in cylindrical bars with damages in the form of notches can be applied to bars of variable lengths and diameters. The technique not only indicates the presence of damage but also gives the exact location and idea about the extent of damage by efficient use of combination of pulse echo and pulse transmission techniques. To assess the practical viability of the technique, the study is further extended to bars embedded in concrete as in RC structures. Ultrasonic testing is carried out on bars embedded in concrete in healthy and damaged states simulating corrosion damages in the form of notches and delamination.

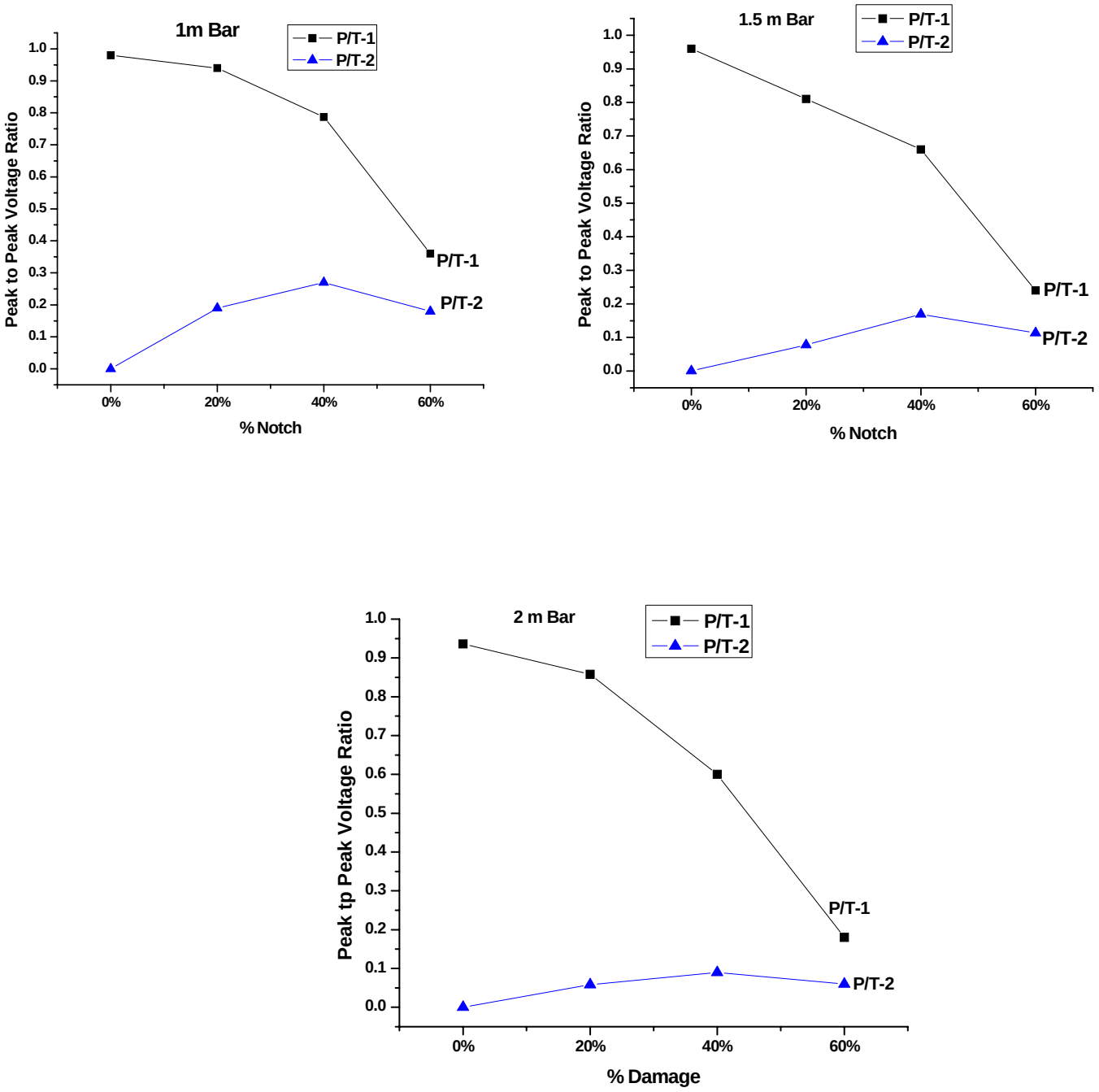

Fig. 4.10: Peak to peak voltage ratio trends of P/T of 12mm diameter bar (1m, 1.5m, 2.0 m) (Notch at L/2)

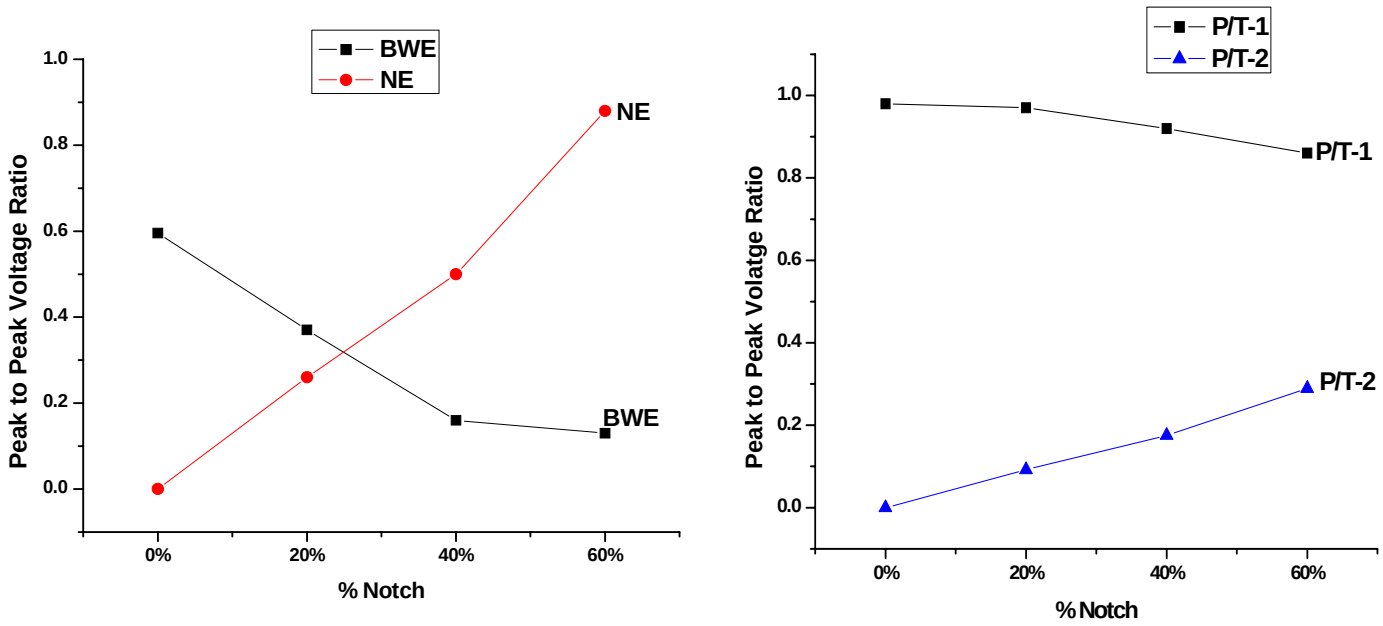

Fig. 4.11: Peak to peak voltage ratio trends in P/E and P/T

(12mm diameter, 1m bar) (Notch at L/3)

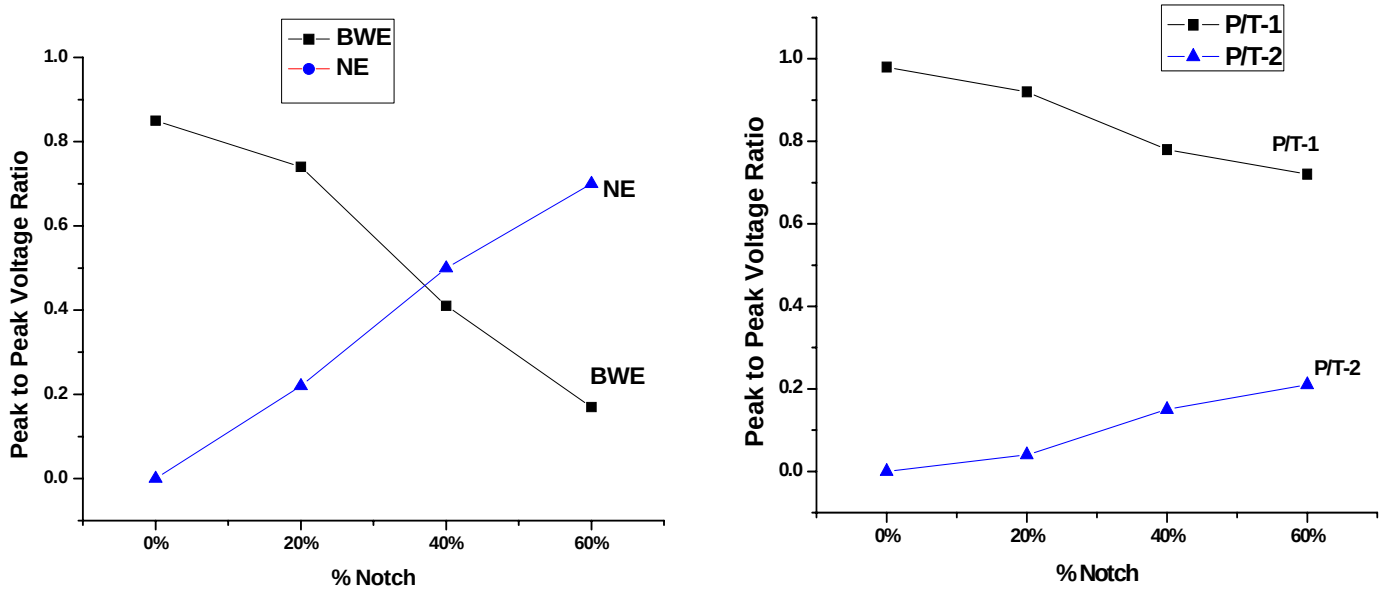

Fig. 4.12: Peak to peak voltage ratio trends in P/E and P/T

(12mm diameter, 1m bar) (Notch at 2L/3)

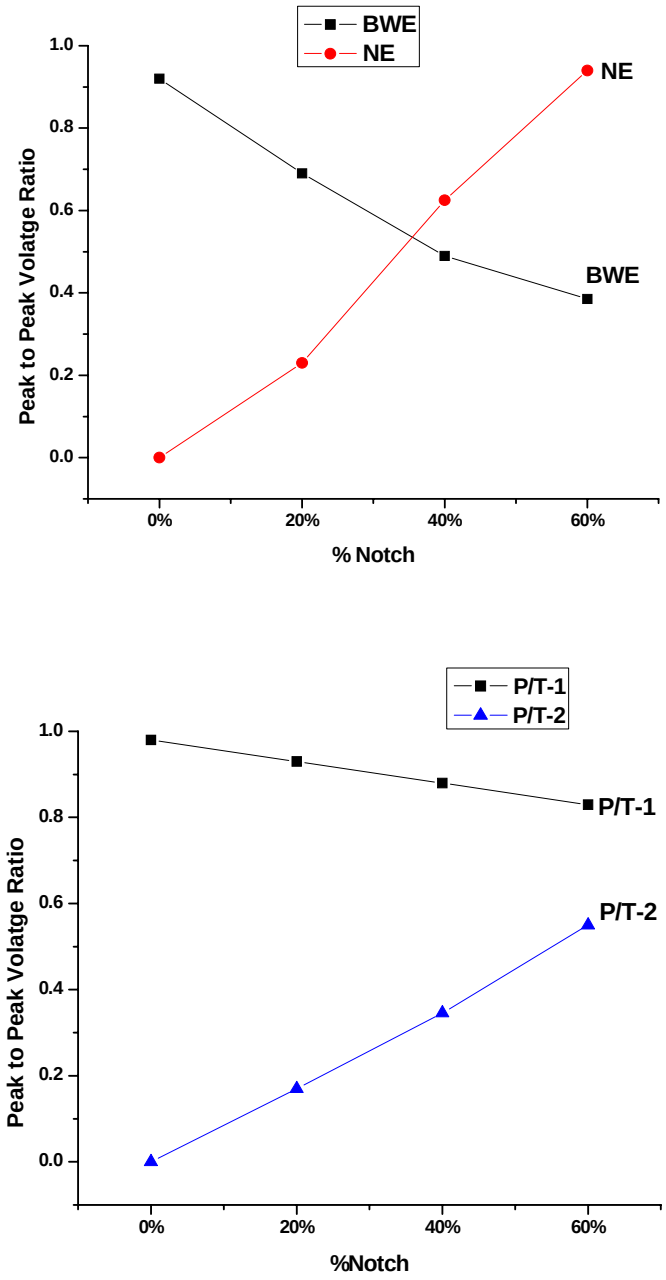

Fig. 4.13: P/E and P/T voltage ratio trends (25 mm diameter, 1m bar) (Notch at L/2)

4.3 BARS EMBEDDED IN CONCRETE

This section investigates the ultrasonic guided wave propagation in reinforcing bars embedded in concrete. Before casting the bars in concrete, they are seeded with damages simulating corrosion. Area loss or pitting is simulated in the form of notches in varying percentages as in case of bars in air. Debonding or delamination of the bar from the surrounding concrete is simulated by wrapping a double sided tape in varying percentages of the length of the bar before casting in concrete. Ultrasonic testing is carried out in both pulse echo and transmission modes to develop a methodology for embedded bars in concrete with simulated corrosion damages.

4.3.1 Selection of Excitation Mode

Reinforcing bars of 12 mm and 25 mm diameter embedded in concrete are used in the study. The selection of excitation mode and frequency for ultrasonic testing of bars in concrete is done using dispersion curves. Dispersion curves for a 12 mm bar embedded in concrete are plotted **(Fig. 4. 14**) for the steel and concrete properties mentioned in **Table 4.6.** Only longitudinal modes have been considered in the study as the flexural and torsional modes experience high theoretical attenuation especially in bars in concrete. Guided longitudinal waves are again produced in the embedded bars by keeping compressional transducers parallel to the guiding configuration at the two ends of the bars embedded in concrete as in case of bars in air. They are validated by experimentally confirming the signal fidelity. For bars embedded in concrete, which is a layered waveguide system, leakage plays an important role. High frequency low attenuating modes with displacement profiles centered in the middle of the bar to minimize leakage (Pavlakovic et al., 2001) are found to be the best for layered systems. The selection of frequencies for testing of embedded reinforcing bars is done based on the phase velocity dispersion curves **(Fig 4.14 a)**.

Phase velocity dispersion curves **(Fig. 4.14 a)** show the fundamental L (0, 1) mode starting at zero frequency with each higher order mode starting from a higher cut off frequency. Each of the higher modes shows a plateau region around the steel longitudinal bulk velocity line. But L (0, 7) mode shows a different pattern. Instead of each plateau region belonging to a single mode, L (0, 7) breaks from this pattern and links the subsequent plateau

regions together to form a single low leakage mode that propagates close to the longitudinal bulk velocity of steel.

Table 4.6: Material properties of steel & concrete used for modeling in Disperse (Pavlakovic et al., 2000)

S.No.	Material Property	Steel	Concrete
1.	Modulus, E (GPa)	210	29.6
2.	Density(ρ),(kg/m^3)	7932	2200
3.	Longitudinal Attenuation (db /m)	0.003	0.2
4.	Shear Attenuation (db/m)	0.008	0.5
5.	Longitudinal Velocity (m/s)	5960	4100
6.	Shear Velocity (m/s)	3260	2300
7.	Poisson's Ratio	0.2865	0.27

The plateau regions correspond to the points of maximum energy velocity **(Fig. 4. 14 b)** and minimum attenuation **(Fig 4.14 c)**. This L (0, 7) mode for 12 mm bar in concrete is chosen for testing because the lowest order low leakage mode has the lowest overall attenuation and is most useful in NDT. At a frequency of 3.5 MHz, the L (0, 7) mode exhibits global attenuation minima of 34.7dB/m and is selected for testing of 12 mm bar in concrete.

Similarly, for a 25 mm bar embedded in concrete, ideal frequency for ultrasonic testing is 1 MHz and L (0, 7) mode **(Fig 4.15).** This mode exhibits global attenuation minima of 22dB/m and is the fastest propagating mode. The phase velocity as obtained from dispersion curve at this frequency is 6 km/s.

Hence, L (0, 7) modes at 1 MHz and 3.5 MHz for 25 mm and 12 mm diameter bars embedded in the concrete are selected for further ultrasonic investigations. These frequencies and modes are utilized for ultrasonic monitoring of simulated and then actually corroding RC specimens as explained in Chapter 5.

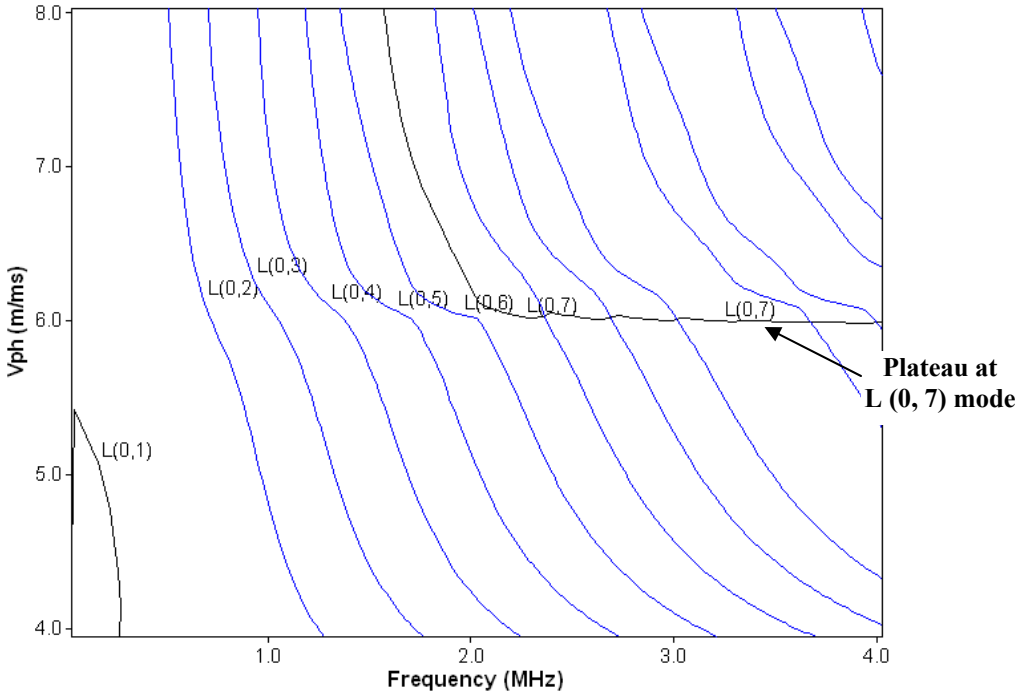

(a) Phase Velocity (Vph) Vs Frequency

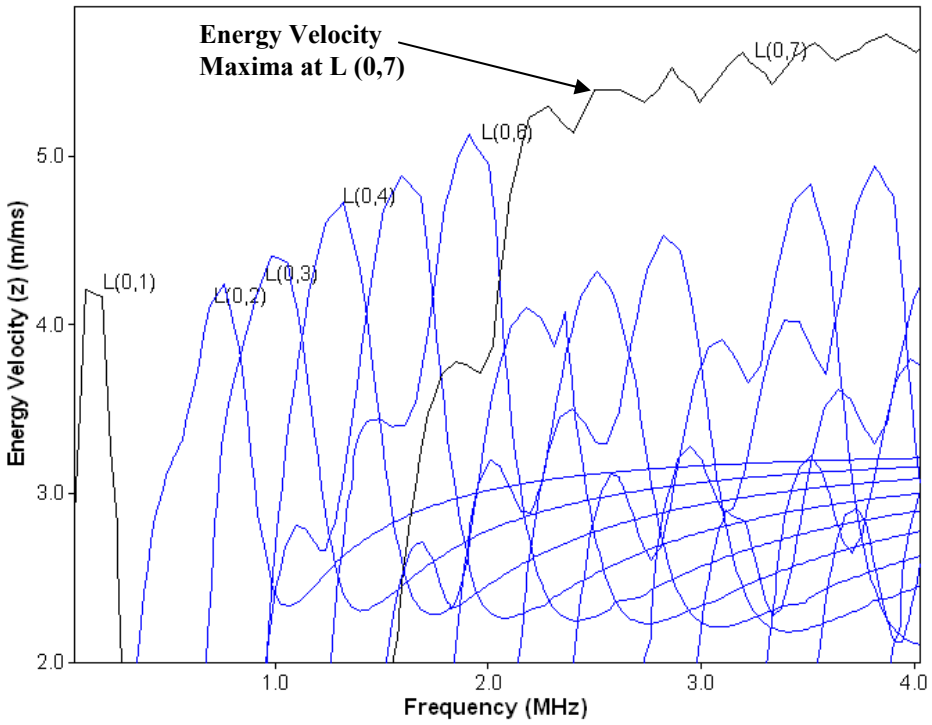

(b) Energy Velocity (z) Vs Frequency

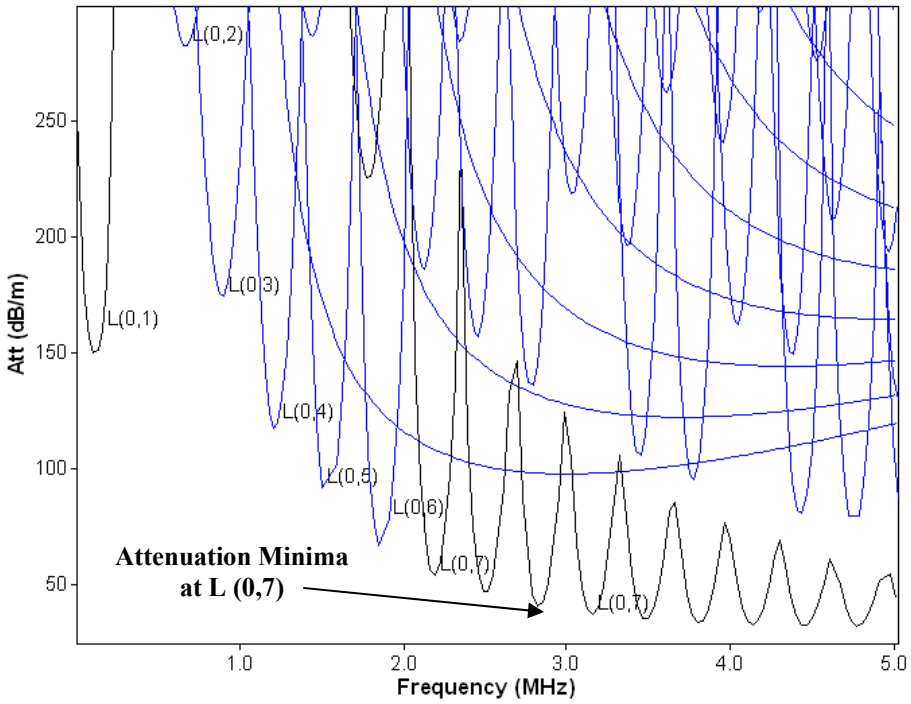

(c) Attenuation Vs Frequency

Fig. 4.14: Dispersion Curves for 12mm bar in concrete

(Pavlakovic et al., 2000)

4.3.2 Description of Experiments

For carrying out ultrasonic testing of embedded bars, the bars are cast in concrete. Concrete mix of M20 grade which is most commonly used for civil engineering applications is designed using IS code method. The designed proportions of cement, sand and stone aggregates are calculated as 1:1.5:2.96 with water cement ratio of 0.45. Standard flexural RC beam models of dimensions 150 mm x 150 mm x 700 mm are cast. 25 mm and 12 mm diameter plain mild steel bars of 1.2 m and 1.0 m length respectively were embedded in the centre of cross-section of the beam at the time of casting. The bar projected out by 250 mm and 150 mm on each side of the beam with 25 mm and 12 mm diameter bar **(Refer Fig 4.16)**.

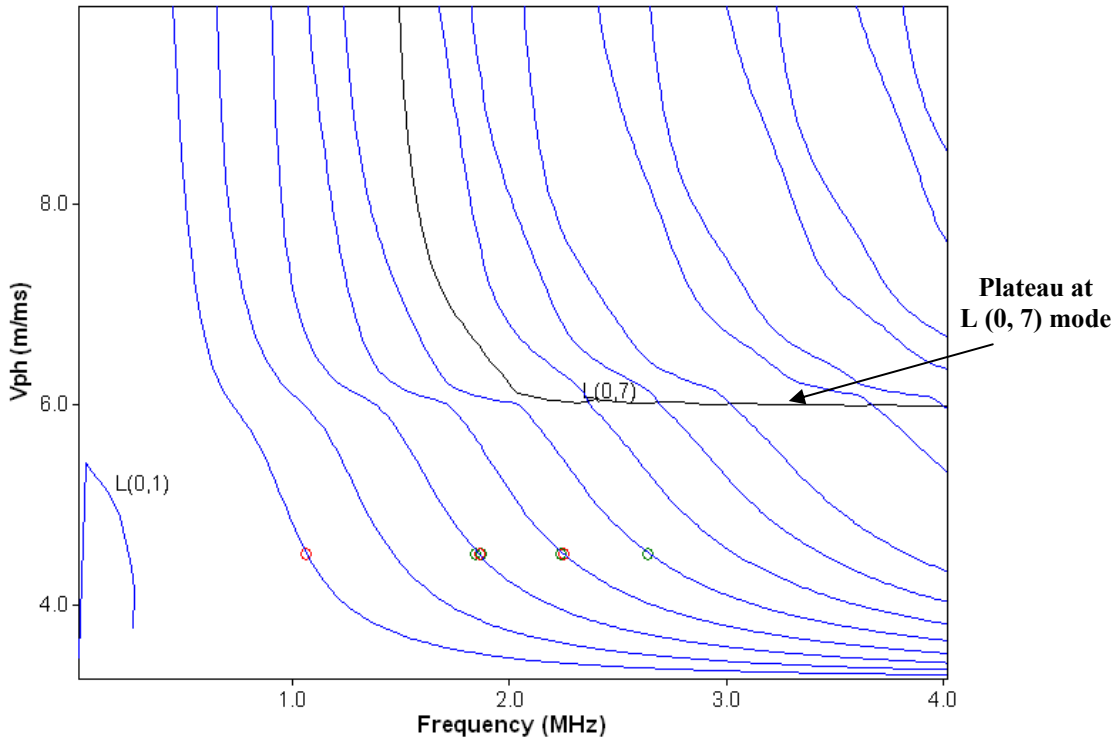

(a) Phase velocity (Vph) Vs Frequency

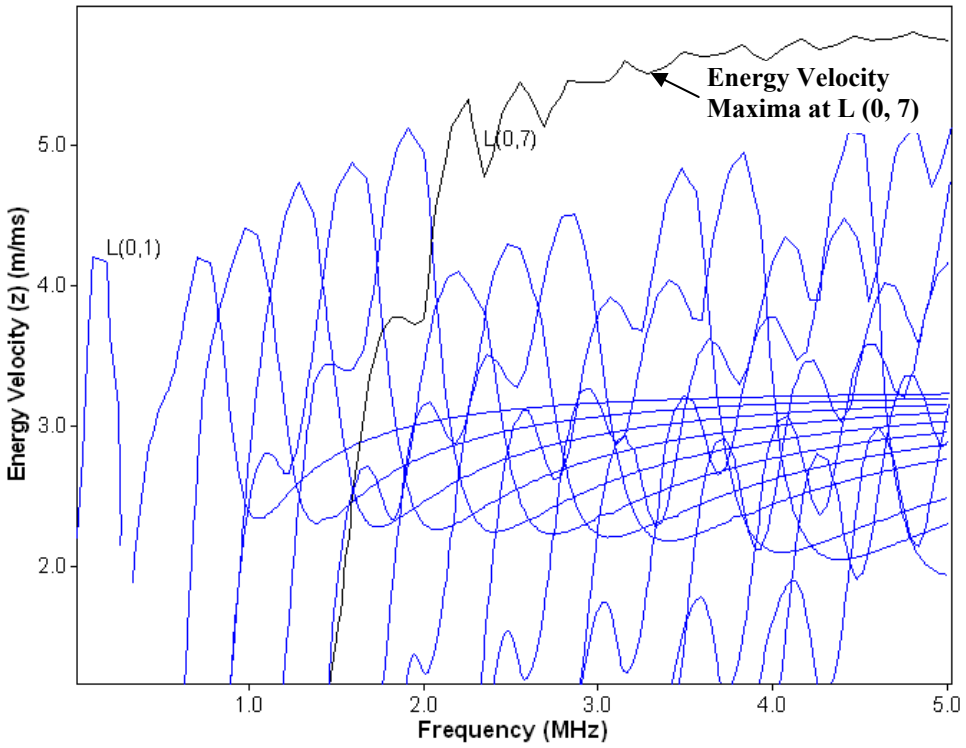

(b) Energy Velocity (z) Vs Frequency

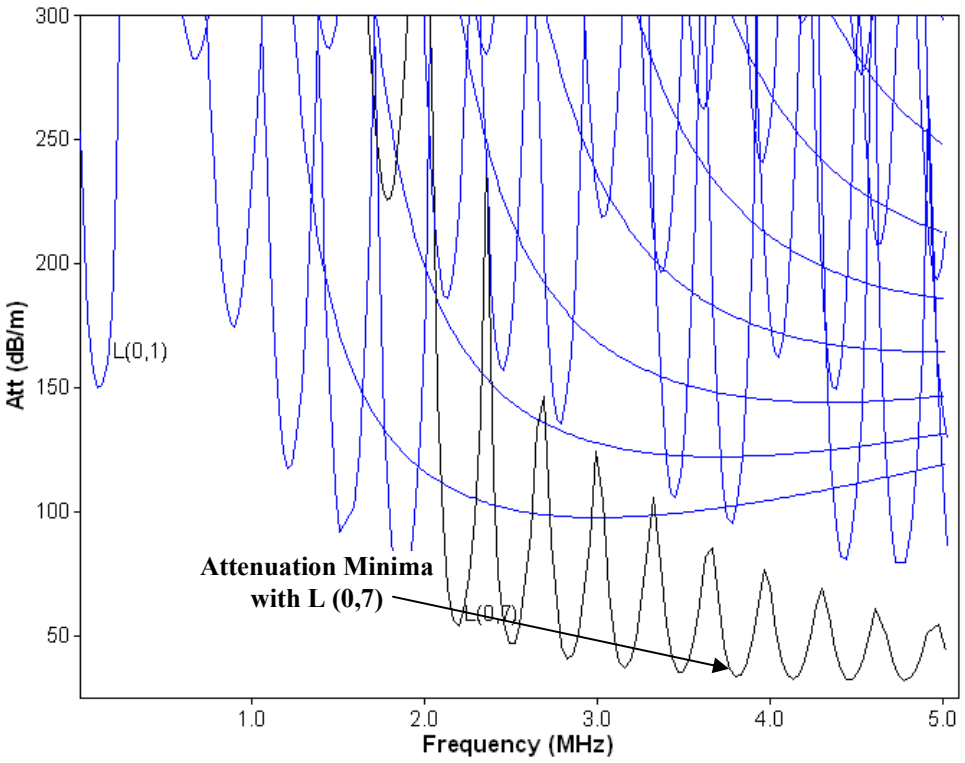

(c) Attenuation Vs Frequency

Fig. 4.15: Dispersion Curves for 25 mm bar in concrete

(Pavlakovic et al., 2000)

Bars are fabricated with two different types of damages, simulating different aspects of corrosion phenomenon. One set of bars embedded in concrete has damage in the form of notches representing pitting effect caused by corrosion. Notches with symmetrical 0%, 20%, 40% and 60% diameter reduction are introduced in the middle of the bars before casting them in concrete. Two samples of each specimen are tested to examine the repeatability and precision of the results. Another set of specimens are fabricated representing delamination between reinforcing bar and surrounding concrete. In this set of specimens, delamination is simulated by a wrapping a double sided tape on the steel bar to different extents of 0%, 6.25%, 12.5%, 25%, 50%, and 75% of the lengths of the bar representing different extents of debonds and then embedded in concrete **(Fig 4.17)**.

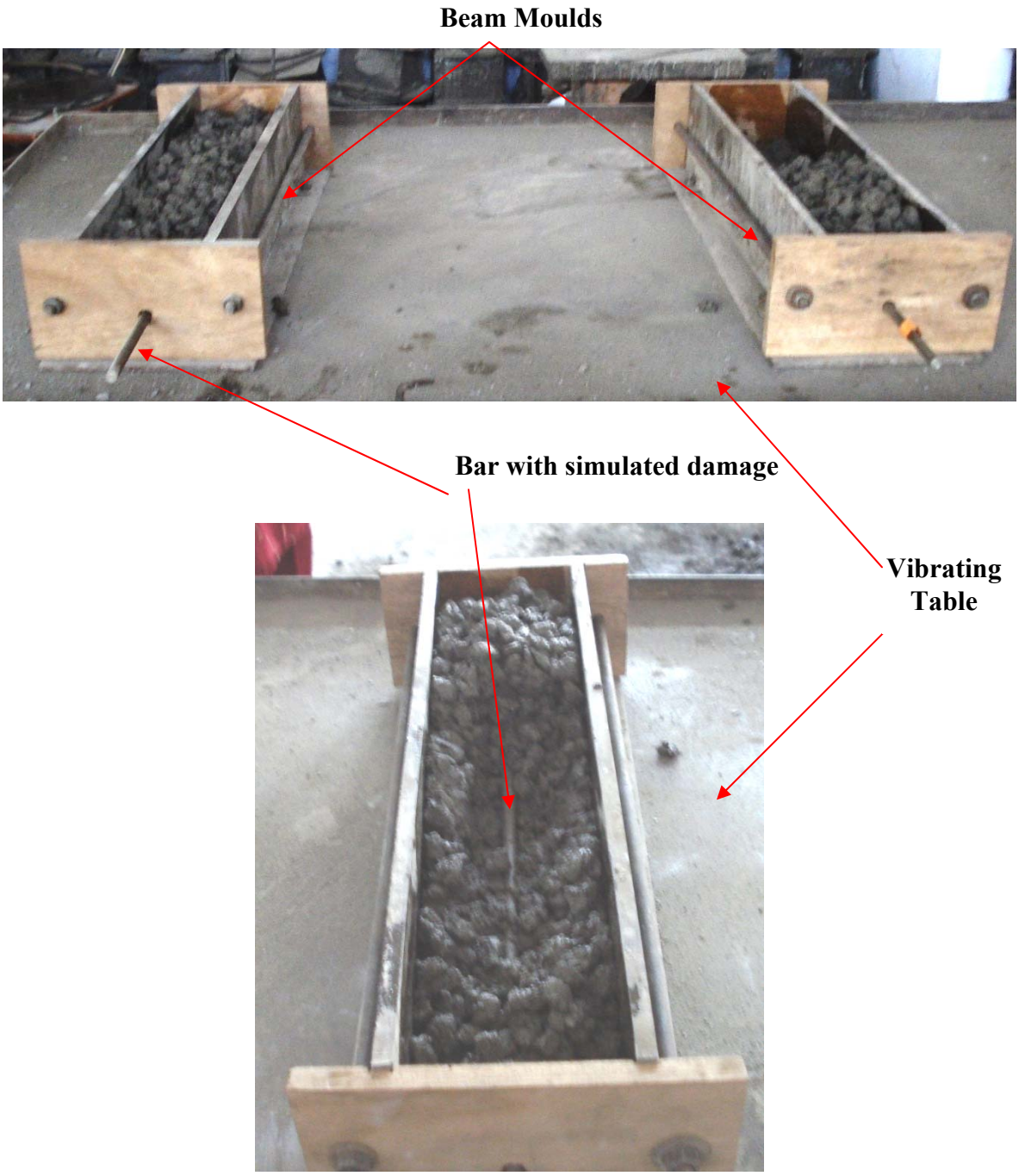

Fig. 4.16: Bar with simulated notch damage in mould during casting of beams

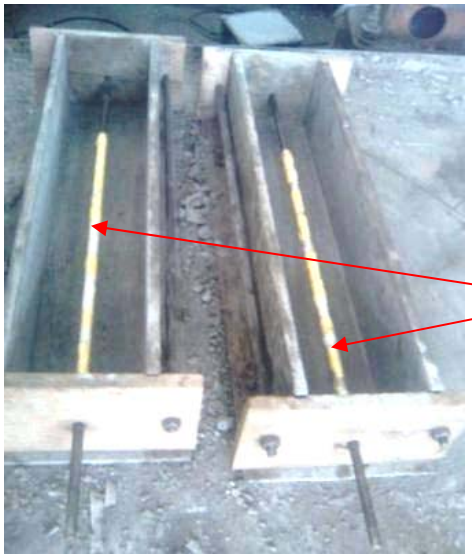

(a) During casting

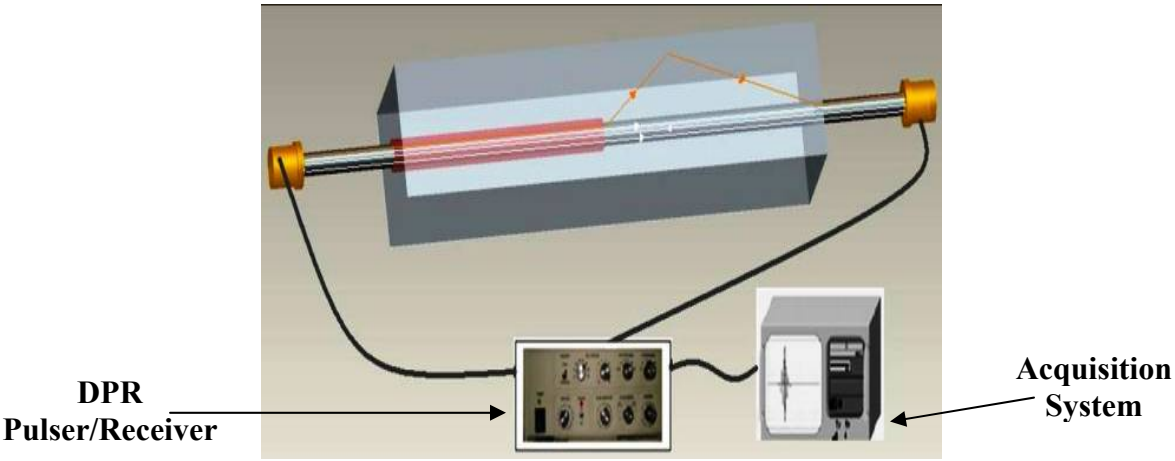

(b) During testing

Fig 4.17: Bar with simulated delamination embedded in concrete

Similar ultrasonic testing set-up as used for testing bars in air is used as shown in **Fig 4.18** for beam specimens**.** The beams with simulated notch damages are ultrasonically monitored in both pulse echo as well as pulse transmission modes.

In Pulse Echo, when there is a notch in the path of the ultrasonic wave, a part of the energy is reflected back from the notch and received by the same transmitting transducer. From the display, the time of flight between the excitation and reflected pulse is measured

and knowing the group velocity of guided wave mode used, the location of defect is exactly ascertained by **Equation 4.12**.

In Pulse Transmission method, an ultrasonic transmitter introduces the wave from one end of the bar and a receiver is placed at the opposite end to record the transmitted pulse. By measuring the relative change of the amplitudes of the input pulse and the received transmitted signals, the relative severity of the damage is assessed. The results are reported in the form of voltage-time curves (V-t) in both tests.

The specimens with simulated debond damages are monitored in pulse transmission mode only, to relate the effect of extent of delamination on input pulse.

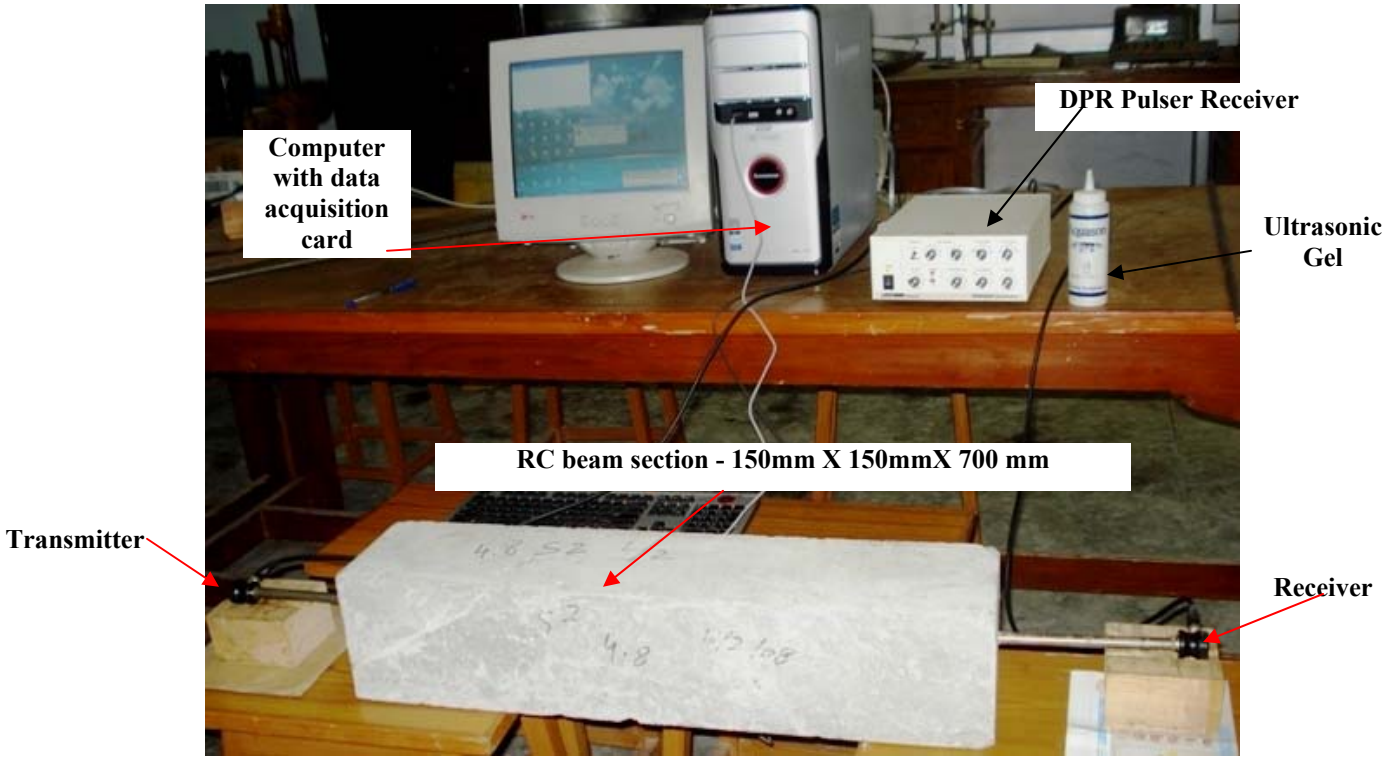

Fig. 4.18: Experimental set up for ultrasonic monitoring of RC beams specimens

4.3.3 Results and Discussions

4.3.3.1 Simulated Notch Damages

For ultrasonic testing of 25 mm bar in concrete, L (0, 7) mode selected for excitation is used. Ultrasonic testing of the embedded bar with notch at L/2 is done in both pulse echo

and pulse transmission modes. Pulse echo records for a 25 mm bar in concrete show the notch echo (NE) as well as the back wall echo (BWE). The voltage-time signatures obtained for a bar embedded in concrete are similar to that obtained for bar in air. In a healthy specimen, the peak is the BWE (**Fig 4.19 a)**. In a notched specimen, the 1st peak is NE and the 2nd peak is BWE **(Fig 4. 19 b)**. Appearance of NE indicates presence of damage in the embedded bar. By knowing the time of flight of this echo, the location of the damage is exactly computed **(Equation 4.12)** as

Notch Location, D = V*t/2 where, V= Group Velocity of excited mode & t= NE time

From **Fig. 4.19,** for a 40% notch in 1.2 m embedded bar in concrete,

t= 0.23 milli-sec (**Fig. 4.19**) V= 5.21 km/s (From Disperse), D = 0.6m i.e Notch is at the centre.

The magnitude of damage is directly related to the magnitude of the peak received after reflection from the notch boundary (NE) as well as BWE. It is observed that the amplitude of NE increased and that of BWE reduces with the increase in the notch dimensions **(Fig 4.21 a)**.

As the magnitude of the notch increases, more signal energy is reflected back from the notch and less of it travels to the back wall. Therefore, the peak-peak voltage amplitudes of NE's and BWE's is related to the extent of damage. However, the NE peak did not rise perceptibly even at 20% damage. Thus, its discernibility to small notches is not very high. This is due to the mode shape of L (0, 7) mode which shows that it is a core seeking mode **(Fig. 4.22)**. The energy is concentrated in the centre of the bar. Hence, this mode is insensitive to surface irregularities.

In the pulse transmission signatures, the peaks observed **(Fig 4.20)** are the transmitted peaks obtained after traveling length 'L' of embedded bar. It may be noted that the arrival time of the pulse is not affected by the presence of the notch. Thus, the notch location is not discernible through pulse transmission. However, studying the relative change in the amplitude of input pulse and the transmitted pulse (P/T-Notch), the severity of the damage can be assessed. The extent of damage in the embedded bar can be ascertained by observing the peak-peak voltage ratio trends of the transmitted peak. As the percent of damage

increased from 0% to 60%, the magnitude of the transmitted peak reduces **(Fig 4.21 b)**. This is because as the notch dimensions increased, more energy is reflected back and less of it travels through the bar to reach the other end. Hence, relative signal attenuation of the transmitted pulse can relate to the extent of the damage in the bar in concrete.

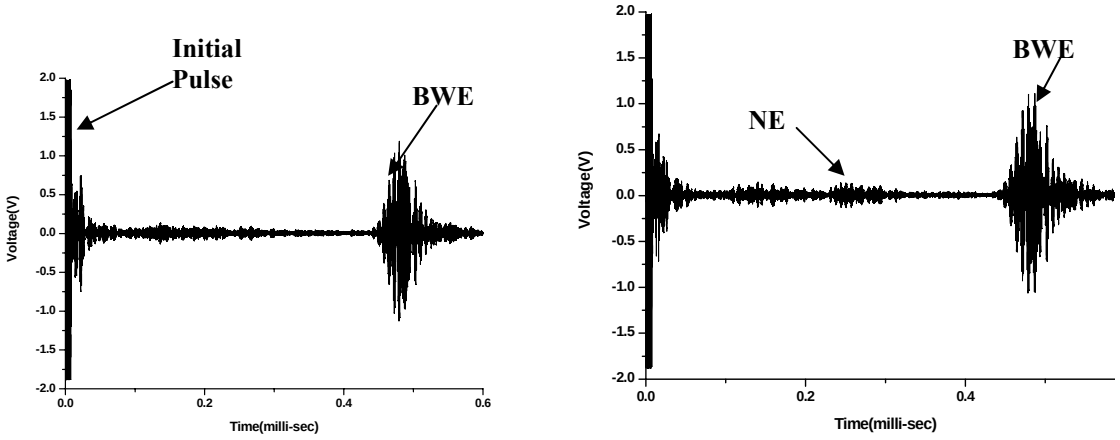

(a) Healthy Beam **(b) 20% notch in embedded bar**

Notch Location from NE Time
Notch Location = (V* t)/2
V = Group Velocity of excited mode

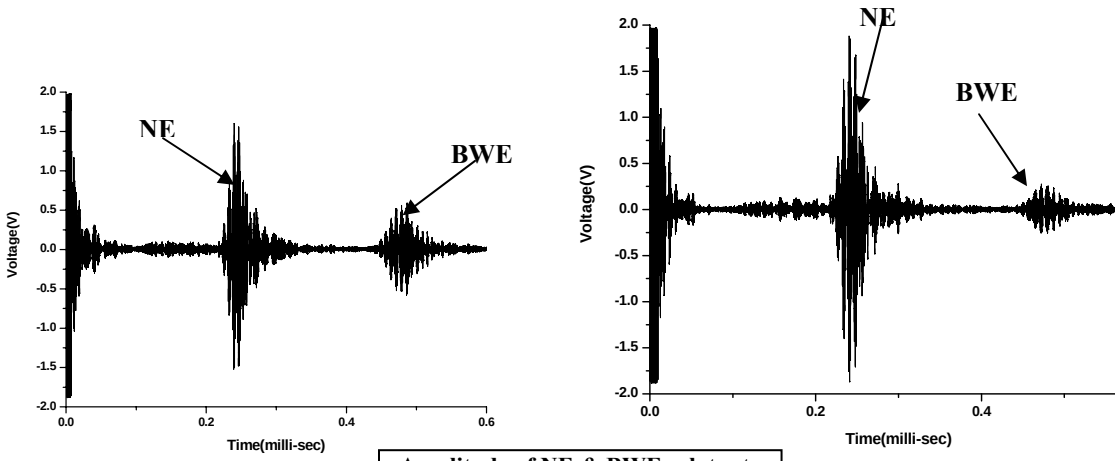

Amplitude of NE & BWE relates to the extent of damage

(c) 40% notch in embedded bar **(d) 60% notch in embedded bar**

Fig 4.19: P/E signatures for simulated notch at L/2 (25mm bar in concrete)

Thus, peak to peak voltage amplitudes of reflected and transmitted peaks in pulse echo and transmission methods respectively, closely relate to the extent of damage. However, the attenuation of the peak is not linearly proportional to the extent of damage. This is again due to the core seeking nature of the mode used. **Fig. 4.20** also shows the rise of the second peak with increase in damage. This peak is due to the reflection of the wave reflected from the notch. The wave reflected from the end of the embedded bar returns and in turn gets reflected from the notch.

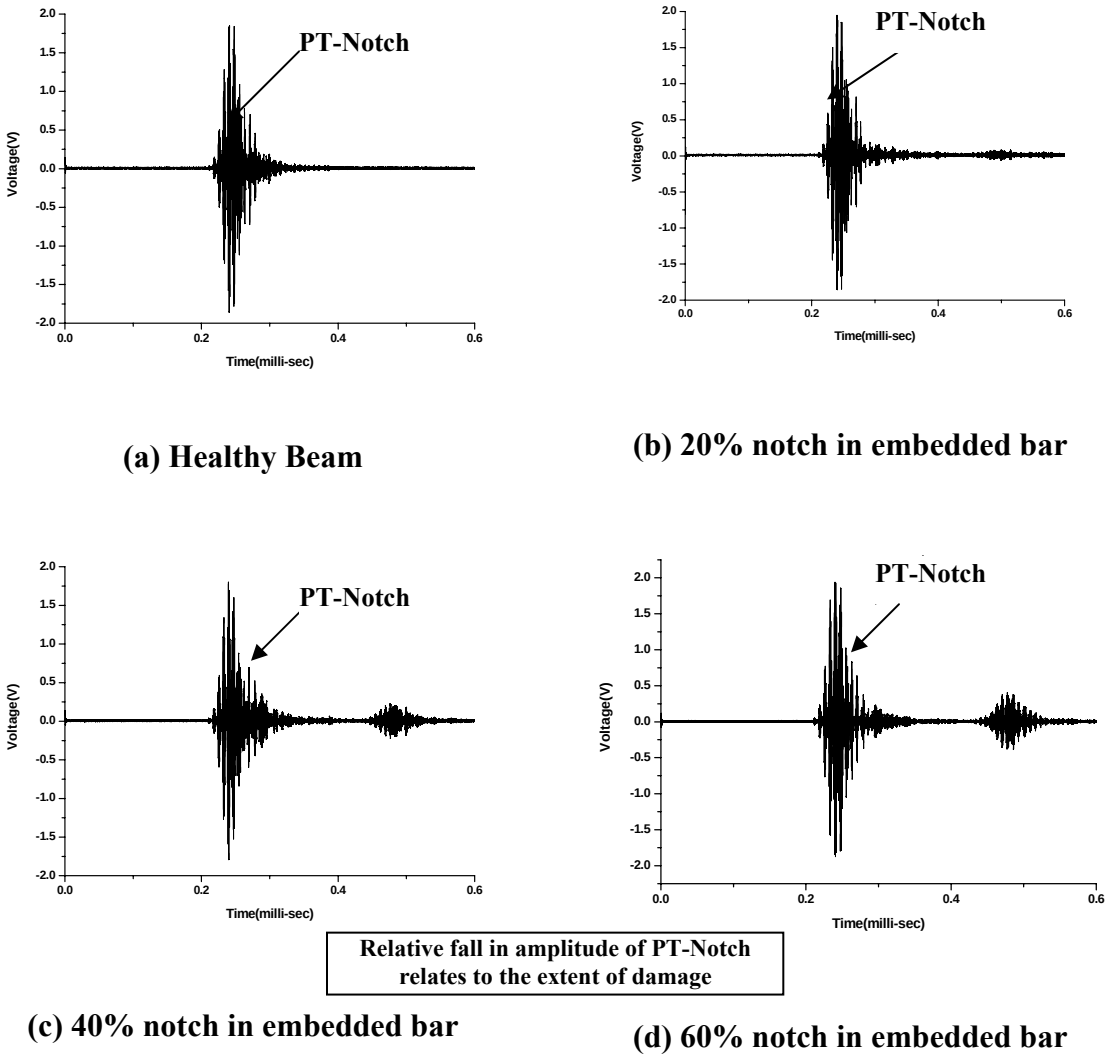

Fig. 4. 20: P/T signatures for simulated notch at L/2 (25mm bar in concrete)

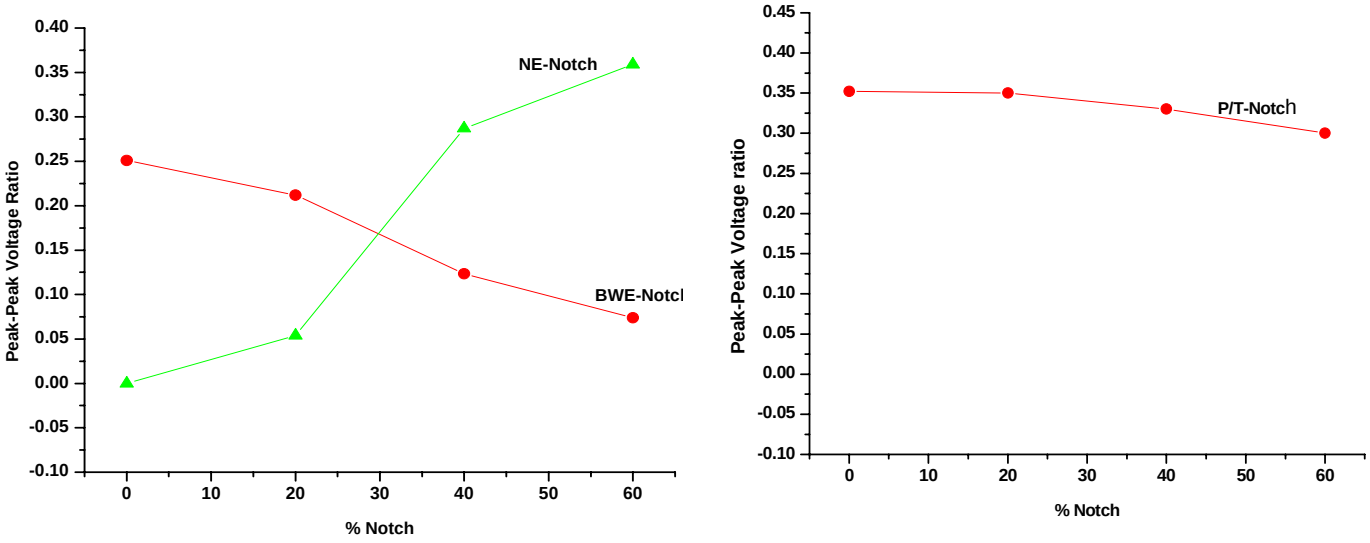

(a) Pulse Echo **(b) Pulse Transmission**

Fig 4.21: Peak-Peak voltage ratio trends of simulated notch specimens at L/2 (25mm bar in concrete)

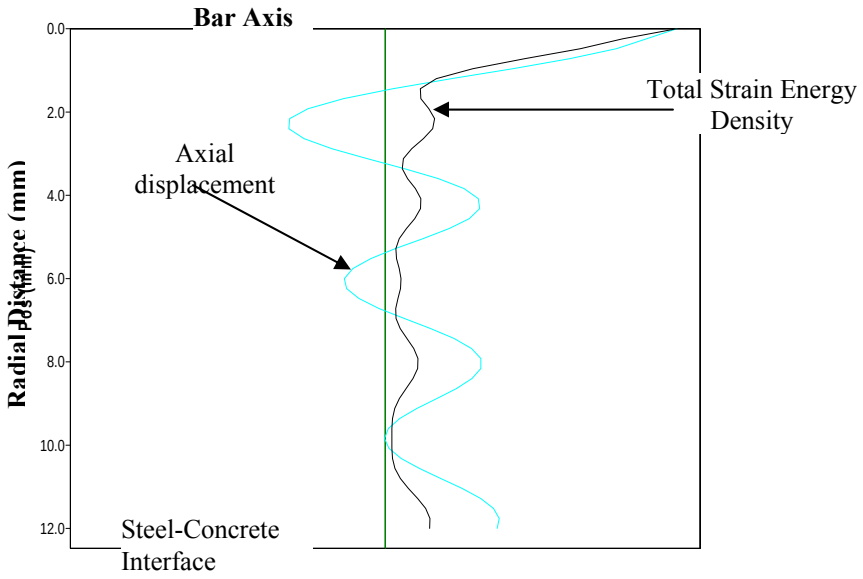

Fig 4.22: Mode shape of Core Seeking Mode - L (0, 7) at 1 MHz (Pavlakovic et al., 2000)

Similarly, ultrasonic testing is carried out for 12 mm bar in concrete. As discussed, same mode L (0, 7) but at a different frequency of 3.5 MHz is used for ultrasonic testing of 12 mm bar in concrete. Signatures of pulse echo and transmission results for 12 mm bar in concrete with simulated notch at L/2 are presented in **Figs 4.23 -4.24.** The reflected and the transmitted signals follow the same trends as for 25 mm bar in concrete. Hence, the methodology for damage detection in notched specimens is similar irrespective of the diameter of the bar. Only excitation frequencies and modes have to be decided judiciously for effective damage monitoring in embedded bars of different diameters.

But a significant observation from these graphs is the huge amount of signal attenuation experienced by the input pulse due to the presence of attenuating concrete in comparison to bar testing in air. Hence, it signifies the importance of selection of an ideal low leakage mode for damage detection in RC structures. Thus, the methodology developed using ultrasonic for damage detection in bars in air can be successfully extended for bars in concrete with simulated notch damages. Due to the presence of highly attenuating concrete, the selection of mode is of prime importance.

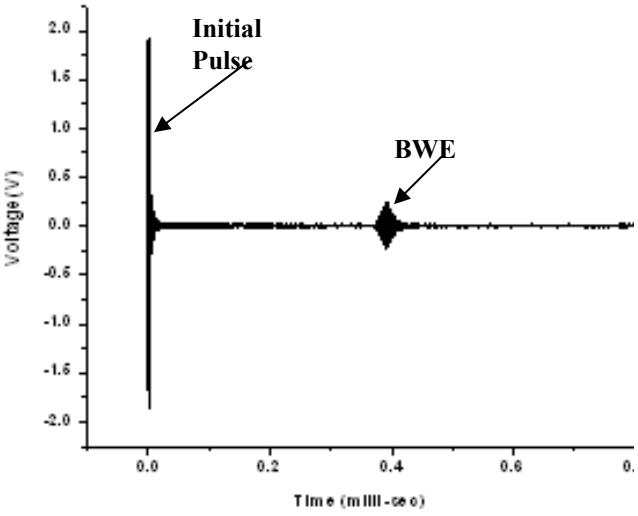

(a) Healthy Specimen

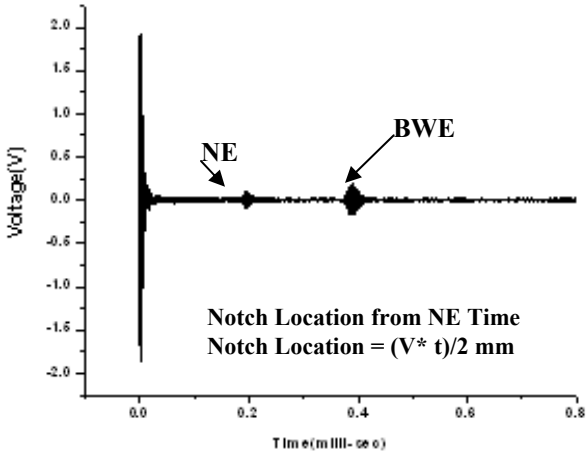

(b) 20% notch in embedded bar

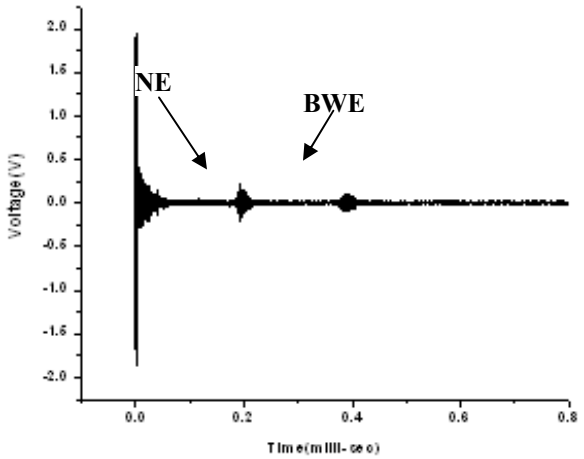

(c) 40% notch in embedded bar

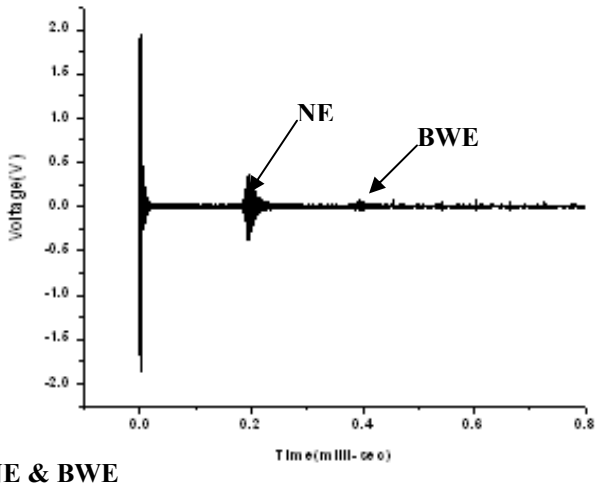

(d) 60% notch in embedded bar

Amplitude of NE & BWE relates to the extent of damage

Fig. 4.23: P/E signatures for simulated notch at L/2 (12mm bar in concrete)

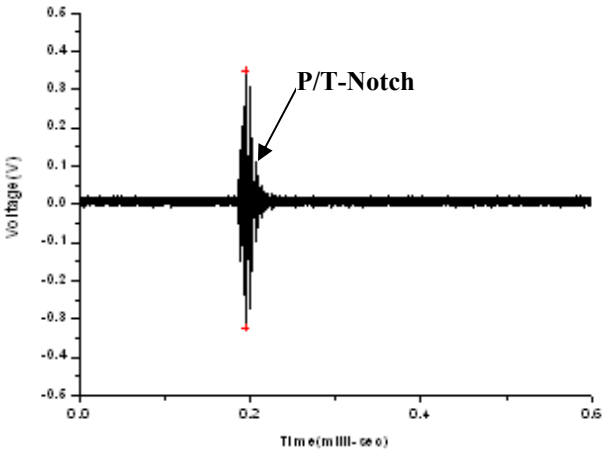

(a) Healthy Specimen

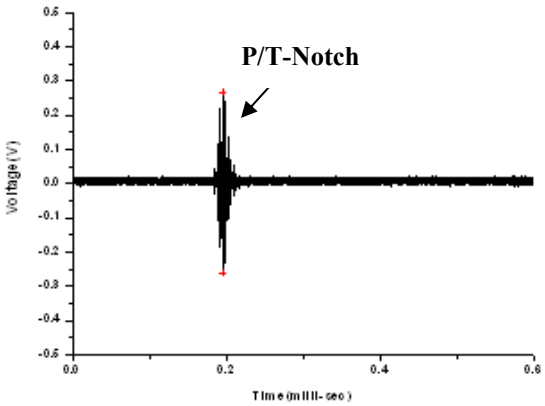

(b) 20% notch in embedded bar

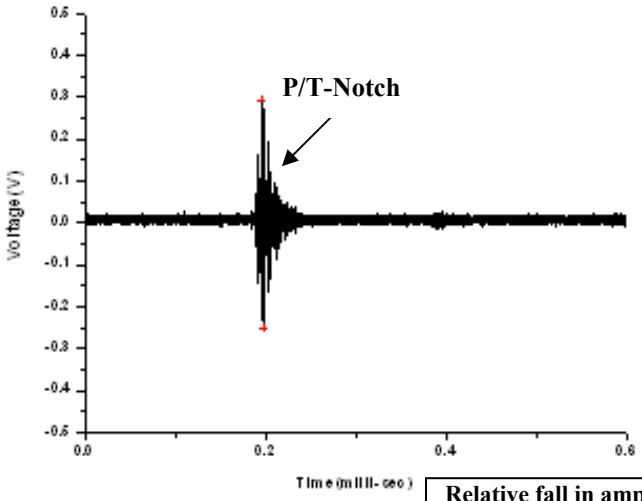

(c) 40% notch in embedded bar

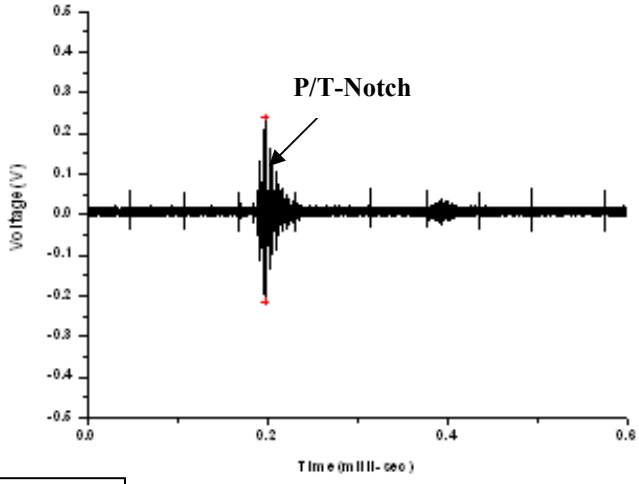

(d) 60% notch in embedded bar

Relative fall in amplitude of PT relates to the extent of damage

Fig. 4.24: P/T signatures for simulated notch at L/2 (12mm bar in concrete)

Another effect of corrosion on the reinforcing bar is the debonding of bar from concrete. Hence, to develop a corrosion monitoring methodology for RC structures, it is important that the developed methodology should also be extended for simulated debond specimens. Debond of the bar from the surrounding concrete due to corrosion should affect the leakage into concrete. The next section reports the results of simulated debond specimens

on ultrasonic wave propagation using the same L (0, 7) mode for 12 mm and 25 mm bar as chosen for the simulated notch testing.

4.3.3.2 Simulated Debond/Delamination Damages

The selected L (0, 7) mode at 3.5 MHz for 12 mm bars and 1 MHz for 25 mm bar is used for pulse transmission testing of beams simulating delamination. The presence of delamination will not affect pulse echo results. Hence, ultrasonic testing of simulated debonding is only carried out in pulse transmission mode. As the percentage of delamination increases, the transmitted signal strength (P/T) keeps on rising for 25 mm **(Fig 4. 25)** and 12 mm **(Fig 4.26)** embedded bars and as plotted in **Fig. 4.27.**

As the percentage of delamination between steel and concrete is increased from 0-100%, transmitted signal strength rises continuously since the amount of energy leaking into the surrounding concrete decreases with increase in percentage delamination **(Fig. 4.27)**. At 100% delamination level, signal is same as received in case of a bar in air. Hence, an increase in the input signal strength in pulse transmission can successfully relate to the presence as well as extent of delamination.

4.3.4 Closing Remarks- Bars embedded in concrete

Ultrasonic guided waves at high frequencies using the low leakage modes can be effectively used for monitoring simulated corrosion damages in reinforcing bars embedded in concrete by utilizing its wave guide effects. In addition to material damping, leakage into the surrounding concrete takes place which emphasizes the selection of ideal low leakage modes in concrete. Corrosion has been simulated as loss of bond and loss of area. The methodology established by the study utilizing the pulse echo and pulse transmission techniques for damage detection in cylindrical bars in air can be successfully extended to bars embedded in concrete. The technique not only indicates the presence of notch damage but also gives the location and magnitude of notch damage by efficient use of combination of pulse echo and pulse transmission techniques. Relative signal attenuation of the transmitted pulse (P/T-1) and rise of the reflected pulse (NE) with increasing notch dimensions can relate to the extent of the damage in the bar in concrete. An increase in the input signal strength in pulse transmission can successfully relate to the presence as well as extent of delamination.

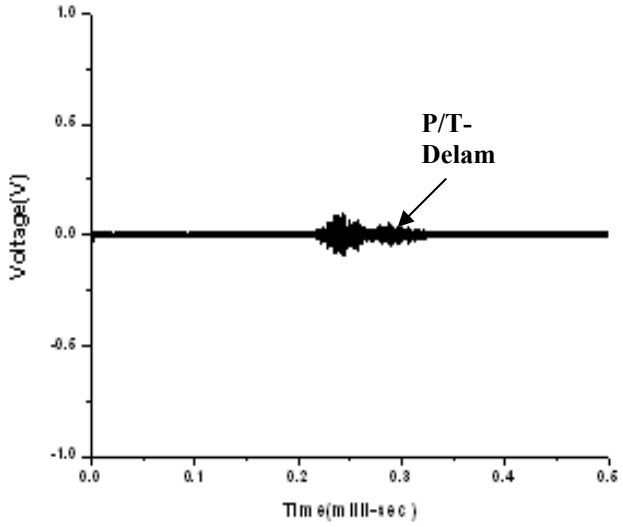

(a) 0% Delamination

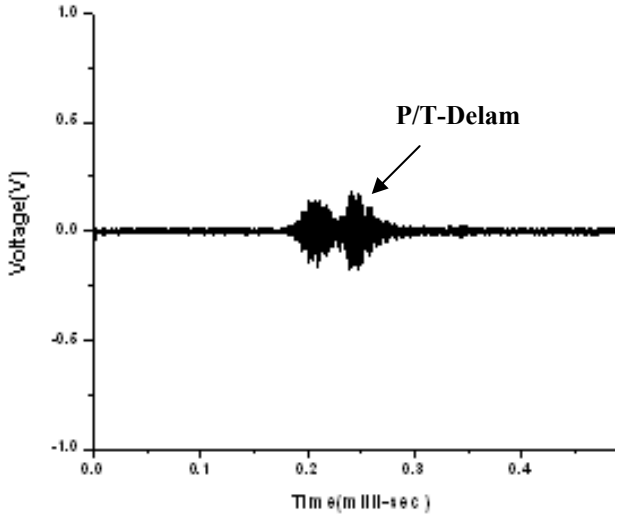

(b) 50% Delamination

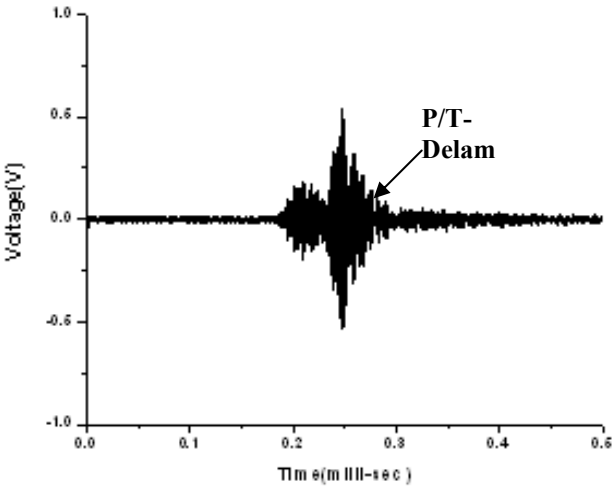

(c) 75% Delamination

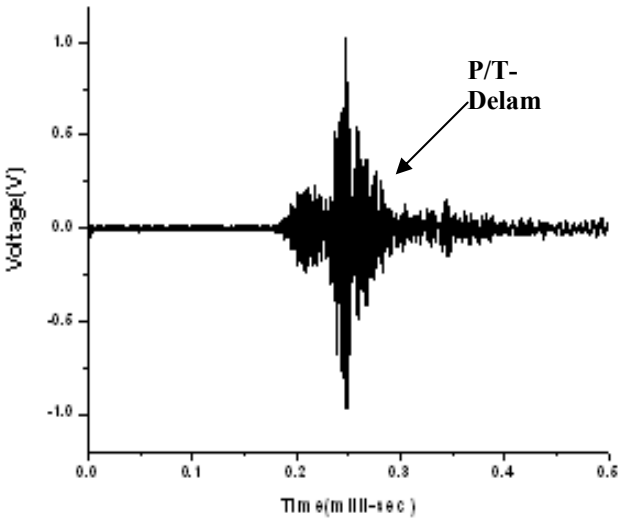

(d) 100% Delamination

Fig. 4.25: P/T signatures for simulated delamination specimens (25mm bar in concrete)

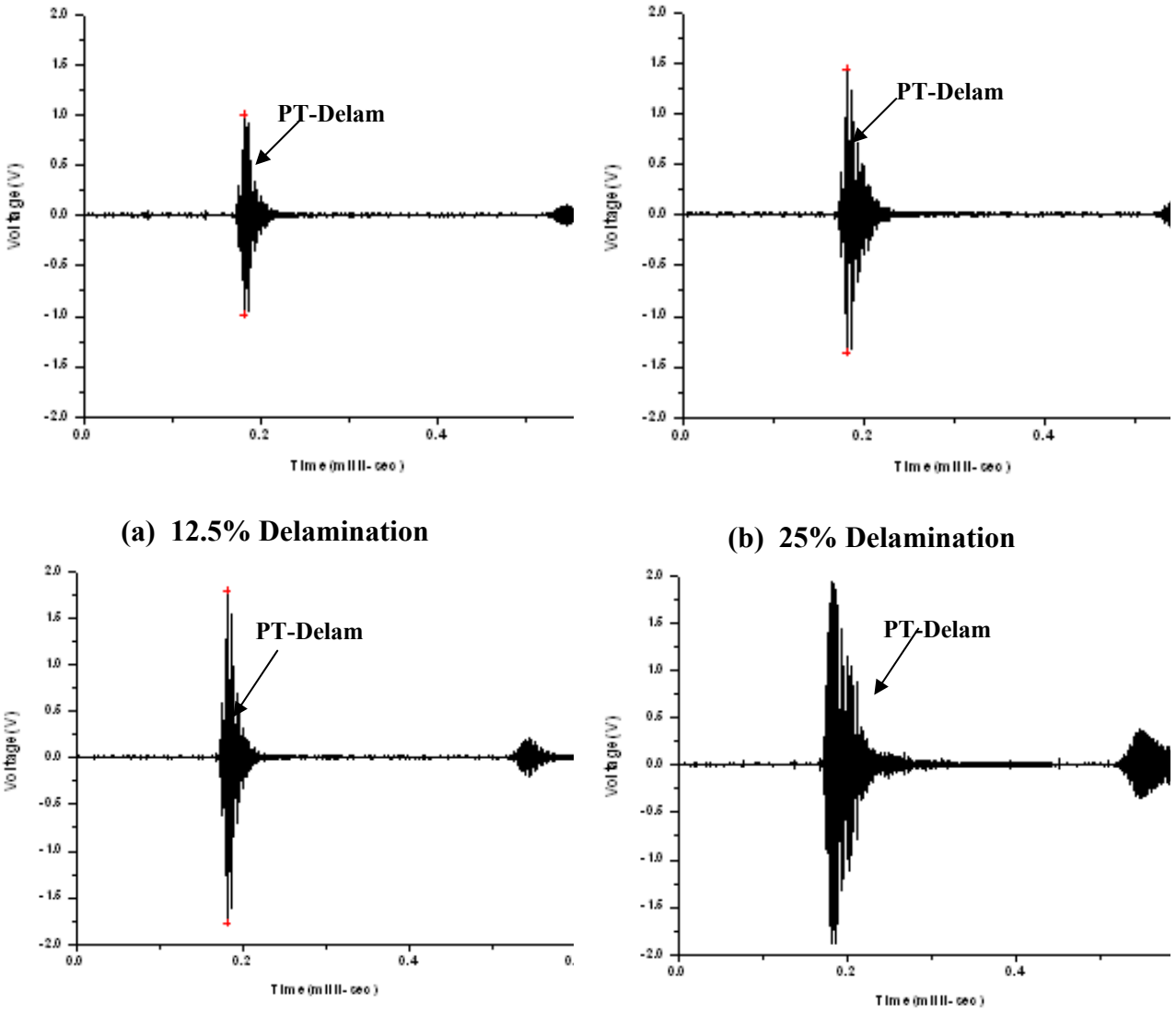

(a) 12.5% Delamination

(b) 25% Delamination

(c) 50% Delamination

(d) 100% Delamination

Fig. 4.26: P/T signatures for simulated delamination specimens (12mm bar in concrete)

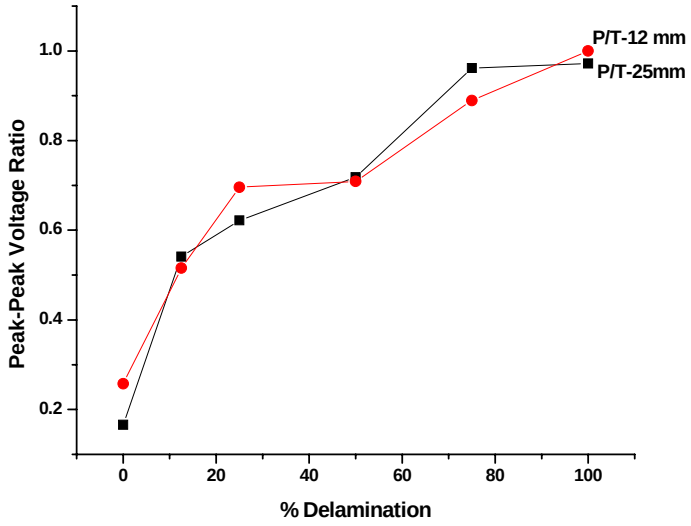

Fig. 4.27: Simulated Delamination P/T trends

CHAPTER 5

RC BEAMS UNDERGOING ACTUAL CORROSION

5.1 INTRODUCTION

The ultrasonic investigations of RC beams for corrosion damages have mainly remained confined to simulated specimens. However, corrosion is a slow process and making meaningful conclusions through controlled corrosion within a reasonable time is difficult. Hence, most of the researchers have concentrated only on simulated corrosion studies. After successfully developing a damage detection methodology in embedded bars with simulated corrosion damages in Chapter 4, this chapter investigates the applicability of ultrasonic guided waves to monitor RC beam specimens undergoing actual corrosion. Since natural corrosion would take decades to occur, it is accelerated by impressing anodic current. As discussed in Chapter 3, the two common types of corrosion mechanisms i.e oxide and chloride corrosion occurring in embedded reinforcements in concrete are considered in the study.

The mechanism of corrosion occurring in RC structures has been discussed in **Section 3.2**. Corrosion occurring because of water and oxygen in the absence of chlorides and carbonates is referred as **Oxide Corrosion (OC)**. The effect of oxide corrosion is the formation of the corrosion products on the surface of the rebar altering the surface. Due to higher volume of rust than the corresponding mass of steel, an outward pressure is generated. This initially improves the interfacial bond but the pressure results in tensile stresses in concrete. As concrete is weak in tension, cracks are developed in it leading to debond. Most researchers have simulated the debond by artificially introducing an element at the interface.

Chloride Corrosion (CC) is the corrosion of steel in concrete due to chlorides present in aggregates, mixing water, admixtures (accelerators), deicing chemicals, and use of sea water for construction. The resulting corrosion products and accompanying processes of cracking, spalling and delamination of concrete occurring in both types of corrosion are same

but the rate and the mode of occurrence of various aspects of corrosion phenomenon are different in the two cases. The rate of chloride corrosion is far higher than oxide corrosion. Although it also leads to debond as described in oxide corrosion, its distinguishing feature is pitting where crevices are formed in the bar leading to locale loss of area. Thus, in addition to debond, chloride corrosion manifests itself in local weakening of the bar. An experiment is carried out to create these two different types of corrosion in RC samples. The process of corrosion can be monitored ultrasonically by observing the signals through the bar while it is corroding. The samples have been ultrasonically monitored throughout the corrosion process.

5.2 EXPERIMENTAL PROCEDURE

5.2.1 Sample Preparation

Concrete with proportions of cement, sand and stone aggregates as 1:1.5:2.96 is taken. The water cement ratio is kept as 0.45. RC beam specimens of dimensions 150 mm x 150mm x 700mm are cast. In one set of specimens, a 25 mm diameter plain mild steel bar of 1.2 m length is placed at the centre of cross-section of the beam at the time of casting. The bar projected out by 250mm on each side of beam. In another set, 12mm diameter bar is used. Plain bar is used to study the effect of corrosion only on bond.

In natural environments, corrosion process takes several years to occur. The process can be accelerated in many ways. The commonly used methods of inducing corrosion in RC specimens can be recalled as salt spray (Berver et al. 2001; Debaiky et al. 2002 and Batis and Rakanta 2005), Chloride diffusion (Tamer et al. 2005; Masoud and Soudki 2006 and Tamer et al. 2006), alternate drying and wetting in salt water (Debaiky et al. 2002 and Soudki 2006) and impressing anodic current (Lee et al. 2000; Tamer et al. 2003 and Wootton et al. 2003). In the salt spray technique a mist with dissolved sodium chloride is created in an enclosed chamber containing the specimens. Previous studies have shown that test specimens kept in a salt spray chamber for more than 100 days did not show any visible signs of corrosion (Berver et al. 2001 and Debaiky et al. 2002). This method is not found suitable considering the time constraint. Method of adding chlorides artificially to the concrete during casting is an effective method of initiating corrosion in an embedded bar. This method is not considered because it did not simulate the present condition of interest. Alternate immersion into NaCl (Sodium Chloride) solution and drying of the specimens also induces corrosion.

However, the quickest method of inducing corrosion is by impressing anodic current. In this method, the specimen is immersed in NaCl solution and a direct current is passed making the reinforcement bar as an anode and another metal nobler than steel in electro-chemical series as cathode. Incidentally, this method has been used by a number of previous investigators (Bonacci 2000; Craig 2002 and Masoud et al. 2005).

Hence, the corrosion process is accelerated using impressed current. Positive terminal of the power supply is attached to the projected bars in the beam. The middle 300mm is selected for exposure to corrosive environment. A thick cotton gauge is placed in this region to keep it moist. Stainless steel wire mesh is wrapped on the cotton gauge. The negative terminal is connected to the wire mesh. A constant voltage of 30V is applied between the two terminals by means of a constant power supply device **(Fig 5.1)**. A dripping mechanism is fitted on the wire mesh to keep the cotton underneath saturated. For Chloride Corrosion (CC), 5% NaCl solution is used as drip. For Oxide Corrosion (OC), plain tap water is used instead of NaCl solution. Cotton gauge below the wire mesh uniformly distributed the water in the central wrapped portion of the beam.

5.2.2 Ultrasonic Investigations

An ultrasonic testing system as used for testing of simulated specimens consisting of a pulser /receiver, contact transducers, and a computer with data acquisition card is used. The transducers are attached at the two ends of the bars by means of a holder and a coupling gel between the bar and the transducer. The holders maintained a constant pressure between the transducer and the bar. Driven by the pulser, the compressional transducer generates an ultrasonic pulse that propagates through the embedded bar in the form of longitudinal waves. The pulse transmitted at the other end of the bar is recorded using a receiving transducer **(Fig 5.1)**. At the time of ultrasonic measurement, the external voltage for accelerated corrosion is switched off. This is done to avoid the interference of noise generated by the anodic current with the ultrasonic signals.

The selection of frequencies for testing is done using the software Disperse (Pavlakovic et al., 2000) and the same modes and frequencies are used as for simulated studies. The modes that are easily distinguishable and have lowest signal attenuation are selected. For a 12mm bar in concrete, L (0, 7) mode at a frequency of 3.5 MHz and for

25mm bar, L (0, 7) modes at a frequency of 1MHz are used. Pulse Transmission and Pulse Echo is monitored once everyday until no significant change in received signal is observed. After exposure, the corroded beams are subjected to pull out test and the extracted bar is checked for mass loss and tensile strength. The ultrasonic test results are compared with those of destructive tests to facilitate calibration of ultrasonic voltages with physical parameters.

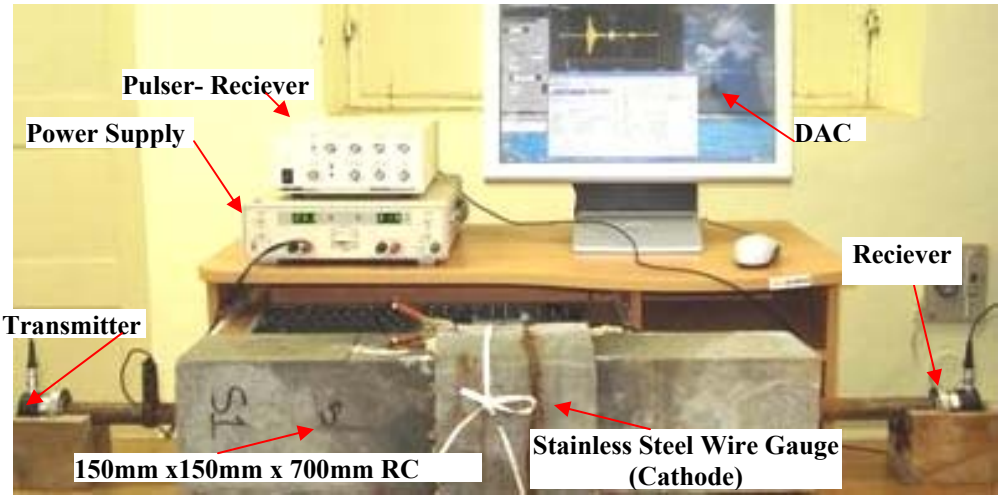

Fig 5.1: Experimental set- up for ultrasonic monitoring of RC beams undergoing accelerated corrosion

5.3 12MM BAR IN CONCRETE

In 12mm bar in concrete, beams are subjected to chloride corrosion only. A pumping mechanism is fitted on the wire mesh to keep the cotton underneath saturated with 5% NaCl solution used as drip. The ultrasonic testing is done for 8 days until the ultrasonic signatures completely vanished. The destructive testing and ultrasonic testing results are discussed below.

5.3.1 Visual Observations

Beams undergoing accelerated chloride corrosion show reddish brown patches of corrosion products and a longitudinal crack parallel to the bar within 3 days. The cracks initiated at the surface of the beam and progressed along the direction of the reinforcement. With the increase in the volume of corrosion products, another crack parallel to the bar

appeared on another face of the beam after 5 days. A reddish brown liquid oozed out of the cracks and the ends of the beam. The crack length and width increased with increase in exposure. At 8 days of corrosion, there are two large and wide longitudinal cracks that divide the entire beam into wedges and the beam is in a highly dilapidated condition **(Fig 5.2a)**.

5.3.2 Ultrasonic Monitoring

5.3.2.1 Pulse Echo testing

Ultrasonic pulse echo signatures are monitored everyday during the exposure to the corrosive environment. In the healthy bar, the signature is characterized by a strong BWE **(Fig 5.3a)**. As the exposure proceeds, BWE attenuates rapidly. It disappeared completely on the 4^{th} day. This is contrary to the expectation if corrosion is manifested through delamination only. Thus, it is clear that corrosion cannot be simulated as simple delamination. It is a well known that in the presence of chlorides, pitting in the form of crevices occur on the steel bars. Moreover, it is likely that due to non-uniform loss of material from the surface, the smooth waveguide is disturbed, thus resulting in scattering of waves.

Another significant observation is the appearance of a peak (NE- Corrosion) between the initial pulse and BWE on the 7^{th} day **(Fig 5.3b).** This indicates that pulses are reflecting from a localized neck formed in the bar due to corrosion. From the time of flight of the peak, the location of the neck is estimated **(Equation 4.12)**.

V= 3.75 km/s (Group Velocity of L (0,7) mode at 3.5 MHz for 12mm bar in concrete)

t = 0.00008 sec

Using **Equation 4.12,** D= V* t/2 = 150mm from the end of bar

i.e just at the bar-beam interface.

After completion of the corrosion process, concrete is removed and the extracted bar is examined **(Fig 5.2b)**. A large notch is indeed seen at the estimated location. As corrosion increased, amplitude of this peak increased indicating increased loss of area from the interface. Corrosion in the presence of chlorides is characterized by pitting and localized loss of material similar to notches. In the present sample, one major notch developed due to corrosion resulting in a close match.

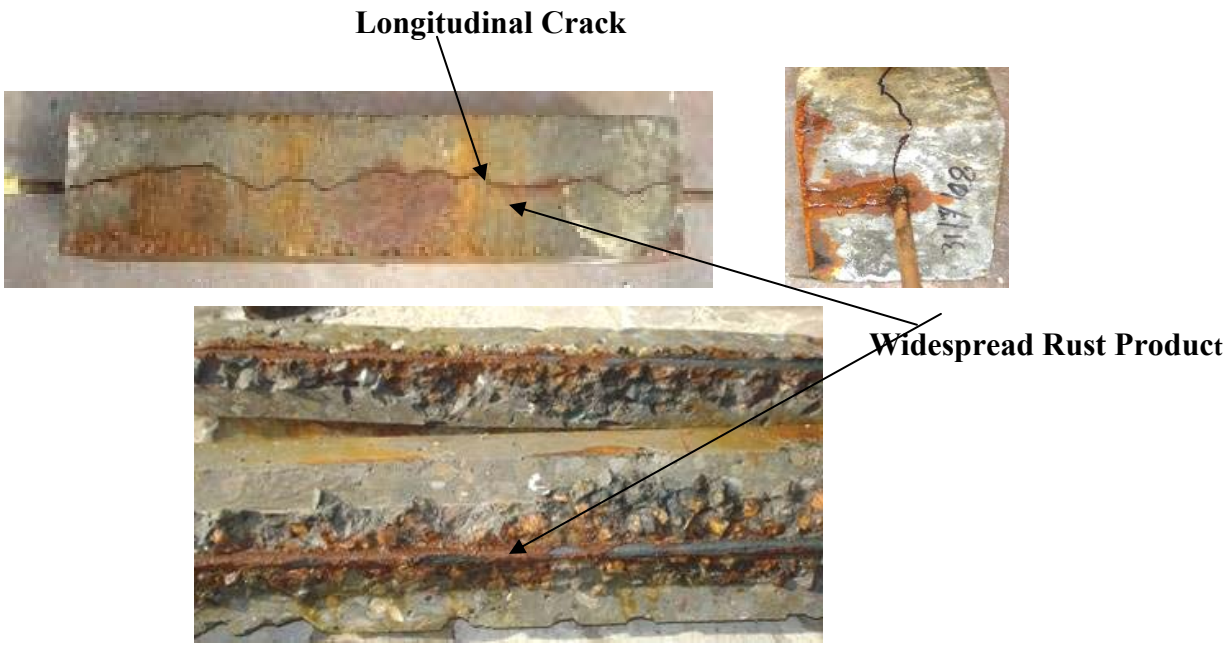

(a) Corroded beam

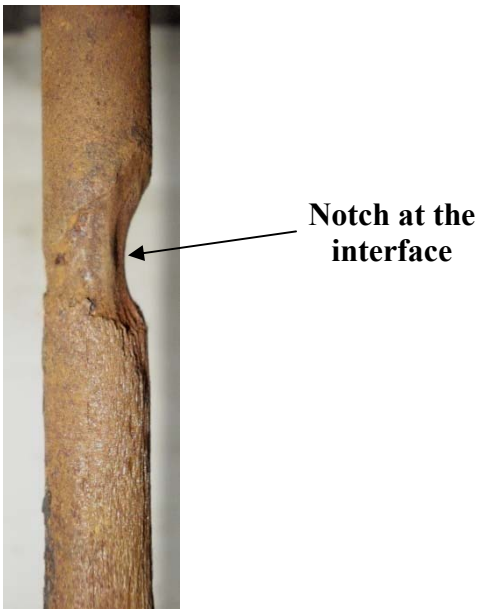

(b) Extracted bar

Fig 5.2: Condition of beam after 8 days of accelerated CC (12mm bar in concrete)

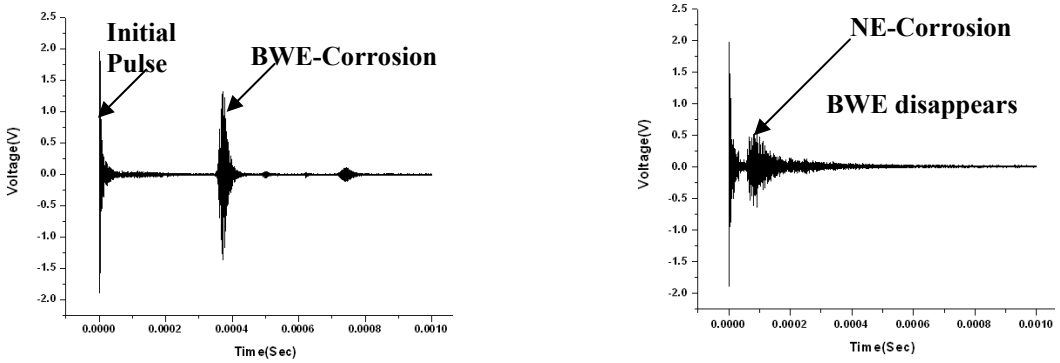

(a) 1st day signature **(b) 7th day signature**

Fig 5.3: Pulse Echo signatures during accelerated corrosion

(12mm bar in concrete)

5.3.2 Pulse Transmission testing

The pulse transmission studies where corrosion is simulated as the loss of bond indicates that the transmitted signal strength goes up due to prevention of leakage into the concrete affected through the loss of bond. Contrary to this observation, the transmitted pulse (P/T-corrosion) steadily losses strength as the corrosion progresses. It disappears completely on the 7th day **(Fig 5.4)**.

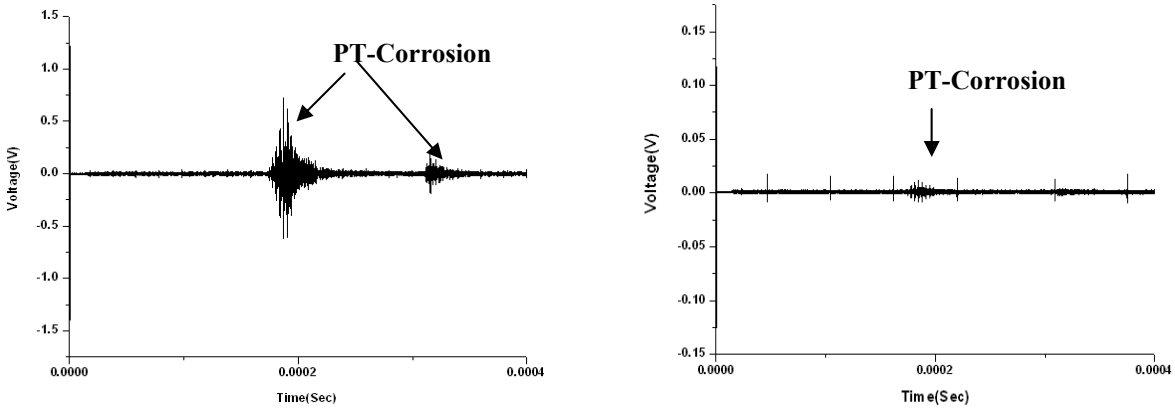

(a) 2nd day Signature **(b) 6th day Signature**

Fig 5.4: Pulse Transmission signatures during accelerated corrosion

(12mm bar in concrete)

The most likely cause of this phenomenon is that corrosion affects the waveguide. In the fresh bar, the diameter is uniform through the length. Thus, a smooth waveguide forms **(Fig 5.5)**. Corrosion reduces the diameter of the bar non-uniformly. Thus, the waveguide is disturbed and scattering takes place from the rough surface.

Moreover, chloride corrosion is characterized by large pittings and area loss which further restricts the passage of waves. While notches restrict the passage of the waves, smooth delamination would facilitate the passage. Thus, pittings and delaminations counteract each other. Thus, chloride corrosion is simulated better as notches rather than delamination.

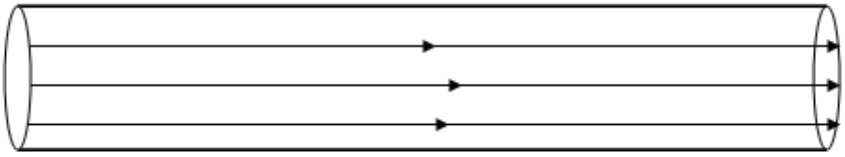

(a) Undamaged Bar

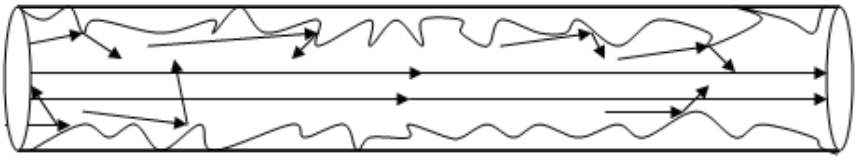

(b) Corroded Bar

Fig 5.5: Effect of corrosion on guided wave

Another contributing factor to the relative sensitivity of ultrasonic waves to pitting and delamination is the selection of mode. **Fig 4.22** shows the displacement mode shape and radial strain energy density distribution for L (0, 7) mode selected in the present investigation. The energy is concentrated in the central core portion of the bar and has relatively less surface component. Hence, it is more sensitive to local bar topography or loss of material changes and not the surface changes. Thus, this mode may not be sensitive to delamination that is more of a surface phenomenon. A mode that has significant surface

component will be sensitive to debonding effect of corrosion of the bar as discussed further in **Section 5.3.2**. Pulse Echo trends showing the BWE-Corrosion and NE-Corrosion are shown in **Fig 5.6.** Pulse Transmission trends depicting peak-to-peak signature voltage ratios P/T –Corrosion are shown in **Fig 5.7.** First and second cracks appeared on the surface of the beam on 3rd and 5th days as observed visually which is also depicted by sudden fall in voltage ratios at the same days.

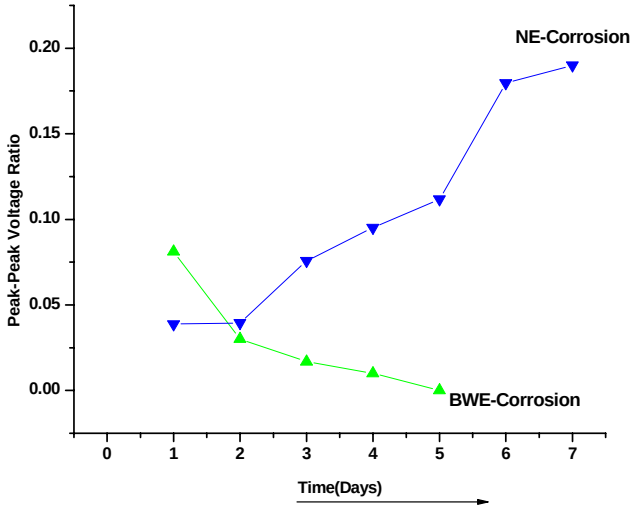

Fig 5.6: Peak to Peak voltage ratio trends in P/E in accelerated corrosion (12mm bar in concrete)

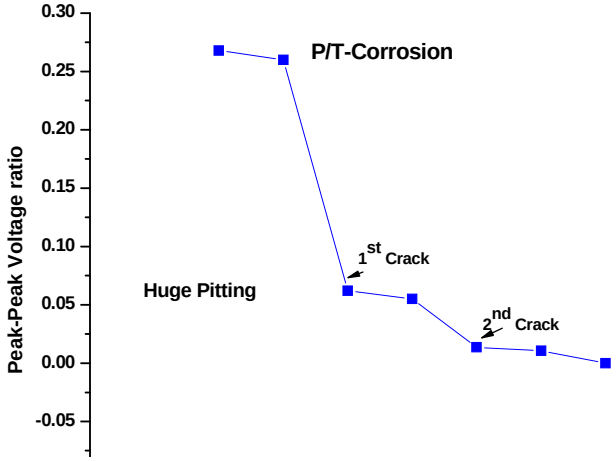

Fig 5.7: Peak to Peak voltage ratio trends in P/T in accelerated corrosion (12mm bar in concrete)

5.3.3 Destructive Tests

The bars are subjected to a series to destructive tests after the period of exposure is completed. After eight days, the bar is removed from concrete and washed with acetone. It is checked for percentage mass loss and tensile strength **(Fig 5.8)**. The bar losses 18.6% of its mass. In tensile test, the bar fails in the region where a huge area loss is observed. Corrosion causes substantial local weakening where the failure is observed. The tensile strength reduces to 20% of that of healthy bar. These reductions in mass and ultimate tensile strengths correlate well with the ultrasonic monitoring results wherein the signal experiences huge signal attenuation both in pulse echo and pulse transmission modes.

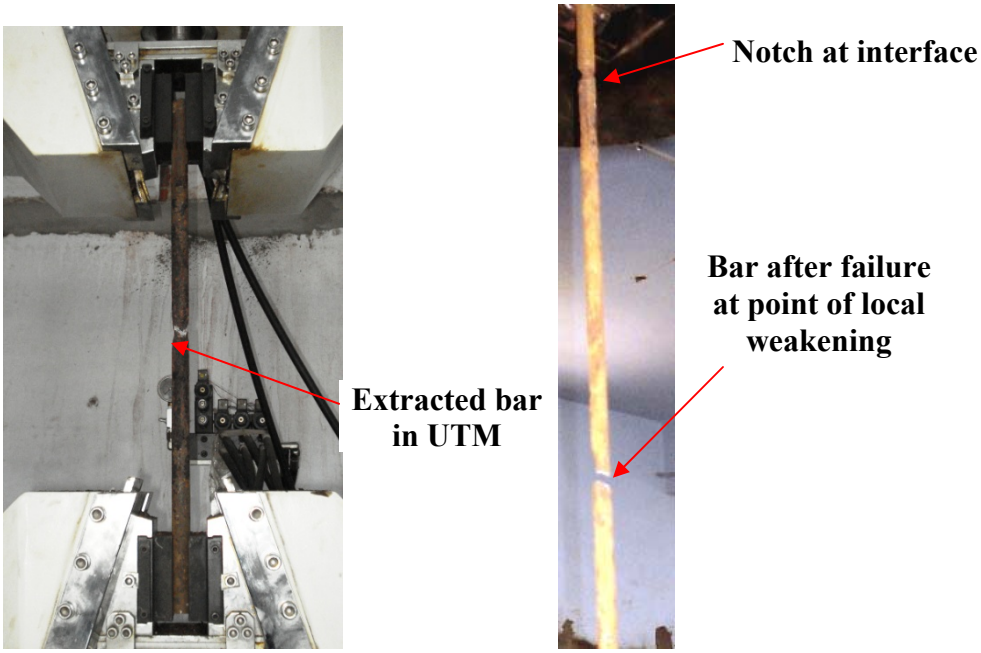

Fig 5.8: Bar undergoing tensile testing in a UTM

5.4 25 MM BAR IN CONCRETE

As observed in the ultrasonic investigations of 12mm bar in concrete, L (0, 7) mode selected could not pick up delamination effect caused by corrosion. As discussed, this is due to the displacement mode shape and radial strain energy density distribution of this mode. L (0, 7) mode is a core seeking mode and the energy is concentrated in the central core portion of the bar and has relatively less surface component. Hence, it is more sensitive to local bar topography or loss of material changes and not the surface changes. Thus, this mode is not

sensitive to delamination that is more of a surface phenomenon. A mode that has significant surface component would be sensitive to debonding effect of corrosion of the bar.

Also, it may be recalled that oxide corrosion and chloride corrosion had different effects on the bar. While oxide corrosion mainly affects the surface of the bar, chloride corrosion leads to pitting inside the bar. Thus, a mode that has significant surface component would be sensitive to oxide corrosion. It is evident that L (0, 1) is such surface seeking mode **(Fig 5.9)**. Hence, for chloride corrosion which would manifest itself in a mode that progresses mainly through the core of the bar and has negligible surface component, L (0, 7) mode is such a core seeking mode. Thus, these two modes have been considered in an attempt to distinguish between oxide and chloride corrosion through ultrasonics and to pick up debonding and pitting effects of corrosion.

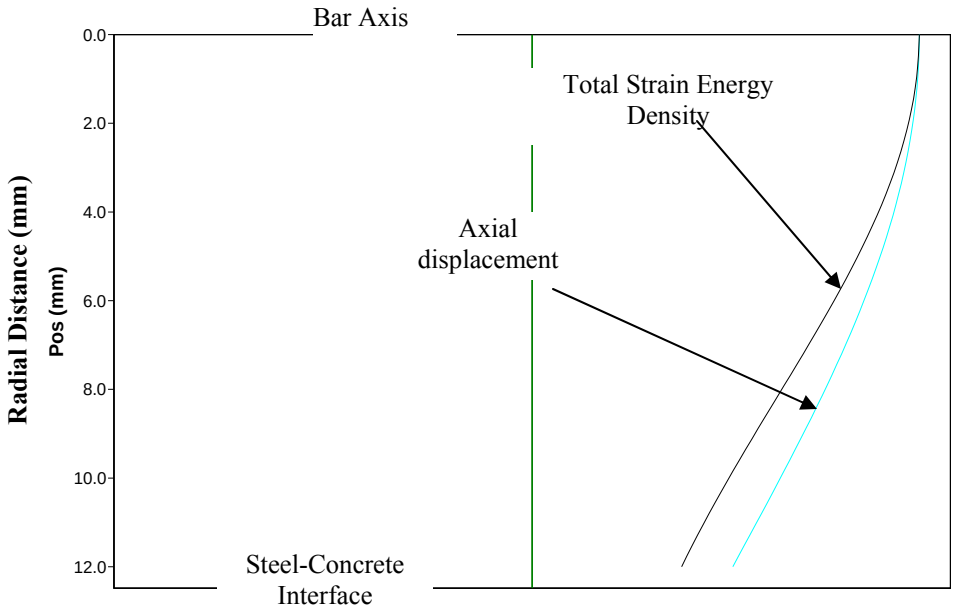

Fig 5.9: Mode shape of Surface Seeking Mode, L (0, 1) at 100 kHz

For 25 mm bar embedded in concrete, beams are subjected to two corrosion environments i.e chloride corrosion and oxide corrosion. For inducing Chloride Corrosion, a dripping mechanism is fitted on the wire mesh to keep the cotton underneath saturated. 5% NaCl solution is used as drip.

In Oxide Corrosion (OC), plain tap water is used instead of NaCl solution. Cotton gauge below the wire mesh uniformly distributed the water in the central wrapped portion of

the beam. The ultrasonic testing is monitored once everyday for 28 days until no significant change in received signal is observed. After 28 days exposure, both the corroded beams are subjected to pull out test and the extracted bar is checked for mass loss and tensile strength. The ultrasonic test results are compared with those of destructive tests.

5.4.1 Visual Observations

Beams undergoing accelerated impressed current CC showed reddish brown patches of corrosion products and a longitudinal crack parallel to the bar. The corrosion product shows different colour from the natural 'brown rust'. This can be attributed to the difference in the chemical composition of the corrosion products formed in natural and impressed current corrosion method (Poursaee et al. 2009; Yuan et al. 2007). Within 7 days, the cracks appear at the surface of the beam and progress along the direction of the reinforcement. With the increase in the volume of corrosion products, another crack parallel to the bar appears on another face of the beam after 15 days. A reddish brown liquid oozes out of the cracks and at the ends of the beam. The crack length and width increases with period of exposure. At 28 days of corrosion, there are two large and wide longitudinal cracks that divide the entire beam into two wedges and the beam is in a highly dilapidated condition **(Fig. 5.10a)**. Hence, chloride corrosion results in formation of large parallel cracks accompanied by oozing out of liquid corrosion product and extensive rust stains. The extracted bar shows significant pits and irregularities on its surface and very minor surface changes **(Fig. 5.10c)**.The loss of metal is irregular and deep pits are noticed at few places.

Contrary to this, in the beam undergoing OC, no visual change is observed until 15 days. Then a longitudinal crack appears parallel to the reinforcement accompanied by a small leakage of corrosion products. The crack increases in length and width but extends to only middle 1/2 length of the beam till 28 days. A significant observation is the appearance of a perpendicular crack at the centre of the beam. It appears on the 22nd day and progresses to divide the length of the beam into halves **(Fig 5.10b)**.

5.4.2 Ultrasonic Monitoring

5.4.2.1 Surface Seeking Mode

With surface seeking L (0, 1) mode, ultrasonic voltages are measured in pulse transmission mode only and pulse echo voltages are not measured. This is because of the

surface seeking nature of mode. It has very less energy for detecting notches produced a s a result of corrosion. **Fig. 5.11** shows ultrasonic voltage trends of the received signal in pulse transmission in both CC and OC specimens using surface seeking mode L (0, 1) at 100 kHz.

In the CC specimen, rise in signal amplitude is observed right from the 1st day indicating loss of bond between steel and concrete and this continues till 12 days. Then the signal amplitude continuously drops until it becomes more or less constant after 21 days. Initially, the formation of flaky rust product having large volume causes delamination of bar from the surrounding concrete resulting in increased signal amplitudes. This continues till the whole bar delaminates from the concrete (12 days). After this, the presence of chlorides results in deterioration of bar in the form of pits leading to attenuation of the signal. This indicates that chloride corrosion begins with bond deterioration and leads to pit formation and area loss as it progresses.

In the OC specimen, the received signal amplitude continues to rise till the end of exposure indicating increasing delamination during the whole period. But the rise in signal strength is slow as compared to CC. This shows that for the same period, OC affects only the surface of the bar causing delamination and no severe pitting or area loss. Corrosion is not as widespread as in CC bars. Delamination dominates the corrosion process and no pits are seen. Visual examination of the bar after conducting the pull out test reveals that there is localized corrosion product, small rust stains and a longitudinal crack in the middle 1/2 length of the beam. Because of this local pressure build up in a small length, a transverse crack appears in the centre of beam.

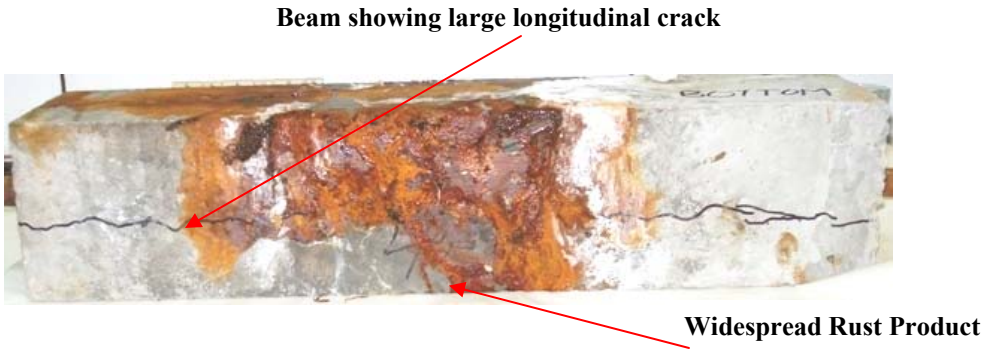

(a) CC Beam

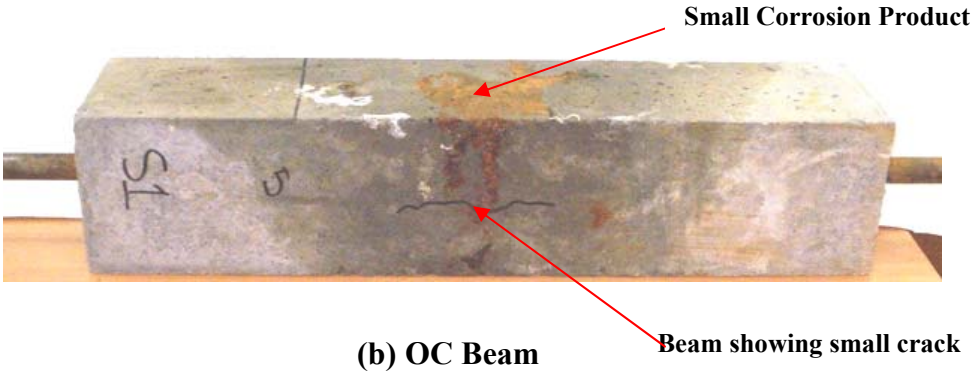

(b) OC Beam

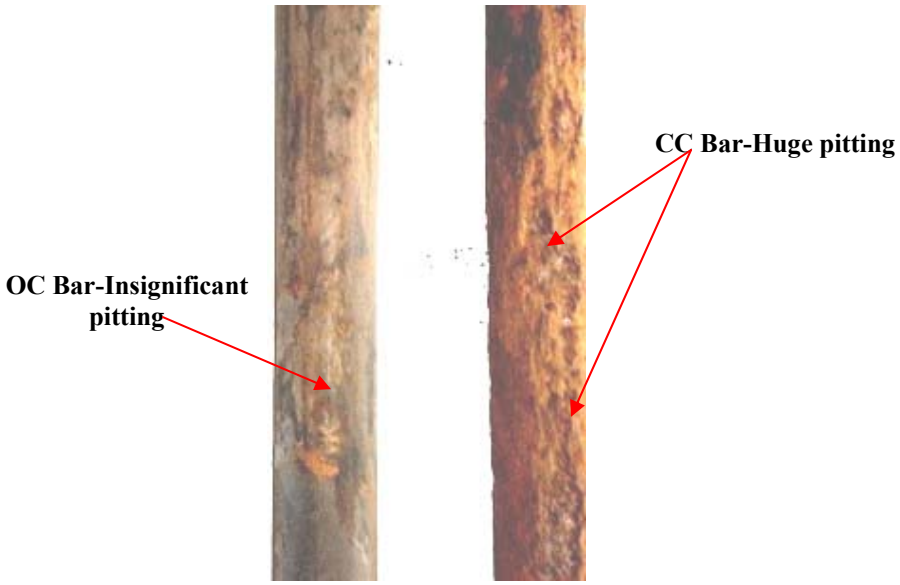

(c) Extracted Bars

Fig. 5. 10: Condition of beam after 28 days of accelerated CC and OC (25 mm bar in concrete)

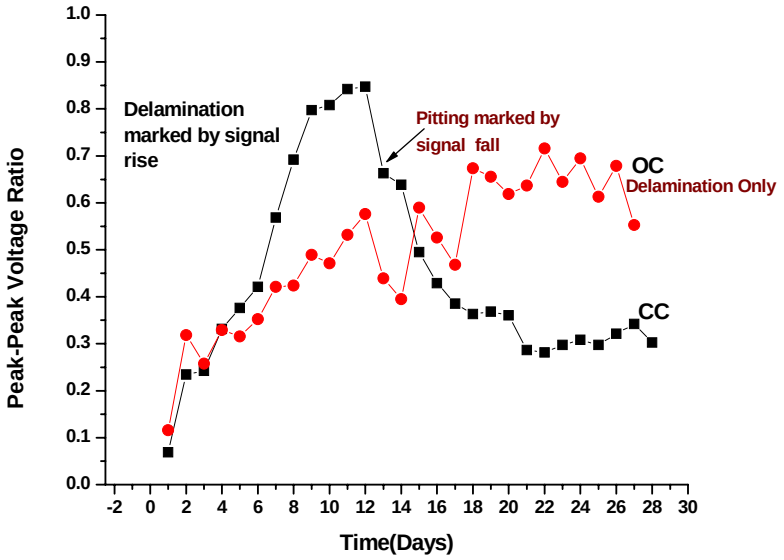

Fig 5.11: Peak to peak voltage ratio trends of transmitted pulse with L (0, 1) mode

(25mm bar in concrete)

5.4.2.2 Core Seeking Mode

With core seeking mode, L (0,7) at 1 MHz ultrasonic measurements are taken in both pulse echo and transmission modes. Ultrasonic pulse echo signatures are recorded everyday during the exposure to the corrosive environment. In the healthy bar, the signature is characterized by a strong back wall echo (BWE-corrosion). As the exposure proceeds, BWE-corrosion attenuates rapidly. It disappears completely on the 28th day **(Fig 5.12a)**. This is contrary to the expectation if corrosion is manifested through delamination only. Thus, it is clear that corrosion cannot be simulated as simple delamanition. It is a well known that in the presence of chlorides, pitting in the form of crevices occur on the steel bars. Moreover, it is likely that due to non-uniform loss of material from the surface, the smooth waveguide is disturbed, resulting in scattering of waves and thus attenuation of signal. It is clear that corrosion in the presence of chlorides is characterized by pitting and localized loss of material resulting in attenuation of BWE-corrosion.

The pulse echo testing of the same beam show no reflections from any localized notch or pit i.e. no NE-Corrosion is observed. Presence of any such damage perpendicular to the axis of the beam due to corrosion would have yielded a notch echo. The extracted bar shows widespread pitting and no local notch formation. Thus, no clear reflection from the notch is observed in a 25mm diameter bar probably due to its large crossectional area.

Fig. 5.12b shows ultrasonic voltage trends of the received signal in pulse transmission in both CC and OC specimens using core seeking mode L (0, 7) at 1 MHz. In CC specimen, the beam shows no significant change in voltage amplitude of the transmitted pulse till 6 days. After 6 days, there is a continuous drop in the amplitude of this pulse till it disappears completely on the 25th day. This point towards drastic non-uniform area loss in the form of pits on the whole length of the bar due to severe chloride corrosion. The widespread loss of area is confirmed visually by opening the beam. As corrosion progresses, there is increase in loss of energy due to scattering, multiple reflections and mode conversions. Hence, there is a drastic fall in signal amplitude. It is worth mentioning that only signal amplitude of this mode L (0, 7) is studied and there is no shift in arrival time of this mode as the exposure continues.

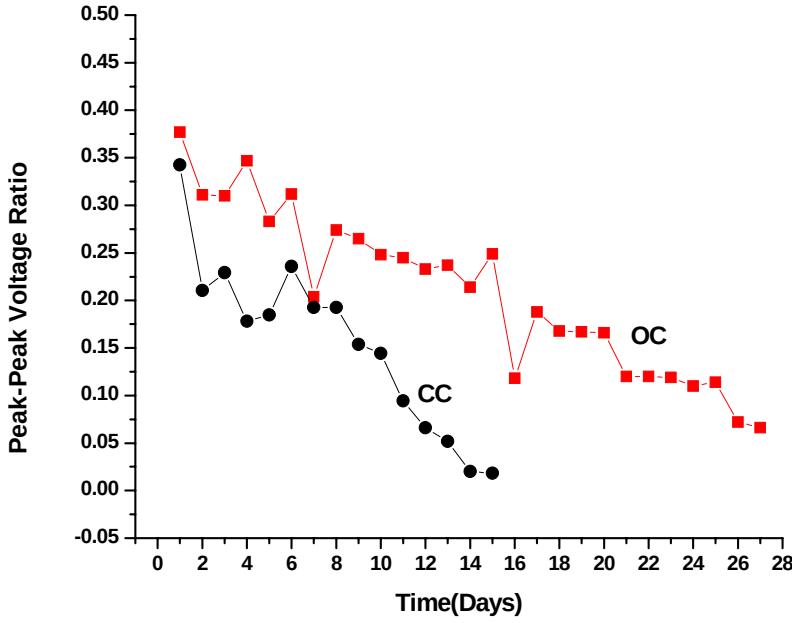

(a) Pulse Echo - BWE trends

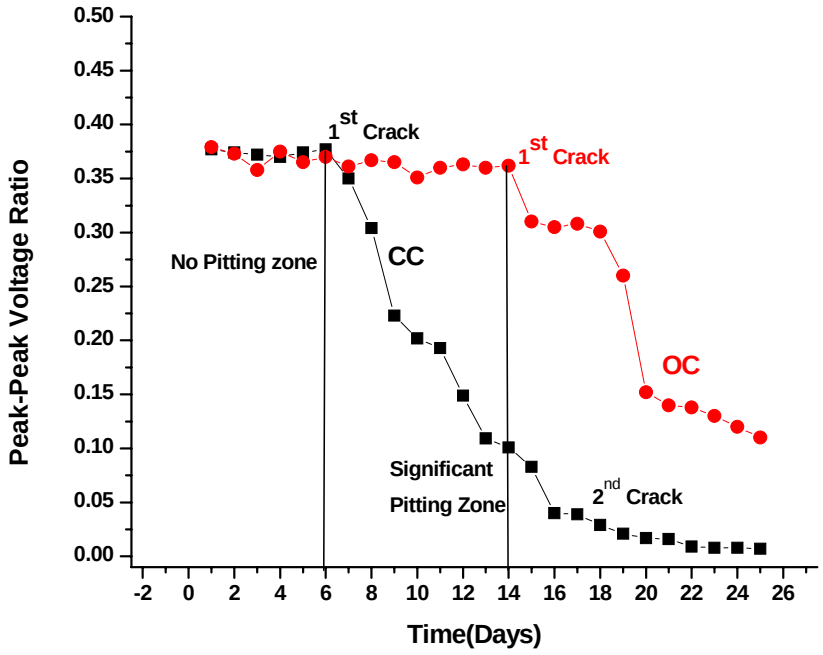

(b) Pulse Transmission- P/T trends

Fig. 5.12: Peak to peak voltage ratio trends of reflected and transmitted peaks with L (0, 7) mode

5.4.3 Study of Corrosion Mechanism using Guided Waves

A test matrix is developed for carrying out accelerated corrosion and ultrasonic monitoring in two environments. This is done to calibrate the ultrasonic data with different ages and stages of accelerated chloride and oxide corrosion by performing destructive tests of mass loss, pullout strength and tensile strength. Further tests for 6, 12, 18 days and 28 days confirm the repeatability of ultrasonic testing results. Ultrasonic signals in CC specimens disappear in 28 days so tests are limited to this period to facilitate comparison of OC and CC environments. To study the complete corrosion process in oxide environment, one OC beam specimen is ultrasonically monitored till the signals vanish in 130 days.

5.4.3.1 Beams undergoing Chloride Corrosion (CC)

From the study of CC ultrasonic signal plots with both surface seeking **(Fig. 5.13)** and core seeking modes **(Fig. 5.14)** and until the signals vanish, three distinct zones are observed:

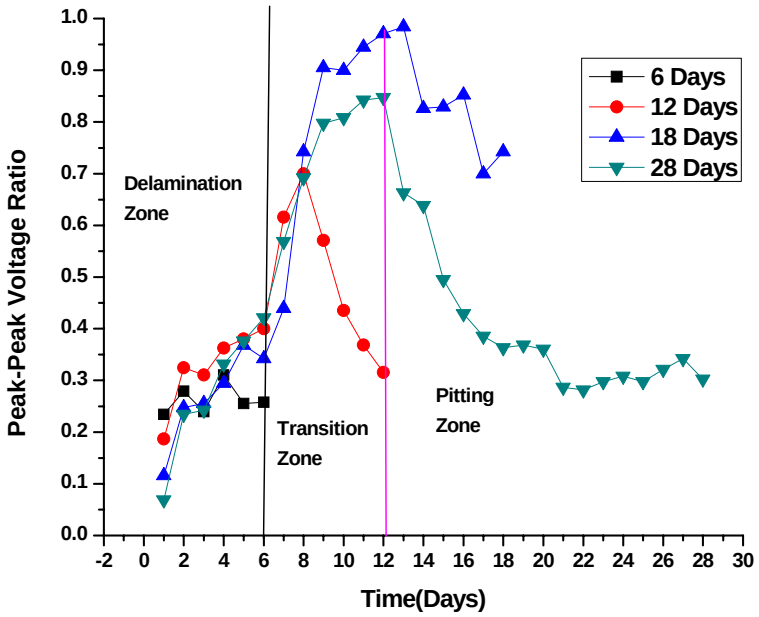

Fig. 5.13: Trends of transmitted pulse with L (0, 1) mode at different stages of CC

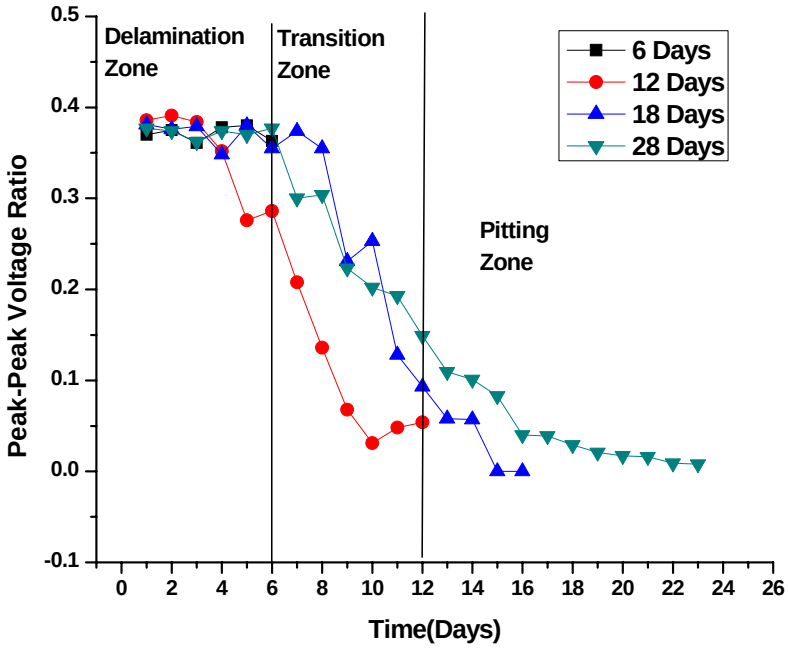

Fig. 5.14: Trends of transmitted pulse with L (0, 7) mode at different stages of CC

- First six days have a rising L (0, 1) signal but steady L (0, 7) signal indicating predominant surface changes but inappreciable core changes. This zone is referred as '*Delamination Zone*'.

- From six to twelve days, the L (0, 1) signal continues to rise but L (0, 7) signal fell significantly. This indicates that the corrosion makes inroads deeper in the bar and it is not restricted to the surface only. Thus, both modes of corrosion are present. This zone is referred as '*Transition Zone*'.

- Beyond the twelfth day, both L (0, 1) and L (0, 7) signals fell continuously exhibiting the same trend. At this stage, pitting of the reinforcing bar is predominant and this zone is referred as '*Pitting Zone*'.

- It is also being observed that the strength of L (0, 1) is significantly higher than that of L (0, 7). Thus, L (0, 1) mode has lower attenuation and it will travel longer distance through the bar.

From the CC ultrasonic plots, the mechanism of corrosion of reinforcing bar in presence of chlorides can be well understood. CC begins with the delamination of bar from the surrounding concrete marked by increased signal amplitudes. The delamination zone marks the onset of corrosion phenomenon in a bar undergoing accelerated CC and is well picked up by the surface seeking mode. As corrosion progresses, it is marked by local loss of area in the form of pitting and crevices along with debonding of bar. It begins in the transition zone shown by signal rise in L (0, 1) mode and signal attenuation in L (0, 7) core seeking mode. It marks the progress of corrosion causing surface modification as well as non-uniform area loss in the form of pits. As exposure increases, there is a drastic fall in signal amplitude in both L (0, 1) and L (0, 7) modes due to increase in loss of energy caused by scattering, multiple reflections and mode conversions. The most likely cause of this phenomenon is that corrosion affects the waveguide. Corrosion reduces the diameter of the bar non-uniformly. Thus, the waveguide is disturbed and scattering takes place from the rough surface.

The trends of peak-peak voltage ratios are same in the samples of different extents of corrosion in L (0, 1) mode **(Fig. 5.13)**. There is a rise in signal strength up to 12 days. This

signifies that corrosion begins with delamination. The drop in signal amplitudes beyond this point confirms the start of pitting phenomenon. The signal strength diminishes from this point till it completely vanishes. It may be noted that the 12 day sample had an early fall in signal strength in comparison to the other samples. This signifies premature pitting which is also captured by the L (0, 7) mode. The L (0, 7) mode that is sensitive to bar profile changes indicates same trends for 6, 12, 18 and 28 days of corrosion **(Fig. 5.14)**. In this case too, the 12 day samples exhibit early departure from other trends. Thus, there is a good correlation between L (0, 1) and L (0, 7) mode results. Hence, the mechanism of corrosion occurring due to chlorides is well picked up by surface and core seeking modes using ultrasonics.

5.4.3.2 Beams undergoing Oxide Corrosion (OC)

In case of beam undergoing OC, similar three zones are observed in ultrasonic signal plots as in CC plots but the process is spread over a vast duration of 130 days and took a long time **(Fig. 5.15, 5.16)**

- L (0, 1) signal continuously rises but very slowly for 50 days indicating predominant surface changes but inappreciable core changes **(Fig. 5.15).** From 1st to 22nd day, there is significant delamination and hence, this zone is called the *'Delamination Zone'*.

- From 22nd day onwards, L (0, 1) signal continues to rise **(Fig. 5.15)** but L (0, 7) signal starts falling though not very significantly as in case of CC **(Fig. 5.16)**. Oxide corrosion is a slow phenomenon resulting in surface modification as shown by L (0, 1) mode along with very slow ingress into the core from 22nd day to 50th day. In this zone, both modes of corrosion are present. This zone is referred as '*Transition Zone*'.

- Beyond the 50th day, both L (0, 1) and L (0, 7) signals fell continuously exhibiting the same trend. At this stage, pitting of the reinforcing bar is predominant and this zone is referred as '*Pitting Zone*'.

- Visual observation of the OC extracted bar after 130 days showed pits in localized length of about middle one third lengths. There is only surface modification in the remaining length of the bar **(Fig. 5.17)**.

- As observed in case of CC, it is also noted that the strength of L (0, 1) is significantly higher than that of L (0, 7) indicating lower attenuation of L (0, 1) mode.

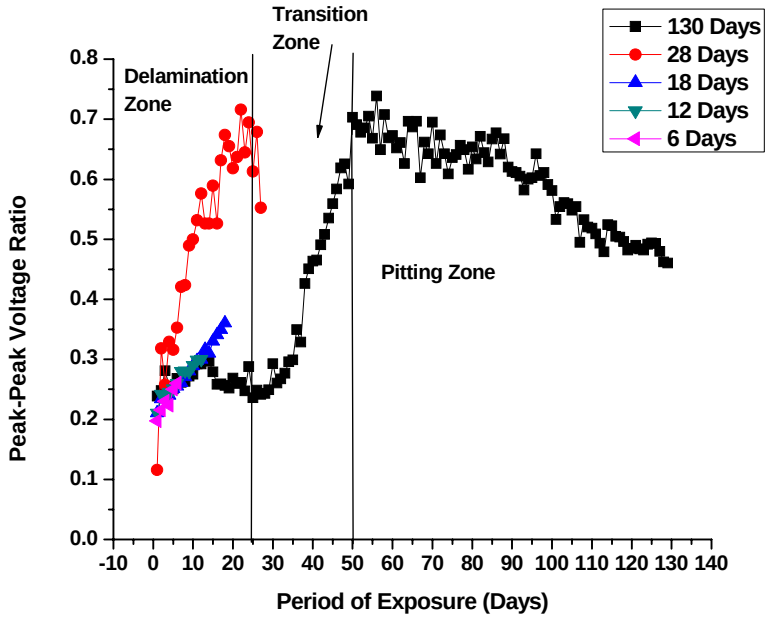

Fig. 5.15: Trends of transmitted pulse with L (0, 1) mode at different stages of OC

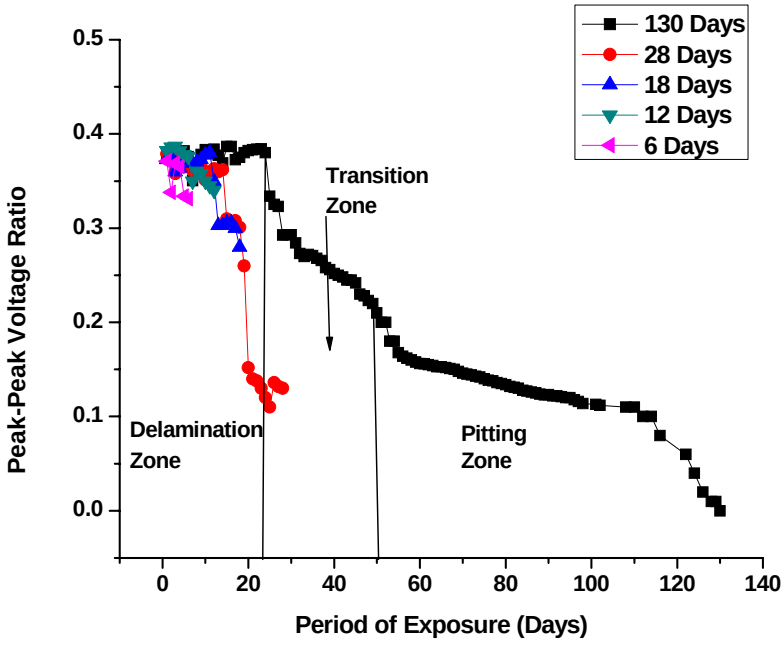

Fig. 5.16: Trends of transmitted pulse with L (0, 7) mode at different stages of OC

Hence, it can be concluded that OC is a slow process mainly resulting in the formation of rust product which is not widespread. It begins with slow delamination of the bar from the surrounding concrete for same period of exposure as CC specimen. Then slowly corrosion progresses towards the core and pitting starts but the pits are localized and the process takes a long time.

Same trends of peak to peak voltage ratios are observed for different periods of exposure in both L (0, 1) and L (0, 7) modes. There is rise in signal strength throughout the period of exposure in L (0, 1) mode indicating delamination for 6, 12, 18 and 22 days **(Fig. 5.15)**. There is no significant signal change observed initially for 22 days by the core sensitive L (0, 7) mode. It indicates no appreciable core changes **(Fig. 5.16)**. After 22 days, fall in signal strength is observed indicating ingress of corrosion into the core. But this fall is not as appreciable and drastic as observed in CC corrosion. Oxide corrosion is a slow phenomenon resulting in surface modification as shown by L (0, 1) mode along with slow ingress into the core from 22nd day to 50th day. After this transition zone, from 50th day onwards, pitting begins till the signal vanishes in 130 days. Hence, OC is well evaluated by both L (0, 1) and L (0, 7) modes.

5.4.4 Destructive Testing and Calibration of Ultrasonic Results

The bars are subjected to a series to destructive tests after the period of exposure is completed. The pullout strength of the interface is determined by securing the specimen in a universal testing machine (UTM) and applying a tensile force on the bar at a rate of 0.02 mm/sec **(Fig. 5.18)**. Tensile testing and mass loss of the extracted bar are performed to establish the effect of corrosion on the mechanical properties. The bar is first cleaned with wire brush and then with acetone to remove all the corrosion products. It is weighed to evaluate its residual mass. The bar is then tested for tensile strength in UTM to determine its residual strength.

5.4.4.1 Beams undergoing Chloride Corrosion (CC)

Destructive Testing Results

After 6 days of exposure, the pullout strength almost doubled **(Table 5.1)**. This is due to the increase in bond as a result of pressure generated by initial formation of corrosion product around the extruded mild steel bar. As the corrosion progresses, pullout strength drops due to debonding of the bar from the surrounding concrete as corrosion increased. For 28 days of

exposure specimen, the pullout strength is 28 % lower in comparison to 6 days exposure specimen. After the pullout strength, the bars are dug out of the beam. The corrosion products are spread in the whole length of the beam accompanied by reddish brown stains and longitudinal cracks. The 28 day bar had lost 5.15 % of its mass and 32.8% of its tensile strength to that of healthy bar. Higher percentage of strength in comparison to the mass indicates that the loss of mass is not uniform and is rather local. The visual inspection also confirms that the bar has experienced severe and widespread pitting.

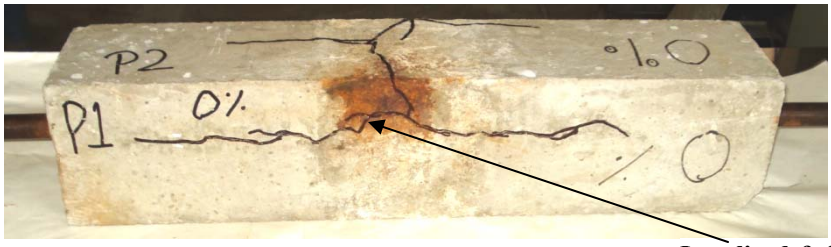

(a) Front & Top Face of Beam

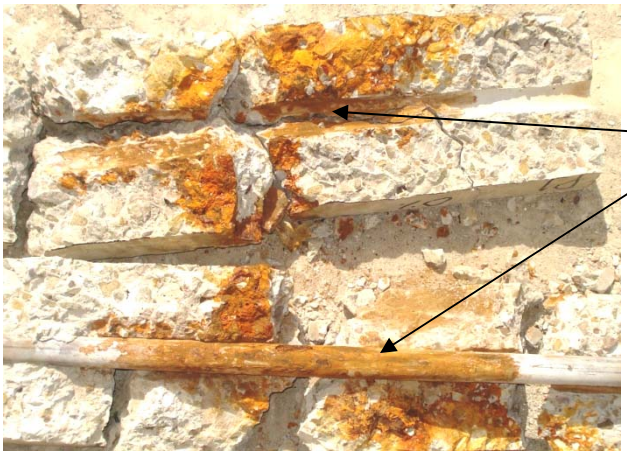

(b) Opened Beam

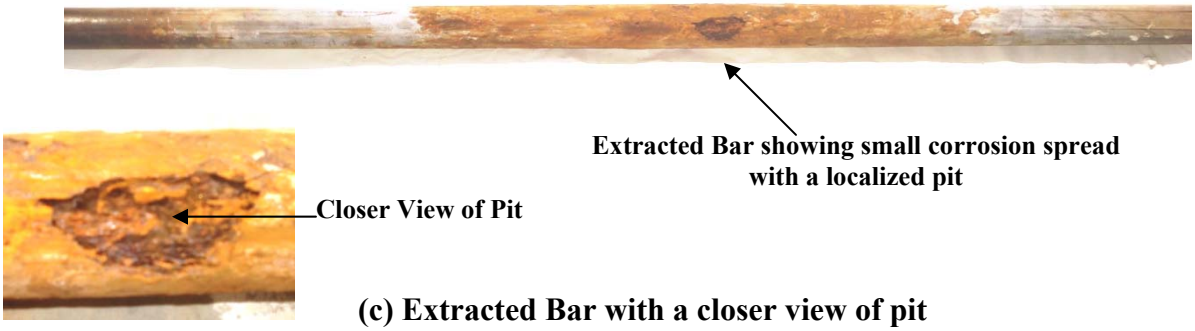

(c) Extracted Bar with a closer view of pit

Fig. 5.17: OC beam specimen after 130 days of corrosion

Fig. 5.18: Beam undergoing pull out test in a UTM

Table 5.1: Destructive Testing Results for beams undergoing CC

Property	**Exposure (Days)**				
	0	**6**	**12**	**18**	**28**
Mass Loss (%)	0	0.141	4.19	5	5.96
Pullout Strength (kN)	25	55	50	47.50	20
Tensile Strength (N/mm^2)	671	660	552.36	511.6	451

As seen from the destructive test results for different days of exposure for CC specimens, loss in mass (ML_t), pullout strength (PO) and tensile strength (f_t) is observed with the increase in the days of exposure. From the mass loss results, it can be seen clearly that the mass loss until the 6^{th} day is marginal. There is a sudden increase in mass loss from 6^{th} – 12^{th} day. After 12^{th} day, increase in mass loss continued but at a slower rate. This signifies that the initial delamination corrosion that takes place at the surface of the bar does not lead to a significant mass loss. At the onset of pitting, after the 6^{th} day, there is significant loss of mass. This is also corroborated by the sudden loss of tensile strength of the bar between 6^{th} and 12^{th} day. The loss of tensile strength indicates the loss of crossectional area of the bar.

The pullout strengths of the beam indicated that there is increase from 0^{th} to 6^{th} day. It may be recalled that the bars used in this experiment are plain extruded bars without any ribs. Thus, the initial bond at the steel – concrete interface is only through friction and there is no mechanical bond. Creation of corrosion products at the surface exert an outward pressure on the concrete. This improves the bond initially. But as corrosion progresses, the soluble corrosion products get washed away creating loss of interfacial bond and fall in pullout strengths.

Correlation of Ultrasonic Voltages with Destructive tests

A correlation is attempted to facilitate non-destructive estimation of the physical condition of the bar. It is important to choose the right mode of ultrasonic wave. It is indicated earlier that L (0, 1) mode is capable of detecting corrosion at early stage. However, it is not very suitable for mapping its output to the physical condition of the bar because the same voltage ratios may be obtained in very different physical conditions of the bar. In case of L (0, 7) mode, the signal decreases monotonically with the deterioration of the bar. Thus, it has one-to-one correspondence between the ultrasonic signal and the physical condition of the bar.

Fig. 5.19 shows the comparison between ultrasonic signals and destructive testing results of mass loss (ML_t), tensile strength (f_t) and pullout (PO) strength. It is clear that L (0, 1) may indicate very the same voltage ratios for very different mass losses. L (0, 7) mode, on the other hand, has a monotonically decreasing voltage ratio with mass loss **(Fig. 5.19 a).** The same trends are seen with other non-destructive parameters of pullout **(Fig. 5.19b)** and tensile strengths **(Fig. 5.19c)** as well. Thus, the calibration of the ultrasonic data with the physical state of the bar has been attempted with L (0, 7) mode only.

Mass Loss (ML_t)

The signal strength is highest at the initial stage and it reduces sharply with the loss of mass finally getting asymptotic once again. Thus, a hyperbolic curve **(Fig. 5.19a)** has been fitted between the voltage ratio and the mass loss given by (5.1).

Mass Loss, (ML_t, %) = ML_{max} /(1+ $100R_0R$) (5.1)

Where

R_0 = Initial peak-peak voltage ratio of the transmitted pulse w.r.t initial pulse

R = peak voltage ratio of the transmitted pulse w.r.t initial pulse at a particular instant

ML_t= Mass loss (%) anticipated at a particular instant

ML_{max}= Maximum % mass loss anticipated for a particular extent/degree of corrosion.

Bond Strength (PO)

It has been already indicated that the bond strength increased initially and then reduced due to corrosion. It is felt that to develop a reliable relationship between the voltage ratio and the bond strength, more data points would be essential **(Fig. 5.19b)**.

Tensile Strength (f_t)

The tensile strength of the bar reduces monotonically with corrosion. Thus, straight linefit **(Fig. 5.19c)** has been attempted for calibrating the residual strength with voltage ratio approx. given by,

$$f_t = \frac{f_0}{R_0} R \quad (5.2)$$

where, f_t = Tensile Strength at any instant (N/mm^2)

f_0 = Initial Tensile Strength (N/mm^2)

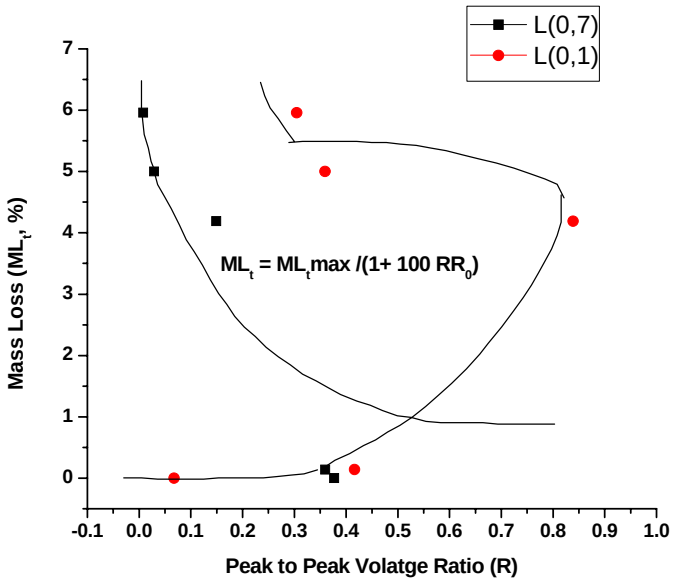

(a) % Mass Loss Vs Peak-Peak Voltage ratio(R)

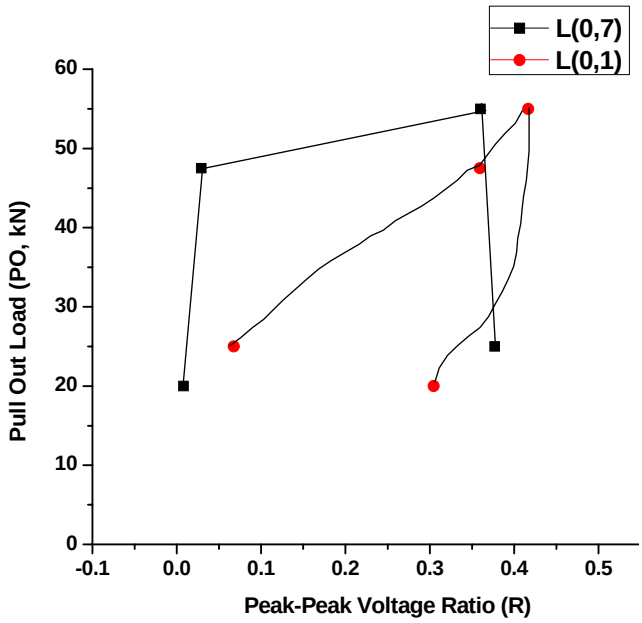

(b) Pullout Load* Vs Peak-Peak Voltage ratio

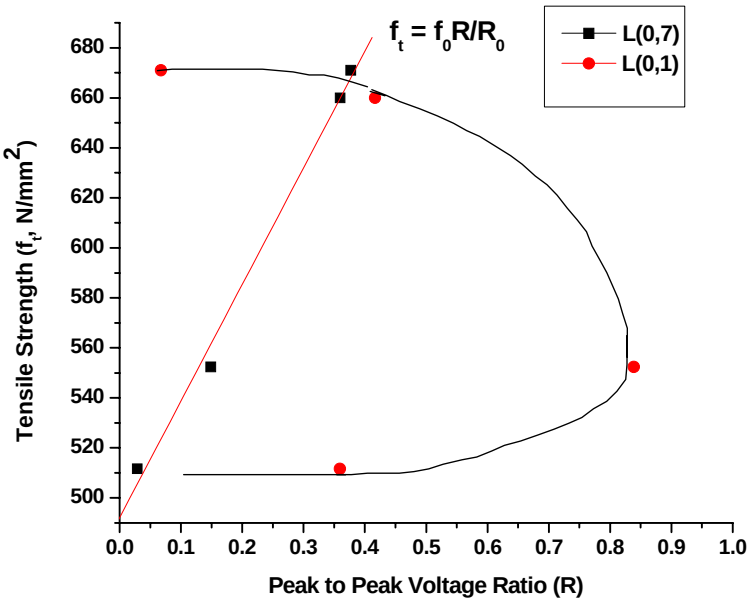

(c)Tensile Strength** Vs Peak-Peak Voltage ratio

Fig. 5.19 : Correlation of destructive CC results with peak to peak voltage ratio (R)

5.4.2.2 Beams undergoing Oxide Corrosion (OC)

Destructive Testing Results

In OC beam specimens **(Table 5.2)** as the exposure increased, the pullout strength continuously increases with the progress of corrosion. This is due to the formation of rust product having large volumes in comparison to the surrounding steel bar resulting in increasing bond strengths. Throughout the slow oxide corrosion process, only surface modification caused by corrosion products formation takes place. An increase in pullout strength by 51% of the healthy beam is observed after 28 days of exposure which increases by 2.6 times in 130 days of corrosion. It is because of the increase in bond of the plain bar to the surrounding concrete as compared to a healthy bar due to rust product formation in oxide corrosion. For the same exposure time, in the beam undergoing CC, corrosion is large, widespread and extensive and the rust product is washed away by chloride solution through the cracks results in release of pressure and decrease of bond. Hence, it experiences loss in pull-out strength.

Table 5. 2: Destructive Testing Results for beams undergoing OC

Property	**Period of Exposure (Days)**					
	0	**6**	**12**	**18**	**28**	**130**
Mass Loss (%)	0	0.1025	0.115	0.12	0.316	2
Pullout Strength (kN)	25	32	34	49	51.5	65
Tensile Strength (N/mm^2)	671	666.7	658.34	650.13	598.23	576.3

Also, the extracted OC bar observed only nominal loss in mass and tensile strength with the increase in corrosion. In 28 days, the bar experiences only 0.316 % and 10.88 % loss of its mass and tensile strength respectively. In 130 days, percentage mass loss and tensile strength increases marginally to 1.5% and 14.1% respectively. The higher percentage of strength and residual mass indicates that oxide corrosion does not lead to severe pitting and loss of metal. The

visual inspection also confirmed that the bar has not experienced large and widespread pitting and area loss.

As seen from the destructive test results for different days of exposure for OC specimens, nominal loss in residual mass (ML_t) and tensile strength (f_t) is observed with the increase in exposure to oxide environment. From the mass loss results, it is seen clearly that the mass loss is marginal. This indicates that delamination corrosion that takes place at the surface of the bar does not lead to a significant mass loss. This is also supported by insignificant loss of tensile strength of the bar. The pullout strengths (PO) of the beam indicate that there has been an increase from 0^{th} to 130^{th} day continuously. The bars as indicated are plain extruded bars where the initial bond at the steel – concrete interface is only through friction and there is no mechanical bond. Creation of corrosion products at the surface exerts an outward pressure on the concrete, thus improving the bond.

Correlation of Ultrasonic Voltages with Destructive tests

A correlation between the ultrasonic peak-peak voltage ratios (R) is done to facilitate non-destructive estimation of the physical condition of the bar. Similar to CC, L (0, 7) mode is mainly capable of detecting oxide corrosion throughout by mapping its output to the physical condition of the bar. In L (0, 1) mode, the voltage ratio increases initially as corrosion progresses with the deterioration of the bar in the form of delamination. Then amplitude shows drop after 50-60 days. Due to the variation in voltage trends with corrosion, L (0, 1) mode is not considered for calibration. With L (0, 7) mode, no initial change for 14 days is observed in voltage ratios when debonding predominates but after this period, the signal amplitude decreases with the deterioration of the bar. Hence, L (0, 7) mode is used to relate the ultrasonic signal voltages with the physical condition of the bar.

Fig. 5.20 shows the comparison between ultrasonic signals and destructive testing results of mass loss (ML_t), tensile strength *(f_t)* and pullout (PO) strength. L (0, 7) mode shows a monotonically decreasing voltage ratio with mass loss **(Fig. 5.20a).** The same trends are seen with other non-destructive parameters of pullout **(Fig. 5.20b)** and tensile strengths **(Fig. 5. 20c)** as well. Thus, the calibration of the ultrasonic data with the physical state of the bar has been attempted mainly with L (0, 7) mode.

Mass Loss (ML_t)

The signal strength of L (0, 1) mode initially increases and then starts falling as corrosion progresses. Since the signal strength shows variation in trends with the degradation of the bar, L (0, 1) mode is not used for calibration of OC. With L (0, 7) mode, as corrosion progresses, signal strength falls causing loss in mass and hence a linear relation between R and % mass loss has been established given by (5.3) and shown in **Fig. 5.20a.**

Mass Loss, ML_t (%) = ML_{max} (1- 100R/R_0) (5.3)

where

R_0 = Initial peak-peak voltage ratio of the transmitted pulse w.r.t initial pulse

R = Peak-peak voltage ratio of the transmitted pulse w.r.t initial pulse at a particular instant

ML_t= Mass loss (%) anticipated at a particular instant

ML_{max}= Maximum % mass loss anticipated for a particular extent/degree of corrosion.

Bond Strength (PO)

It has been already indicated that the bond strength increased as corrosion progresses with fall in signal strength in L (0, 7) mode. But the increase in bond strength is very nominal and a scatter of data points is obtained. Hence, it is felt that to develop a reliable relationship between the voltage ratio and the bond strength in OC as in case of CC, more data points would be essential **(Fig. 5.20b)**.

Tensile Strength (f_t)

The tensile strength of the bar reduces with corrosion indicated by fall in strength of L(0,7) mode. A linear fit is attempted between R and f_t in L (0, 7) mode as given in (5.4). A relationship of tensile strength with L (0, 1) mode is not attempted since the signal shows deviation in trends with progress of corrosion as in case of mass loss.

Tensile Strength, ft ($N/mm^{2)}$ = f_0 R/R_0 (5.4)

Where

f_t = Tensile Strength at any instant (N/mm^2)

f_0 = Initial Tensile Strength (N/mm^2)

Thus, it is confirmed that ultrasonics are capable of discerning the type and mechanism of corrosion of bars in RC structures. Also calibration of the ultrasonic voltages with some parameters relating to the physical condition of the bar is attempted. It is worth mentioning that

calibration of ultrasonic data is an initial attempt based on initial results obtained in limited tests and they would require further confirmation and fine tuning.

5.5 CLOSING REMARKS

Ultrasonic guided waves utilizing core and surface seeking modes can successfully be utilized for monitoring of corrosion in a bar embedded in concrete. In general, huge pitting and non-uniform area loss highlighted by severe signal attenuation marks chloride corrosion is well picked up by core seeking mode. It begins with delamination shown by signal rise with surface seeking mode. In oxide corrosion, the rate of corrosion is slow, localized and marked by slow bond deterioration as depicted by signal strength rise in surface seeking mode. Pitting is insignificant as shown by very slow signal fall in core seeking mode in OC. Thus, through a judicious selection of ultrasonic modes not only the corrosion phenomenon can be monitored but also different types of corrosion in RC structures can be successfully identified. The ultrasonic testing of the bar at different stages and ages of corrosion and the correlation between ultrasonic and destructive tests of mass loss, pull out strength and tensile strength justifies the ability of ultrasonics to predict the level of deterioration of the embedded bars in reinforced concrete. Thus, a mapping between the physical condition of the bar with the voltage ratios is successfully attempted in the form of algebraic equations. These should facilitate non-destructive evaluation of reinforcements embedded in concrete. However, the relationships presented here are based on limited early results.

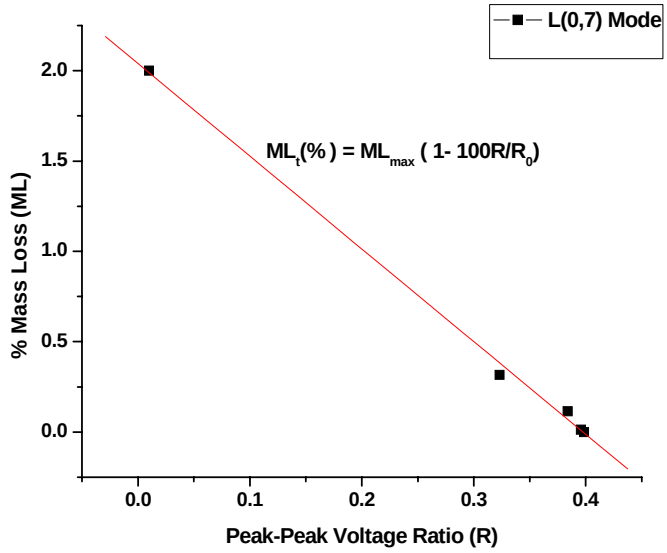

(a) % Mass Loss Vs Peak-Peak Voltage ratio(R)

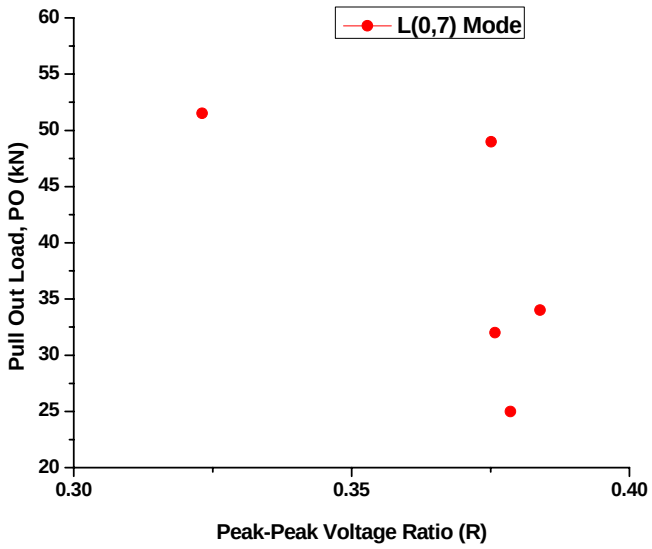

(b) Pullout Load Vs Peak-Peak Voltage ratio(R)

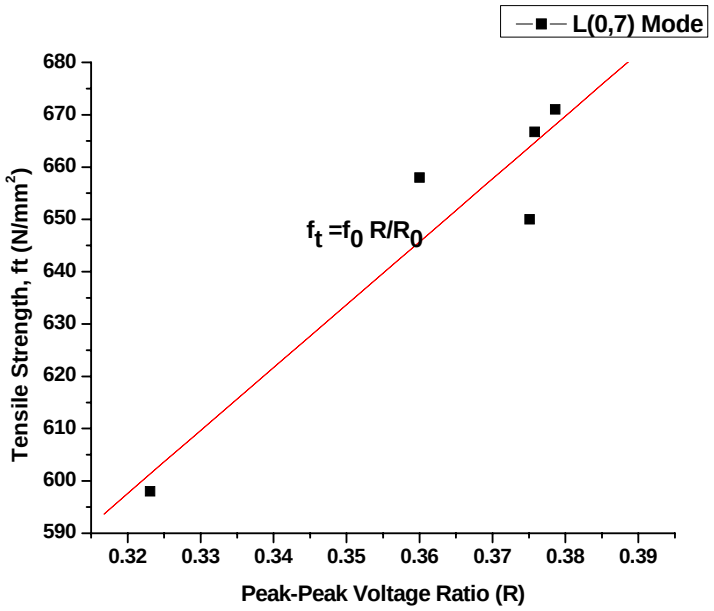

(c)Tensile Strength Vs Peak-Peak Voltage ratio(R)

Fig. 5.20: Correlation of destructive OC results with peak to peak voltage ratio (R)

CHAPTER 6

COMPARISON OF SIMULATED AND ACTUAL CORROSION

6.1 INTRODUCTION

Ultrasonic guided waves have been successfully used to develop a corrosion monitoring methodology for embedded reinforcements in concrete. However, it is important to excite the right mode for detection of particular type of damage. Both simulated and actually corroded bars have been investigated as described in preceding chapters.

Chapter 4 investigates the effect of local loss of material and loss of bond on the propagation of ultrasonic waves on simulated RC beam specimens. Simulated pitting effects are created by notches on the surface of the bar in varying percentages of its cross-sectional area. Simulated debond is generated by wrapping a double sided tape of varying length on the bar embedded in concrete. Ultrasonic guided waves utilizing pulse echo and pulse transmission techniques are used in combination to predict the presence, location and magnitude of the notch defects. Pulse transmission can relate to the percentage delamination very efficiently.

The ultrasonic monitoring technique developed in simulated studies is applied in-situ to bars embedded in concrete undergoing accelerated Chloride and Oxide corrosion in Chapter 5. Corrosion in the absence (OC) and presence of chlorides (CC) has been investigated. The rate of chloride corrosion is far higher and faster than oxide corrosion and its distinguishing feature is pitting right from the beginning, where crevices are formed in the bar leading to local loss of area. The developed guided wave monitoring methodology can identify both phenomena of pitting and debonding in embedded reinforcing bars. It can not only monitor the condition of embedded steel but also identify the type of corrosion undergone by the reinforcing steel. In the present chapter, the results of simulated and actually corroded bars for ultrasonic investigations are compared. The comparison has been done to estimate the suitability of simulation techniques.

6.2 12 MM BAR IN CONCRETE

Ultrasonic monitoring in pulse echo and transmission is carried out on 12 mm plain mild steel of 1.1 m length bar embedded in concrete. RC beam specimens of dimensions 150 mm x 150 mm x 700 mm are cast. As discussed in Section 4.3.2., one set of bars with simulated damages in the form of notches (with symmetrical 0%, 20%, 40% and 60% diameter reduction) are introduced in the middle of the bar before casting them in concrete. Another set of bars is wrapped with a double sided tape in varying percentages of 0%, 12.5%, 25%, 50%, 75% and 100% simulating delamination and are cast in concrete. As discussed in Section 4.2.1, L (0, 7) mode at a frequency of 3.5 MHz is chosen for study, being the fastest and lowest attenuating mode.

To estimate the suitability of the simulated corrosion experiments, RC beams undergoing accelerated chloride corrosion are created. The process is accelerated using impressed current as explained in Section 5.2.1. Both the simulated and beams undergoing accelerated chloride corrosion are ultrasonically monitored both in pulse echo and pulse transmission modes. A comparison is carried out to assess the suitability of the simulation technique used.

6.2.1 Comparison of Simulated and Actual Corrosion Studies

6.2.2.1 Pulse Echo testing

In simulated notch specimens, pulse echo records show the notch echo (NE- Notch) as well as the back wall echo (BWE-Notch). The appearance of NE indicates presence of the damage in the embedded bar. By knowing the time of flight of this echo, the location of the damage can be exactly computed. The magnitude of damage can be directly related to the magnitude of the NE as well as BWE. It is observed that the amplitude of NE increased and that of BWE reduced with the increase in the notch dimensions **(Fig 6.1)**. Therefore, the peak-peak voltage amplitudes of NE's and BWE's can be related to the extent of damage.

In specimens undergoing actual accelerated chloride corrosion, monitoring is done everyday during the exposure to the corrosive environment. In the healthy bar, the signature is characterized by a strong BWE. As the exposure proceeded, BWE attenuated rapidly (BWE-Corrosion). This is contrary to the expectation if corrosion is manifested through delamination only. Hence, in the presence of chlorides, pitting in the form of crevices occur

on the steel bars, and it cannot be manifested as delamination only. Moreover, it is likely that due to non-uniform loss of material from the surface, the smooth waveguide is disturbed, thus resulting in scattering of waves. Also, a NE appeared between the initial pulse and BWE on the 2nd day (NE- Corrosion). This indicates that pulses are reflecting from a localized neck formed in the bar due to corrosion. From the time of flight of the peak, the location of the neck can be estimated. It is at the bar-beam interface. After completion of the corrosion process, concrete is removed and the extracted bar is observed. A large notch is indeed seen at the estimated location. As corrosion increased, amplitude of this peak increased indicating increased loss of area from the interface.

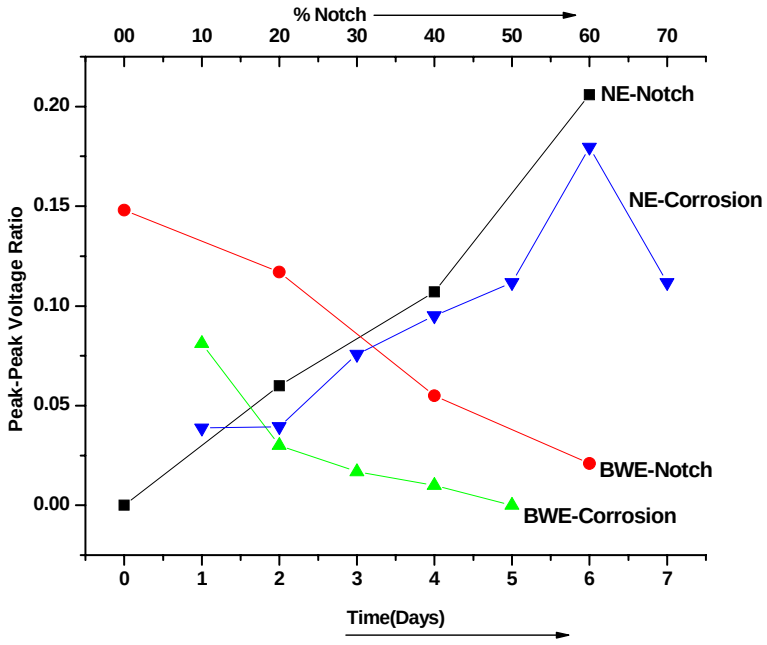

Fig 6.1: Peak to Peak voltage ratio trends in Pulse Echo

(12mm bar in concrete)

Fig 6.1 compares the pulse echo results of simulated and actual corrosion. The pulse echo testing methodology developed in simulated studies closely matches with the actual chloride corrosion phenomenon. As in the case of simulated studies, with the increase in percentage of damage, BWE falls and NE rises which is also observed in actual corrosion of bar. As corrosion progresses, BWE falls and NE rises. The location of NE can also be ascertained at the bar-beam interface as in case of notch location in simulated notch

specimens. It is clear that the actual corrosion results match closely with that of the notched samples. Corrosion in the presence of chlorides is characterized by pitting and localized loss of material similar to notches. In the present sample, one major notch developed due to corrosion resulting in a close match.

6.2.2.2 Pulse Transmission testing

In the pulse transmission records of simulated notch specimens, the peaks observed are the transmitted peaks obtained after traveling length 'L' of embedded bar. Arrival time of the pulse is not affected by the presence of the notch. Thus, the notch location is not discernible through pulse transmission. However, relative signal attenuation of the transmitted pulse (P/T-Notch analogous to P/T-1) can relate to the extent of the damage in the bar. The extent of damage in embedded bar can be ascertained by observing the peak-peak voltage trends of the transmitted peak. As the percent of damage increased from 0% to 60%, the magnitude of the transmitted peak reduces **(Fig 6.2)**.

In simulated debond specimens, as the percentage of delamination increases, the transmitted signal strength (P/T-Debond) keeps on rising. As the percentage of delamination between steel and concrete is increased from 0-75%, transmitted signal strength rises continuously since the amount of energy leaking into the surrounding concrete decreases with increase in percentage delamination.

The pulse transmission studies where corrosion is simulated as the loss of bond indicate that the transmitted signal strength goes up due to prevention of leakage into the concrete affected through the loss of bond. Contrary to this observation, the transmitted pulse steadily lost strength as the corrosion progressed. It disappeared completely on the 8^{th} day. The most likely cause of this phenomenon is that corrosion affects the waveguide. In a fresh bar the diameter is uniform through the length. Thus, a smooth waveguide forms. Corrosion reduces the diameter of the bar non-uniformly. Thus, the waveguide is disturbed and scattering takes place from the rough surface. Moreover, chloride corrosion is characterized by large pittings that further restricts the passage of waves. While notches restrict the passage of the waves, smooth delamination will facilitate the passage. Thus, pittings and delaminations counteract each other. **Fig 6.2** compares the peak-peak voltage ratios of simulated and actually corroded bars in pulse transmission. Clearly the results of notch

specimens are in closer agreement with the actual corrosion results. Thus, chloride corrosion is simulated better as notches rather than delamination.

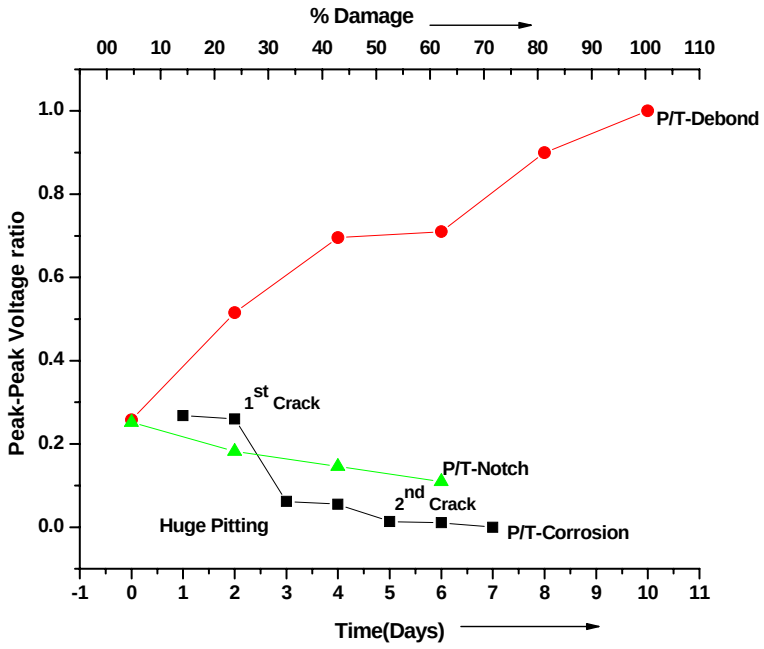

Fig 6.2: Peak to Peak voltage ratio trends in Pulse Transmission (12mm bar in concrete)

Another contributing factor to the relative sensitivity of ultrasonic waves to pitting and delamination is the selection of mode. The displacement mode shape and radial strain energy density distribution for L (0, 7) mode (**Fig. 5.6)** shows that it is a core seeking mode and has relatively less surface component. Hence, it is more sensitive to local bar topography or loss of material changes and not to surface changes. Thus, this mode may not be sensitive to delamination that is more of a surface phenomenon. A mode that has significant surface component should be selected for studying the debonding effect of corrosion of the bar.

6.2.2 Closing Remarks- 12mm bar in concrete

Ultrasonic guided waves at high frequencies can be effectively used for monitoring corrosion damages in reinforcing bars embedded in concrete by utilizing its wave guide effects. Corrosion is simulated as loss of bond and loss of area. The results have been compared with that of a bar undergoing accelerated chloride corrosion. The notch specimens had a closer agreement with the corroded bars than the debonded specimens. Chloride

corrosion roughens up the surface of the bar and creates large pittings. Thus, the effect of chloride corrosion is closer to that of a notched bar. In addition, the mode shapes of the selected wave have a profound effect on the sensitivity of the wave to the type of defect. For 12 mm bars in concrete, a centre seeking mode has been used. Thus, it is more sensitive to local defects rather than surface delamination. A surface seeking mode is more appropriate to study surface changes in the embedded bars. This is investigated in the subsequent section. By means of a judicious selection of ultrasonic modes, corrosion in RC structures can be successfully identified and monitored.

6.3 25 MM BAR IN CONCRETE

Ultrasonic monitoring in pulse echo and transmission is also carried out on 25 mm plain mild steel of 1.2 m length bar embedded in concrete. RC beam specimens of dimensions 150 mm x 150 mm x 700 mm are cast. As discussed in Section 6.2, similar specimens are manufactured in simulated as well as actual corrosion studies. As discussed in Section 5.3.2, for monitoring two different phenomena of pitting and delamination occurring as a result of corrosion, two different frequencies and modes have been identified. These modes of L (0, 7) and L (0, 1) are utilized for ultrasonic monitoring of simulated and actually corroding RC specimens in 25 mm bar specimens embedded in concrete. L (0,7) mode is sensitive to core changes while L(0,1) at low frequencies is sensitive to bar profile changes. It is a surface seeking mode as is evident from **Fig. 5.9.**

Two different types of corrosion i.e CC and OC samples are ultrasonically monitored both in pulse echo and transmission modes as discussed in Section 5.3.2. Both the simulated and beams undergoing accelerated chloride and oxide corrosion were ultrasonically monitored in pulse echo and pulse transmission modes and the results are compared.

6.3.1 Comparison of Simulated and Actual Corrosion Studies

6.3.1.1.1 Pulse Echo testing

In simulated specimens, pulse echo records for a 25 mm bar in concrete also shows NE as well as BWE. Appearance of NE-Notch indicates presence of the defect in the embedded bar. By knowing the time of flight of this echo, the location of the damage can be exactly computed. The magnitude of damage can be directly related NE as well as BWE. It is

observed that the amplitude of NE-Notch increased and that of BWE-Notch reduced with the increase in the notch dimensions. Therefore, the peak-peak voltage amplitudes of NE and BWE can be related to the extent of damage.

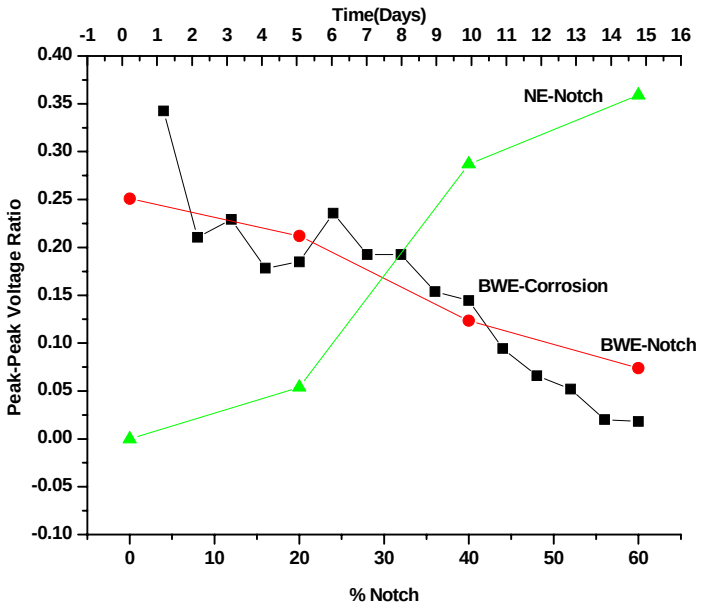

Fig 6.3: Peak-Peak voltage ratio trends of BWE & NE with L (0, 7) mode in CC (25mm bar in concrete)

In actual corrosion monitoring of specimens undergoing accelerated CC, ultrasonic pulse echo signatures are recorded everyday during the exposure to the corrosive environment. As in case of simulated notch specimens, as the exposure proceeds, BWE-corrosion attenuates rapidly. It disappears completely on the 28th day in CC specimen. These observations are similar to those observed in 12 mm bar. **Fig 6.3** compares the pulse echo results of simulated and actual CC corrosion specimens. It is clear that the actual corrosion results match closely with that of the notched samples. Corrosion in the presence of chlorides is characterized by pitting and localized loss of material resulting in attenuation of BWE-corrosion.

In specimens undergoing OC, the BWE-corrosion follows same trends but the fall is not very rapid as in CC specimens. This is because CC is pitting dominated phenomenon while OC results in more of surface irregularities. **Fig 6.4** compares the pulse echo results of simulated and actual OC corrosion specimens. Hence, OC cannot be simulated as notches.

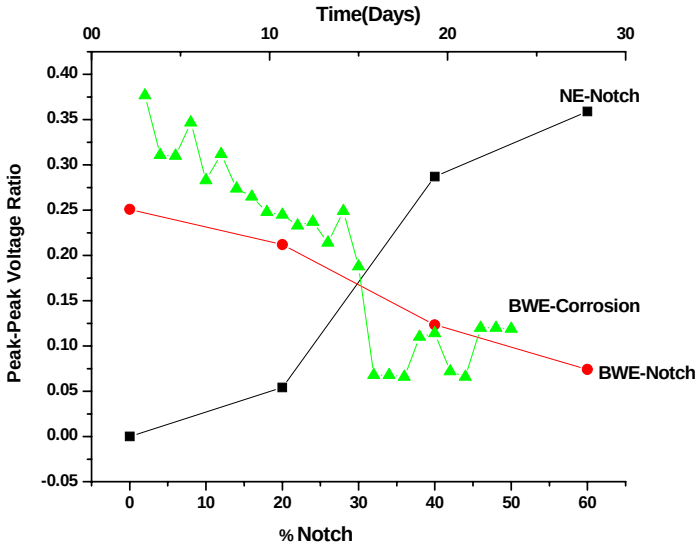

Fig 6.4: Peak-Peak voltage ratio trends of BWE & NE with L (0, 7) mode in OC (25mm bar in concrete)

The pulse echo testing of the same CC and OC beams showed no reflections from any localized notch or pit. Presence of any such damage perpendicular to the axis of the beam due to corrosion would have yielded a notch echo. This is confirmed by appearance of a notch echo in pulse echo testing of a 12 mm diameter bar embedded in beam subjected to same corrosion conditions as discussed in Section 6.2. Huge pit formation and hence, notch echo is not observed in a 25 mm diameter bar due to its large crossectional area.

6.3.1.2 Pulse Transmission testing

Core Seeking Mode

In the pulse transmission records, the peaks observed by L(0,7) mode are the transmitted peaks obtained after traveling length 'L' of embedded bar. As explained in 12mm bar case, the notch location is not discernible through pulse transmission. However, studying the relative change in the amplitude of input pulse and the transmitted pulse (P/T-Notch), an idea about the severity of the damage can be made. The extent of damage in embedded bar can be ascertained by observing the peak-peak voltage trends of the transmitted peak.

Pulse transmission studies of CC specimens with L (0, 7) mode where corrosion has been simulated as the loss of bond, indicate that the transmitted signal strength goes up due to prevention of leakage into the concrete affected through the loss of bond. Contrary to this observation, the transmitted pulse (P/T-corrosion) steadily lost strength as the corrosion progressed as in case of 12 mm bar. It disappeared completely on the 25^{th} day**.** Corrosion reduces the diameter of the bar non-uniformly. Thus, the waveguide is disturbed and scattering takes place from the rough surface**.** Moreover, as explained chloride corrosion is characterized by large pittings that further restricts the passage of waves. While notches restrict the passage of the waves, smooth delamination would facilitate the passage. Thus, pittings and delaminations counteract each other. **Fig 6.5** compares the peak-peak voltage ratios of simulated and actually CC corroded bars. Clearly the results of notch specimens are in closer agreement with the actual CC results at high frequencies. Thus, chloride corrosion is simulated better as notches rather than delamination with high frequency core seeking guided wave modes.

With OC specimens, the comparison of simulated and actual corrosion specimens is shown in **Fig 6.6.** With L (0, 7) mode which is a core seeking mode sensitive to surface changes in the embedded bar, there is no change in received signal strength till 15 days. Even after this time duration, the fall in voltage amplitude is insignificant. This is because OC results only in surface changes rather than huge pittings as observed in CC. Since this mode is insensitive to delamination, hence no drastic changes are observed in signal amplitudes. OC cannot be represented as notches with center seeking L(0,7) mode. It would be better simulated as delaminated specimens with a surface seeking mode.

Surface Seeking Mode

In L (0, 1) mode of testing on simulated specimens, as the percentage of delamination increases, the transmitted signal strength (P/T-Delam-Simulated) keeps on rising. As the percentage of delamination between steel and concrete is increased from 0-75%, transmitted signal strength rises continuously since the amount of energy leaking into the surrounding concrete decreases with increase in percentage delamination. At 100% delamination level, signal is same as received in case of a bar in air. Hence, an increase in the input signal

strength in pulse transmission in L (0, 1) mode can successfully relate to the presence as well as extent of delamination.

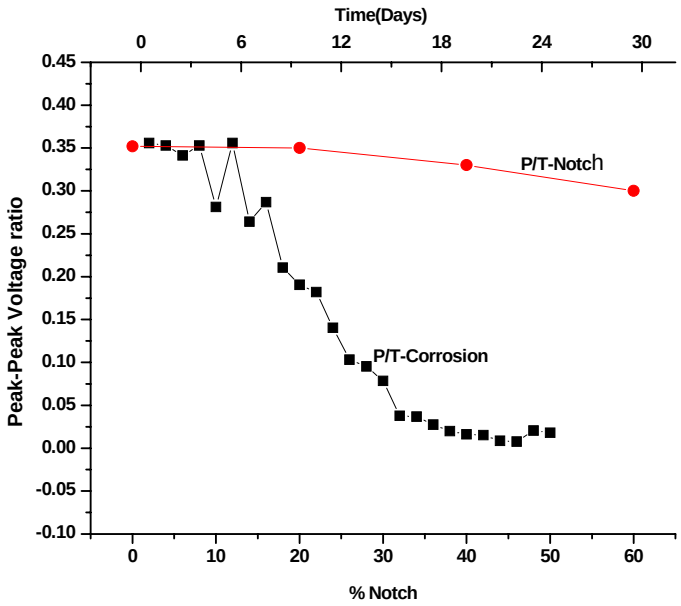

Fig 6.5: Peak-Peak voltage ratio trends of P/T with L (0, 7) mode in CC (25mm bar in concrete)

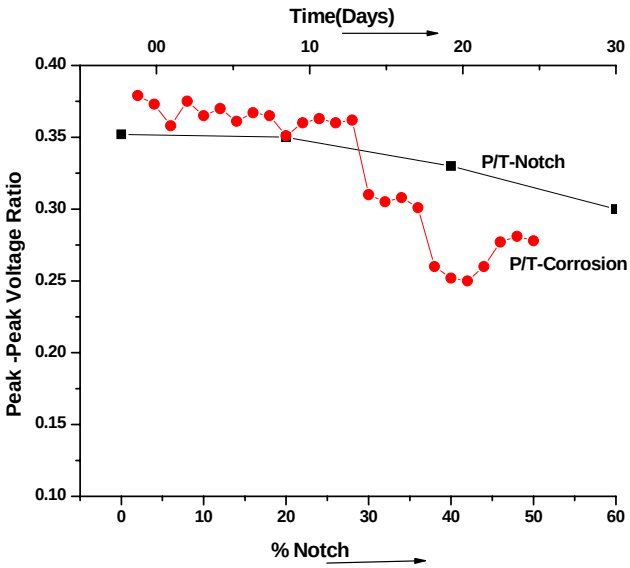

Fig 6.6: Peak-Peak voltage ratio trends of P/T with L (0, 7) mode in OC (25mm bar in concrete)

With L (0,1) monitoring of the beam specimen undergoing CC, rise in signal amplitude (P/T-Delam-Corrosion) is observed right from the 1st day indicating loss of bond between steel and concrete and this continued till the 12th day **(Fig 6.7)**. Then the signal amplitude continuously drops until it becomes more or less constant after 21 days. Initially, the formation of flaky rust product having large volume causes delamination of bar from the surrounding concrete resulting in increased signal amplitudes. This continues till the whole bar delaminates from the concrete (12 days). Thereafter, the presence of chlorides results in deterioration of bar in the form of pits and mode shows continuous fall. This indicates that chloride corrosion begins with bond deterioration and is well picked up by surface seeking L (0,1) mode. Thereafter, it leads to pit formation and area loss as it progresses and is simulated better as notches with L(0,7) mode.

In the OC specimen, the received signal amplitude continues to rise till the end of exposure indicating increasing delamination during the whole period. But the rise in signal strength is slow as compared to CC **(Fig 6.8)**. This shows that for the same period, OC affects only the surface of the bar causing delamination and no severe pitting or area loss. Corrosion was not as widespread as in CC bars. Delamination dominates the corrosion process and no pits were seen. Comparison of P/T-Delam-Simulated and P/T-Corrosion shows that OC roughens up the surface of the bar and the effect is closer to a delaminated bar.

6.4 CLOSING REMARKS

Ultrasonic guided wave methodology established in the study using low and high frequency ultrasonic pulse echo and pulse transmission on simulated notch and debond damages can be successfully applied for in-situ corrosion monitoring of embedded reinforcements in RC beams. It not only indicates the presence of damage but also gives the exact location and magnitude of damage by efficient combination of the two ultrasonic monitoring techniques. Ultrasonic guided wave monitoring utilizing specific core and surface seeking modes successfully identifies corrosion mechanism in a bar embedded in concrete. In general, huge pitting and non-uniform area loss highlighted by severe initial signal attenuation marks chloride corrosion is well picked up by core seeking mode. It begins with delamination shown by signal rise with surface seeking mode. It progresses in the form of huge pitting and crevices which is well picked up by core seeking mode. Chloride corrosion

roughens up the surface of the bar and creates large pittings. Thus, the effect of chloride corrosion is closer to that of a notched bar.

Oxide corrosion is a slow phenomenon which basically results in initial surface modification of the embedded bar undergoing corrosion. It is well picked up by surface seeking modes at low frequencies. Oxide corrosion roughens up the surface of the bar and and the effect is closer to that of a delaminated bar initially. Thus, through a judicious selection of ultrasonic modes, the complete corrosion mechanism and type of corrosion in RC structures can be successfully identified.

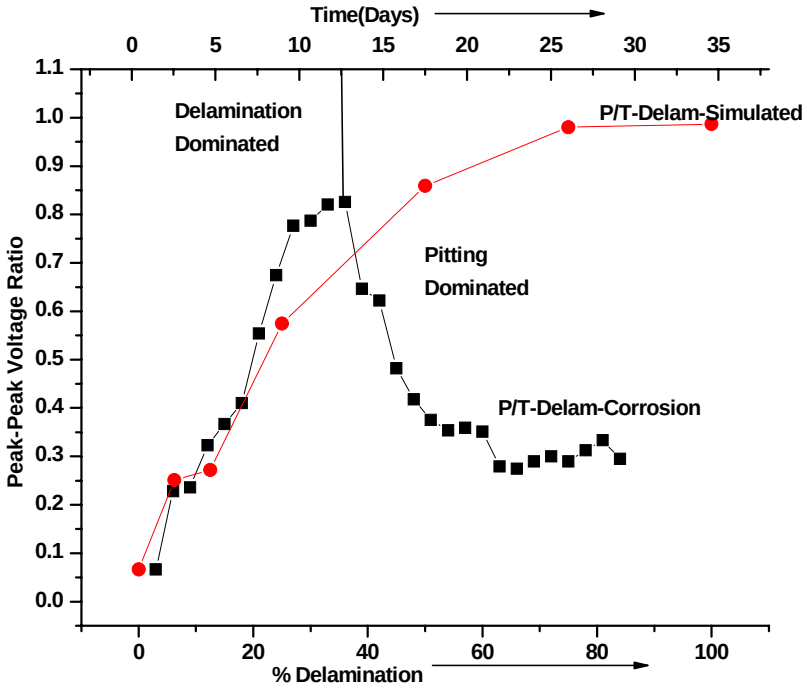

Fig 6.7: Peak-Peak voltage ratio trends of P/T with L (0, 1) mode in CC

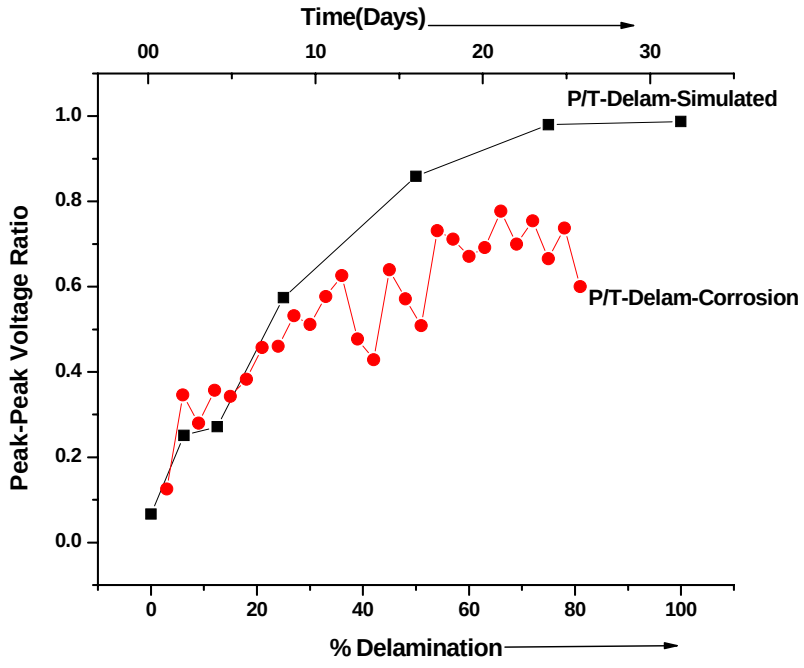

Fig 6.8: Peak-Peak voltage ratio trends of P/T with L (0, 1) mode in OC

CHAPTER 7

SUMMARY AND CONCLUSIONS

7.1 INTRODUCTION

There is an urgent need for a corrosion monitoring technique that can discern the location and map the extent of corrosion damages in embedded reinforcing bars in concrete. In this work, ultrasonic guided waves have been identified as a potentially effective technique for the same. Corrosion damage is simulated in the form of area loss (notches) and delamination (tape wrapped on embedded bar) from the surrounding concrete. Two ultrasonic techniques of pulse echo and pulse transmission are used to monitor healthy and damaged steel bars in air and then embedded in RC beam specimens. The methodology is then successfully applied to reinforced concrete beams specimens undergoing accelerated corrosion in two corrosive environments- i.e in presence of chlorides and in absence of it. The simulated and actual corrosion results are compared to study the effectiveness of simulation techniques. Effective combination of ultrasonic guided wave modes could identify the onset as well as other stages of both types of corrosion. The ultrasonic signals are calibrated to estimate the physical condition of the bars in terms of residual mass, tensile strength and pullout strength. The conclusions spread over the entire research have been summarized in the following sections.

7.2 SIMULATED CORROSION

Guided ultrasonic wave modes that are least attenuative and gave best signal outputs are used for ultrasonic investigations of reinforcing bars in air and embedded in concrete with simulated corrosion damages. The simulation of corrosion is carried out in two ways- loss of area (analogous to pitting) and loss of bond (analogous to debonding of the bar). For bars in air, pitting is simulated as area loss in varying percentages of area reduction. The embedded bars are seeded with a range of simulated notches and debond defects in the varying percentages of area reduction and delamination respectively. Pulse Echo and Pulse Transmission are used in combination to predict the presence, location and magnitude of the

corrosion damages. Following conclusions are drawn from the ultrasonic investigations of simulated corrosion studies:

7.2.1 Bars in Air

- The different longitudinal modes at the ends of the bar are produced by varying the excitation frequencies. Selection of frequencies is done based on the dispersion curves. They can be validated by experimentally confirming the signal fidelity. High frequency low loss modes are found to be the best.
- For bar with simulated pitting damage two techniques, pulse echo and pulse transmission are used for ultrasonic testing. In pulse echo testing, appearance of a peak corresponding to the notch, called notch echo (NE) indicates the presence of pitting damage in the bar. Time of flight measurement of NE indicates the damage location accurately. The magnitude of damage is directly related to the magnitude of the reflected peak received n from the notch (NE) as well as back wall echo (BWE). The amplitude of NE increases and that of BWE reduces with the increase in the notch dimensions.
- Pulse echo is a better indicator of the presence of the notch rather than the pulse transmission technique.
- In pulse transmission, the arrival time of the transmitted pulse remains unchanged due to varying location of notch. Thus, it is not feasible to ascertain the location of the damage using pulse transmission technique.
- Pulse echo is a preferred method for damage location since NE is more discernible and it directly gives the location.
- The extent of damage in the bar is ascertained by observing the peak to peak voltage trends of the transmitted pulse (P/T-1). As the percentage of damage increases from 0 to 60, the magnitude of the transmitted peak reduces continuously. Hence, relative signal attenuation of P/T-1 relates to the extent of the damage in the bar.
- The signal attenuation is not linear with the depth of notch. P/T-1 values drop very gradually with increase in notch dimensions. This is attributed to the parabolic input pressure profile generated by the transducer with the peak at its centre. Most of the

energy is able to pass through the core portion of the bar even though its periphery is notched.

- The amplitude of received signal in both pulse echo and pulse transmission is a measure of extent of damage. The two techniques when used in combination can predict the existence, location as well as the extent of damage in bars in air.
- The methodology developed utilizing the pulse echo and pulse transmission techniques for damage detection in cylindrical bars with damages in the form of notches is applied successfully to bars of variable lengths and diameters.

7.2.2 Bars Embedded in Concrete

Bars fabricated with notch and delamination damages simulating different aspects of corrosion are embedded in concrete and tested ultrasonically using the frequencies and modes selected using dispersion curves. Notches with symmetrical 0%, 20%, 40% and 60% diameter reduction are introduced in the middle of the bars before casting them in concrete and tested in pulse echo and pulse transmission modes. To simulate debonding of bar from concrete due to corrosion, another set of specimens is fabricated in which delamination is simulated by a wrapping a double sided tape on the steel bar to different extents of 0%, 6.25%, 12.5%, 25%, 50%, and 75% representing different extents of debonds and then embedded in concrete. As in case of bars in air, similar methodology can be applied for damage detection in bars in concrete. The following important observations and conclusions have been drawn:

- For bars embedded in concrete, which is a layered waveguide system, leakage plays an important role. High frequency low attenuation modes with displacement profiles centered in the middle of bar to minimize leakage are selected for layered systems.
- The modes selected for testing of bars embedded in concrete are high frequency modes corresponding to the points of maximum energy velocity and minimum attenuation. These modes are utilized for ultrasonic monitoring of simulated and then actually corroding RC specimens.

Simulated Notch Damages

- Appearance of NE in pulse echo testing indicates presence of notch damage in the embedded bar. By knowing the time of flight of this echo, the location of the damage is computed.
- The magnitude of damage is directly related to the magnitude of the peak received after reflection from the notch boundary (NE) as well as BWE. It is observed that the amplitude of NE increases and that of BWE reduces with the increase in the notch dimensions. Therefore, the peak-peak voltage amplitudes of NE and BWE are related to the extent of damage.
- It is observed that NE peak in Pulse Echo testing did not rise perceptibly even at 20% damage. Thus, its discernibilty to small notches is not very high. This is due to the mode shape of L (0, 7) mode which is a core seeking mode. The energy is concentrated in the centre of the bar and this mode is insensitive to minor surface irregularities.
- Studying the relative change in the amplitude of input pulse and the transmitted pulse (P/T-Notch), the severity of the damage is assessed. As the percent of damage increases from 0% to 60%, the magnitude of the transmitted peak (P/T-Notch) reduces. Hence, relative signal attenuation of the transmitted pulse is related to the extent of the damage in the bar.
- Peak to peak voltage amplitudes of reflected (NE) and transmitted peaks (P/T-Notch) in pulse echo and transmission methods respectively closely relate to the extent of damage. However, the attenuation of the peak is not linearly proportional to the extent of damage. This is again due to the core seeking nature of the mode used.
- The methodology for damage detection in notched specimens is similar irrespective of the diameter of the bar. Only excitation frequencies and modes have to be decided judiously for effective damage monitoring in embedded bars of different diameters.
- It is important to select an ideal low leakage mode for damage detection in RC structures. This is because of the huge amount of signal attenuation experienced by the input pulse due to the presence of attenuating concrete in comparison to bars.

Simulated Delamination Damages

- The presence of delamination did not affect pulse echo results. Hence, ultrasonic testing of simulated debonding is only carried out in pulse transmission mode.
- As the percentage of delamination increases, the transmitted signal strength (P/T-Delam) keeps on rising. As the percentage of delamination between steel and concrete increases from 0-75%, transmitted signal strength rises continuously since the amount of energy leaking into the surrounding concrete decreases with increase in percentage delamination. At 100% delamination level, the signal is same as received in case of a bar in air. Hence, an increase in the input signal strength in pulse transmission is successfully related to the presence as well as extent of delamination.

7.3 ACTUAL CORROSION

Ultrasonic investigations on RC beams that are reported earlier for corrosion damages have mainly remained confined to simulated scorrosion. After successfully developing a damage detection methodology in embedded bars with simulated corrosion damages, the present study is extended to investigate the applicability of ultrasonic guided waves to monitor RC beam specimens undergoing actual corrosion. Since natural corrosion would take decades to occur, it is accelerated by impressing anodic current. Two common types of corrosion mechanisms i.e oxide (OC) and chloride corrosion (CC) occurring in embedded reinforcements in concrete are considered in the study. The same modes and frequencies are used for testing as for simulated studies. The modes that are easily distinguishable and have lowest signal attenuation are selected. For the 12mm bar in concrete, L (0, 7) mode at a frequency of 3.5 MHz and for the 25mm bar, L (0, 7) mode at a frequency of 1MHz is used. Pulse transmission and pulse echo are monitored once everyday until no significant change in received signal is observed. The following major conclusions are drawn from ultrasonic investigations of actually corroding RC beam specimens:

7.3.1 Beams undergoing CC

- Visual observations of 12mm bar in RC beam undergoing accelerated chloride corrosion shows reddish brown patches of corrosion products and a longitudinal crack parallel to

the bar within 2 days. The cracks initiated at the center of the beam and progressed along the direction of the reinforcement.

- As the volume of corrosion products increased, another crack parallel to the bar appeared on another face of the beam after 6 days. A reddish brown liquid oozed out of the cracks and the ends of the beam. The crack length and width increased with increase in exposure. At 8 days of corrosion, two large and wide longitudinal cracks that divided the entire beam into wedges were observed and the beam was in a highly dilapidated condition.
- Pulse echo signatures of the healthy bar in RC beam are characterized by a strong BWE. As the exposure proceeds, BWE attenuates rapidly. It disappears completely on the 4^{th} day. This is contrary to the expectation if corrosion is manifested through delamination only.
- This indicates that corrosion cannot be simulated as simple delamination.
- Another significant observation is the appearance of a peak (NE) between the initial pulse and BWE on the 2^{nd} day. This indicates that pulses are reflecting from a localized neck formed in the bar due to corrosion. From the time of flight of the peak, the location of the neck can be estimated. It is at the bar-beam interface. After completion of the corrosion process, concrete is removed and the extracted bar is visually examined. A large notch is indeed seen at the estimated location.
- As corrosion increases, amplitude of NE increases indicating increased loss of area from the interface. Hence, corrosion in the presence of chlorides is characterized by pitting and localized loss of material similar to notches.
- Pulse transmission studies where corrosion is simulated as loss of bond indicates that the transmitted signal strength goes up due to prevention of leakage into the concrete affected through the loss of bond. Contrary to this observation, the transmitted pulse steadily loses strength as the corrosion progresses. It disappears completely on the 8^{th} day.
- The most likely cause of this phenomenon is that corrosion affects the waveguide. In the fresh bar the diameter is uniform through the length. Thus, a smooth waveguide forms.

Corrosion reduces the diameter of the bar non-uniformly. Thus, the waveguide is disturbed and scattering takes place from the rough surface.

- Chloride corrosion is characterized by large pittings and area loss which restricts the passage of waves. While notches restrict the passage of the waves, smooth delamination will facilitate the passage. Thus, pittings and delaminations counteract each other. Thus, CC is simulated better as notches rather than delamination.
- Another contributing factor to the relative sensitivity of ultrasonic waves to pitting and delamination is the selection of mode. The L (0, 7) mode selected for testing is a core seeking mode with the energy concentrated in the central core portion of the bar and has relatively less surface component. It is more sensitive to local bar topography or loss of material changes and not the surface changes. Hence, this mode is not sensitive to delamination which is more of a surface phenomenon.
- For 25 mm bars in concrete undergoing CC same observations are made with L(0,7) mode in both Pulse Echo and Pulse Transmission. Ultrasonic pulse echo signatures are characterized by a strong back wall echo (BWE-corrosion). As the exposure proceeds, BWE-corrosion attenuates rapidly. It disappears completely on 28th day. Ultrasonic voltage trends of the received signal in pulse transmission shows no significant change in voltage amplitude of the transmitted pulse till 6 days. After 6 days, there is a continuous drop in the amplitude of this pulse till it disappears completely on 25^{th} day. This points towards drastic non-uniform area loss in the form of pits due to severe chloride corrosion.
- The widespread loss of area is confirmed visually by opening up the beam. As corrosion progresses, there is increase in loss of energy due to scattering, multiple reflections and mode conversions. Hence, there is a drastic fall in signal amplitude.
- With surface seeking mode L (0,1), rise in signal amplitude of the transmitted pulse is observed right from the 1^{st} day indicating loss of bond between steel and concrete and it continues till 12 days. Then the signal amplitude continuously drops until it becomes more or less constant after 21 days. The reason for such signals is that initially, the formation of flaky rust product having large volume causes delamination of bar from the surrounding concrete resulting in increased signal amplitudes. This continues till the

whole bar delaminates from the concrete (12 days). After this, the presence of chlorides results in deterioration of bar in the form of pits leading to attenuation of the signal. This indicates that CC begins with bond deterioration and leads to pit formation and area loss as it progresses.

- From the peak to peak voltage ratio plots, the mechanism of corrosion of reinforcing bar in presence of chlorides can be well understood. Corrosion begins with formation of flaky rust product having large volume causing the delamination of bar from the surrounding concrete resulting in increased signal amplitudes. The delamination marks the onset of corrosion phenomenon in a bar undergoing accelerated corrosion and is clearly indicated by the surface seeking mode.
- As corrosion progresses, it is marked by local loss of area in the form of pitting and crevices as well as the debonding of bar. It begins in the transition zone shown by signal rise in L (0, 1) mode and signal attenuation in L (0, 7) mode. It marks the progress of corrosion causing surface modification as well as non-uniform area loss in the form of pits. As exposure increases, there is a drastic fall in signal amplitude in both L (0, 1) and L (0, 7) modes due to increase in loss of energy caused by scattering, multiple reflections and mode conversions.

7.3.2 Beams undergoing OC

- Two different modes are to be selected to distinguish between OC and CC through ultrasonics and to pick up debonding and pitting effects of corrosion.
- Corrosion in the presence and absence of chlorides (referred as Chloride Corrosion, CC) and Oxide Corrosion, OC respectively) had different effects on the bar. While OC mainly affects the surface of the bar, CC leads to pitting inside the bar. Thus, a mode having significant surface component will be sensitive to OC and L (0, 1) is such a surface seeking mode. CC manifests itself in a mode that progresses mainly through the core of the bar and has negligible surface component. L (0, 7) mode is such a mode. Therefore it is suitable for identifying CC.
- In the beam undergoing OC, no visual change is observed until 15 days. Then a longitudinal crack appears parallel to the reinforcement accompanied by a small leakage

of corrosion products. The crack increased in length and width but extended to only middle 1/2 length of the beam till 28 days. A significant observation is the appearance of a perpendicular crack at the centre of the beam. It appears on the 22nd day and progresses to divide the length of the beam into halves.

- With surface seeking mode L (0, 1), in the OC specimen, the received signal amplitude continues to rise till the end of exposure indicating increasing delamination during the whole period. But the rise in signal strength is slow as compared to CC.
- For the same period, OC affects only the surface of the bar causing delamination and no severe pitting or area loss is observed. Corrosion is not as widespread as in CC bars. Delamination dominates the corrosion process and no pits are seen.
- Visual examination of the bar after conducting the pull out test revealed that there is localized corrosion product, small rust stains and a longitudinal crack in the middle 1/2 length of the beam. Because of this local pressure build up in a small length, a transverse crack appeared in the centre of beam.
- Ultrasonic monitoring of the OC beam with L (0, 7) mode shows no drop in signal till 12 days. Then it starts dropping slowly but the fall is not drastic as observed in CC testing. This clearly differentiates the corrosion mechanism in the two kinds of corrosion process. Corrosion mechanism in OC specimen shows insignificant core modification of the embedded bar in the form of pitting as against huge drops in voltages in chloride corrosion.
- Ultrasonic guided wave monitoring utilizing specific core and surface seeking modes successfully identifies the type, rate and mechanism of corrosion in a reinforcing bar in concrete subjected to different exposure conditions. In general, huge pitting and non-uniform area loss highlighted by severe signal attenuation marks CC and is well picked up by core seeking mode. It begins with delamination shown by signal rise with surface seeking mode. In OC, the rate of corrosion is slow, localized and marked by slow bond deterioration as depicted by signal strength rise in surface seeking mode. Pitting is insignificant as shown by very slow signal fall in core seeking mode in OC.
- Through a judicious selection of ultrasonic modes different types of corrosion in RC structures can be successfully identified.

7.4 DESTRUCTIVE TESTING AND CALIBRATION WITH ULTRASONICS

Ultrasonics is a non-destructive technique and its results must be calibrated with the results of destructive tests such as mass loss, bond strength and residual tensile strength of the reinforcement. Ensembles of samples at different stages of corrosion in two environments are monitored ultrasonically followed by destructive tests. The ultrasonic voltages at particular instants are mapped to percentage mass loss, tensile strength and pullout strength and the following conclusions were drawn:

7.4.1 Beams undergoing CC

- From the destructive test results for different days of exposure for CC specimens, loss in residual mass (ML_t), pullout strength (PO) and tensile strength (f_t) is observed with the increase in the days of exposure.
- It is observed that the mass loss until the 6^{th} day is marginal. There is a sudden increase in mass loss from 6^{th} – 12^{th} day. After 12^{th} day, increase in mass loss continues but at a slower rate. This signifies that the initial delamination corrosion that takes place at the surface of the bar does not lead to a significant mass loss.
- At the onset of pitting after the 6^{th} day, there is a significant loss of mass. This is also corroborated by the sudden loss of tensile strength of the bar between 6^{th} and 12^{th} day. The loss of tensile strength indicates the loss of crossectional area of the bar.
- The pullout strengths of the beam indicate that there has been an increase from 0^{th} to 6^{th} day. It is because the bars used in the experiments are plain extruded bars without any ribs. Thus, the initial bond at the steel – concrete interface is only through friction and there is no mechanical bond. Creation of corrosion products at the surface exerts an outward pressure on the concrete. This improves the bond initially. But as corrosion progresses, the soluble corrosion products get washed away creating loss of interfacial bond and fall in pullout strengths.
- A correlation is attempted to facilitate non-destructive estimation of the physical condition of the bar. It is important to choose the right mode of ultrasonic wave. It is indicated earlier that L (0, 1) mode is capable of detecting corrosion at early stage. However, it is not very suitable

for mapping its output to the physical condition of the bar because the same voltage ratios are obtained in very different physical conditions of the bar.

- With L (0, 7) mode, the signal strength decreases monotonically with the deterioration of the bar. Hence, one-to-one correspondence between the ultrasonic signal and the physical condition of the bar can be established. Thus, the calibration of the ultrasonic CC data with the physical state of the bar is attempted with L (0, 7) mode only.
- The signal strength of L (0, 7) mode is highest at the initial stage and it reduces sharply with the loss of mass finally getting asymptotic once again. Thus, a hyperbolic curve is fitted between the voltage ratio and the mass loss.
- It has been already indicated that the bond strength increases initially and then reduces due to corrosion. It is felt that to develop a reliable relationship between the voltage ratio and the bond strength, more data points would be essential.
- The tensile strength of the bar reduces monotonically with corrosion. Thus, straight line fit is attempted for calibrating the residual strength with voltage ratio.

7.4.2 Beams undergoing OC

After destructive tests of mass loss, tensile strength and pull out with OC beams, following conclusions are drawn:

- In OC beam specimens, as the exposure increased, the pullout strength increases with the progress of corrosion. This is due to the formation of rust product having large volumes in comparison to the surrounding steel bar resulting in increasing bond strengths. Throughout the slow oxide corrosion process, only surface modification caused by corrosion products formation takes place. An increase in pullout strength by 51% of the healthy beam is observed after 28 days of exposure which increased by 2.6 times in 130 days of corrosion.
- Also, the extracted OC bar observed only nominal loss in mass and tensile strength with the increase in corrosion. In 28 days, the bar experienced only 0.316 % and 10.88 % loss of its mass and tensile strength respectively. In 130 days, percentage mass loss and tensile strength increased marginally to 1.5% and 14.1% respectively. The higher percentage of strength and residual mass indicates that OC does not lead to severe pitting and loss of metal. The visual inspection also confirmed that the bar had not experienced large and widespread pitting and area loss.

- A correlation between the ultrasonic peak-peak voltage ratios is done to facilitate non-destructive estimation of the physical condition of the bar. Similar to CC, L (0, 7) mode is mainly capable of detecting OC throughout by mapping its signal output to the physical condition of the bar.
- In L (0, 1) mode, the voltage ratio increases initially as corrosion progresses with the deterioration of the bar in the form of delamination. Then amplitude shows drop after 50-60 days. Due to the variation in voltage trends with corrosion, L (0, 1) mode is not considered for calibration. With L (0, 7) mode, no initial change for 14 days is observed in voltage ratios when debonding predominates but after this period, the signal amplitude decreases with the deterioration of the bar. Hence, L (0, 7) mode is used to relate the ultrasonic signal voltages with the physical condition of the bar.
- With L (0, 7) mode, as corrosion progresses, signal strength falls. Also loss in mass is observed with progress of corrosion and hence a linear relation between R and % mass loss is established.
- It has been already indicated that the bond strength increases as corrosion progresses with fall in signal strength in L (0, 7) mode. Hence, a parabolic relationship has been established between PO and R with L (0, 7) mode.
- The tensile strength of the bar reduces with corrosion indicated by fall in strength of L (0, 7) mode. A linear fit is attempted between R and f_t in L (0,7) mode.

7.5 SCOPE OF FUTURE WORK

Ultrasonic guided waves utilizing specific core and surface seeking modes can be successfully used for real time monitoring the corrosion phenomenon in a bar in concrete. Through a judicious selection of ultrasonic modes, it not only identifies the type of corrosion mechanism but also the rate of corrosion. The ability of ultrasonics to predict the level of deterioration of the bars and to correlate with its physical condition of the bars at different stages of corrosion in the two environments is successfully explored. In the course of investigation, a few open issues have been identified. Ultrasonic guided waves can be implemented for health monitoring of civil infrastructure systems and there is a lot of potential future research in this area:

- Extension of the above developed corrosion monitoring methodology using ultrasonic guided waves to large scale testing of RC beams
- To apply the developed methodology to real reinforcing bars i.e. ribbed bars in concrete and study the effect of ribs on ultrasonic voltages
- Ensembles of samples at different stages of corrosion in two environments to be monitored ultrasonically followed by destructive tests to seek more data points to sketch and develop perfect equations
- Developing a theoretical/numerical model to analyze the corrosion phenomenon in RC structures
- Application of guided waves to detect damages in the form of wire breaks and corrosion damages in prestressing tendons embedded in grout.
- To study the effect of curvature and presence of multiple wires in the tendons on ultrasonic voltages.

7.6 CLOSING REMARKS

The present study indicates that ultrasonic guided waves can be successfully utilized for corrosion monitoring of reinforcing bars in concrete. Specific core and surface seeking modes can identify the type, rate and mechanism of corrosion in a reinforcing bar in concrete subjected to different exposure conditions. Thus, through a judicious selection of ultrasonic modes different types of corrosion in RC structures can be successfully identified. The ability of ultrasonics to predict the level of deterioration of the bars can be done successfully by correlating ultrasonic voltage ratios with destructive parameters of mass loss, tensile strength and bond strength in the two common corrosion environments. These would facilitate non-destructive evaluation of reinforcements embedded in concrete.

REFERENCES

Ahmad, S. and Bhattacharjee, B. (1995), 'A simple arrangement and procedure for in-situ measurement of corrosion rate of rebar embedded in concrete', Corrosion Science, 37(5), pp. 781–91.

Ahmad, S. (2003), 'Reinforcement Corrosion in concrete structures, its monitoring and service life prediction- A Review', Cement and Concrete Composites, 25, pp. 459-471.

Aktan, A.E. and Grimmelsan, K.A. (1999), 'The Role of NDE in bridge health monitoring, Proc. SPIE, 3587, pp. 2-15.

Alleyne, D.N., Cawley, P., Lank, A.M. and Mudge, P.J. (1997), 'The Lamb wave inspection of chemical plant pipe network', Review of Progress in QNDE, Plenum Press New York, 16, pp. 1269-1276.

Alleyne, D.N., Lowe M.J.S. and Cawley, P. (1998), 'The reflection of guided waves from circumferential notches in pipes', ASME Journal of Applied Mechanics, 65, pp. 635-641.

American Society of Testing and Materials, Standard Test Method for Half Cell Potentials of Uncoated Reinforcing Steel in Concrete, ASTM C876, 1987.

Amos, D.E. (1995), 'A Remark on algorithm 644: a portable package for Bessel's functions of a complex argument and non-negative order', ACM Transactions on Mathematical Software, 21(4), pp. 388-393.

Andrade, C., Alonso, C. and Molina, F. J. (1993), 'Cover cracking as a function of rebar corrosion: Part I-Experimental Test', Materials and Structures, 26 (162), pp. 453–464.

Andrade, C. and Alonso, C. (1996), 'Corrosion rate monitoring in the laboratory and on-site', Construction and Building Materials, 10 (5), pp. 315-328.

Andrade, C., Alonso, C. and Sarría, J. (2002), 'Corrosion rate evolution in concrete structures exposed to the atmosphere', Institute of Construction Science "Eduardo Torroja", CSIC, Serrano Galvache s/n, Apdo 19002, E-28033 Madrid, Spain.

Badawi, M. and Soudki, K. (2005), ' Control of corrosion-induced damage in reinforced concrete beams using carbon fiber-reinforced polymer laminates', Journal of Composites for Construction., 9(2), pp. 195-201.

Batis, G. and Rakanta, E. (2005), 'Corrosion of steel reinforcement due to atmospheric

pollution', Cement and Concrete Composites, 27, pp. 269–275.

Bazant, Z. P. (1979), 'Physical model for steel corrosion in concrete sea structures—Theory', Journal of Structures, ASCE, 105, pp. 1137–1153.

Beard, M.D. (2002), 'Guided wave inspection of embedded cylindrical structures', PhD Thesis, Department of Mechanical Engineering, Imperial College of Science, Technology and Medicine, London, UK.

Beard, M.D., Lowe, M.J.S. and Cawley, P. (2003), 'Ultrasonic guided waves for inspection of grouted tendons and bolts', Journal of Materials in Civil Engineering, 15, pp. 212-218.

Bentur. A., Diamond, S. and Berke, N. S., 'Steel Corrosion in Concrete: Fundamental and Civil Engineering Practice,' London, E & FN Spon.,1997.

Berkely K.G.C. and Pathmanaban, S., 'Cathodic protection of reinforcement steel in concrete', London, Butterworths & Co. Ltd. , 1990.

Berke, N.S. and Hicks, M. (1992), 'Corrosion forms and control for infrastructure", V.Chaker Editor, ASTM STP 1137, American Society of Testing and Materials, Philadelphia, pp. 207.

Berliner, M. and Solecki, R. (1996), 'Wave propagation in a fluid - loaded transversely isotropic cylinder: Part 1. Analytical Formulation', Journal of Acoustical Society of America, 99 (4), pp. 1841- 1847.

Bernard, A., Lowe, M.J.S. and Deschamps, M. (2000), 'Guided waves energy velocity in absorbing and non-absorbing plates', Journal of the Acoustical Society of America, 110, pp.186-196.

Berver, E., Fowler, D., Jirsa, J. and Wheat, H. (2002), 'Composite wrapping as a means of corrosion mitigation', Proc., of Twelfth International Offshore and Polar Engineering Conference, International Society of Offshore and Polar Engineers, Kitakyushu, Japan, pp. 137-142.

Bennett, J., Schue, T. J., Clear, K. C., Lankard, D. L., Hartt, W. H. and Swiat, W. J. (1993), 'Electrochemical chloride removal and protection of concrete bridge components: laboratory studies,' Strategic Highway Research Program Report, (SHRP-S-657).

Bindal, V.N., 'Transducers for ultrasonic flaw detection', Narosa Publishing House, 1999.

Bjegovic, D., Stipanovic, I., Skazlic, M., Feric, K. and Barbalic, I. (2009), 'Case study – Corrosion monitoring in marine environment in Croatia', Courtesy-Google Search.

Bonacci, J. (2000), 'Rehabilitation of corrosion-damaged RC infrastructure using externally-

bonded FRP', Proc. 3rd Int. Conf. on Advanced Composite Materials in Bridges and Structures, Canadian Society for Civil Engineering, Ottawa, pp. 679-686.

Broomfield, J.P. and Tinnear, J. S., (1992), 'Cathodic protection of reinforced concrete bridge components', Strategic Highway Research Program Report, (SHRP-92-618).

Broomfield, J.P., 'Corrosion of Steel in Concrete: Understanding, Investigation and Repair', London, UK: E & FN Spon., 1997.

Broomfield, J.P., Davies, K. and Hladky, K. (2002), 'The use of permanent corrosion monitoring in new and existing reinforced concrete structures' Cement and Concrete Composites, 24, pp. 27-34.

Browne, R.D. (1982), 'Design prediction of life for reinforced concrete in marine and other chloride environment', Durability of Building Materials, 1, pp. 113-125.

Bungey, J.H., 'The testing of concrete in structures', Surrey University Press, London, 1989.

Carino, N. J. (2001), 'Impact-echo method: An overview', Proc. Structures Congress and Exposition, American Society of Civil Engineers (ASCE), Washington D.C., pp. 1-18.

Chree, C. (1889), 'The equations of an isotropic elastic solid in polar and cylindrical coordinates, their solutions and applications', Transactions of the Cambridge Philosophical Society, 14, pp. 250-369.

Craig, B., C. (2002), 'Confining effects of FRP laminates on corroded concrete members,' MS thesis, Univ. of Waterloo, Ontario, Canada.

Cullington, D. W., MacNeil, D., Paulson, P. and Elliot, J. (2001), 'Continuous acoustic monitoring of grouted post-tensioned concrete bridges', International Journal of Non-Destructive Testing & Evaluation , 34, pp. 95-106.

Davies, R.M. (1948), 'A Critical Study of the Hopkins on pressure bar', Phil. Transactions of Royal Society, London, 240, pp. 375- 457.

Dayal, V. (1993), 'Longitudinal waves in homogenous anisotropic cylindrical bars immersed in fluid', Journal of Acoustical Society of America, 93 (3), pp. 1249.

Doyle, J. F, 'Wave Propagation in Structures', Springer, New York, 1989.

Debaiky, A., Green, M.C. and Hope, B.B. (2002 a). Carbon fiber-reinforced polymer wraps for corrosion control and rehabilitation of reinforced concrete columns, ACI Journal of Materials, 99(2), pp. 142–152.

Debaiky, A., Green, M. C. and Hope, B. B (2002 b), 'Proceedings of Annual Conference -

Canadian Society for Civil Engineering, 30th Annual Conference: 2002 Challenges Ahead', Jun 5-8 2002, Montreal, QB, Canada.

Ervin, B. L. and Reis, H. (2008), ' Longitudinal guided waves for monitoring corrosion in reinforced mortar', Measurement. Science &. Technology, 19(1), pp. 1-19.

Ervin, B. L., Kuchma, D. A., Bernhard, J. T. and Reis, H. (2009), 'Monitoring corrosion of rebar embedded in mortar using high frequency guided ultrasonic waves', Journal of Engineering Mechanics, 135(1), pp. 9-19.

Fang, C., Lundgren, K., Chen, L. and Zhu, C. (2004), 'Corrosion influence on bond in reinforced concrete', Cement and Concrete Research, 34, pp. 2159–2167.

Feliu, S., Andrade. C., Gonzalez, J.A. and Alonso, C. (1996), 'A new method for in-situ measurement of electrical resistivity of reinforced concrete', Journal of Materials & Structures, 29 (190), pp. 362-365.

Fontana, M., G., and Greene, N. D. 'Corrosion Engineering**',** McGraw-Hill, New York, New York, 1967.

Fitch, A.H., (1963), 'Observation of elastic – pulse propagation in axially symmetric symmetric and non-axially symmetric longitudinal modes of hollow cylinders' , Journal of Acoustical Society of America, 35(5), pp. 706-708.

Flis, J., Sehgal, A., Li, D., Young, Tai K., Sabotl, S., Pickering, H., Osseo-Asare, K. and Cady , P. (1993), 'Condition evaluation of concrete bridges relative to reinforcement corrosion method for measuring corrosion rate of reinforcing steel', SHRP-S-324, National Research Council. Washington, DC.

Gadve, S., (2008), 'Corrosion protection of steel reinforcement in concrete with externally applied FRP sheets', PhD Thesis, IIT Powai, Bombay, India.

Gadve, S., Mukherjee, A. and Malhotra, S. N. (2009), 'Corrosion of steel reinforcements embedded in FRP wrapped concrete," Journal of Construction & Building Materials, 23(1), pp. 153-161.

Gaydecki, P. A., Burdekin, F. M., Damaj, W. , John , D. G and Payne, P. A. (1992), ' Digital deconvolution analysis of ultrasonic signals influenced by the presence of longitudinally aligned steel cables in pre-stressed concrete', Measurement. Science &. Technology, 3(9), pp. 909-917.

Gazis, D.C.(1959), 'Three Dimensional investigation of the propagation of waves in hollow

circular cylinders', Journal of Acoustical Society of America, 31(5), pp. 568-578.

Griffiths, R.W. (1998), 'Recent and current developments in distributed fiber optic sensing for structural monitoring', Proc. SPIE. , 985, pp. 69-76.

Glass, G., Page, C. and Short, N. (1991), 'Factors affecting steel corrosion in carbonated mortars', Corrosion Science, 32, pp.1283-1394.

Gu, P., Gu, Y., Xie, P. and Beaudoin., J.J. (1994), 'Significance of pre-existing cracks on nucleation of secondary enttringite in steam cured cement paste', Cement and Concrete Research, 24(6), pp. 1015-1024.

Hay, T. R. and Rose, J. L. (2004), 'Interfacing guided wave ultrasound with wireless technology', Proc. SPIE, 5391 , pp. 314–20.

Hachani, L., Fiaud , C., Triki, E. and Raharinaivo, A.(1994), ' Characteristics of steel/concrete interface by electrochemical impedance spectroscopy', British Corrosion Journal, 29 , pp. 122-127.

He, C., Van Velsor, J. K., Lee, C. M. and Rose, J. L. (2006), ' Health Monitoring of rock bolts using ultrasonic guided waves', Quantitative Nondestructive Evaluation (AIP Conf. Proc. 820), ed D.O. Thompson and D.E. Chimenti , pp. 195-201.

Hong, H.W. and Saraswathy, V. (2007), 'Corrosion monitoring of reinforced concrete structures – a review', International Journal of Electrochemical Science, 2, pp. 1-28.

Hope, B.B., Ip, A.K. and Manning, D.G. (1985), 'Corrosion and Electrical Impedance in concrete', Cement and Concrete Research, 15(3), pp. 525-534.

Hussain, S.E., Rasheeduzzafar, M., Al-Musallan, A. and Al-Gahtani. A.S. (1995), 'Factors affecting threshold chloride for reinforcement corrosion in concrete', Cement and Concrete Research, 25, pp.1543-1555.

Husain, A., Al-Bahar, S., Abdul Salam, S. and Al-Shamali, O. (2004),'Accelerated A.C impedance testing for prequalification of marine construction materials', Desalination, 16 (5), 377-384.

Hudson, G.E. (1943), 'Dispersion of Elastic Waves in solid circular cylinders', Physics Review, 63, pp. 46-51.

Idrissi, H. and Limam, A. (2003), 'Study and characterization by acoustic emission and electrochemical measurements of concrete deterioration caused by reinforcement steel

corrosion', NDT & E International, 36, pp. 563–569.

Ijsseling F.P. (1986), 'Application of electrochemical methods of corrosion rate determination to system involving corrosion product layers, British Journal of Corrosion, 21(2), pp. 95–101.

John, D.G., Searson, P.C. and Dawson, J.L. (1981), 'Use of AC impedance technique in studies on steel in concrete in immersed conditions', British Corrosion Journal, 16, pp. 102-106.

Kranc, S.C. and Sagues, A.A. (1993), 'Polarization current distribution and electrochemical impedance responseof reinforced concrete when using guard ring electrodes', Electrochemica Acta, 38 (14), pp. 2055-2061. .

Kumar, R. (1971), 'Flexural vibrations of fluid-filled circular cylindrical shells', Acoustica, 24, pp.137-146.

Kumar, R. (1972), 'Dispersion of axially symmetric waves in empty and fluid-filled cylindrical shells', Acoustica, 27(6), pp. 317-329.

Kundu, T., Na, W.B. and Ehsani , M. R. (2002), 'Ultrasonic guided waves for steel bar concrete interface testing', Materials Evaluations, 60(3), pp. 437-444.

Kundu T. (2004), 'Ultrasonic Nondestructive Evaluation: Engineering and Biological Material Characterization, Pub. CRC Press, USA.

Kundu, T. , Banerjee, S. and Jata, K. V. (2006), ' An experimental investigation of guided wave propagation in corrugated plates showing stop and pass bands', Journal of Acoustical Society of America, 12093, pp. 1217-1226.

Kundu, T. and Placko, D. , 'Advanced Ultrasonic Methods for Material and Structure Inspection', ISTE Ltd., Newport Beach, CA 92663, USA, 2007.

Lay, P., Lawrence, P.F., Winkins, N.J.M. and Williams. D.E. (1985), 'An A.C impedance steady of steel in concrete', Journal of Applied Electrochemistry, 50, pp. 755

Lee, C., Bonacci , J., Thomas, M., Khajenpour, S. and Hearn N. (2000), 'Accelerated corrosion and repair of reinforced concrete columns using CFRP sheets', Canadian Journal of. Civil Engineering, 27(5), pp. 949-959.

Lowe, M.J.S. (1995), 'Matrix techniques for modeling ultrasonic waves in multilayered media', IEEE Trans., Ultrasonics, Ferroelectrics and Frequency Control, 42(4), pp. 525-542.

Lopez, W., and Gonzalez, J.A. (1993), 'Influence of degree of pore saturation on the resistivity of concrete and corrosion rate of steel reinforcement', Cement and Concrete Research, 23, pp.

368-376.

MacDonald, D.D., Mckubre, M.C.H. and Urquidi-Macdonald, M. (1988), 'Theoretical assessment of AC impedance spectroscopy for detecting corrosion of rebar in reinforced concrete corrosion of metal in concrete', Corrosion, 44(2).

Macdonald, D.D., El-Tantawy, Y.A., Rocha-Filho, R.C. and Urquidi-Macdonald, M. (1991), 'Evaluation of Electrochemical Impedance Techniques for Detecting Corrosion on Rebar in Reinforced Concrete', National Research Council , Washington, DC, SHRP-ID/UFR-91-524.

Martínez, I. and Andrade, C. (2009), 'Examples of reinforcement corrosion monitoring by embedded sensors in concrete structures', Cement & Concrete Composites, 31, pp. 545–554.

Masoud, S., Soudki, K. and Topper, T. (2005), 'Post-repair fatigue performance of FRP-repaired corroded RC beams: Experimental and Analytical Investigations', Journal of Composites for Construction, 9(5), pp. 441-449.

Masoud, S. and Soudki, K. (2006), 'Evaluation of corrosion activity in FRP repaired RC beams', Cement & Concrete Composites, 28, pp. 969–977.

Matt, P. (2001), ' Non-destructive evaluation and monitoring of post-tensioning tendons', *fib Bull. 15:* Durability of post-tensioning tendon, pp. 100-108.

Meeker T.R. and Meitzler, A.H. (1972), 'Guided wave propagation in elongated cylinders and plates', Physical Acoustics – Principals and Methods, eds. W.P. Mason and R.N. Thurton, Academic Press New York , pp. 111-167.

Millard, S., Harrison, J. and Edwards, A. (1989), 'Measurement of electrical resistivity of reinforced concrete structure for assessment of corrosion risk', Non- Destructive Testing, 31, pp. 617-621.

Miller, T., Hauser, C. J. and Kundu, T. (2002), 'Non- destructive inspection of corrosion and delamination at the concrete-steel reinforcement interface', Proceedings of. ASME NDE Division. Symposium, 23, pp. 121-128.

Mirsky, I. (1954), 'Wave propagation in transversely isotropic circular cylinders Part 1: Theory', Journal of Acoustical Society of America, 37 (6), pp. 1016-1021.

Morcous, G. and Lounis, Z. (2005), 'Prediction of onset of corrosion in concrete bridge decks using neural networks and case-based reasoning', Computer Aided Civil Infrastructural. Engineering, 20, pp. 108–117.

Montemor, M.F., Simoes, A.M.P., Salta, M.M. and Ferreira, M.G.S. (1993), 'The assessment

of electrochemical behavior of flyash- containing concrete by impedance spectroscopy', Corrosion Science, 35, pp. 1571-1578.

Morse, R. (1954), 'Compressional Waves along an anisotropic circular cylinder having hexagonal symmetry,' Journal of Acoustical Society of America, 26 (6), pp. 1018-1021.

Morris, W., Vico, A., Vazquez, M. and Sánchez De, S.R. (2002), 'Corrosion of reinforcing steel evaluated by means of concrete resistivity measurements', Corrosion Science, 44(1), pp. 81-99.

Nagy, P. (1995), 'Longitudinal guided wave propagation in a transversely isotropic rod immersed in fluid', Journal of Acoustical Society of America, 98 (1), pp. 454- 457.

Na, W., Kundu , T. and Ehsani, M. R. (2002) , 'Ultrasonic guided waves for steel bar concrete interface testing' , Materials Evaluation , 60, pp. 437-444.

Newton, C.J. and Sykes, J. M. (1988), 'A Galvanic Pulse Technique for investigation of steel corrosion in concrete,' Corrosion Science, 28, 1051-1073.

Okba, S., El-Dieb, A., El-Shafle, H., Rashad, A. (2003), 'Evaluation of corrosion protection for reinforced concrete wrapped by FRP', Proceedings of ICPCM-2003 Conference, Cairo, Egypt, pp. 18-20.

Onoe, M., McNiven, H.D. and. Mindlin, R.D. (1962), 'Dispersion of axially symmetric waves in elastic solids', Journal of Applied Mechanics, 29, pp. 729-734.

Pao, Y.H. and Mindlin, R. (1960), 'Disperison of flexural waves in an elastic, circular cylinder', Journal of Applied Mechanics, 27, pp. 513-520.

Pao, Y.H. (1962), 'The dispersion of waves in an elastic, circular cylinder - Part 2', Journal of Applied Mechanics, 29, pp. 61-64.

Pavlakovic, B.N. (1998), 'Leaky guided ultrasonic waves in NDT', PhD Thesis, Department of Mechanical Engineering, Imperial College of Science Technology and Medicine, London.

Pavlakovic, B.N., Lowe, M.J.S. and Cawley, P. (1998), 'Guided ultrasonic waves for the inspection of post-tensioned concrete bridges', Review of Progress in QNDE, eds.D.O. Thompson and D.E. Chimenti, 17, pp.1557-1564, Plenum Press, New York.

Pavlakovic, B.N., Lowe, M.J.S. and Cawley, P. (1999), 'Inspection of tendons in post-tensioned concrete using guided ultrasonic waves', Insight, 41(7), pp. 446-452.

Pavlakovic, B.N. and Cawley, P. (2000), DISPERSE User's Manual Version 2.0.1.1, Imperial College, University of London.

Pavlakovic, B.N., Lowe, M.J.S. and Cawley, P. (2001), 'High frequency low loss ultrasonic modes in imbedded bars', International Journal of Applied Mechanics, 68, pp. 67-75.

Pochhammer, J. (1876),Ueber die Fortpflanzungsgeschwindigkeiten kleiner Schwingungen in einem unbegrenzten isotropen Kreiszylinder, Journal fuer reine und angewandte Math, 81,pp. 324-336.

Poursaee, A. and Hansson, C. M. (2009), 'Potential pitfalls in assessing chloride –induced corrosion of steel in concrete', Cement and Concrete Research, 39, pp. 391-400.

Pullar-Strecker, P., 'Corrosion damaged concrete: assessment and repair,' London: Butterworths, 1987.

PUNDIT 6 , Operating Manual, CNS Farnell, Manor Way, Borehamwood, Hertfordshire, UK.

Reis, H., Ervin, B. L., Kuchma, D. A. and Bernhar, J. T. (2005), 'Estimation of corrosion damage in steel reinforced mortar using guided waves', Journal of Pressure Vessel Technology, 127, pp. 255-261.

Rens, K. L., Transue, D. J. and Schuller, M. P. (2000), 'Acoustic tomographic imaging of concrete infrastructure', ASCE Journal of Infrastructure Systems, 6(1), pp. 15-23.

Rodríguez, P., Ramirez, E. and Gonzalez, J.A. (1994), 'Methods for studying corrosion in reinforced concrete', Magazine of Concrete Research, 46(167), pp. 81–90.

Rostam, S. (2003), 'Reinforced concrete structures—shall concrete remain the dominating means of corrosion prevention?', Materials Corrosion, 54, pp. 369–378.

Safaai-Jazi, A., Jen, C.K. and Farnell, G.W. (1986), 'Cutoff conditions in an acoustic fiber with infinitely thick cladding', IEEE Transactions on Ultrasonics, Ferroelectrics and Frequency Control, 33(1), pp.69-73.

Sanjurjo, A., Hettiarachchi, S., Lau, K., Wood, B. and Cox, P. (1993), 'Development of metallic coatings for corrosion protection of steel rebars', Strategic Highway Research Program Report, (SHRP-I-622).

Sathiyanarayanan, S., Natarajan, Patanjali, Saravanan, K., Srinivasan, S. and Venkatachari, G. (2006), 'Corrosion Monitoring of steel in concrete by galvanostatic pulse technique', Cement and Concrete Composites, 28, pp. 630-637.

Sato, D. (2001), 'Measurement technique of acquiring sodium chloride concentration by using near-infrared spectrum', Proceedings of JSCE Annual Conference, 56, pp.844-845.

Schiessl, P. (1975), 'Admissible crack width in reinforced concrete structures', Contribution

II, International Colloquium on the Behavior in Service of Concrete Structures, pp. 3-17.

Schiessl, P. (1988), 'Corrosion of steel in concrete', Report of the Technical Committee, 60-CSC, RILEM.

Scheel, H. and Hillemeier, B. (1995), 'The capacity of the remanent magnetism methods to detect fractures of steel in tendons embedded in prestressed concrete', Proceedings of International Symposium on Non-Destructive Testing in Civil Engineering, Berlin, 1, pp. 211-218.

Silk, M.G. and Bainton, K.F. (1979), 'The propagation in metal tubing of ultrasonic wave modes equivalent to Lamb waves', Ultrasonics, pp.11-19.

Simmons, J.A., Drescher-Krasicka, E. and Wadley, H.N.G. (1992), 'Leaky axisymmetric modes in infinite clad rods', Journal of the Acoustical Society of America, 92(2), pp.1061-1090.

Silk, M.G. and Bainton, K.F. (1979), 'The propagation in metal tubing of ultrasonic wave modes equivalent to Lamb waves', Ultrasonics, pp.11-19.

Shamsad, A. (2003), 'Reinforcement corrosion in concrete structures, its monitoring and service life prediction – a review', Cement & Concrete Composites, 25, pp. 459-471.

Stratfull, R.F. (1957), 'Corrosion of steel in a Reinforced Concrete Bridge: Corrosion', 13, pp. 173-179.

Stratfull, R.F. (1974), 'Experimental cathodic protection of a bridge deck', Materials Protection, 8 , pp.1-15.

Stern, M. and Geary, A. L. (1957), 'Electrochemical Polarization, I-. A Theoretical analysis of shape of polarization curves', Journal of Electrochemical Society, 104, pp. 56-63.

Tamer, E., M. and Soudki, K. (2003), 'Effectiveness of impressed current technique to simulate corrosion of steel reinforcement in concrete', Journal of Materials in Civil Engineering, 15(1), pp. 41-47.

Tamer, E. M. and Soudki, K. (2005), 'Carbon-Fiber-Reinforced polymer repair to extend service life of corroded reinforced concrete beams', Journal of Composites for Construction, 9(2), pp.187-194.

Tamer, E. M., Chahrour, A. and Soudki, K. (2006), 'Effect of Fiber-Reinforced polymer wraps on corrosion activity and concrete cracking in chloride-contaminated concrete cylinders', Journal of Composites for Construction, 10(2), pp. 139-147.

Thurston, R. (1978), 'Elastic waves in rods and clad rods', Journal of the Acoustical Society of America, 64(1), pp.1-37.

Tutti, K., 'Corrosion of steel in concrete,' Swedish Cement and Concrete Research Institute, Sweden, Stockholm, 1982.

Valle, S. and Zanzi, L. (1997-1998),' Travel time radar tomography for NDT on masonry and concrete structures', European Journal of Environmental Engineering Geo-Phys., 2, pp. 229-246.

Viens, M., Tshukahara, Y., Jen, C.K. and Cheeke, J.D.N. (1994), 'Leaky torsional modes in infinite clad rods', Journal of the Acoustical Society of America, 95(2), pp. 701-707.

Vurpillot, S., Inaudi, D. and Ducret, J. M. (1996), 'Bridge monitoring by fiber optic deformation sensors: Design, Emplacement And Results', Proceedings of SPIE. , 2719, pp. 141-149.

Wootton, I. A., Spainhour, L. K. and Yazdani, N. (2003), 'Corrosion of steel reinforcement in carbon fiber-reinforced polymer wrapped concrete cylinders', Journal of Composites in Construction, 7, pp. 339–347.

Wenger, F. and Galland , J.(1990), ' Analysis of local corrosion of large metallic structures or reinforced concrete structures by electrochemical impedance spectroscopy,' Electrochemica Acta, 35 , pp. 1573-1578.

Weight, J. (1994), 'High Frequency Ultrasonic Tests on grouted Tendons', Unpublished Report supplied to Transport Research Laboratory, US.

Wu , F. and Chang, F. K. (2006), ' Debond Detection using embedded piezoelectric elements in reinforced concrete structures: I. Experiment,' Structural Health Monitoring, 5, pp. 5-15.

www.ndt.net

www.ndt.org

www.googleimages.com

Xu, P.C. and Datta, S. (1991), 'Characterization of Fiber-Matrix interface by Guided Waves: Axisymmetric Case', Journal of Acoustical Society of America, 89 (6), pp. 2573-2583.

Yuan, Y., Ji, Y. and Shah, S. P. (2007), 'Comparison of two accelerated corrosion techniques for concrete structures', ACI Structural Journal, pp. 344-347.